Mathematical modelling and systems analysis of intracellular signalling networks and the budding yeast cell cycle

A thesis presented for the degree of

Doctor of Philosophy of the University of London

and the

Diploma of Imperial College

by

Daniel D. Seaton

Department of Chemical Engineering

Imperial College

180 Queen's Gate, London SW7 2AZ

JULY 9, 2013

I certify that this thesis, and the research to which it refers, are the product of my own work, and that any ideas or quotations from the work of other people, published or otherwise, are fully acknowledged in accordance with the standard referencing practices of the discipline.

Signed:

Copyright

Abstract

Cellular signalling networks are responsible for coordinating a cell's response to internal and external perturbations. In order to do this, these networks make use of a wide variety of molecular mechanisms, including allostery, gene regulation, and post-translational modifications. Mathematical modelling and systems approaches have been useful in understanding the signal processing capabilities and potential behaviours of such networks.

In this thesis, a series of mathematical modelling and systems investigations are presented into the potential regulation of a variety of cellular systems. These systems range from ubiquitously seen mechanisms and motifs, common to a wide variety of signalling pathways across many organisms, to the study of a particular process in a particular cell type - the cell cycle in *Saccharomyces cerevisiae*.

The first part of the thesis involves the analysis of ubiquitous signalling mechanisms and behaviours. The potential behaviours of these systems are examined, with particular attention paid to properties such as adaptive and switch-like signalling. This series of investigations is followed by a study of the dynamic regulation of cell cycle oscillators by external signalling pathways. A methodology is developed for the study of mathematical models of the cell cycle, based on linear sensitivity analysis, and this methodology is then applied to a range of models of the cell cycle in *Saccharomyces cerevisiae*. This allows the description of some interesting generic behaviours, such as nonmonotonic approach of cell cycle characteristics to their eventual values, as well as allowing identification of potential principles of dynamic regulation of the cell cycle.

Acknowledgements

I owe a debt of gratitude to the many people who have helped me through my PhD, beginning with the staff and fellow students at Imperial College. I am grateful to my advisor, Krishnan, for his invaluable advice, supervision, and patience over the last four years. I would also like to thank my fellow students in the research group - Aiman Alam-Nazki, Liu Cong, Nuri Purswani and others, with special thanks to Aiman Alam-Nazki for her help and advice on many occasions. I am also grateful to my fellow PhD students in the Center for Process Systems Engineering - Pedro Rivotti, Alexandra Krieger, Ines Cecilio, Anna Voelker, Maria Fuentes, and others, for their continual support and friendship. I would also like to acknowledge the EPSRC for funding my PhD on a DTA studentship.

Finally, I owe a great deal to my family and friends for their support during my PhD. My parents, Roxana and Nigel, have been supportive and encouraging of my education and ambitions over not only the last four years, but my whole life, and I owe them a great deal. To my friends in London (and especially those with whom I have lived) - Giovanni, Joanna, Alicia, Kathryn, Patrizia, Arne, Yuki, Lyndsey, Domenico, Dominic, Bene, and Olivier - I am grateful for putting up with me, and to my friends back home in Scotland - Ian, Sean, Julz, and Abi - I thank for the frequent source of escapism.

Table of contents

Abstract **4**

Table of Contents **6**

List of Figures **10**

List of Tables **24**

1 Introduction **27**

2 Background **30**
2.1 Introduction 30
2.2 Biochemical mechanisms of cellular signal transduction 31
2.2.1 Ligand binding 31
2.2.2 Post-translational modification 32
2.2.3 Complex formation 33
2.2.4 Transcriptional regulation 33
2.3 Prototypical behaviours of cellular signalling networks 34
2.3.1 Switch-like signalling 35
2.3.2 Adaptive signalling 35
2.3.3 Oscillatory signalling 36
2.4 Systems characteristics of cellular signalling networks 37
2.4.1 Network modularity 37
2.4.2 Robustness 38
2.4.3 Signalling crosstalk 39
2.5 Mathematical modelling and analysis of signalling networks 39
2.5.1 Ordinary differential equation representations of biochemistry . . . 40
2.5.2 Mass action kinetics 41
2.5.3 Michaelis-Menten kinetics 42
2.5.4 General cooperativity 43

3 Coupling of pathways and processes through shared components 45
3.1 Introduction . . . 45
3.2 Models . . . 48
3.2.1 A basic model of coupling between signalling pathways . . . 48
3.2.2 Models of reversible phosphorylation . . . 51
3.3 Results and discussion . . . 54
3.3.1 Modulation of the shared component . . . 54
3.3.2 Modulation of each pathway alone and together . . . 61
3.3.3 Combinatorial signalling and the influence of complex formation mechanisms and allostery . . . 62
3.3.4 Coupling of switches . . . 66
3.3.5 Spatial signalling . . . 69
3.4 Conclusions . . . 71

4 Effects of multiple enzyme-substrate interactions in basic units of cellular signal processing 77
4.1 Introduction . . . 77
4.2 Modelling and methods . . . 79
4.3 Results . . . 87
4.3.1 Product Inhibition . . . 88
4.3.2 Inactive Enzyme Interference . . . 93
4.3.3 The interaction between inactive enzyme and modified substrate . . . 98
4.3.4 Combinations of additional interactions . . . 99
4.3.5 Double Modification of Substrate . . . 100
4.3.6 Scaffold-mediated modification . . . 101
4.4 Conclusions . . . 102

5 A modular systems approach to understanding the interaction of adaptive, monostable, and bistable threshold processes 106
5.1 Introduction . . . 106
5.2 Models . . . 109
5.2.1 Modules of adaptation . . . 109
5.2.2 Modules of monostable thresholds . . . 111
5.2.3 Modules of bistable thresholds . . . 113
5.2.4 Example equations for interconnected modules . . . 115
5.3 Results . . . 116
5.3.1 Interaction of adaptive and monostable threshold modules . . . 116
5.3.2 Interaction of adaptive and bistable threshold modules . . . 117
5.3.3 Consequences of under- and overadaptation . . . 121
5.3.4 The processing of multiple-pulse (pulse train) signals by threshold modules . . . 123
5.3.5 Inducing switching in bistable networks . . . 127

5.3.6 Analysis of the processing of time-varying signals 130
5.3.7 Alternate interconnection of modules 131
5.4 Conclusions 133

6 Principles of dynamic regulation of the budding yeast cell cycle 136
6.1 Introduction 136
6.2 Models of the cell cycle 140
6.2.1 Basic mathematical description of the cell cycle 140
6.2.2 Selection of suitable models to investigate 141
6.2.3 Adapting models to include the effects of budding 144
6.3 Steady state sensitivity analysis 144
6.4 Dynamic response of the cell cycle to changes in parameters 152
6.4.1 Methodology 152
6.4.2 Dynamic sensitivity to changes in individual parameters 154
6.4.3 Dynamic sensitivity to changes in combinations of parameters . . . 162
6.4.4 Response to steadily increasing or decreasing signals 172
6.5 Case study: Glucose regulation of the cell cycle 174
6.6 Comparison of sensitivities for analogous parameters across models 177
6.6.1 Starter cyclin production 178
6.6.2 Mitotic cyclin production 178
6.7 Application of analysis to subpopulations of cells 180
6.8 System-wide comparisons of models 184
6.8.1 Comparison of model flexibility 184
6.8.2 Post-G1-phase dynamics as a source of biphasic responses 188
6.9 Conclusions 190

7 Conclusions and future work 195

A Coupling of pathways: Parameter values 198
A.0.1 Figure 3.4 198

B Multiple enzyme-substrate interactions: Parameter values 201

C Interaction of modules: Parameter values 204

D Cell cycle: additional plots 206

E Description of digital appendices - MATLAB simulation code 210
E.0.2 Chapter 3: Coupling of pathways and processes through shared components 210
E.0.3 Chapter 4:Effects of multiple enzyme-substrate interactions in basic units of cellular signal processing 211

E.0.4 Chapter 5: A modular systems approach to understanding the interaction of adaptive, monostable, and bistable threshold processes . 212
E.0.5 Chapter 6: Principles of dynamic regulation of the budding yeast cell cycle 213

References **215**

References **239**

List of Figures

2.1 Representations of some simple behaviours exhibited by a wide range of biochemical signalling networks. 45

3.1 Schematic of the basic model of coupling of two processes through a shared component. 51
3.2 Steady-state response of basic coupling model to changes in production of X. 56
3.3 Dynamic response of basic coupling model to a step-change in production of X. 62
3.4 Dynamic response of basic coupling model to pulsatile change in production of X. 63
3.5 Dynamic response of basic coupling model to change in production of A or B alone. 64
3.6 Dynamic response of basic coupling model to change in production of A and B together. 65
3.7 Schematic of combinatorial signalling through shared components. 67
3.8 Effects if combinatorial signalling on signal specificity. 68
3.9 Effects of competition on signal specificity. 72
3.10 Effects of competition on timing. 72
3.11 Coordinated switching of pathways through coupling by a shared component. 74
3.12 Response of basic spatial model to localized production of X. 76
3.13 Response of basic spatial model to localized production of B. 77
3.14 Response of basic spatial model when affinities are varied. 78

4.1 Schematics of models of signal transduction involving additional interactions. 88
4.2 Modified behaviour of the pathway in the presence of product inhibition. . . 98
4.3 Response to different strengths of product inhibition for the basic model with the alternative parameter set. 99
4.4 Response of the system to changes in $[A_T]$ and $[S_T]$ when product inhibition is present. 102
4.5 Change in behaviour induced by increasing strengths of product inhibition for cases where the enzyme-substrate affinity is varied. 103

4.6 The potential dynamics of the basic model in the presence of product inhibition. . . . 104
4.7 The modified behaviour of the basic model in the presence of inactive enzyme interference. . . . 107
4.8 The modified behaviour of the pathway in the presence of inactive enzyme interference for the alternative parameter set. . . . 107
4.9 The conversion of a graded response to a threshold response by increasing the strength of inactive enzyme interference. . . . 108
4.10 The increased sensitivity introduced by inactive enzyme interference for a case in which $[B_T] > [A_T]$. . . . 110
4.11 The changes in free concentration of upstream enzyme, A*, with the strength of inactive enzyme interference. . . . 110
4.12 The change in behaviour induced by increasing strengths of inactive enzyme interference for cases where the enzyme-substrate affinity is varied. . . . 111
4.13 The slow down in signalling dynamics with increasing inactive enzyme interference. . . . 112
4.14 The change in behaviour with the strength of interaction between inactive enzyme and modified substrate. . . . 113
4.15 The steady state response of the system under different strengths of the combined interactions are shown. . . . 114
4.16 The effects of product inhibition and inactive enzyme interference on the concentration of modified substrate. . . . 116
4.17 The effects of inactive enzyme interference and product inhibition on scaffold-mediated signalling. . . . 117

5.1 Schematic of the interaction of the adaptive and threshold (monostable/bistable) modules. . . . 124
5.2 Interaction topologies of the biochemical models of adaptation and thresholds studied. . . . 126
5.3 Interaction of the adaptive module with monostable threshold modules. . . . 134
5.4 Interaction of the adaptive module with the bistable threshold module. . . . 136
5.5 Switching thresholds in input pulse amplitudes and durations. . . . 138
5.6 Interaction of underadapting adaptive module with a bistable threshold module. . . . 142
5.7 Response of the monostable Goldbeter-Koshland switch to multiple-pulse inputs. . . . 144
5.8 Response of the bistable threshold module to multiple-pulse inputs. . . . 147
5.9 Switching in a bistable threshold module without leaving the bistable regime. 150
5.10 Response of combined adaptive and bistable module to gradually increasing input signals. . . . 153
5.11 Response of the system in alternate interconnection of modules is shown, with a threshold module upstream of an adaptive module. . . . 155

5.12 Summary of how the functionality of the system depends on the interconnection of system modules and on their relative timescales, in some limiting cases. 156

6.1 A schematic of the essential characteristics of the budding yeast cell cycle is shown, illustrating the coordination between cell cycle progression and changes in cell morphology (i.e. budding). 161
6.2 The cumulative distribution of the proportion of parameters in the Barik model for which a relative parameter change of less than $x(= \Delta k/k)$ (i.e. $x = 1$ corresponds to a 100% change in the parameter) results in difference in the estimates of less than 10%. 171
6.3 Examples of how the first- and second-order estimates of parameter sensitivities diverge for some example parameters are shown. 172
6.4 The $C_k^{T_{div}}$ and $C_k^{V_{div}}$ for parameters in all cell cycle models. 174
6.5 The sensitivity of some cell cycle characteristics down generations to a perturbation of the parameter determining the rate of translation of starter cyclins k_{sn3} applied at $t = 83mins$ during the first generation. 179
6.6 The sensitivity of some cell cycle characteristics down generations to a perturbation of the parameter determining the rate of translation of mitotic cyclins k_{sbM} applied at $t = 41mins$ during the first generation. 180
6.7 The sensitivity of some cell cycle characteristics down generations to a perturbation of the parameter determining the rate of translation of starter cyclins k_{sbM}, as a function of the cell cycle time at which it is applied. . . . 182
6.8 The sensitivity of some cell cycle characteristics down generations to a perturbation of the parameter determining the rate of translation of starter cyclins k_{sn3}, as a function of the cell cycle time at which it is applied. . . . 183
6.9 The phase response curves ($R_k(t)$) and changes in mass fraction donated to the first daughter cell after the perturbation is applied is shown as a function of the time at which that perturbation is applied. 184
6.10 The combination of regulation of two parameters (k_{dcm} in blue and k_{dnt} in green) with monophasic sensitivities. 187
6.11 Changes in daughter size down three generations for different combinations of different sets of three parameters which achieve the same eventual change in behaviour, and all of which achieve minimal M_{dau} compared to other combinations of those three parameters. 191
6.12 Changes in cell cycle period down three generations for different combinations of different sets of three parameters which achieve the same eventual change in behaviour, and all of which achieve minimal M_{period} compared to other combinations of those three parameters. 192
6.13 The dynamic responses of V_{dau} over the first generation are compared for the examples considered in figures 6.11 and 6.12. 193

6.14 The phase responses for different combinations of the three parameters k_{sbS}, k_{pcmp}, and k_{dt1} are plotted alongside the change in the mass fraction donated to the daughter cell in the first generation for cases of increasing and decreasing daughter sizes. 194
6.15 Another example of the case plotted in figure 6.14 is shown, for a different choice of three parameters (in this case, k_{dbMi}, k_{pi5p}, and k_{sn3}). 195
6.16 The correspondence between the sensitivity to step changes ($S_k^Q(t)$) and the sensitivity to temporally graded perturbations ($W_k^Q(t)$) is shown. 197
6.17 Investigation of glucose regulation, feasible forms of regulation, and dynamic sensitivity. 202
6.18 Comparison of parameter sensitivities between models - starter cyclin production parameters. 204
6.19 Comparison of parameter sensitivities between models - mitotic cyclin production parameters. 205
6.20 The phase responses of the system in response to the three example parameters, and the partial synchronisation of cells subjected to perturbations of these parameters. 208
6.21 The flexibility of the models, plotted according to the fraction of singular values σ_i of the matrix A which obey the relationship $\sigma_i/\sigma_{max} > \lambda$. 211
6.22 Fraction of parameters for each model with a biphasic response below the threshold γ in the post-budded phase compared to the fraction with biphasic response in the pre-budded phase. 213

D.1 Changes in daughter size down three generations for different combinations of different sets of three parameters (from the Sriram model) which achieve the same eventual change in behaviour, and all of which achieve minimal M_{dau} compared to other combinations of those three parameters. 231
D.2 Changes in cell cycle period down three generations for different combinations of different sets of three parameters (from the Sriram model) which achieve the same eventual change in behaviour, and all of which achieve minimal M_{period} compared to other combinations of those three parameters. 232
D.3 The dynamic responses of V_{dau} over the first generation in the Sriram model are compared for the examples considered in figures D.1 and D.2. 233

List of Tables

3.1 **Summary of results for the basic model** We consider the case where the shared component, X, binds with high affinity to component A, forming the complex AX, and with low affinity to component B, forming the complex BX. 63

3.2 **Summary of results for variations on the basic model** A summary of results for the biologically motivated variations on the basic model is presented. These demonstrate how the effects considered may play a role in diverse biological contexts. 72

6.1 Flexibility of modulation of V_{div} and T_{div} 187

List of papers

Some of the research presented in this thesis can also be found in the following list of publications:

- D. Seaton and J. Krishnan. Modular systems approach to understanding the interaction of adaptive and monostable and bistable threshold processes. *IET Systems Biology*, 5:2, 2011
- D. D. Seaton and J. Krishnan. The coupling of pathways and processes through shared components. *BMC Systems Biology*, 5:103, 2011
- D. D. Seaton and J. Krishnan. Effects of multiple enzyme–substrate interactions in basic units of cellular signal processing. *Physical Biology*, 9, 2012
- D. D. Seaton and J. Krishnan. Principles of dynamic regulation of the budding yeast cell cycle. *In preparation*

Chapter 1

Introduction

Signalling networks allow cells to convert information about their environment into instructions for cellular behaviour. They allow single-cell organisms to adapt to new environments, and allow the correct development of multicellular organisms through intercellular communication. Understanding of cellular signalling networks has involved a variety of theoretical and biological work.

In this thesis, two strands of work on this theme are laid out. The first is a sequence of investigations into some of the signalling behaviours which some generic signalling networks are capable of, while the second strand of work encompasses a detailed investigation into one relatively well-characterised process - the budding yeast cell cycle - and how it is controlled by the environment through the signalling networks which interact with it.

The first strand, investigating generic signalling networks, follows a broad thematic progression from the coupling of different biochemical signalling modules to the details of how a particular module might operate. These investigations are not specific to any one biological system, but are motivated by patterns of behaviour and biochemical mechanisms that are expected to be ubiquitous in biological systems. This expectation is established by thorough reference to the relevant experimental literature.

This strand of work begins with an investigation into the consequences of two pathways being coupled by the sharing of a single component (chapter 3). In this chapter a basic modelling framework for understanding the coupling of processes and pathways through shared components is developed. This framework starts with the interaction of two components with a common third component and includes production and degradation of all these components. This model is then analysed to identify possible signalling

behaviours, including ultrasensitive and adaptive responses. The basic model is then elaborated with additional control regulation, including switch-like signal processing, and spatial signalling. In the process, a way in which allosteric regulation may contribute to signalling specificity is identified. Further, the role of competitive effects in coupling parallel switch-like signalling mechanisms in an enzymatic signalling cascade is analysed to show how an enzyme might robustly coordinate and time the activation of parallel pathways.

One interesting theme arising from this work is how the details of protein-protein interactions can affect signalling behaviours, as noted particularly in the examination of an enzyme regulating two signalling pathways in parallel. This observation, which has not in general been appreciated in the construction and analysis of models of signalling networks leads naturally to consideration of how the behaviour of models of signalling networks might be affected by the inclusion of protein-protein interactions which are not generally included. This is investigated in some prototypical signalling systems in chapter 4. The basic signalling system chosen for investigation is an enzymatic signalling cascade in which each successive protein is reversibly modified by an upstream enzyme. In these systems, the interaction of an active enzyme with the unmodified form of its substrate is essential for signalling to occur. However, a myriad of other enzyme-substrate interactions are possible, such as the interaction of an active enzyme with the modified form of its substrate (i.e. product inhibition), examples of which are found in the experimental literature. Thus, in this chapter, the behaviour of a basic model of signalling in which such additional, non-essential enzyme–substrate interactions are possible is analysed. These interactions include those between the inactive form of an enzyme and its substrate, and between the active form of an enzyme and its product. It is shown that these additional interactions can result in increased sensitivity and biphasic responses, respectively. The dynamics of the responses are also significantly altered by the presence of additional interactions. Finally, the consequences of these interactions are investigated in two variations of the basic model, involving double modification of substrate and scaffold-mediated signalling, respectively. It is concluded that the molecular details of protein–protein interactions are important in determining the signalling properties of enzymatic signalling pathways.

Thus, in summary, chapters 3 and 4 can be seen as investigating the signalling capabilities of generic, small, modules. In chapter 5 this approach is extended by analysing the signalling capabilities of two modules, with typical and widely seen signalling behaviours, when combined. The modules combined are an adaptive signalling module and a threshold signalling module. Representative models of these processes are used to examine and

analyse various aspects of their interaction including the order of interconnection, the role of relative time-scales, the difference between monostable and bistable thresholds in this context, and how threshold modules may act as a switch induced by transient signals. Numerical simulations, bifurcation analysis and analytical work are employed to address these questions. Overall, this analysis is a first step towards a detailed systems engineering understanding of the different kinds of interactions between these ubiquitous elements in cellular signal transduction.

The work on interacting modules leads into the detailed investigation of the regulation of a specific module in a specific system - the cell cycle of the budding yeast, *Saccharomyces cerevisiae*, in chapter 6. This is a good model system for understanding cell cycle regulation in a wide variety of other organisms. In this chapter, a framework is built for the analysis of the dynamic regulation of the cell cycle, based around sensitivity analysis and inspired by work on neural and circadian oscillators. This framework is applied to a selection of models of the budding yeast cell cycle from literature, and some general conclusions about the possibilities of dynamic regulation are made. These include the independent controllability of cell size and cell cycle period, complex dynamic responses after step-changes in conditions, flexibility in these responses for a given choice of signalling mechanisms, and the potential for phase shifting through asymmetric division. While some of these results are specific to budding yeast, the general approach and methods are expected to be applicable to other systems, and have relevance to investigations of population-level properties of many cell types.

Chapter 2

Background

2.1 Introduction

Cellular signalling networks are responsible for coordinating cellular responses with extra- and intracellular signals, and consequently display an enormous variety of behaviours. Here, "signalling networks" are given the broad definition of any biochemical network which is responsible for producing a particular response to a given stimulus, regardless of whether the origin of the stimulus is intra- or extracellular. These networks are composed of a variety of protein and non-protein components, which interact with each other in a variety of ways.

In this chapter, background is provided to the study of cell signalling, with a particular focus placed on areas in which mathematical modelling and analysis has been useful. An overview of some basic mathematical modelling techniques is also supplied, along with a discussion of the relevance of each approach to different scenarios.

Given the broad scope of analysis in subsequent chapters, the description of key themes here is necessarily general. The intention is to give an idea of the range of different mechanisms and behaviours of cellular signalling systems, and the ways in which they are commonly modelled. These principles will then be utilised repeatedly to investigate both generic signalling behaviours and an example of a complex cellular process (the cell cycle).

2.2 Biochemical mechanisms of cellular signal transduction

In order to give an idea of the diversity of biochemical mechanisms that are involved in cellular signalling pathways, a brief overview of some very common mechanisms is given below. These mechanisms are: ligand binding, complex formation, post-translational modification, and transcriptional regulation. These mechanisms provide the core signalling capabilities of many signalling pathways, and a discussion of their basic properties gives an indication of some of the variety that can be expected in the mathematical models of signalling that will be explored and analysed later. Note that the listed mechanisms are not exhaustive. Other important mechanisms of regulation in biological systems include ion channels, mRNA binding proteins, mRNA degradation, protein transport channels, and translational regulation.

2.2.1 Ligand binding

One of the most basic mechanisms of regulation is the binding of a ligand to a receptor or other protein. Ligand receptors can be either extracellular or intracellular. An example of the former is the epidermal growth factor (EGF) receptor family, including the ERBB family (Citri and Yarden, 2006). The ERBB signalling network is one of the most extensively studied areas of signal transduction, and of great interest as an anti-cancer drug target. An example of intracellular ligand binding is signalling through the soluble gas nitric oxide. Nitric oxide is capable of passing through cellular membranes, and binds reversibly to iron in the active site of guanylyl cyclase in cellular cytoplasm, stimulating its enzymatic activity to produce the second messenger cyclic GMP. Another example of a class of intracellular ligand receptors is the family of nuclear hormone receptors. These mediate ligand regulation of gene activity by binding to specific DNA sequences in a ligand-dependent manner. The ligands for nuclear receptors in higher eukaryotes are often hormones, such as cortisol and vitamin D.

The above examples have considered cases in which an initially extracellular ligand is allowed to pass through the membrane before instigating signalling through binding to an intracellular signalling protein. In other cases, an intracellular ligand is produced as a result of extracellular signalling. Such ligands are termed “second messengers”. A prototypical example of such a ligand is cyclic AMP (cAMP), which regulates a diverse range of processes in the cell. These include transcription of a range of genes (through

the CREB family of transcription factors (Sands and Palmer, 2008)) and post-translational modifications (through the cAMP-dependent kinase PKA (McConnachie et al., 2006)).

More sophisticated examples of ligand binding come in the form of allosteric regulation. This refers to the ability of a ligand to selectively stabilise a particular conformation of the protein. Depending on the conformation stabilised, this can increase or decrease the affinity of the protein for another ligand at another site. The prototypical example for this type of interaction is the binding of oxygen to haemoglobin. In this case, allostery allows cooperative binding of successive oxygen molecules, greatly enhancing oxygen transport. This mechanism is also of use in signalling, where it allows proteins to integrate multiple signals through cooperative binding of different ligands. An example of this is seen in PLCβ (Philip et al., 2010), which is responsible for integrating signals from G-protein coupled receptors to produce the second messenger species IP3.

2.2.2 Post-translational modification

The reversible post-translational modification of proteins is a ubiquitously utilised and versatile mechanism of biochemical signal transmission. Such modifications include phosphorylation, acetylation, O-GlcNacylation, and ubiquitination. Of these, phosphorylation has been the most widely studied as a result of the availability of experimental techniques, and it has been shown to be occur widely in many systems (e.g. (Gnad et al., 2009; Mayya et al., 2009; Sugiyama et al., 2008)). However, as technology has developed, other modifications such as acetylation have also been demonstrated to be similarly widespread (Choudhary et al., 2009). Cascades of enzymes regulating one another through post-translational modification, such as the MAPK cascade, have provided some of the most well-studied examples of cellular signalling.

Post-translational modification of a protein can provide a signal in several different ways. For example, a modification can create a binding site for another protein, prevent binding of another protein, or change the structure of the protein in a way that activates its catalytic capabilities (). The combination of multiple modifications - both of the same type and different types - on different sites of the same protein has been suggested to allow a high degree of signal integration (Hunter, 2007).

The basic mechanism of post-translational modification in eukaryotes usually involves an enzyme binding to the target site on a protein and catalysing a reaction between an amino acid at the target site and the substrate required for the relevant modification (e.g.

ATP in the case of phosphorylation). Another mechanism of post-translational modification involves a modified protein passing on its own modification to a downstream substrate. An example of such a modification is the phosphorelay, which is common in bacterial systems (Stock et al., 2000).

2.2.3 Complex formation

In addition to the transient interactions between enzymes and substrates upon which signalling through post-translational modifications relies, proteins are capable of forming longer-lived interactions as part of protein complexes. These form the core of many cellular processes (Gavin et al., 2006).

Some of the most well-studied examples of protein complexes are those involved in the basic processes of the cell. These include ribosome, RNA polymerase, and protease complexes. Regulation of the composition and activity of these complexes can have global consequences for cellular processes, including signalling, but their primary function is not to process signals. At the smaller scale, a well-studied example of protein complexes involved in signalling is that of the G-protein coupled receptors (GPCRs) (Rosenbaum et al., 2009). The dynamics of complex formation between the α and $\beta\gamma$ subunits of these complexes transmit information to a wide range of second-messenger systems at the cell membrane. In this case, the regulated binding properties of the complex confer signalling abilities which can be dynamically modulated.

Other classical examples of signalling complexes are receptor and transcription factor dimers. Transcription factors often form homo- or heterodimers before they can bind DNA and perform their gene regulatory function. This is a highly regulatable process (Seo et al., 2011). The complexes formed by a particular transcription factor depend on its binding specificities for available monomers, and the identity of the complex then determines which binding sites it can bind to (Amoutzias et al., 2008). This allows flexibility in the responses that can be induced by a single transcription factor, depending on the coincidence with other signals.

2.2.4 Transcriptional regulation

Regulation of gene transcription is a fundamental mechanism of signal transduction, by which a cell can modify the rate at which a transcript from a particular gene is produced.

Networks of genes involving only regulation at the transcriptional level are capable of complex behaviours, for example self-sustained oscillations (Elowitz and Leibler, 2000; Stricker et al., 2008) or pulse-like responses (Mangan and Alon, 2003). The most well-studied and basic model of transcriptional regulation involves the binding of transcription factors to the promoter of a gene, and either aiding the recruitment of RNA polymerase (i.e. the transcription factor behaves as an activator) or preventing it (i.e. the transcription factor behaves as a repressor). More recently, regulation of transcription through mechanisms outside this well understood mechanism, such as modification of chromatin structures, have been investigated (MacQuarrie et al., 2011).

It is important to note that, while transcriptional regulation is important and widespread, the ultimate level of expression of a gene is only partially determined by levels of transcription - it is also influenced by transcript degradation. This itself is a highly regulated process capable of responding to external stimuli in a transcript-specific manner (Fabian et al., 2010; Shyu et al., 2008).

2.3 Prototypical behaviours of cellular signalling networks

Cellular signalling networks are sophisticated networks of biochemical reactions that have evolved to coordinate cellular responses with the vast array of external signals. In this section, a brief overview of some of the behaviours observed in signalling networks is provided. These behaviours are: switch-like signalling, where a small change in stimulus can result in a large change in the pathway output; adaptive signalling, in which changes in the stimulus may provide only a transient change in the pathway output, before it relaxes to close to its original level; oscillatory signalling, in which a sequence of cellular events is coordinated repeatedly in time by an oscillating signal; and signalling specificity, in which a network with multiple inputs, outputs, and sources of crosstalk is capable of responding specifically to some combinations of inputs.

While the above list of behaviours is in no sense complete, it does describe what can be considered prototypical examples of biochemical signal processing, all of which will be elaborated on in further chapters. In each case, the essential behaviour will be discussed, followed by a summary of how understanding of these basic elements of signal processing have been useful in understanding systems with more complex overall behaviours.

2.3.1 Switch-like signalling

Switch-like signalling behaviour is observed in many situations in which a sensitive response to a signal is required. These include, for example, the response of the Janus kinase (JNK) signalling cascade (Bagowski et al., 2003), or the mitogen activated protein kinase (MAPK) cascade (Huang and Ferrell, 1996). More recently, this behaviour has also been engineered into signalling systems. For example, a molecular titration mechanism has been used to create switches in transcription factor activity (Buchler and Cross, 2009), modification of a protein's modular domains has been used to introduce sensitive allosteric regulation of catalytic activity (Dueber et al., 2007), and eukaryotic signalling proteins have been used to create a switch based on post-translational modifications in *Escherichia coli* (Takahashi et al., 2012). These examples are interesting for their diversity of mechanisms, and for the fact that the behaviour is the result of relatively local interactions between proteins - there are no complex feedback structures built into these systems.

In real systems, however, positive feedback is a commonly seen mechanism for enhancing sensitivity of switch-like behaviour, and for introducing hysteresis (Ferrell, 2002). This means that they have different thresholds for switching "up" and "down", and so have a region of bistability in which the switch is capable of existing in either state. The difference between monostable and bistable switches is depicted in figure 2.1. This has been suggested to enhance the robustness of switches in cell states. This is of clear utility in the cell cycle, for example - the cell should only undertake DNA replication once per cycle, so the transitions through phases must be irreversible (Charvin et al., 2010; He et al., 2011). Another classic example of a bistable switch is the switch to a lysogenic state in phage lambda (Ptashne, 2011).

2.3.2 Adaptive signalling

Adaptive signalling behaviour is the (possibly approximate) maintenance of a given output level after a change in input, after any transient response has subsided (Drengstig et al., 2008; Ma et al., 2009). A schematic of this behaviour, displaying perfect adaptation, is shown in 2.1. Such signalling patterns are common in a wide range of systems. Some good examples are found in stress responses (El-Samad et al., 2005; Muzzey et al., 2009; Ni et al., 2009; Zhang and Andersen, 2007). In these cases, the application of a stress stimulates activation of signalling pathways, leading to an appropriate cellular response.

This response counteracts the effects of the stress, leading to a subsequent deactivation of the relevant signalling pathways, with the resultant pulse-like response in their activity. Another good example of adaptive signalling occurs in sensory systems (Friedlander and Brenner, 2009; Wark et al., 2007) and chemotactic systems (Levchenko and Iglesias, 2002; Yi et al., 2000). In these cases, adaptation to the level of a stimulus allows the pathway to maintain a dynamic range of signalling to new changes in the stimulus (i.e. the pathway response is not susceptible to saturation).

2.3.3 Oscillatory signalling

Cellular rhythms have been identified in a wide range of processes across a wide range of timescales (Goldbeter et al., 2012). Oscillatory signals are characterised by a period and an amplitude (see figure 2.1c) for an illustration), both of which may change with time and may encode their own information for downstream processes to interpret.

Some examples of oscillatory signalling systems include oscillations in Ca^2+ (Dupont and Croisier, 2010) and p53 (Batchelor et al., 2009). Along with these examples of oscillating signals encoding information to downstream processes are canonical examples of self-sustained oscillators in biological systems, such as circadian clocks (Zhang and Kay, 2010), cell-cycle oscillators (Tyson and Novak, 2008), and segmentation clocks (Oates et al., 2012). These oscillating systems are able to regulate various forms of coordination. In particular, the cell cycle coordinates the internal state of the cell so that specific stages of development (e.g. duplication of DNA) occur only once and in the correct order, while segmentation clocks coordinate the development of sets of cells within one organism, and circadian clocks coordinate organism timing in response to external 24-hour-periodic stimuli.

In addition to the oscillators identified above, it is interesting to note synthetic examples of oscillators. Genetic circuits displaying rhythmic behaviour have been designed, including a three-negative-feedback loop oscillator (known as the *repressilator* (Elowitz and Leibler, 2000)), a simple self-repressing feedback loop (Stricker et al., 2008), and a synthetic gene-metabolic oscillator (Fung et al., 2005).

Similarly to adaptive behaviour, oscillatory signalling is interesting and non-trivial to investigate because of its dynamic behaviour (Novak and Tyson, 2008). In this way, oscillators provide a good example of systems in which mathematical modelling has been especially instructive in establishing an understanding of the basic mechanisms behind the

behaviour.

Despite differences in the purpose of these various cellular oscillators, there are clear similarities in the structure of the networks responsible for generating their essential oscillatory behaviour. In particular, the examples listed all contain at least one negative feedback, which help facilitate oscillations.

2.4 Systems characteristics of cellular signalling networks

While examples of biochemical signalling mechanisms and behaviours are interesting to consider, it is also important to ask what system-level properties are commonly exhibited by cellular signalling networks. These are considered here, and provide some necessary background to justify the approaches taken in subsequent section. This is especially true of the discussion of network modularity, which is taken advantage of in every chapter, and is, in fact, implicit in the majority of experimental approaches.

2.4.1 Network modularity

One common property observed in biology as a whole is modularity - the property that a complex whole can be subdivided into parts with distinct, relatively independent functions. This is not to say that the behaviour of the whole can be understood by merely studying subsystems in isolation. Rather, the existence of modularity is required for any subsystems to be identified in the first place. This property has been key to much of the success that has been possible up to this point in understanding biological processes at the molecular level, as it allows for the possibility of reverse engineering and the informative study of processes in relative isolation.

Modularity is observed at essentially all levels of biology. Genes contain sequences responsible for regulating their expression (i.e. promoters) distinct from their protein-coding regions, while proteins may have different domains and motifs which are responsible for different aspects of the protein function (Bhattacharyya et al., 2006; Del Sol et al., 2007). At the whole-organism level, functions of metabolism and reproduction are frequently segregated into distinct compartments and/or organs. Another excellent example at this scale is the specialisation of regions of the brain to perform specific functions. Of particular importance for the investigation of cellular signalling behaviour, however, is modularity at the intermediate scale of biochemical signalling networks.

This has been observed in network-level analyses, for example in the case of coexpression of functional modules (Barabasi and Oltvai, 2004; Tanay et al., 2004) or sets of interacting proteins (Luo et al., 2007), and is also clear from investigations of specific pathways and processes. For example, it is seen in oxygen signalling pathways (Crosson et al., 2005), and epidermal growth factor signalling (Citri and Yarden, 2006). Separation of functions into modules has also been detected at the evolutionary level in the cases of stress response networks (Singh et al., 2008). While the above examples refer mostly to networks of interacting proteins, modularity is also clear at the level of gene regulatory networks, for example in development (Davidson, 2010). This ability to separate functions in this way has recently been taken advantage of to produce a model of a cell at the whole-organism level in *Mycoplasma genitalium* (Karr et al., 2012) - an endeavour which would not have been possible if an appropriate modular decomposition of functions did not exist.

In all cases, the observation of modularity is of course merely a useful abstraction - no biological module is truly independent of the system in which it resides. Nevertheless, while the evolutionary origins and posited selective advantage of modularity have been questioned (Lynch, 2007), the existence of network modularity has been vital for the successful investigation of these systems.

2.4.2 Robustness

Another property which has been suggested to be widespread in biological system is that of "robustness". This has been defined as "a property that allows a system to maintain its functions against internal and external perturbations." (Kitano, 2004), or similarly as "the ability to maintain performance in the face of perturbations and uncertainty" (Stelling et al., 2004). As a result of the myriad perturbations and challenges faced by organisms in dynamically changing environments, this property has been seen as a key property of biological systems. Classic examples of robustness include the adaptive dynamics of the chemotaxis system in *e. coli* (Yi et al., 2000) and the temperature compensation observed in circadian systems (Ukai and Ueda, 2010).

Apart from the theoretical interest in how a system maintains a behaviour across a range of conditions, it should also be pointed out that this property has been of great use experimentally, since it has meant that many labs can study essentially the same phenomena independently and without exact duplication of conditions.

2.4.3 Signalling crosstalk

Signalling networks contain many components, each of which may interact with many others. This means that signalling from inputs to outputs does not occur through linear signalling pathways of unconnected components, but through complicated networks which branch, combine, and feed back on one another. It is interesting, then, that such networks are capable of responding in a specific manner to a given input signal. By this, we mean that an output provides information about a particular input independently of other inputs, even if those inputs are utilising some of the same components of the signalling network to transmit information.

2.5 Mathematical modelling and analysis of signalling networks

Mathematical modelling has become an increasingly useful tool for understanding the mechanisms and principles around which biological systems are organised. This is due in part to the inherent complexity of these systems, meaning that intuition and verbal reasoning alone are of limited utility, and also in part to the rapid advancement of experimental technology, which has led to a dramatic increase in quantitative characterisation.

Mathematical modelling provides a way of formalising knowledge about a biological system. This can allow intuition about mechanisms to be checked and confirmed (i.e. "is the mechanism I have suggested actually capable of producing the observations?"). In cases where data are difficult to reconcile with the current model, the models can also be useful for suggesting additional experiments or gaps in understanding. Finally, investigation of the properties of the model may suggest principles of operation which may be shared by other systems.

In this section, a brief overview is given of approaches to the mathematical modelling and analysis of signalling networks. This overview focuses on deterministic dynamical modelling of biochemical networks using ordinary differential equations (ODEs), since it is this approach which is used throughout the thesis. Other approaches may be more suitable for other types of investigation. For example, stochastic models have seen widespread use in biochemical modelling, and enable investigation of the consequences of molecular noise in biological systems (Wilkinson, 2009).

The objective in this section is merely to give an idea of how such models are constructed. Small, self-contained models of some of the basic signalling mechanisms dis-

cussed above are included here as examples.

2.5.1 Ordinary differential equation representations of biochemistry

The ordinary differential equation (ODE) formalism is one of the most commonly used modelling formalisms for biological systems. An ODE model of a system, involving the dynamic change in time (denoted t) of state variables $\mathbf{x}$, is given by:

$$\frac{d\mathbf{x}}{dt} = f(\mathbf{x}, t, \theta) \tag{2.1}$$

The solution to this equation is given by $\mathbf{x}(t)$. Here, $\mathbf{x}$ is a vector of state variables, which could be, for example, concentrations of species, or absolute number of molecules of a particular species. The vector θ provides a set of parameters, describing fixed properties such as rate constants and binding affinities. The time is specified by t, meaning that $\mathbf{x}_0 = \mathbf{x}(0)$ provides the initial conditions of the system.

There are many advantages to using this formalism. It is flexible, and able to represent a wide range of mechanisms. In addition, there are theoretical tools available for the exact solution of ODEs, and for the investigation of properties such as stability and oscillatory behaviour (through bifurcation analysis and dynamical systems theory). For cases in which it is not possible to derive exact solutions, there are excellent numerical tools available for the approximate solution of these problems. These numerical tools are, in general, not very computationally expensive (e.g. when compared to simulations of stochastic models). They are also naturally extensible to the spatial domain by the inclusion of diffusion effects (so they become partial differential equations (PDEs)).

As will become clear by the range of different examples considered below, it is possible to use this basic modelling formalism to describe biological systems at varying levels of abstraction.

2.5.2 Mass action kinetics

Mass-action kinetics describe the rates of reactions through products of concentrations combination of two species. For example, in the case of ligand-mediated signalling, the association between a receptor R and a ligand L has the reaction equation:

$$R + L \Leftrightarrow R.L \tag{2.2}$$

This can be modelled by mass-action kinetics of the form:

$$\begin{aligned}\frac{d[R]}{dt} &= k_d[R.L] - k_a[R][L] \\ \frac{d[L]}{dt} &= k_d[R.L] - k_a[R][L] \\ \frac{d[R.L]}{dt} &= k_a[R][L] - k_d[R.L]\end{aligned} \tag{2.3}$$

Here, k_a represents the rate of association, and k_d represents the rate of dissociation. The dynamics of this model, and the eventual steady state, are then fully specified once the initial conditions are specified. In modelling real biological systems, it is also common to include processes leading to the production and degradation of all components. A simple, mass-action model of this process would include constant production and a constant rate of dilution of protein (as a result of cell growth - the rate of which is commonly denoted by μ):

$$\begin{aligned}\frac{d[R]}{dt} &= k_{sa} + k_d[R.L] - k_a[R][L] - \mu[R] \\ \frac{d[L]}{dt} &= k_{sl} + k_d[R.L] - k_a[R][L] - \mu \\ \frac{d[R.L]}{dt} &= k_a[R][L] - k_d[R.L] - \mu\end{aligned} \tag{2.4}$$

Here, k_{sa} and k_{sl} denote the rates of production of receptor and ligand, respectively. Interestingly, while the dynamics described by equation 2.4 depend on the initial conditions, the eventual steady state is insensitive to the initial conditions. This is a common property of models which include constitutive production and degradation terms.

From this brief overview, it is possible to evaluate a few advantages and disadvantages of this modelling approach. Its main advantages are derived from the explicit representation of proteins in their various bound and unbound states. This means that knowledge about the protein-protein interactions can be specified in detail. It also means that such models can be used directly to perform stochastic simulations of the system using the Gillespie algorithm (or similar). On the other hand, it should be noted that detailed mass-action kinetic models are likely to be overcomplicated in many cases, and will usually involve many more parameters than can reasonably be identified from available data. These factors have

led to simplified representations of large sets of reactions, which are nonetheless capable of capturing the main behaviours.

2.5.3 Michaelis-Menten kinetics

Michaelis-Menten kinetics are the best-known case of a simplified representation of mass-action kinetics. This was derived in order to describe the kinetics of a simple reaction:

$$E + S \Leftrightarrow E.S \Rightarrow E + P \tag{2.5}$$

This reaction describes the reversible binding of an enzyme to its substrate, followed by a reaction, leaving product and the original enzyme. This is a common way to represent the post-translational modification of a protein by some signalling enzyme, as described above - the reverse reaction may be treated in a similar way. Clearly, in many cases the actual reaction kinetics are more complicated. For example, phosphorylation of a substrate by a kinase also requires the binding of ATP to the appropriate site on the kinase. However, this provides a useful working model for these types of reaction in many cases. The mass-action kinetics of this reaction are given by:

$$\begin{aligned}
\frac{d[E]}{dt} &= k_r[E.S] - k_f[E][S] + k_{cat}[E.S] \\
\frac{d[S]}{dt} &= k_r[E.S] - k_f[E][S] \\
\frac{d[E.S]}{dt} &= k_f[E][S] - k_r[E.S] - k_{cat}[E.S] \\
\frac{d[P]}{dt} &= k_{cat}[E.S]
\end{aligned} \tag{2.6}$$

These equations can be simplified by assuming that the concentration of the complex $E.S$ does not change on the timescale of product formation (i.e. $\frac{d[E.S]}{dt} = 0$). This is known as the quasi-steady-state assumption, and allows the concentration of $E.S$ to be expressed as a function of substrate and enzyme concentrations, so a simple expression is obtained for the rate of product formation:

$$\frac{d[P]}{dt} = \frac{V_{max}[S]}{K_m + [S]} \tag{2.7}$$

Where $V_max = k_{cat}[E]$ (the enzyme capacity), and $K_m = (k_r + k_{cat})/k_f$ (the so-called "Michaelis-Menten constant", related to the affinity of enzyme for substrate. The above is an example of a more general approach to the simplification of mass-action equations, making use of the quasi-steady-state assumption (for more information, see (Ciliberto et al., 2007; Segel, 1988)).

2.5.4 General cooperativity

At a further level of abstraction, it has been observed that many biological systems display a high degree of cooperativity, meaning that a nonlinear response, sensitive to a stimulus is observed, as discussed above in the context of switch-like signalling. This can occur at the level of a single protein complex, for example through the mechanism of allostery, a classical example of which is the binding of oxygen to hemoglobin (Perutz, 1970). It is also observed at the level of complex formation and binding of transcription factors to DNA, and at the whole-pathway level (e.g. in the response of MAPK cascades (Ferrell, 1996)).

A common way to model this qualitative behaviour in biological systems is to simply represent the response by a Hill function, which has a sigmoidal response function, as defined by:

$$f(x) = \frac{x^n}{x^n + K^n} \tag{2.8}$$

The "steepness" of this function is determined by the value of the cooperativity coefficient n (higher values of n lead to more nonlinear input-output functions), while the input (denoted x) required to achieve half-maximal output is given by the parameter K. While this represents a monotonically increasing function, indicating activation with increasing x, it is equally straightforward to represent repression:

$$f(x) = \frac{K^n}{x^n + K^n} \tag{2.9}$$

As an example application of this approach, we take a model of gene expression in which a gene (Y) is regulated at the transcriptional level by both an activator (A) and a repressor (R):

$$\frac{d[Y]}{dt} = k_s . \frac{[A]^{n_A}}{[A]^{n_A} + K_A^{n_A}} . \frac{K_R^{n_R}}{[R]^{n_R} + K_R^{n_R}} - k_d[Y] \tag{2.10}$$

Here, k_s and k_d give the rates of production and degradation of Y, respectively, while n_A, K_A and n_R, K_R describe the activation and repression responses to A and R, respectively.

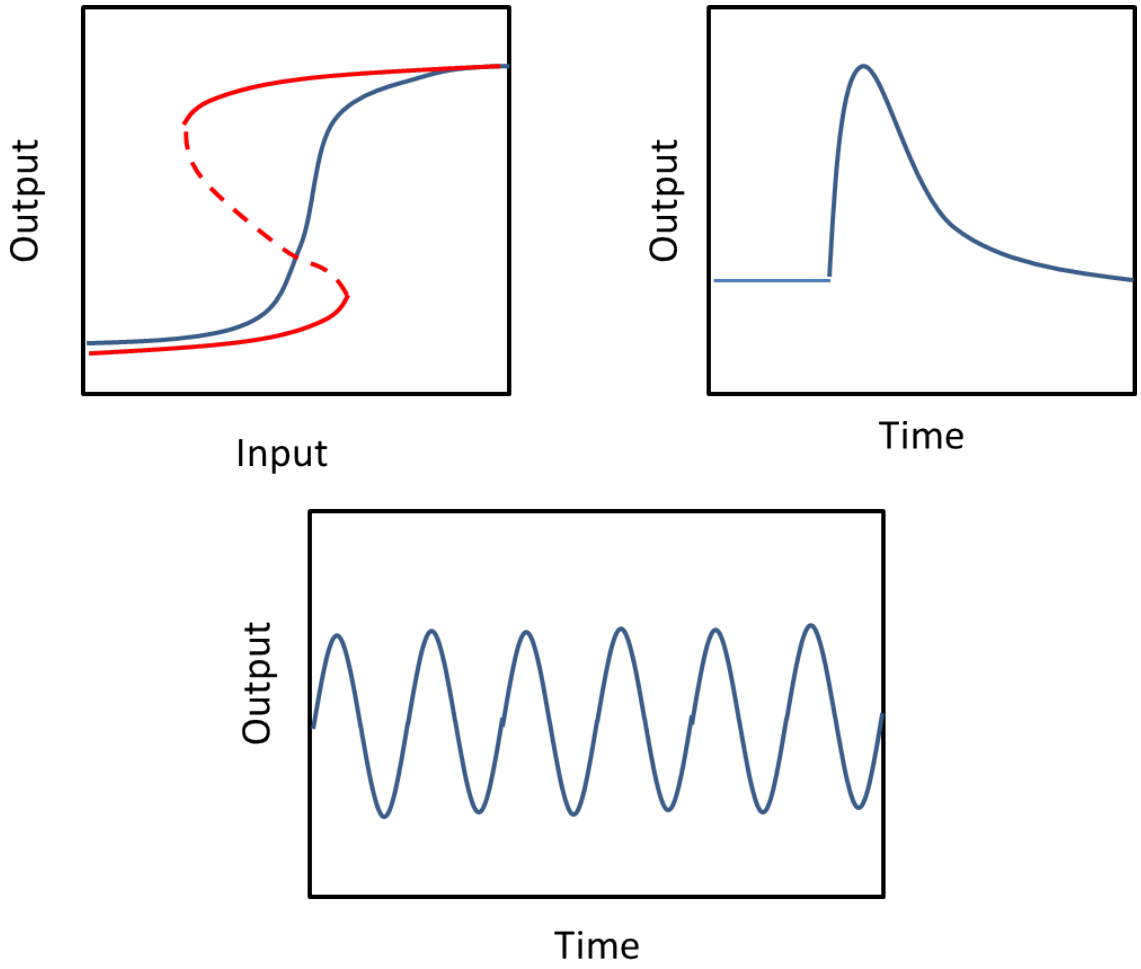

Figure 2.1: Some simple behaviours exhibited by a wide range of biochemical signalling networks are represented. a) a threshold response is shown, in which at some input value, a small change in input results in a large change in output. The thresholds displayed are monostable (blue) and bistable (red). b) an adaptive response is shown, in which a sudden change in input causes a change in output which eventually returns to its original value. c) an oscillatory response is shown, characterised by an amplitude, offset, and oscillatory frequency.

Chapter 3

Coupling of pathways and processes through shared components

3.1 Introduction

Components of intracellular signalling networks often interact with multiple entities at multiple locations, allowing them to receive and send multiple signals. This property is seen, for example, in proteins capable of multiple allosteric interactions such as n-WASP Padrick and Rosen (2010), WAVE Beene and Scott (2007), Cdk-2 Prehoda and Lim (2002), and PLC Philip et al. (2010). There are also many examples of enzymes capable of modifying multiple substrates Copley (2003); Hult and Berglund (2007); Kim et al. (2010, 2011); Nobeli et al. (2009), including signalling proteins such as cyclin-dependent kinases Bloom and Cross (2007); Csikasz-Nagy et al. (2009), and ubiquitin ligases Peters (2006). Similarly, substrates may be modified by multiple enzymes, as is the case for the p53 tumour suppressor Lavin and Gueven (2006) and many GTPases. Each of these reactions may take place while bound to various adaptor and scaffold structures, as is common for instance in MAPK cascades Dhanasekaran et al. (2007). Finally, all of these interactions and reactions may take place in diverse cellular locations, with many proteins having been identified as having multiple subcellular localizations Huh et al. (2003). Commonly known examples of this are cell-cycle proteins such as cyclins, which shuttle between the nucleus and cytoplasm, and a wide variety of membrane-binding signalling proteins, which may also be present in the cytoplasm. The sharing of components between pathways and locations is widespread and one of the most basic ways in which processes may be coupled. A notable

aspect of signalling in biological systems, and one which distinguishes them from many engineered systems, is that it is inherently bidirectional. Whenever a signal is being sent or received, components must interact with one another, and/or change location, and are occupied by those actions for finite periods of time. Therefore a signal is itself modified when it is perceived by a downstream signalling element. The extent of bidirectional signalling has been termed retroactivity Del Vecchio et al. (2008). While retroactivity may be low in some cases, and while there may be reasons for systems minimising it in some cases, it is nonetheless likely to have a non-trivial effect in other cases. This is particularly true, and especially significant, in networks containing elements with multiple interactions. Signalling networks involve many proteins with multiple interactions and multispecific enzymes, where many of the elements are similar in concentration. Therefore, proteins may be shared between multiple pathways, and the question arises as to what functional roles these multiple interactions and consequent bidirectionality might play in cellular signal processing in biological systems.

The most important aspect of signalling networks which may be affected by multiple interactions is their ability to perceive and integrate signals, and thereby perform logical operations. Multiple interactions and bidirectional signalling may affect the input-output response of pathways, and may be particularly relevant to investigating signalling crosstalk Bardwell (2006); Bardwell et al. (2007); Haney et al. (2010). Crosstalk occurs when multiple pathways share components. Despite this coupling, signalling networks are often seen to allow one input to specifically regulate only one or a few outputs. This is termed signalling specificity. Likewise, it is observed that in some networks particular outputs are regulated by only one or a few inputs, termed signalling fidelity. It is important to understand the role of crosstalk in such networks and how signalling specificity and fidelity may be maintained. Another phenomenon observed in signalling is the temporal coordination of processes with one another. Examples include events such as mitosis Georgi et al. (2002) and the assembly of large protein complexes involved in flagellar motors Kalir et al. (2001). Bidirectional aspects of signalling may affect or even contribute to these properties in a very non-trivial manner, and therefore are of direct biological relevance. Overall our studies provide important insights which help bridge descriptions of networks at local and global levels.

Further to the biological implications discussed above, there are important implications for the ways in which biological signalling circuits are modelled. Mathematical modelling has been used to analyse and understand many signalling networks. Such models

frequently consider enzyme-substrate complexes only implicitly, often using Michaelis-Menten kinetics or other simplifications such as the quasi-steady state assumption (QSSA) (Borghans et al., 1996; Ciliberto et al., 2007; Segel, 1988). It has been recognised that these simplifications may have significant effects on the behaviour of models, as seen recently in analyses of ultrasensitive and multistable reaction networks (Gunawardena, 2005; Sabouri-Ghomi et al., 2008; Thomson and Gunawardena, 2009). Another implication is that modular decompositions of networks, which may allow rapid simulation and more straightforward analysis, must be undertaken with care. The analysis which we present is relevant to both these aspects.

In order to focus on the essential aspects of coupling of processes through shared components, and hence provide insights into the various issues mentioned above, we develop an appropriate modelling/systems framework. The modelling framework incorporates two components which bind exclusively to a common third component, and are therefore indirectly affected by each other. The model incorporates the production and degradation of all components, thus allowing each component to serve as a "signalling port". Having developed the basic model, we proceed to systematically examine the signal processing through this module, as this sheds direct light on the above issues. It is worth emphasizing that in this minimal general setting, systems analysis provides transparent and important insights which are relevant to a wide range of systems/contexts where the above feature(s) occur. We further build on the study of the basic model to include additional features such as spatial diffusion/localization, and other complexities in signal propagation such as threshold effects. Throughout, we focus on the effects of coupling signalling elements through shared components, revealing different facets of such generic coupling.

This chapter is organized as follows. In the next section, we present the basic modelling framework which we employ. Following this, we systematically examine the steady state and temporal signal processing in this module in turn. We illustrate the relevance of the analysis in specific biological contexts. We then examine the effect of the additional elements mentioned above. Finally we conclude with a synthesis and discuss additional applications and extensions.

3.2 Models

3.2.1 A basic model of coupling between signalling pathways

Here, we develop a basic model of pathway coupling – the sharing of one component between processes. In its most basic form, the coupling of processes and signalling can be studied via a simplified ordinary differential equation model, which involves the interaction of three species A, B and X. A and B each bind exclusively to X, and thus X serves as a factor which couples the dynamics of A and B. We formulate the model in a general form, so that the essential insights can be extracted in a transparent and generalisable way. We begin by modelling the interaction of A and X alone. The processes which are modelled are the binding of A and X to produce a complex AX, the dissociation of the complex, and the independent production and degradation of A and X. The dynamics of this system are governed by the equations:

$$\begin{aligned} \frac{d[X]}{dt} &= k_{a2}[AX] - k_{a1}[A][X] + k_{px} - k_{dx}[X] \\ \frac{d[A]}{dt} &= k_{a2}[AX] - k_{a1}[A][X] + k_{pa} - k_{da}[A] \\ \frac{d[AX]}{dt} &= k_{a1}[A][X] - k_{a2}[AX] - k_{dax}[AX] \end{aligned} \tag{3.1}$$

Here, $[X]$, $[A]$, and $[AX]$ denote the concentrations of each species A, X and the complex AX. In the above equation, ka1 and ka2 denote the binding and unbinding rate constants, kpx, kpa denote the production rates of the species X and A respectively, and kdx, kda denote the degradation rates of these species. This model is, in general, non-trivial to solve analytically, although this may be facilitated if the degradation rates of all species are equal (Buchler and Louis, 2008). There are, however, several reasonable simplifications which allow some initial analysis to be performed. First of all, if production and degradation of species may be assumed to occur on a longer timescale than complex formation, then these terms may be neglected and this results in the equations (in dimensionless form):

$$\begin{aligned}
\frac{d[X]}{dt} &= k_{a2}[AX] - k_{a1}[A][X] \\
\frac{d[A]}{dt} &= k_{a2}[AX] - k_{a1}[A][X] \\
\frac{d[AX]}{dt} &= k_{a1}[A][X] - k_{a2}[AX]
\end{aligned} \tag{3.2}$$

Note that in these simplified equations, the total amounts of A and X are conserved, and hence information about the availability of these species is contained in the initial conditions. These expressions may be condensed by applying conservation conditions using the total quantities of A, and X (denoted $[A_T]$ and $[X_T]$, respectively).

All we have done up to this point is describe the dynamics of a protein, X, involved in one process, A, as has been modelled previously (Buchler and Louis, 2008). However, we are primarily interested in what happens when X is involved in more than one process, since it is these cases in which the coupling comes into play. Therefore, we introduce a second process, B, and can make use of the same model to describe its interactions with X (see figure 3.1):

$$\begin{aligned}
\frac{d[X]}{dt} &= k_{a2}[AX] - k_{a1}[A][X] + k_{b2}[BX] - k_{b1}[B][X] + k_{px} - k_{dx}[X] \\
\frac{d[A]}{dt} &= k_{a2}[AX] - k_{a1}[A][X] + k_{pa} - k_{da}[A] \\
\frac{d[AX]}{dt} &= k_{a1}[A][X] - k_{a2}[AX] - k_{dax}[AX] \\
\frac{d[B]}{dt} &= k_{b2}[BX] - k_{b1}[B][X] + k_{pb} - k_{db}[A] \\
\frac{d[BX]}{dt} &= k_{b1}[B][X] - k_{b2}[BX] - k_{dbx}[BX]
\end{aligned} \tag{3.3}$$

The above model incorporates the binding of B to X to form a complex BX, as well as the dissociation, and in addition includes the production and degradation of B (rate constants k_{b1},k_{b2},k_{pb}, and k_{db} respectively). While we have described the production and degradation of species, we stress that this need not be taken as protein synthesis and degradation – it includes, for example, the rate of formation of a particular post-translationally modified form of a protein. This is significant because these processes may occur on a much faster timescale than protein synthesis and degradation.

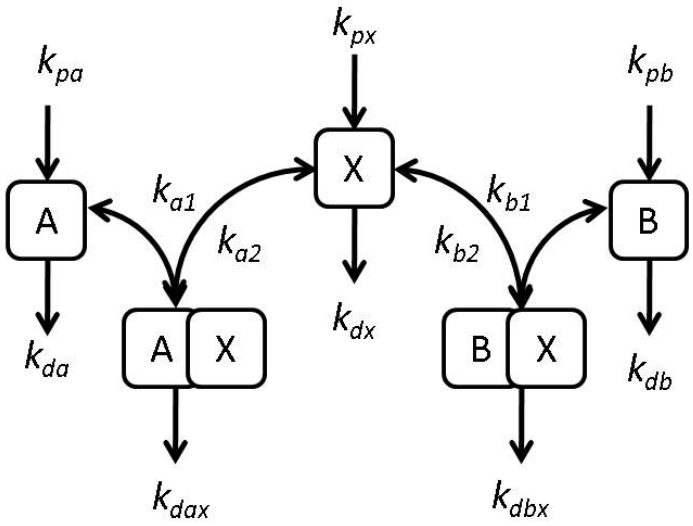

Figure 3.1: **Basic model schematic.** A schematic of the basic model is shown here. The species X interacts with both A and B. All species undergo constant production and degradation.

Some of the analysis will be concerned with the steady-state of these models. In this, the equilibrium constants for the complex formation of A and B with X (the ratio of binding to dissociation rate constants) become relevant parameters of interest. We denote these $K_A(= k_{a1}/k_{a2})$ and $K_B(= k_{b1}/k_{b2})$, respectively.

Variation of inputs and outputs

We note at the outset that the model is a general model of components A and B, interacting through competitive binding with the element X. This model allows modulation of the levels of each of these components by external signals through their rates of production and degradation. Throughout the chapter, we are primarily interested in two essentially different ways in which the levels of components are modulated by external signals. In the first case, we examine how changes in production of the shared component, X, are propagated to affect the levels of free A and B, and the levels of the complexes AX and BX, and therefore modify both pathways in which X participates. In the second case, we examine how changes in the production of the components A and B affect the levels of all components and complexes. This corresponds to the pathways being controlled while the shared component remains constant. Through this analysis, we hope to understand the range of behaviours available to such systems, and their possible biological significance. In particular, we examine how shared components may coordinate processes, and how

processes may remain independent despite sharing components.

At this stage we make very few assumptions about the nature of the downstream processes involving the complexes AX and BX. Later in the chapter, we build on the existing modelling framework to examine certain additional features in the downstream processes from our perspective.

Choice of parameters

Since we are concerned with investigating the effects of binding in a general context, we choose parameters that allow straightforward demonstration of the important behaviours. To this end, the binding affinities of the species for one another are chosen to be high, while remaining within a biologically feasible range. In general, the total concentrations of each component are of $O(1)$, while the affinities are of $O(10^3)$ ($K_A = 10^3$ and $K_B = 70$ for most simulations, see below). The concentrations and parameter values are dimensionless, and therefore represent a range of possible scenarios. To give an idea of a corresponding real-unit scenario in the case of the higher-affinity interaction between A and X, the parameters used here could correspond to concentrations of $10\mu M$ with $K_A = 10^4 nM^{-1}$. These affinities are high compared to typical affinities of enzyme-substrate interactions, but are still biologically feasible in this case (see, for example, (Bae et al., 2009; Huynh et al., 2009)), and may be more typical of other systems, since enzyme-substrate interactions are expected to be transient (and therefore low affinity) by their very nature.

Our results involve analysing the models using simulations (performed in MATLAB using ode15s) and analytical results. The MATLAB code used to generate the figures is provided as part of the digital appendices (described in Appendix E.0.2), with the parameter values used in each case additionally supplied in Appendix A.

3.2.2 Models of reversible phosphorylation

In order to investigate the effects of multiple interactions in the case of enyzmes with multiple substrates (so-called "multispecific enzymes"), we simulate two models of reversible phosphorylation. Given the abstract representation of phosphorylation in these models, they may be considered representative of any number of other reversible post-translational modifications, such as methylation or ubiquitination. The models we use consist of single- and double-modification of a substrate by an enzyme.

Model of single reversible phosphorylation

A single reversible phosphorylation, with uptake of the kinase, can be described by combining a mass-action based phosphorylation reaction with a Michaelis-Menten type dephosphorylation reaction (as in (Goldbeter and Koshland, 1981)). This gives the equations:

$$\begin{aligned} \frac{d[E]}{dt} &= v_2 + v_3 - v_1 \\ \frac{d[AE]}{dt} &= v_1 + v_2 - v_3 \\ \frac{d[A_p]}{dt} &= v_3 - v_4 \\ \frac{d[A]}{dt} &= v_2 + v_4 - v_1 \end{aligned} \tag{3.4}$$

Where:

$$\begin{aligned} v_1 &= k_{a1}[A][E] \\ v_2 &= k_{a2}[AE] \\ v_3 &= k_{a3}[AE] \\ v_4 &= \frac{k_a 4[A_p]}{K_{ma4} + [A_p]} \end{aligned} \tag{3.5}$$

Similar equations are obtained for the phosphorylation of B by the same enzyme.

Model of double phosphorylation

Modification cycles consisting of multiple phosphorylations may behave similarly to modification cycles involving only one phosphorylation. Therefore, by including a model of double phosphorylation, we are especially interested in a behaviour that it is capable of exhibiting that is not possible in the case of single phosphorylation - bistability. A model of double phosphorylation has been shown to exhibit bistability Markevich et al. (2004), and we use this model as published. This model is described by the equations:

$$
\begin{aligned}
\frac{d[E]}{dt} &= u_2 - u_1 + u_4 - u_2 \\
\frac{d[F]}{dt} &= w_3 - w_1 + w_6 - w_4 \\
\frac{d[A]}{dt} &= w_6 - u_1 \\
\frac{d[Ap]}{dt} &= u_2 - u_3 + w_3 - w_4 \\
\frac{d[A_{pp}]}{dt} &= u_4 - w_1 \\
\frac{d[AE]}{dt} &= u_1 - u_2 \\
\frac{d[A_pE]}{dt} &= u_3 - u_4 \\
\frac{d[A_{pp}F]}{dt} &= w_1 - w_2 \\
\frac{d[A_pF}{dt} &= w_2 - w_3 \\
\frac{d[A_pF^*}{dt} &= w_4 - w_5 \\
\frac{d[AF]}{dt} &= w_5 - w_6
\end{aligned}
\tag{3.6}
$$

Where:

$$
\begin{aligned}
u_1 &= k_1[A][E] - k_{-1}[AE] \\
u_2 &= k_2[AE] \\
u_3 &= k_3[A_p][E] - k_{-3}[A_pE] \\
u_4 &= k_4[A_pE] \\
w_1 &= h_1[A_{pp}][F] - h_{-1}[A_{pp}F] \\
w_2 &= h_2[A_{pp}F] \\
w_3 &= h_3[A_pF] - h_{-3}[A_p][F] \\
w_4 &= h_4[A_p][F] - h_{-4}[A_pF] \\
w_5 &= h_5[A_pF^*] \\
w_6 &= h_6[AF] - h_{-6}[A][F]
\end{aligned} \tag{3.7}
$$

3.3 Results and discussion

The results are organized as follows: we use our modelling framework to study how the system responds to different signals from both steady state and temporal perspectives. We then build on our analysis to examine a number of biologically motivated variations to our structure, which include additional components, downstream switching elements and spatial signal transduction, and discuss their possible biological significance. We start by examining the case where a signal modulates the production of the shared component, X, and continue by examining the case where signals modulate the components A and B, both separately and simultaneously. As discussed above, the MATLAB code used to generate the figures is provided as part of the digital appendices (described in Appendix E.0.2), with the parameter values used in each case additionally supplied in Appendix A.

3.3.1 Modulation of the shared component

We begin by analysing the steady state response of the system to changes in the production of X. From the perspective of signal propagation, this may be regarded as signal processing through "diverging pathways". Assuming that the rates of degradation of all components are equal, we can write the total quantity of each component in terms of the production and degradation rates ($[X_T] = k_{px}/k_d$, $[A_T] = k_{pa}/k_d$, $[B_T] = k_{pb}/k_d$, where $[X_T]$, $[A_T]$,

and $[B_T]$ refer to the total concentrations of X, A, and B, respectively). This allows us to analyse the model in terms of its response to $[X_T]$, allowing more transparent explanation of the results.

Figure 3.2 shows the response of the system when A and B are produced and degraded at equal rates, for the case where X binds more strongly to A than to B. We note that there are essentially three regimes of response. In the first regime, all processes are unsaturated and X is mostly taken up by A, since . In the second regime, process A has become saturated, and X is taken up by B. In the third regime, both processes have become saturated and X accumulates in its free form. These regimes show an "ultrasensitive" response of BX and free X, where a threshold in the total amount of X present must be reached before a significant response is observed. For our purposes, it is sufficient to think of "ultrasensitivity" as an effect involving increased relative sensitivity, along with a concomitant threshold effect, and see (Gunawardena, 2005) for a discussion of technical definitions of "ultrasensitivity").

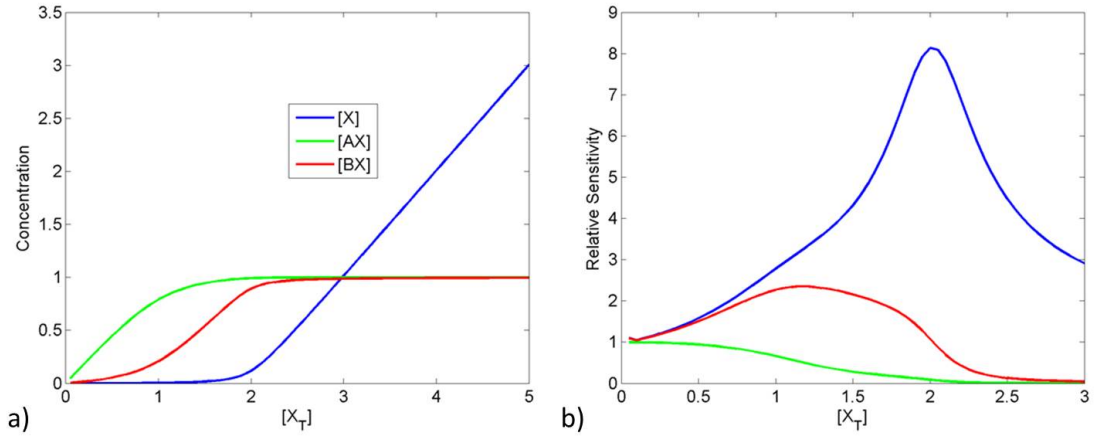

Figure 3.2: **Steady-state response to changes in production of X** a) The pattern of linear and saturating responses to changes in $[XT]$ is shown for the case $K_A \gg K_B \gg 1$. b) The relative sensitivity of each component with respect to $[XT]$ is plotted showing how it peaks above one for free X and BX, but decreases to zero for AX.

Some basic analysis provides direct quantitative insight. For simplicity, the analysis is performed for the case where the production and degradation of X, A and B are neglected. In this case, the behaviour of the system is monitored for the case where an addition of free X (and hence total X) is imposed at t=0. An inspection of the steady state equations reveals that the concentration of the complexes is proportional to the total amount of X, $[X_T]$. At steady state, each of the complex formation/dissociation reactions is at equilibrium (derived

from Equation 3.3):

$$\begin{aligned}[AX] &= K_A[A][X] \\ [BX] &= K_B[B][X]\end{aligned} \tag{3.8}$$

At steady state and using the conservation condition , we get the following equations for the response of AX, BX and free X to changes in the total concentration of X:

$$\begin{aligned}\frac{[X]}{[X_T]} &= \frac{1}{K_A[A] + K_B[B] + 1} \\ \frac{[AX]}{[X_T]} &= \frac{K_A[A]}{K_A[A] + K_B[B] + 1} \\ \frac{[BX]}{[X_T]} &= \frac{K_B[B]}{K_A[A] + K_B[B] + 1}\end{aligned} \tag{3.9}$$

Note that $[A]$ and $[B]$ are the concentrations of free A and free B and hence implicitly depend on the total X in the system. As mentioned above, for our purposes ultrasensitivity involves heightened relative sensitivity to $[X_T]$ along with any concomitant threshold effects. The absolute sensitivity of a concentration to $[X_T]$ is defined as its derivative with respect to $[X_T]$, while the relative sensitivity is this quantity scaled by the ratio of the relevant concentrations. Here, we analyse the steady state response of the model in terms of the absolute and relative sensitivities to the total quantity of X, $[X_T]$. In particular, we look at how these quantities behave in particular limits, when there is a significant difference in the affinities K_A and K_B.

We begin by deriving expressions for the absolute and relative sensitivities. Differentiating the steady state expressions given in equation 3.9 with respect to $[X_T]$ gives the absolute sensitivities

$$\begin{aligned}d[X]d[X_T] &= \frac{1}{K_A[A] + K_B[B] + 1} + [X_T]\frac{d}{d[X_T]}\left(\frac{1}{K_A[A] + K_B[B] + 1}\right) \\ \frac{d[AX]}{d[X_T]} &= \frac{K_A[A]}{K_A[A] + K_B[B] + 1} + [X_T]\frac{d}{d[X_T]}\left(\frac{K_A[A]}{K_A[A] + K_B[B] + 1}\right) \\ \frac{d[BX]}{d[X_T]} &= \frac{K_B[B]}{K_A[A] + K_B[B] + 1} + [X_T]\frac{d}{d[X_T]}\left(\frac{K_B[B]}{K_A[A] + K_B[B] + 1}\right)\end{aligned} \tag{3.10}$$

The relative sensitivities are then given by:

$$\begin{aligned}
S^{[X_T]}_{[X]} &= \frac{d[X]}{d[X_T]}\frac{[X_T]}{[X]} \\
&= 1 + \frac{[X_T]^2}{[X]}\frac{d}{d[X_T]}\left(\frac{1}{K_A[A] + K_B[B] + 1}\right) \\
S^{[X_T]}_{[AX]} &= \frac{d[AX]}{d[X_T]}\frac{[X_T]}{[AX]} \\
&= 1 + \frac{[X_T]^2}{[AX]}\frac{d}{d[X_T]}\left(\frac{K_A[A]}{K_A[A] + K_B[B] + 1}\right) \\
S^{[X_T]}_{[BX]} &= \frac{d[BX]}{d[X_T]}\frac{[X_T]}{[BX]} \\
&= 1 + \frac{[X_T]^2}{[BX]}\frac{d}{d[X_T]}\left(\frac{K_B[B]}{K_A[A] + K_B[B] + 1}\right)
\end{aligned} \tag{3.11}$$

From these expressions, we can explain the pattern in relative sensitivities shown in figure 3.2b. First, when there is very little X present, very little complex is formed, and we have $[A] \approx [AT]$, $[B] \approx [BT]$, and $[X_T] \ll 1$ (the amount of different complexes is proportional to the available X). At this point, noting that the derivatives in the above expressions are bounded, we simply have $S^{[X_T]}_{[X]} = S^{[X_T]}_{[AX]} = S^{[X_T]}_{[BX]} = 1$.

We can consider what happens at intermediate, albeit low, values of $[X_T]$ for the case of comparable $[A_T]$ and $[B_T]$, with $K_A >> K_B >> 1$. This is similar to the case considered in figure 3.2. Here, at low levels of $[X_T]$, $K_A[A] >> K_B[B] + 1$, meaning that the absolute sensitivities are given by: $d[X]/d[X_T] \approx 0$, $d[AX]/d[X_T] \approx 1$, and $d[BX]/d[X_T] \approx 0$. Taking the relative sensitivities, as given by equation 3.11, and evaluating the derivatives (substituting $(-d[AX]/d[X_T])$ for $d[A]/d[X_T]$ and $-(d[BX]/d[X_T])$ for $d[B]/d[X_T]$, as given by the conservation conditions) gives:

$$\begin{aligned}
S^{[X_T]}_{[X]} &= 1 + \frac{[X_T]^2}{[X]}\frac{\left(K_A\frac{d[AX]}{d[X_T]} + K_B\frac{d[BX]}{d[X_T]}\right)}{(K_A[A] + K_B[B] + 1)^2} \\
S^{[X_T]}_{[AX]} &= 1 + \frac{[X_T]^2}{[AX]}\frac{\left(K_A[A]\left(K_A\frac{d[AX]}{d[X_T]} + K_B\frac{d[BX]}{d[X_T]}\right) - K_A\frac{d[AX]}{d[X_T]}(K_A[A] + K_B[B] + 1)\right)}{(K_A[A] + K_B[B] + 1)^2} \\
S^{[X_T]}_{[BX]} &= 1 + \frac{[X_T]^2}{[BX]}\frac{\left(K_B[B]\left(K_A\frac{d[AX]}{d[X_T]} + K_B\frac{d[BX]}{d[X_T]}\right) - K_B\frac{d[BX]}{d[X_T]}(K_A[A] + K_B[B] + 1)\right)}{(K_A[A] + K_B[B] + 1)^2}
\end{aligned} \tag{3.12}$$

Substituting the above approximations for the absolute sensitivities then gives:

$$\begin{aligned} S_{[X]}^{[X_T]} &= 1 + \frac{[X_T]^2}{[X]} \frac{K_A}{(K_A[A] + K_B[B] + 1)^2} \\ S_{[AX]}^{[X_T]} &= 1 - \frac{[X_T]^2}{[AX]} \frac{K_A(K_B[B] + 1)}{(K_A[A] + K_B[B] + 1)^2} \\ S_{[BX]}^{[X_T]} &= 1 + \frac{[X_T]^2}{[BX]} \frac{K_A K_B[B]}{(K_A[A] + K_B[B] + 1)^2} \end{aligned} \tag{3.13}$$

This shows that, before A becomes saturated (i.e. while $K_A[A] \gg K_B[B] + 1$ holds), the relative sensitivities of both $[X]$ and $[BX]$ to $[XT]$ increase from 1, while that of $[AX]$ decreases from 1. This is observed in simulations, as shown in Fig. 2b.

In the limit of very high $[XT]$, we can consider that $[XT] \approx [X]$, as the proportion of X taken up in complexes becomes small. Under these conditions, the equilibrium expressions in equation 3.8 can be rearranged to give:

$$\begin{aligned} [A] &= \frac{[AX]}{K_A[X_T]} \\ [B] &= \frac{[BX]}{K_B[X_T]} \end{aligned} \tag{3.14}$$

where the numerators approach a constant value. This indicates the asymptotics for $[A]$ and $[B]$ as the total X becomes large (this can be justified carefully).

These expressions are small for high $[XT]$, so we can consider that $K_A[A] + K_B[B] \ll 1$, so $1 + K_A[A] + K_B[B] \approx 1$. Using this and equation 3.12 in equation 3.11 and evaluating the derivatives gives:

$$\begin{aligned} S_{[X]}^{[X_T]} &\to 1 \\ S_{[AX]}^{[X_T]} &\to 0 \\ S_{[BX]}^{[X_T]} &\to 0 \end{aligned} \tag{3.15}$$

This result can also be obtained by incorporating the asymptotic expression for $[A]$ and $[B]$ for large $[XT]$ and evaluating the relevant expressions.

This demonstrates what we expect intuitively – as $[XT]$ becomes large, the relative sensitivity of free X asymptotes to one, while the relative sensitivities of the complexes AX and BX asymptote to zero.

In summary, assuming that the binding affinity of A is much greater than that of B, we can discern three regimes in the response. These three regimes can be described in terms of the saturation of A and B. Initially, since the binding affinity of A is much greater than B and A and B are present in equal amounts, $K_A[A] + K_B[B] + 1 \approx K_A[A]$, and most of the available X forms complexes with A (this implicitly assumes that the available A and B is in excess of X). Once A is depleted, the quantity $K_A[A]$ becomes dwarfed by $K_B[B]$, and so $K_B[B] + 1 \approx K_B[B]$, and most of the available X forms complexes with B. This is what underlies an ultrasensitive response in BX as the total concentration of X is increased. This parallels the effects discussed by Buchler et al (Buchler and Cross, 2009; Buchler and Louis, 2008), although we note that the relative sensitivity (the sensitivity scaled by concentrations, see (Seaton and Krishnan, 2011b) for details) in the complex BX is less than the relative sensitivity observed in the free X (see figure 3.2). Once B is depleted, all remaining X is added to the free pool. We note that the ultrasensitivity in response of the B pathway depends on suppression of signal at low values of the input (in this case $[X_T]$) by the A pathway. This requires that $K_A[A] \gg K_B[B]$, which is a condition on relative affinities rather than absolute affinities. However, the absolute sensitivity in also depends upon a high linear response once A is depleted and that suppression is overcome, requiring $K_B[B] \gg 1$. Therefore, the response observed requires the system to satisfy the condition $K_A[A] \gg K_B[B] \gg 1$. The results are illustrated in figure 3.2.

Other classes of regime may similarly be discerned, depending on the relative amounts of A and B initially and the affinities. For instance suppose $K_A[A] \gg 1 \gg K_B[B]$, then we see that as $[X_T]$ increases, A is largely taken up, but as A depletes, much of the extra X remains free rather than bound to B. The other case, where $1 \gg K_A[A] \gg K_B[B]$ throughout is one where most of the X is unbound, and is hence of less interest.

Returning to the above analysis for the case when $K_A[A] \gg K_B[B] \gg 1$, we note that our analysis and conclusions were based on a steady state analysis and the factors which enter the analysis are the equilibrium constants. We now examine how such a network responds to temporal signals.

In order to do this, we take the full system at steady state and change the production rate of X at $t = 0$. Note that a slow change in the quantity of X would leave the system in a quasi-steady state, and the results would follow directly from the steady state analysis pre-

sented above. Thus, we examine cases where rapid changes in the quantity of X available are induced.

If we apply a step increase in the production of X, we find that A responds first, followed by B as discussed above – this is illustrated in figure 3.3. This is for the case where the relative affinity of A is greater than that of B and where the timescales of the pathway A are much faster than that of B. In this case the dynamic signal processing in this circuit essentially mirrors the steady state signalling and response discussed above. This can also be demonstrated analytically (Seaton and Krishnan, 2011b). We further note that, when X is present at low levels, an increase in the production of X will primarily affect A, with little dynamic response in B.

Also shown in figure 3.3 is that, in the opposite case, if the relative time scales of the high affinity binding/unbinding are changed (keeping the equilibrium constant fixed) it is possible to saturate the low-affinity component, B, more rapidly than the high-affinity component. In figure 3.3, a case where a sufficiently high change in X is considered so that both A and B are essentially saturated at steady state. For intermediate levels of X, what can be observed is that the low affinity component complex is rapidly formed before a gradual redistribution of X between the pathways. Thus if the low affinity component B is the faster responding component, then a step change in X (in this range) will affect B first, before it gradually reduces with the X "leaking" back to the A pathway. Thus in this regime, a step change in X results in a marked but essentially transient response for BX, and a much more gradual response for AX. Thus BX displays a faster but adaptive response, while AX displays a slower but persistent response. We further note that if the total X is increased past a level which ensures saturation of the component A, then BX displays a response which is partially adaptive. This partial adaptation (underadaptation) can be traced to the saturation of the "inhibitory" pathway A. This illustrates the importance of kinetics in addition to steady state and quasi-steady state analysis in understanding the temporal order of activation of the pathways.

To further examine the temporal response, we input a square pulse in the production of X. The response is seen in figure 3.4, where the faster of the two pathways responds quickly, but also recovers more quickly. In contrast, the slower pathway registers a more prolonged but shallower response. Again, the insights from the numerical simulations can be complemented by analytical studies.

Overall, the analysis above provides insight into how the coupled pathways process steady and temporal signals through their shared component and propagate them down-

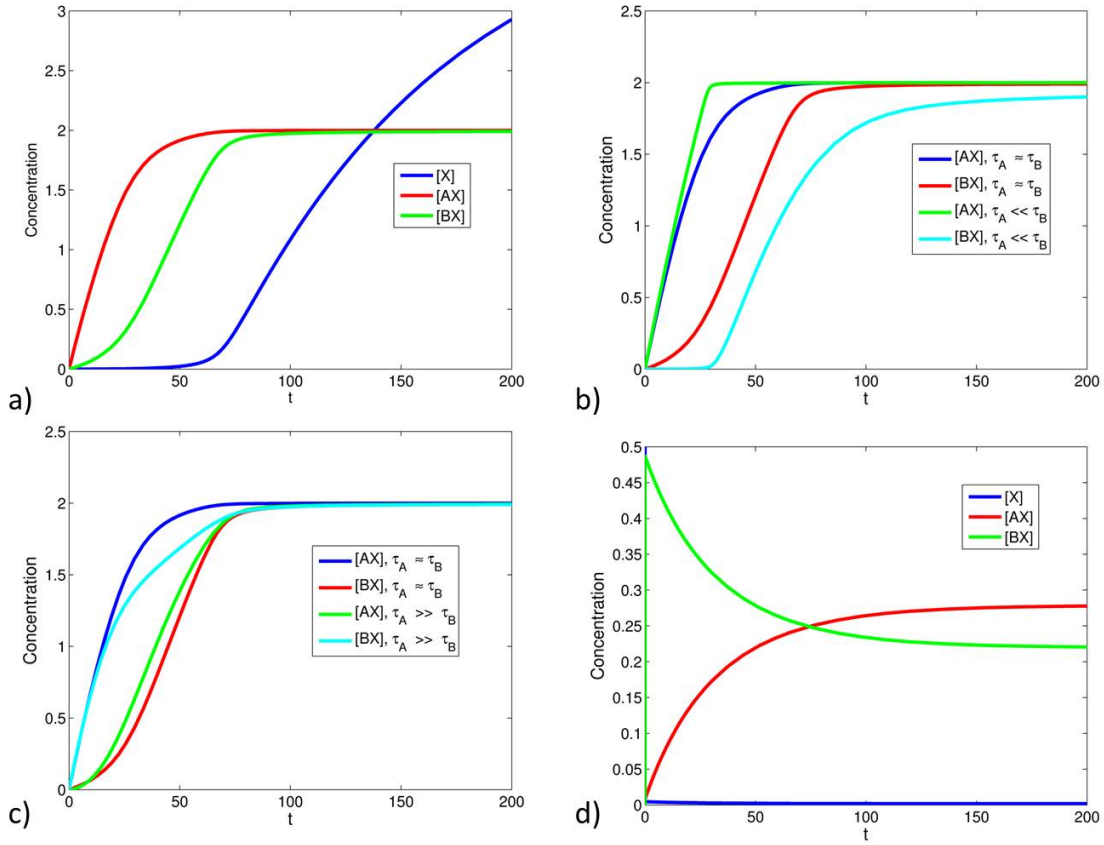

Figure 3.3: **Dynamic response to a step-change in production of X** a). This figure shows how a step change in production rate of X (starting from 0) imposed at $t = 0$, affects the concentration of all different components. Here,$K_A \gg K_B \gg 1$. Note that eventually the concentration of free X also reaches a steady state. b) When the timescale of the lower-affinity interaction (interaction of X with B) is lengthened, the higher-affinity interaction saturates at earlier times, and the lower-affinity interaction saturates at later times. c) When the timescale of the higher-affinity interaction (interaction of X with A) is lengthened, the order in which the complexes are formed can be reversed, so that the lower-affinity interaction saturates at an earlier time than the higher-affinity interaction. Note that in this case the total amount of X in the system finally is clearly greater than the total of A and B put together, so that eventually, most of A and B are present in complexed form. (d) The case where the lower affinity component is faster is shown. Here a sudden change in production of X is imposed so that the total X does not exceed the total amount of A and B. Here we see that at early times B takes up most of the X, while at longer times, the concentration of the complex BX gradually decreases and that of AX eventually increases.

stream, and the role of other factors in modulating this process.

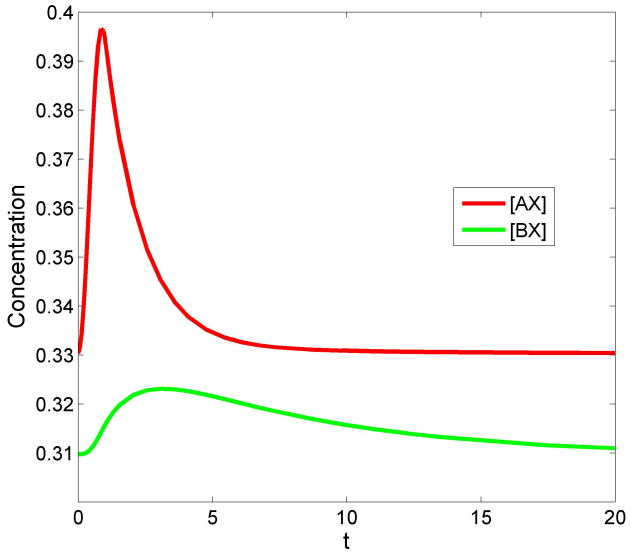

Figure 3.4: **Dynamic response to pulsatile change in production of X** The response to a rectangular pulse of X imposed starting at $t = 0$ is considered here. Here the affinities of the interactions are equal ($K_A = K_B = 1$), but the timescales are different ($\tau_A \ll \tau_B$). The faster interaction (with A) takes up X more quickly, but also releases it more quickly.

3.3.2 Modulation of each pathway alone and together

We now use our modelling framework to examine the case where input signals "converge" on a common target. This is done in our model by changing the production of A and B, and keeping the production of X fixed. We first consider the case when the input is applied only to A (the high affinity component). Figure 3.5 shows the result wherein the concentration of the complex AX increases and the concentration of free X decreases followed by that of the complex BX. This shows how signalling through one of two "converging pathways" may affect the second one. Also shown is the case where the step input is applied to the low affinity component. Here BX builds up, depleting X, and then AX, but overall the AX concentration doesn't decrease as substantially as before simply because the low affinity component isn't able to outcompete the high affinity component as effectively. Thus here the retroactivity effect of pathway B on pathway A is weak, when compared to that of pathway A on B.

Now we consider the effect of simultaneous step changes provided to A and B (figure

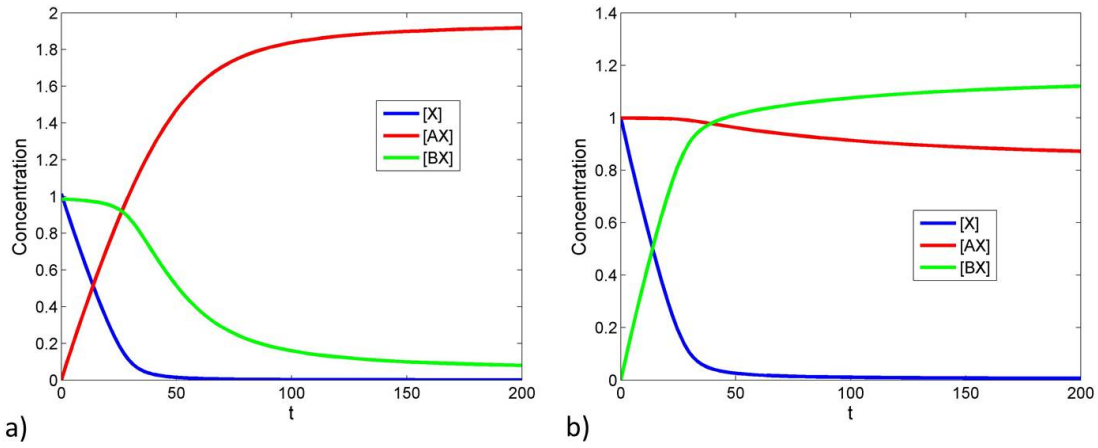

Figure 3.5: **Dynamic response to change in production of A or B alone** The response to step change in production of A (starting from zero) is shown in a), with $K_A \gg K_B \gg 1$. The steady state analysis shows that this should result in a depletion of BX and X. The temporal analysis shows the expected ordering of this depletion: first X is depleted, then BX. Note that the initial conditions correspond to a steady state with a non-zero production rate of B. The response of the system to a step change in production of B (starting from zero) is shown in b). The initial conditions here correspond to a steady state with a non-zero production of A. The result is qualitatively similar, except production of B is less able to deplete AX, since $K_A \gg K_B$.

3.6). We find that the concentrations of both complexes initially rise, but that eventually the concentration of the complex of the low affinity component is depleted by the retroactivity effect. We thus see how a step change in production and A and B together results in a partially adapting response of BX, purely due to competition effects.

We have examined a variety of ways in which this basic system may be modulated by a external signals, both at steady state and dynamically (see Table 3.1 for a summary). We now build on this to examine how the basic network structure and dynamics may be affected by other additional elements or features. We begin by examining how an additional component can affect the system by forming a complex with A and X.

3.3.3 Combinatorial signalling and the influence of complex formation mechanisms and allostery

It was shown above that, in essence, processes which share a component may act to inhibit one another. The above analysis of the mass-action model applies to situations where A and B form complexes with X by simple independent interactions. In many cases a protein may bind cooperatively, and it may be affected by further binding proteins. In this section

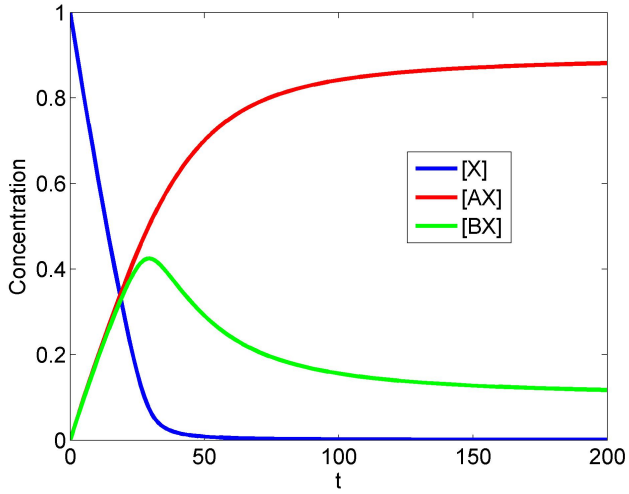

Figure 3.6: **Dynamic response to change in production of A and B together** The response to a simultaneous step change in production of A and B (both starting from zero) is shown, where $K_A \gg K_B \gg 1$. We observe that both $[AX]$ and $[BX]$ rise initially. However, as $[X]$ decreases competition between A and B becomes significant, and the higher affinity interaction of X with A means that it outcompetes B at later times.

Scenario	Result
Changing the rate of production of the shared component, X	At steady state, ultrasensitivity may be observed in the response of the lower affinity component, and of free X. When one examines the dynamics of the response of the two pathways, the relative timescales of the interactions are important. Depending on this, the dynamics may mirror the steady state response; alternatively, an adaptive response may be observed in the low affinity component.
Changing the rate of production of A and B.	The two pathways may inhibit one another, with the high affinity component having a greater inhibitory effect. Depending on the timescales of the interactions, the dynamics may either mirror the steady state response, or result in an adaptive response in the lower affinity pathway.

Table 3.1: **Summary of results for the basic model** We consider the case where the shared component, X, binds with high affinity to component A, forming the complex AX, and with low affinity to component B, forming the complex BX.

we show how such mechanisms influence the potential interaction and coupling between processes. We then suggest a role for this in effect in insulating pathways against crosstalk. In particular, since these mechanisms allow single proteins to behave as "AND" gates – active only when receiving both input signals – they allow tuning of specificity through combinatorial signalling.

In this section, we will consider X as an input affecting A and B; the only difference is that we will have an additional input Y which affects the activation of the A pathway by X. This can occur in different ways: for instance Y can bind with A before it is targeted by X. Alternatively Y can bind with the complex AX only. A third way is if X and Y co-operatively interact with A. Schematic diagrams of all these cases are shown in figure 3.7. All of these cases represent a modification of one of the coupled pathways by an extra element Y. Having understood the behaviour of the simpler model previously we can examine what the role of the extra element Y is in coupling the two pathways. Here, we consider the X and Y to be two inputs, with the complexes AXY and BX the outputs.

As a simple example of the effect complex formation mechanisms can have, consider that the binding of X to A precedes binding by Y (Fig. 3.7b). We denote this, the sequential-binding model of complex formation. A good example of such a mechanism is the binding of substrate to CDK-cyclin complexes, where the cyclin must bind to CDK before the substrate (Rabiller et al., 2010). In this case, two unbinding events must occur before X is free. Y, which corresponds to the CDK-cyclin substrate, is effectively locking in X, which corresponds to the CDK (which may bind to many different cyclins, corresponding to A and B). An analysis of this network reveals the highly non-trivial impact which Y has: this will impact on both the steady state and dynamic behaviour as seen in figure 3.8. What is observed is that without Y, the signalling pathway involving A is inactive, and in the presence of Y it is active. Further, in the presence of Y, not only is the A pathway activated but the B pathway is inhibited. In our modelling framework, the introduction of Y can be seen as effectively reducing the dissociation rate of X from the complex AX, modulating the response by further suppressing BX formation at low concentrations of X.

Thus, such a complex formation mechanism can act to increase signalling specificity by effectively combining the cross inhibition and combinatorial signalling methods of reducing crosstalk. In the case of CDK-cyclin complexes mentioned above, given that different cyclins result in different substrate specificities (Bloom and Cross, 2007), sequestration provides a mechanism for the presence of substrates for a particular cyclin-CDK complex to favour the formation of that complex rather than other cyclin-CDK complexes. Further,

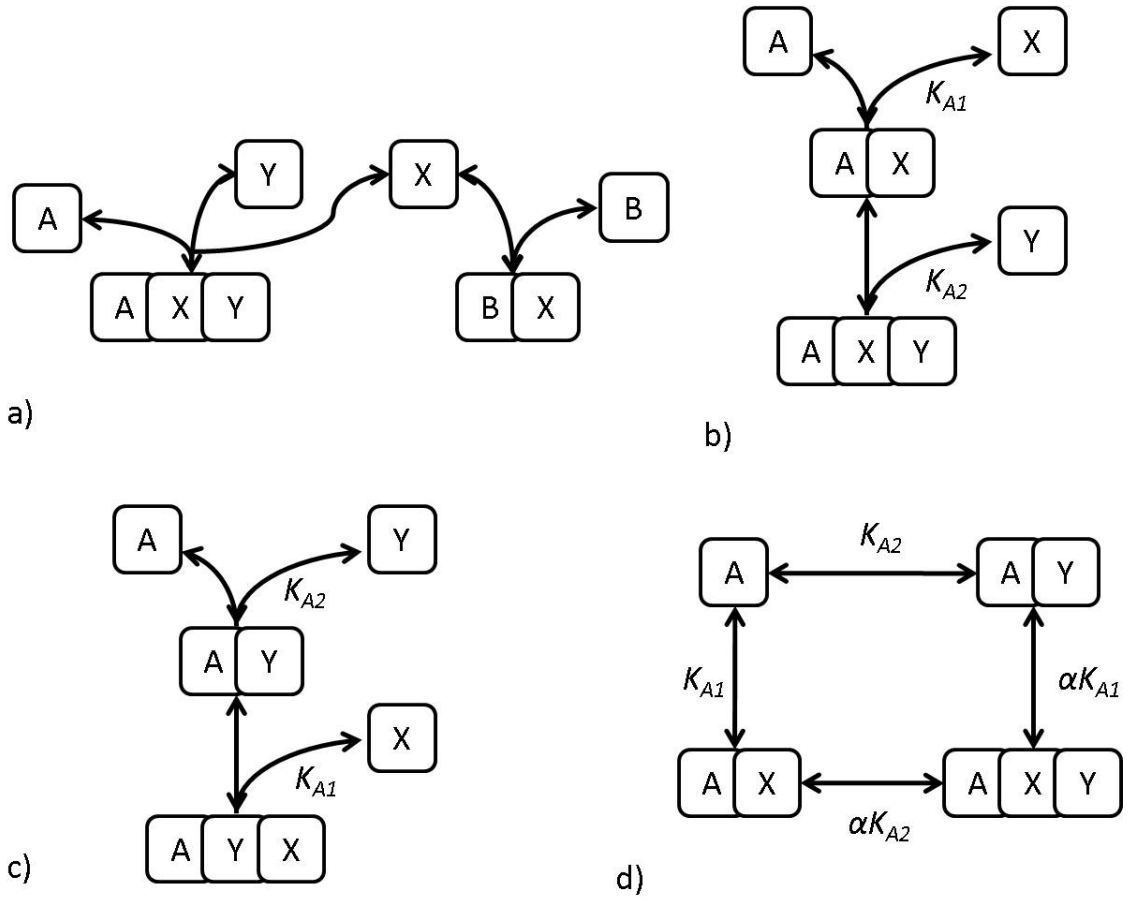

Figure 3.7: **Schematic of combinatorial signalling** A situation where an extra player Y is involved in regulating/interacting with pathway X is considered. The signals X and Y combine to form an active complex with A, but X also participates in a complex with B, as shown in a). This involves the formation of a tertiary complex, AXY. Three distinct mechanisms for the formation of this complex are illustrated in b)-d). In b), A binding to X precedes its binding to Y. In c), A binding to Y precedes its binding to X. In d) X and Y bind to A cooperatively, stabilizing it in its active conformation.

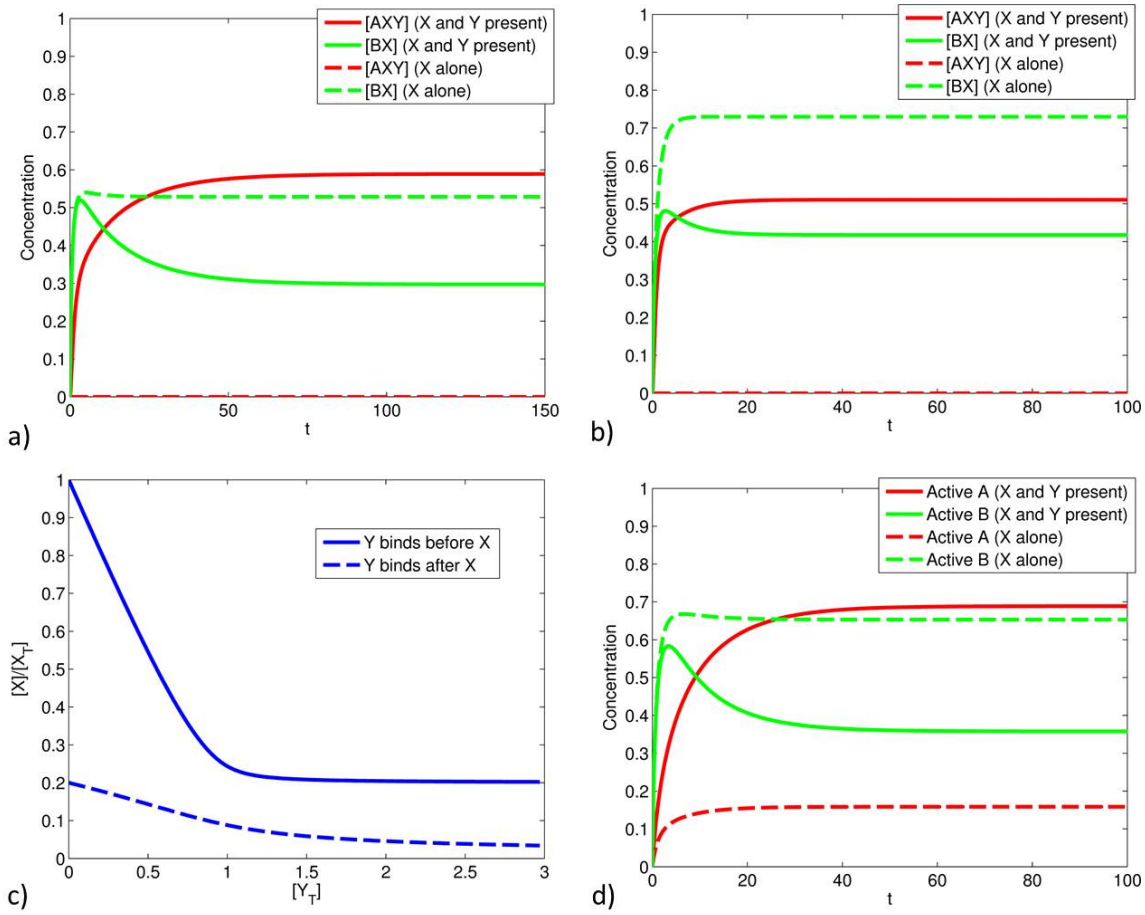

Figure 3.8: **Combinatorial signalling and specificity** Combinatorial signalling can increase signalling specificity through competitive inhibition of parallel pathways. This figure depicts the outputs of the A and B pathways when subject (at $t = 0$) to a change in production rate of X, starting from zero. Solid curves represent the response to both X and Y together, while dashed curves represent the response to X alone. a) shows the response when X binding to A precedes Y binding, b) shows the response when Y binding to A precedes X binding, c) shows how the amount of available Y affects the fraction of free X and d) shows the response when X and Y bind to A cooperatively. In all cases, it is seen that the presence of X and Y together not only activates the A pathway but also inhibits the B pathway, and thus leads to improved signalling specificity. In (a) and (b), the absence of Y leads to zero output from the A pathway. While the qualitative results from (a) and (b) are similar, we some differences in how the total availability of Y affects the results. In the case where Y binds to A before X binds to it, we see that a low availability of Y substantially increases the fraction of free X. This is not the case when Y binds to A after X is bound to it.

deletion of a cyclin may lead to compensation effects from the binding of substitute cyclins, as many are present at significant levels at the same time (Cross et al., 2002).

The other case, where binding of Y to A precedes binding of X to form the active complex AXY, can also be considered within our framework (figure 3.7c)). In this case, addition of Y allows binding of X, and so performs the same role in modulating B as A alone did in the basic model. Figure 3.8 shows again that the presence of Y, increases specificity of A and leads to greater inhibition of B. On the other hand, we see that the presence of Y acts to insulate A from the crosstalk through B via the common connection X. While in both cases an increased Y acts to inhibit BX formation at steady state, there are some differences. In one case (Y binding with A before binding with X) we see that the amount of Y limits the amount of X involved in this pathway. Thus a low level of Y will substantially reduce the amount of X involved in this pathway. This is not the case for the scenario where Y binds to the complex AX. The contrasting effects of the two mechanisms on the uptake of X in response to Y are shown in figure 3.8.

The above mechanism essentially allows one component to lock another into the complex. Another view of protein complex formation comes from allostery. Here, it is possible for two inputs to act on one protein in a synergistic way, so that they are both in some sense locked in by one another, simply through the stabilization of a high affinity conformation. Examples in which this might be significant are widely available, and include the WASP family of proteins (Padrick and Rosen, 2010), A-kinase anchoring proteins (Beene and Scott, 2007), and phospholipase C (Philip et al., 2010). This can be captured by a model of co-operative interaction between X and Y in binding A in which the preferential binding of the proteins to the active conformation shifts the population towards this active state. A simple representation of such a model is the following (see schematic in figure 3.7d)).

$$\begin{aligned}
\frac{[AX]}{[A][X]} &= K_{A1} \\
\frac{[AY]}{[A][Y]} &= K_{A2} \\
\frac{[AXY]}{[AY][X]} &= \alpha K_{A1} \\
\frac{[AXY]}{[AX][Y]} &= \alpha K_{A2}
\end{aligned} \tag{3.16}$$

Where K_{A1} and K_{A2} are association constants and α is the cooperativity constant between X and Y. Note that in the above model the same co-operativity constant appears in the last two expressions. This is done for simplicity, and ensures that the steady state of binding in the network corresponds to equilibrium conditions. Again, we see that signalling specificity may be increased through this mechanism. Just as in the previous cases, we find that the presence of Y increases the active output from pathway A but also inhibits pathway B (figure 3.8).

It is worth pointing out that allosteric models of complex formation predict that this mechanism of crosstalk inhibition can occur bidirectionally, meaning that Y affects uptake of X and vice versa. This is in contrast to the sequential-binding model discussed above, where the component which binds first can affect uptake of the other, but not the other way round. It should also be noted that, while allosteric mechanisms are often proposed due to observed synergistic activation of a protein, the crosstalk inhibition effect identified here does not require such synergy. In the case considered here, if Y can activate A on its own, then allosteric effects may not appear to be significant. However, they can still allow cross-inhibition of pathways, and therefore signalling specificity.

Taken together we have seen how the presence of an extra element Y to the simple pathway coupling can lead to the activation of the relevant pathway and inhibition of the other (competing) pathway. Thus mechanisms of complex formation provide control settings to determine how pathways and processes may inhibit one another. Overall, additional elements can modulate the pathway structures in highly non-trivial ways, and this provides some insight into how additional elements in cellular signalling systems may act to modulate and control signal splitting between pathways.

3.3.4 Coupling of switches

The basic model presented here made no assumptions about the nature of the pathways in which A and B are involved, and merely represented the binding of species to one another. However, in many cases proteins with multispecificity are also capable of enzymatically modifying the proteins with which they interact (Copley, 2003; Csikasz-Nagy et al., 2009; Hult and Berglund, 2007; Kim et al., 2010, 2011; Nobeli et al., 2009). In this section we extend our model to examine some of the consequences which reversible multispecific posttranslational modification might have on the signalling properties of the system. We examine two generic cases of signalling through post-translational modifications – one

involving only single reversible modifications of the substrates, and the other involving a double modification of one substrate. The first case is shown in Fig. 3.9 and involves two switch-like pathways of Goldbeter-Koshland type (Goldbeter and Koshland, 1981), involving a single reversible posttranslational modification of each substrate (A and B) by the shared enzyme X. As previously, we begin by examining the steady state situation in terms of the conserved total quantities of X. The enzyme kinetics are chosen such that the affinity of X for A is higher than that for B, while keeping the overall steady state response of the switches in isolation very similar, as shown in Fig. 3.9. Now, when the two switches are connected via the common upstream component, we see that the high affinity pathway (A) is activated at a lower input level than the low affinity pathway (B). Thus the coupling of switches allows for a sequential activation in a well-defined order of the two pathways. In the model under consideration, we examined the effect of availability of A and B on the input dose difference between the activation of the switches, over a wide range of abundances of A and B (Fig. 3.10). We note that this difference varies significantly when there are low concentrations of one component – this is the result of the uptake of X by the component being insufficient to couple to switches effectively. However, higher concentrations of A and B ensure suitable conditions for the coupling to occur effectively, and little difference is observed in their activation dosage-gap. Thus it is possible to have a sequenced activation of coupled switches arising from their activation through a common source.

Further to the steady state analysis, we can look at the effects of the system dynamics on signalling. As expected from the dynamic analysis of the response of coupled pathways to modulation of the shared component X, if the timescale of interaction between A and X (the high affinity interaction) is faster than the interaction between B and X, the dynamic pattern is similar to the steady state one – activation of A preceding that of B. Likewise, if the timescale of interaction between B and X is faster than the interaction between A and X, we get the reversed pattern, where at first B is active, followed by A. Again, adaptive behaviour in the low-affinity component, B, can result due if the faster pathway is the lower affinity pathway(results not shown).

We now examine a different coupling of switches, of the enzyme with a single reversible modification of the substrate B, but two sequential reversible modifications of the substrate A (which we refer to as the multiphosphorylation switch), by the common enzyme X. The multiphosphorylation switch is capable of a range of behaviours – it is also capable of the switch-like monostable response of single phosphorylation (Liu et al., 2010), but is further

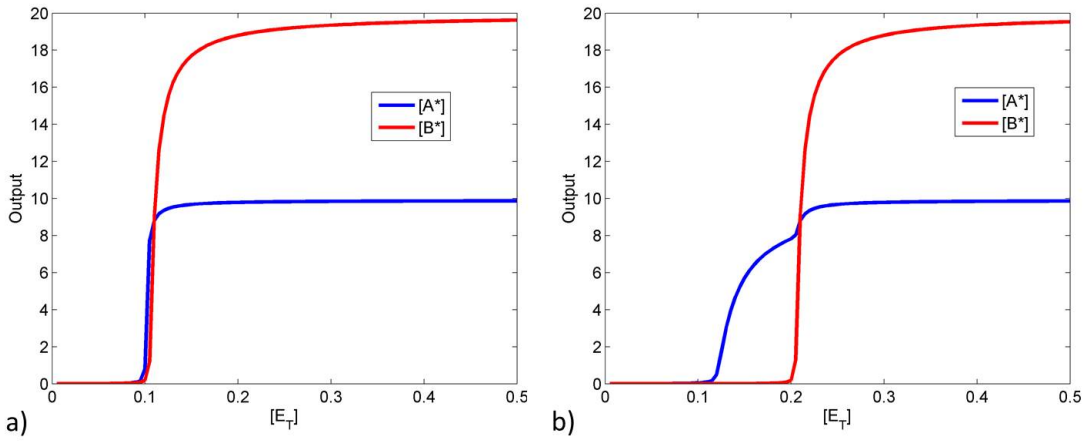

Figure 3.9: **Competition and specificity** This figure shows how signalling specificity may be improved by competition effects. It considers the case of two switches which are regulated by the same upstream component. Each of the switches in isolation display switching behaviour at the same input dosage. a) shows the response of the switches in isolation, and b) shows the switches operating together. It is clear that it is not possible to choose input values for the isolated case which would result in mutual specificity. However, when they operate together mutual specificity can be obtained by having low inputs activating A and high inputs activating B, triggering the relevant switch.

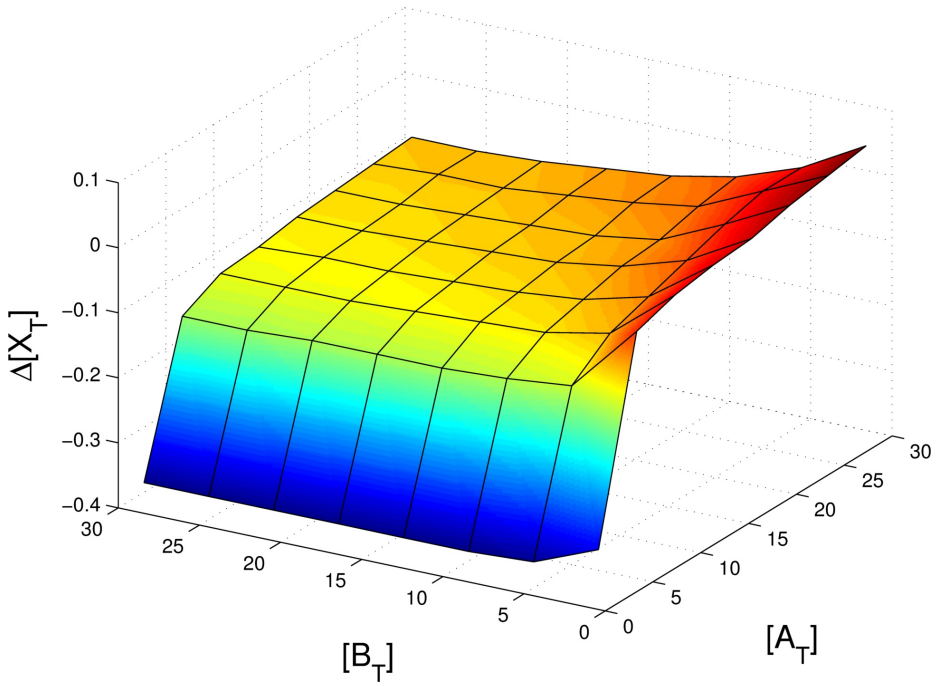

Figure 3.10: **Competition and timing** This figure further examines the case presented in Figure 3.9 and shows how the difference in total enzyme ($[X_T]$) concentrations at which the two switches become activated is kept consistent over a wide range of total concentrations of A and B. The difference plotted is the difference in input concentration between that where the A pathway is triggered and that where the B pathway is triggered.

capable of exhibiting bistability (Markevich et al., 2004) (see above for model equations and parameter values). When exhibiting a monostable response, the behaviour of the combined system is as described above. However, when exhibiting a bistable response, a qualitative change in the behaviour is observed. The behaviour of the two switches in isolation and together is shown in Fig. 3.11. We note that, when isolated from one another, pathway B displays only a slightly sigmoidal response, while pathway A displays a dramatic shift in response as a result of its bistability. In this case by coupling these two pathways via a common upstream regulator X, we see that as the upstream signal is increased past a threshold the multiphosphorylation switch is switched on. It is evident that at this point the switch involved in pathway A is also triggered, in fact in a more dramatic fashion than the regular switching of pathway A itself, and this is purely due to the coupling of the switches. The reason for this switching is seen in the shift in the available X observed when the bistability threshold is crossed (see Fig. 3.10) – this shift is not observed when a monostable signalling threshold is crossed. Bistability in this case therefore results in significant qualitative changes to bidirectional signalling, as well as to the input-output response. Thus this example reveals that a strong switching behaviour in a pathway need not necessarily arise from characteristics embodied in that pathway, but may instead arise from coupling with other switches through shared components. Taken together the examples show how it is possible to get sequential spaced switching from the coupling of switches with identical thresholds and also to get coordinated switching of pathways in a striking manner.

3.3.5 Spatial signalling

This chapter thus far has studied the coupling of pathways/processes through shared components and focussed exclusively on temporal signal processing. Many cellular processes involve aspects of spatial signal transduction, and the importance of spatial aspects in signalling is being increasingly recognized. In the context of our analysis, we systematically investigate phenomena introduced purely by differences in the diffusivity and localization of the components.

In order to do this, we assume that all components exist in a spatial domain. For specificity, we take this to be a 1-dimensional periodic domain, although most of the essential results remain valid in other domains. We now include the spatial element, by including spatial variation in one or more elements. Additionally, we examine the effects of one of the components being highly diffusible to see if this changes the effect of the interaction of

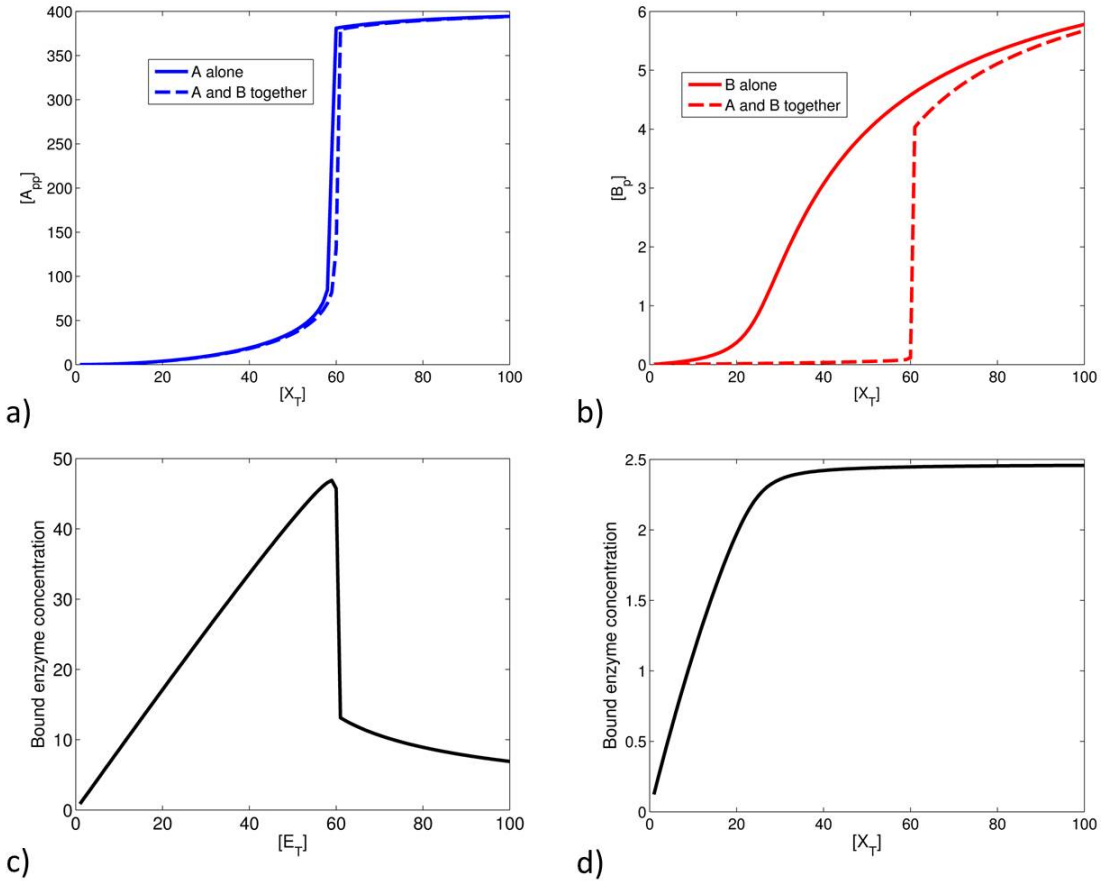

Figure 3.11: **Coordinated switching** This figure illustrates another aspect related to the coupling of two switches through common upstream regulation. One of the switches (A) is a multiphosphorylation switch while the other (B) is a monophosphorylation switch. The response of the multiphosphorylation and monophosphorylation switches are shown in a) and b), respectively. The solid curves show their response to $[XT]$ in isolation, while dashed curves show their response to $[XT]$ when together. We see that the sharp switching of the multiphosphorylation switch can be "transmitted" to the monophosphorylation switch, resulting in coordinated switching at a well defined location. The reason for this is the sharp change in the uptake of enzyme by the multiphosphorylation switch, as the threshold is crossed, as shown in c), resulting in an increase in free enzyme. The response of the single phosphorylation switch does not exhibit this behaviour, as shown in d).

the pathways in a non-trivial way. In this case, we will assume that A is highly diffusible, and likewise so is the complex AX. We emphasize that while we perform simulations and analysis in a 1-D periodic domain, our analysis and main conclusions are also relevant to other situations, for instance where X is initially present only in the membrane of the cell , while A is present, along with its complex, both in the membrane as well freely diffusible in the cytosol. We will examine some scenarios which draw a direct contrast with the purely temporal signal processing in the case where the shared component, X, is modulated. We start by examining the situation where X is present only in part of the domain. A concrete example is if X is present at a non-zero level only in a specific region initially (for example having a square-pulse like spatial profile). No species is either produced or degraded. Now if all entities are non-diffusible then we expect that, in the region where X is present, at steady state there exists a balance between the concentrations of free X and complexes AX and BX, and this is determined exactly as above. Overall the conclusion therefore is that the complexes AX and BX are present only in the region where X is present, and the balance between these complexes is determined just as in previous sections.

We now build on this to examine a related case where X is being actively produced in a inhomogeneous manner with a Gaussian like profile centred around the middle of the domain. All species are assumed to be degraded equally quickly. Analysis reveals again that the total A and B attain a uniform constant profile, that the complex AX attains a uniform profile, while both X and the complex BX are inhomogeneous. Increasing the production of X actually leads to an elevation in the level of BX at every spatial location, while only weakly reflecting the pronounced asymmetry in the spatial profile of X. This is shown in Fig. 3.12. Complementary analytical results are performed in (Seaton and Krishnan, 2011b).

In the above case, the activating signal was spatially inhomogeneous and this was the source of the spatial aspect of signalling. A slightly different case can be also examined, which fits naturally into our framework. This is the case where the activating signal is spatially homogeneous, but a localized sequestration reaction occurs. Thus in the above case we let the production of X be spatially homogeneous, but we regard the activation of the B pathway as occurring only locally in a restricted region. This can be described either by starting with homogeneous X in the domain, and B present only in a localized region, with no production or degradation of any species or alternatively by having homogeneous production of X (and A) and highly inhomogeneous production of B and having degradation of all species. Both situations provide essentially similar results.

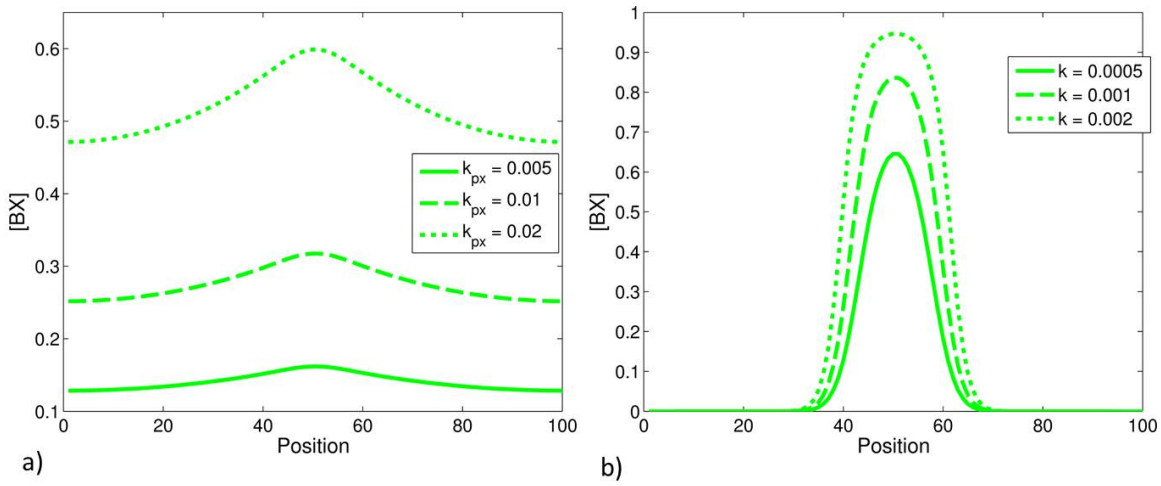

Figure 3.12: **Response to localized production of X** This figure shows how the steady state spatial distribution of the complexes in response to varying rates of production of nondiffusible X. A and B are produced at a uniform rate across the domain, while X is produced in a localized region. a) shows the spatial distribution of BX as production of X changes, where both A and AX are diffusible. This allows BX to spread over the whole cell, even though it is not diffusible. The distribution of BX is almost uniform for low levels of production of X. b) shows the spatial distribution of BX as production of X changes, where A is the only diffusible component. Here a pronounced localization is observed. In both cases the AX profile is spatially uniform (not shown).

Now, if the A pathway is highly diffusible, at steady state the AX profile becomes homogeneous and an analysis of the X profile reveals that it too becomes homogeneous. The BX profile reflects the pronounced heterogeneity, and now there is a global coupling between the levels of X and AX, and the profile of BX, which arises from a global conservation condition.

Simulations describing this case are shown in Fig. 3.13. In this case, if the X binding to B is strong, the net effect is a localized activation of B, and a consequently less strong regulation of A, which is nevertheless spatially homogeneous. It is also worth pointing out that for moderate levels of X production, the spatial profile of free X is itself close to uniform (and under these conditions are in agreement with analytical results performed for the case of no production/degradation of X) although as the rate of production is substantially increased the free X profile starts to reflect a dip in the region where B is present.

Finally, we can consider the effects of differing affinities in this system. These effects are demonstrated in Fig. 3.14, showing the response of AX and BX to a fixed, localised production of X, in the cases of A alone being diffusible, and A and AX both diffusing. In all cases, increasing the binding affinity of a complex increases its concentration globally,

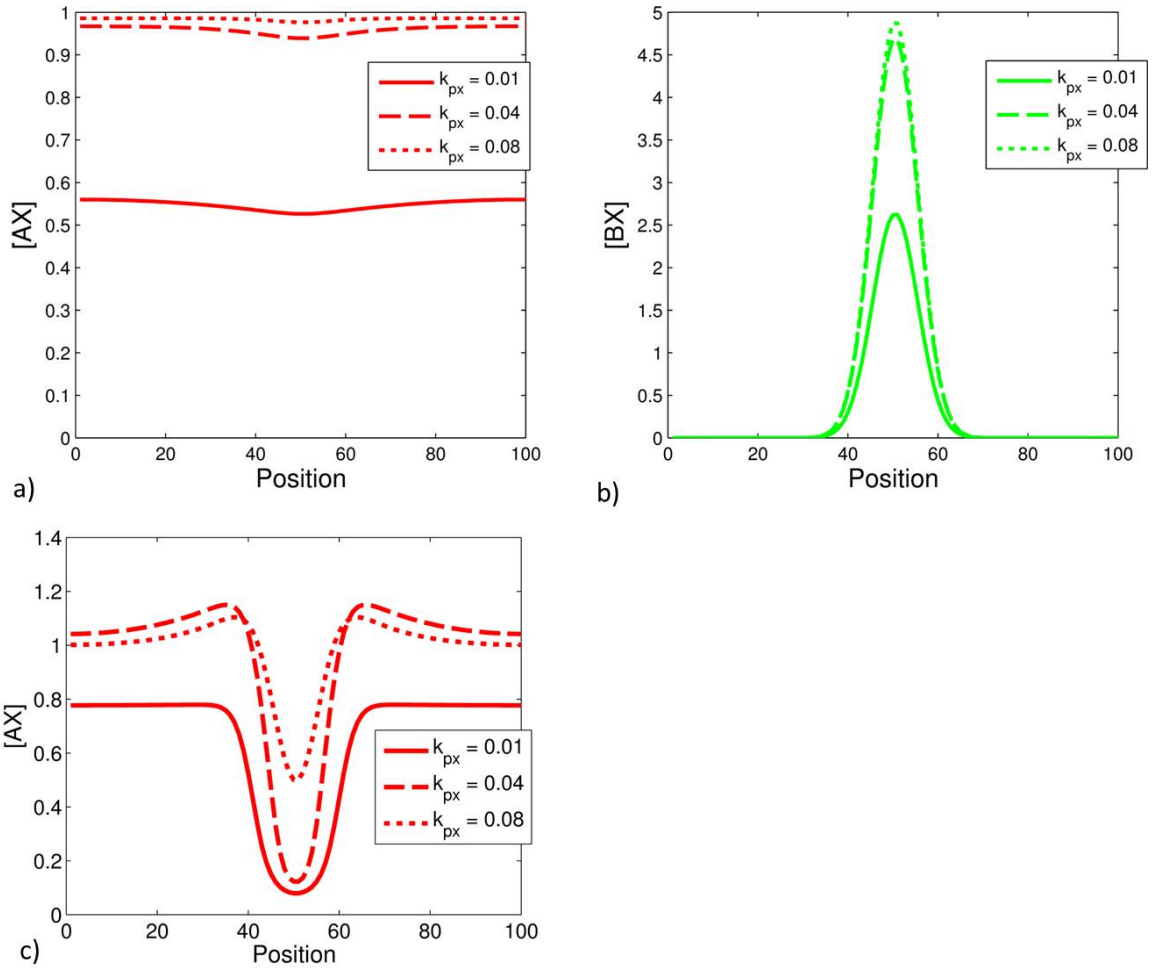

Figure 3.13: **Response of pathways when production of B is localized** This figure shows how the steady state spatial distribution of the complexes AX and BX change in response to varying rates of production of nondiffusible X. A and X are produced at a uniform rate across the domain, while B is produced in a localized region (described by a sharp Gaussian profile centred around the middle of the domain). The spatial distribution of AX and BX as production of X changes is shown in a) and b), respectively. Localized production of B causes a very mild reduction in the production of AX around the centre and a sharp increase in BX there. Both A and AX are diffusible. In part c), only A is diffusible. Localized production of B causes a sharp reduction in the production of AX around the location at which B is produced.

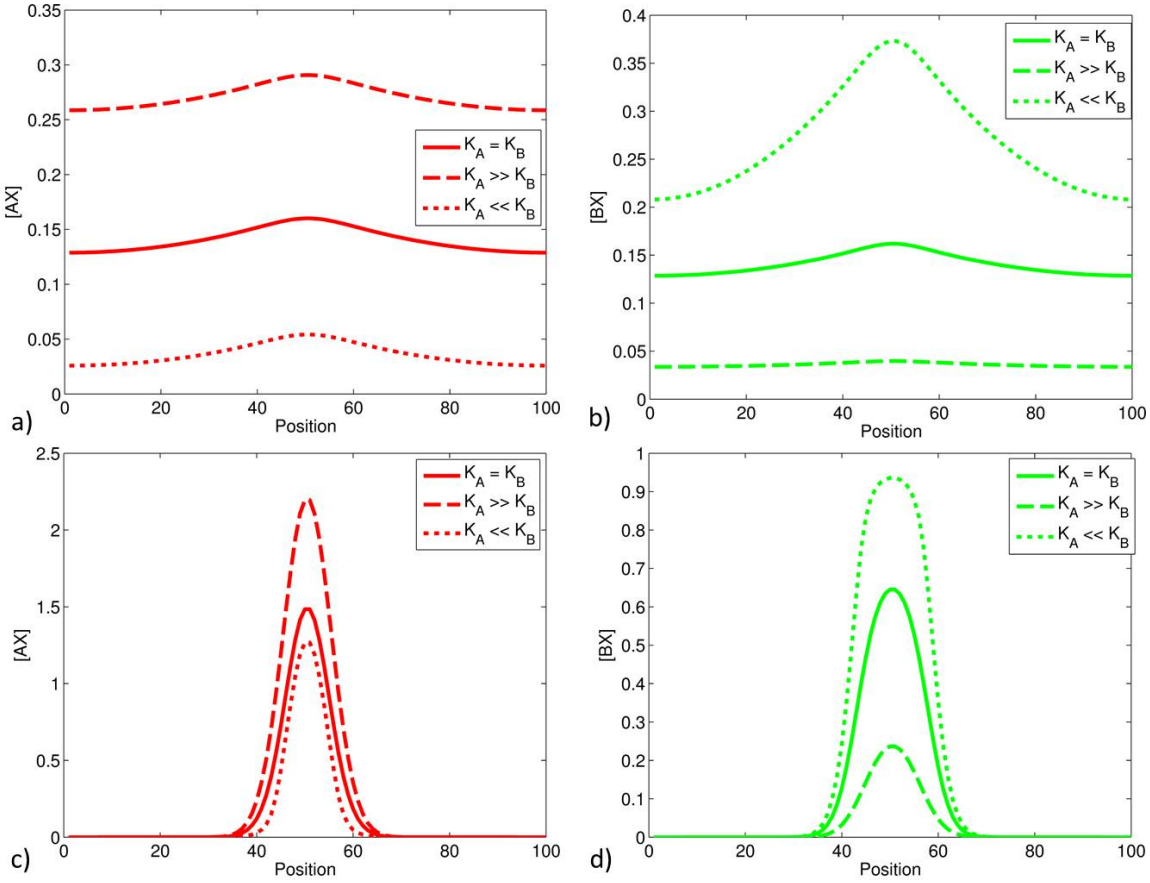

Figure 3.14: **Response when affinities are varied** This figure shows how the steady state spatial distributions of the complexes AX and BX change with the relative affinities of A and B for X. In a) and b), both A and AX are the only diffusible components, while X is locally produced. In c) and d), only A is diffusible, while X is locally produced. It is seen that increasing the binding affinity of a particular complex increases its concentration, and that this effect is most significant for the nondiffusible complex, BX, which exhibits a more pronounced spatial variation.

as expected. However, there is a difference in the behaviour of AX and BX to the difference in affinities – BX is more sensitive to changes in affinities than AX. The reason for this is that diffusion of A (or A and AX) allows the concentration of free A, and therefore the concentration of complexes, to remain relatively constant, while any uptake from a local pool of B cannot be compensated by the same mechanism. Therefore, AX is merely responding to changes in availability of X, while BX responds to changes in availability of X and B, and its sensitivity is consequently greater. In the above, when we have considered the effects of a diffusible pathway, we have assumed that both A and AX are diffusible. One may also examine the case where A is the only diffusible component, and not AX. In this case, the response is similar to non-diffusible case, and AX exhibits a non-trivial spatial profile. The main difference when X is inhomogeneous arises in the fact that X is no longer limited by the local availability of A in contrast to the results in the purely temporal case.

Overall the above cases provide an illustration of the coupling of signalling pathways with shared components, where spatial aspects of signalling are important.

Scenario	Result
An additional component is involved the uptake of X by one of the two pathways through a complex formation mechanism.	The additional component can control how signalling through X is divided between the two pathways. This may enhance signalling specificity. The degree of control the additional component has depends on the mechanism of complex formation.
The shared component is involved in two downstream pathways which display switching behaviour.	Where uptake of the shared component is significant, the switching behaviour of one pathway may influence that of the other. This can result in either a specific ordering of activation, or coordinated activation, of the two pathways.
One of the downstream components, and its complex with the shared component, is diffusible.	The shared component is spread across the domain. This results in uptake being significant across the domain, with the spatial distribution of the nondiffusible components also affected.

Table 3.2: **Summary of results for variations on the basic model** A summary of results for the biologically motivated variations on the basic model is presented. These demonstrate how the effects considered may play a role in diverse biological contexts.

3.4 Conclusions

This chapter focussed on analyzing the interaction and coupling of pathways through shared components, a ubiquitous phenomenon in cellular networks. In this chapter we examined this basic branching structure from a modelling and systems perspective. We believe that a detailed systems analysis of signal processing in this setting is useful for multiple reasons. Firstly, it allows us to explicitly analyze the different features which affect signal processing, without being distracted by the details of a particular signalling context. Secondly, since such structures are repeatedly encountered biologically, it is only to be expected that different variations around this basic theme will be encountered, and the results here provide a platform and framework for analyzing these subsequently.

We developed a minimal modelling framework where we could examine the interaction of pathways with shared components. Since we include the possibility of production of all components, we were able to examine both dynamic and steady state responses to a variety of signals. More complex cases such as temporally regulated interacting pathways, with buffering of one pathway also form part of the framework. Each of the pathways of necessity interacted with the other, because of the shared component. These results were obtained using simulations and analytical work (see Table 3.1 for a summary of the main results).

We first examined the case where the common component is regulated by some external signal. Building on the work of Buchler et al (Buchler and Cross, 2009; Buchler and Louis, 2008), our studies reveal how, depending on the affinities of the common activating component to the two pathways, it is possible to obtain "ultrasensitivity" in the response of the component with a weaker affinity. We also showed how depending on the kinetic rates of binding/unbinding, the pathways could get activated in either temporal order or even concurrently. If there is a clear separation of affinities, and the low affinity pathway is the faster pathway, then for certain ranges of the input signal, the response of this pathway to a persistent stimulus is adaptive: this adaptation may be close to being exact if enough quantity of the high affinity component is present. A significant departure from the adaptive response is observed if the high affinity component is consumed. The saturation effect leading to inexact adaptation in this case is the consumption of the additional "inhibitory" high affinity component, and this is qualitatively similar to other saturating mechanisms leading to inexact adaptation (see the discussion in [41]).

In a similar manner we examined the case where the two other components, A and B,

are regulated by external signals. Our framework allowed us to naturally apply and extend our analysis to this case too. We found that at steady state the high affinity pathway dominates. However, temporally, if the low affinity pathway was the faster pathway, then the response of this pathway was (for certain stimulus levels) partially adaptive (either underadaptive or overadaptive) and this was entirely due to the added high affinity component acting as an inhibitory component. If one regards the components A and B to be stimulated externally through some common source, then the signal transduction of the low affinity pathway in this regime is qualitatively similar to a feedforward adaptive signalling module.

Although our analysis was performed for the case of two pathways sharing a common component, the insights naturally generalize to the case where there are multiple pathways sharing a common component. Our results indicate that depending on the relative affinities, kinetics, and amounts of the individual components, different combinations of steady state responses (including possible "ultrasensitivity") and different kinds of temporal responses will be observed for the different complexes. This will be examined in detail subsequently. Our results have natural relevance for the (competitive) binding/activation of different entities by a common factor. Further, it is possible to predict the effect of modulating individual pathways here. Additionally, since many components are subject to temporal modulation (for instance, in concert with the progression with the cell cycle), this framework provides a natural platform for examining such effects systematically.

We then built on our basic analysis by examining additional factors built over the basic model structure (see Table 3.2 for a summary of models and findings). This is motivated by the fact that such additional elements modulating such pathways are naturally expected to be present in different ways in different contexts.

In the first case we examined the effect of an additional component modulating one of the two pathways. It was shown that this could allow for greater specificity in signalling, effectively through inhibition of the one pathway by the other. Different modes of interaction via the extra component were considered, including sequential binding either before or after binding with the target, as well as co-operative binding to the target species. Analysis reveals that many of the relevant conclusions for all these cases were similar. This indicates how cellular systems may have naturally exploited their pre-existing set of molecules to add further layers of control and separation/differentiation between diverging pathways. We additionally examined the effect of coupling of pathways which are involved non-trivial and highly non-linear signal processing. Thus we built on our existing modelling structure to include switch-like signalling in each pathway. Our analysis reveals that coupling two

switches even with identical switching thresholds, can result in a well-defined order in the switching response, and further that under many conditions it is possible to maintain a robust "dosage gap" in the switching of the pathways. In other cases the interaction of two switches can lead to one switch being highly accentuated by coupling to a multiphosphorylation switch which is bistable. This is an example of co-ordinated switching in two pathways which arises from their coupling through shared components, and suggests that in some cases switch-like behaviour in some pathways can arise from their coupling to other pathways rather than their intrinsic switch-like behaviour.

Finally we expanded our model in a natural way to include spatial aspects in signalling and built on our early studies to examine signal processing in coupled pathways in spatial signal transduction. We showed that the coupling of a highly diffusible pathway to a non-diffusible pathway, could lead to effective redistribution, even of the non-diffusible complexes and hence provide a completely different spatial signalling profile. This reveals another facet of the coupling between pathways through shared components. Our framework and analysis is relevant in a range of cellular settings. The activating of elements involved in controlling multiple pathways is observed in different settings, especially for proteins which interact promiscuously with a range of downstream targets (eg. Cyclin-dependent kinases (Bloom and Cross, 2007) and ubiquitin ligases (Peters, 2006)). A special case is that of protein which interacts with different isoforms of downstream proteins. One example of an effect similar to the response we have analyzed here occurs with anaphase promoting complex (APC)–mediated ubiquitination of cyclin A, securin and geminin: securin and geminin are ubiquitinated, and thus degraded, earlier than cyclin A (Rape et al., 2006). Further, the presence of securin and geminin delays the ubiquitination of cyclin A. Other examples include the multiple GEFs (Guanine Exchange Factors) which target RhoGTPases. Our analysis of the is also relevant to competitive exclusive binding of multiple ligands to the same receptor, and is of special interest when the binding of each ligand triggers opposite responses (for e.g. CAMP and 8-CPT CAMP to CAR1 receptors in Dictyostelium [42]).

In the case of the two separate components being modulated together, our framework provides insight into how different elements are targeted by multiple pathways, and how cells may have evolved strategies to reinforce or minimize the concurrence of signals. The presence of a host of additional proteins providing combinatorial control and selective tuning of individual pathways is a key aspect to be investigated to understand signal processing through classes of hub proteins, and is also likely to be highly relevant to selective targeting

of pathways intended as drug targets. Our analysis is also relevant to the assessment of the deleterious effects of increased gene dosage (suggested to be the result of the promiscuous interaction of certain proteins, which is suppressed at low copy numbers) as well as their mitigation by selective degradation of unbound proteins which are also promiscuous (Oberdorf and Kortemme, 2009; Vavouri et al., 2009; Veitia et al., 2008).

The spatial aspect of signalling we have considered here is relevant to enzyme regulation of multiple components, all or some of which may shuttle between different compartments (for eg. membrane, cytosol, nucleus, ER) as well as the enzyme regulation of multiple components, some of which may be highly diffusible (eg. cGMP). Likewise the localized sequestration is observed when certain enzymes which are otherwise freely mobile, partially bind to anchor proteins at specific regions on the cell membrane or elsewhere in the cell. An example of this is the case of PKA which may be partially anchored in certain regions by suitable anchor proteins. Analogues of these spatial effects at the tissue level also exist. In developing Drosophila embryos it has been suggested that substrate competition for MAPK (itself present in a spatial pattern) coordinates the anterior and terminal patterning systems (Kim et al., 2010).

The presence of a common element between two pathways can serve to couple them. If the signal transduction in either or both pathways is highly non-linear, this can lead to a significant interference between the signal processing and distortion as a result. In which situations this actually happens due to the natural wiring of the cell, and under which conditions this is effectively minimized, is a topic which needs much more thorough investigation. It will be of interest to see how shared components may affect the interaction of other modules (e.g. (Seaton and Krishnan, 2011b)) and this is something which will be examined in the future.

Our results and insights have been obtained in a general setting, and thus we expect that many of these insights to be relevant of a wide range of systems. Using this framework, it is possible to build additional features like multiple-component signalling, combined converging and diverging signals as well as coupling of more complex downstream processes. Additionally, the analysis here provides insight into understanding to what extent control or temporal modulation of upstream signals may be propagated through multiple pathways and how this affects the manner in which pathways interact with one another. It is worth pointing out that the analysis here is relevant not only to natural signalling circuits but to synthetic circuits as well. In synthetic circuits a major challenge is to how a synthetically constructed circuit may interact with the host cell. One of the most basic interactions is the

possibility of components in the synthetic circuit being also involved in other pathways in the host cell.

The network structure which embodies the diverging/converging pathways we have studied is ubiquitously observed. By examining the signal processing in this "splitter" or "converger" element from a systems perspective we can examine how such elements may be interfaced with other signal transduction elements both upstream and downstream. This will be invaluable both in understanding complex dynamics and control regulation and coupling of signalling in systems biology, but also be vital for starting to build synthetic circuits which usefully and optimally channelize signals for a range of purposes.

Chapter 4

Effects of multiple enzyme-substrate interactions in basic units of cellular signal processing

4.1 Introduction

Cellular signalling networks are responsible for coordinating a cell's response to internal and external perturbations. In order to do this, these networks make use of a wide variety of molecular mechanisms, including allostery, gene regulation, and post-translational modifications. Post-translational modifications are ubiquitous in signalling networks, and are frequently viewed as basic units of signal transduction, in which activated enzymes provide a signal to downstream substrates through their catalytic activity. The basic signalling system which we consider here involves signal activating an enzyme which in turn modifies its substrate.

The essential signalling interaction in this system involves the interaction of the active enzyme with the unmodified substrate, since it is this interaction which allows catalysis to take place. Similar signalling cascades have been the subject of much experimental and theoretical investigation Ferrell (1996); Goldbeter and Koshland (1981); Huang and Ferrell (1996); Kholodenko (2000); Salazar and Hofer (2006), and it has been demonstrated that these systems are capable of producing switch-like responses, amongst other things. Furthermore, recent investigations have demonstrated some of the ways in which uptake of enzyme by substrate can significantly modulate the behaviour of these signalling networks

Ciliberto et al. (2007); Kim and Ferrell (2007); Kim et al. (2010); Rape et al. (2006); Seaton and Krishnan (2011b); Vecchio et al. (2008). In these cases, the affinities and abundances of the signalling components are such that interesting signalling behaviours arise from the details of the enzyme-substrate interactions. There is huge diversity in the patterns of enzyme-substrate interactions, as they often involve multiple domains and protein-protein interfaces Bhattacharyya et al. (2006); Endicott et al. (2012); Goldsmith et al. (2007), and their occurrence may be regulated by a variety of mechanisms including allostery Canals et al. (2011); Goodey and Benkovic (2008); Seco et al. (2012) and post-translational modification Chen et al. (2011); Narayanan and Jacobson (2009); Pawson and Kofler (2009). It is therefore of interest to explore in some detail how the precise nature of the rules governing the occurrence of enzyme-substrate interactions affects simple signalling systems such as the one described above. Here, we examine how some simple and biologically realistic additional enzyme-substrate interactions, beyond those typically considered, might affect signalling in this system.

The first such interaction considered is the interaction between active enzyme and modified substrate. This corresponds to product inhibition, as is commonly seen in enzymes involved in metabolism. Some signalling enzymes involved in such interactions are Ca^{2+}/calmodulin dependent protein kinases Huynh and Pagratis (2011), kinases in the MAPK pathway Schindler et al. (2002), and protein kinase D Huynh and McKinsey (2006). In these cases, the phosphorylation of the substrate protein is not a sufficient modification to prevent binding between enzyme and substrate. Kinases are a particularly good example system for diverse protein-protein interactions because they mediate their many interactions through a variety of different domains, motifs, and scaffolds, that are located away from the interface between the active site of the enzyme and the modification site of the substrate Bhattacharyya et al. (2006); Endicott et al. (2012); Goldsmith et al. (2007).

The second additional interaction considered here is the interaction between inactive enzyme and unmodified substrate, which we term "inactive enzyme interference". This occurs when regulation of an enzyme's catalytic activity is separated from regulation of its substrate binding affinity. Some examples of such enzymes are the protein kinases Btk Lin et al. (2009), PKA Steichen et al. (2010), and JNK1β1 Figuera-Losada and LoGrasso (2012). In these cases, activation of their conserved catalytic domains takes place through phosphorylation of the activation loop. This phosphorylation allows the active site residues to adopt a catalysis-competent conformation Kornev et al. (2006); Taylor and Kornev (2011). In the kinases listed above, dephosphorylation of the activation loop leads to a

dramatic reduction in the k_{cat}, but not the K_m, of the enzyme, meaning that substrate binding can still occur. This binding may prevent the active form of the enzyme from modifying the substrate, hence "inactive enzyme interference". As with product inhibition, inactive enzyme interference can be seen as a natural consequence of the regulation of protein-protein interactions by many different binding domains and docking motifs. While the examples given for both of the additional enzyme-substrate interactions have come from one well-studied class of signalling enzymes (the protein kinases), they are likely not limited to this class, but may occur more generally when an enzyme's activity is regulated at its active site while using other protein-protein interfaces to bind substrate. We also examine a third additional interaction, between the inactive enzyme and the modified substrate.

In this work, we aim to build a predictive framework to elucidate the potential effects of additional protein-protein interactions in this basic unit of signal transduction. By including these additional interactions in our models, we are able to consider how they modify the basic nature of signal transduction - the main objective of this chapter. In addition, we are able to investigate the effects of introducing analogous additional interactions in two variations of this basic model, involving multiple modification of substrate, and scaffold-mediated modification of substrate. These are both commonly seen in signalling systems involving post-translational modifications.

4.2 Modelling and methods

In this chapter, we analyse a model of a two-stage signalling cascade in which enzyme and substrate interact in multiple ways (see Fig. 4.1 for a schematic). The basic system consists of an enzyme, A, which in its active form (denoted by A*) modifies a downstream substrate, B, producing B* (the modified form of B). The enzyme A is itself activated by an upstream signal, S, and deactivated by another protein, X. The modification of the substrate B is removed by another protein, Y. In our model, all elementary reactions are modelled by mass action kinetics, so that the effects of enzyme uptake and competitive binding are taken into account, and so that additional interactions may be unambiguously introduced. The input to this system is taken to be the total concentration of signal S, denoted $[S_T]$, while the output is taken to be the free concentration of modified substrate B*, denoted $[B^*]$. Implicit in this choice of output is the idea that the interaction of B* with other species (e.g. with Y) prevents it from participating in other processes downstream.

The additional interactions we examine are an interaction between the active enzyme,

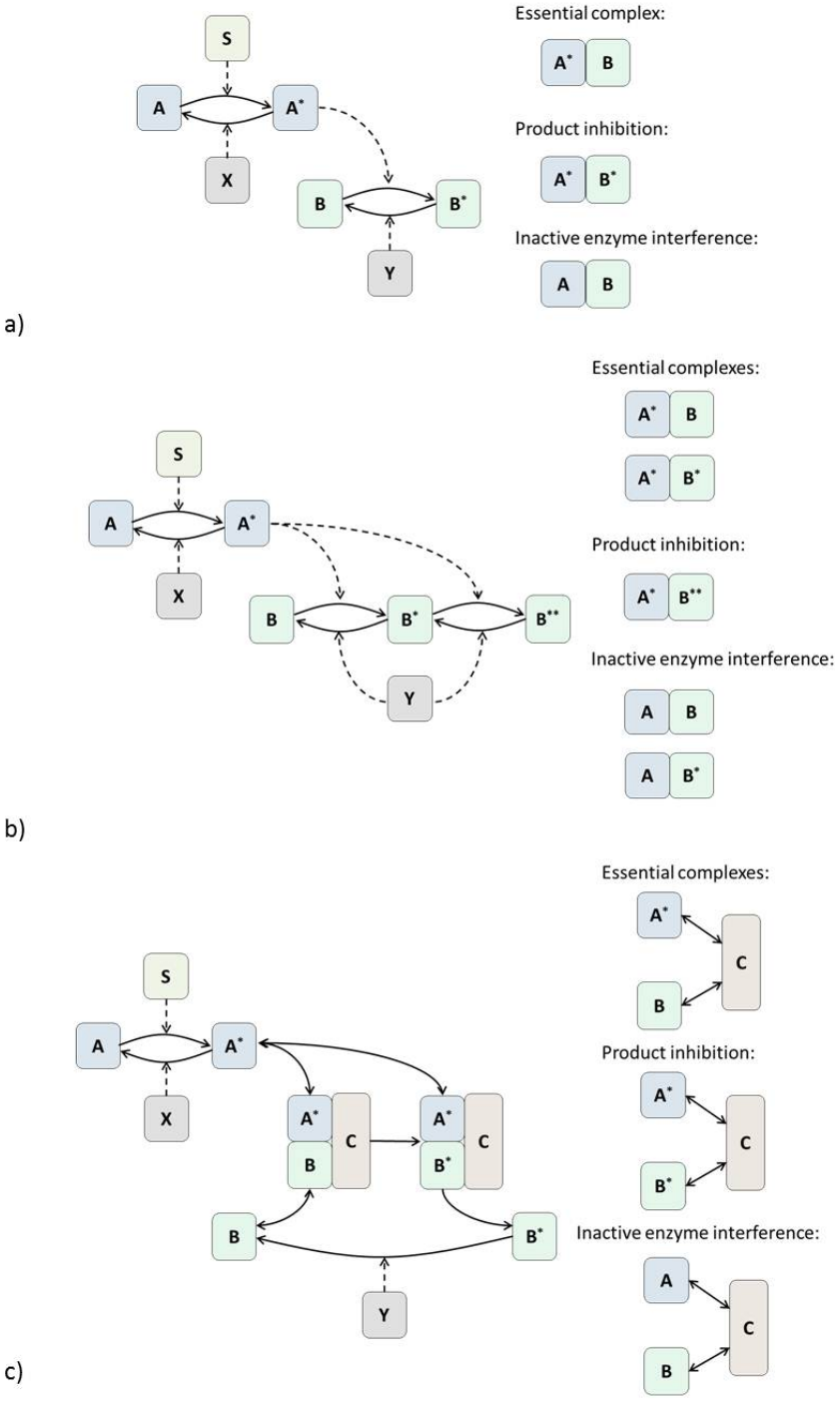

Figure 4.1: Schematics of the models analysed are shown, along with the additional interactions which occur in the cases of product inhibition and inactive enzyme interference. a) shows the basic model, in which the enzyme A is activated by the signal S, and modifies the substrate B. X and Y reverse the activation of A and the modification of B, respectively. b) shows the double modification model, in which an additional reaction occurs to modify B again after its first modification. c) shows the scaffold model, in which the interaction between A and B is mediated by the scaffold, C.

A*, and the modified substrate, B* (this is the case of product inhibition), and an interaction between the inactive enzyme, A, and the unmodified substrate, B (this is the case of inactive enzyme interference). We also briefly examine the effects of another interaction, between A and B*. There are many other interactions which may be thought to occur but which, for the purposes of simplicity, we exclude from occurring. These include, for example, the binding of X and Y to their products, A and B, respectively, and the formation of ternary complexes. An example of a ternary complex would be a complex containing S, A, and B, and not allowing this complex to form means that an inactive enzyme cannot be activated once it is bound to the substrate.

The first model we consider is a mass action model of the basic, two-stage signalling cascade with the additional interactions described above. The model equations below describe the concentration dynamics of all species (active and inactive forms), and their complexes, with mass action kinetics. The equations for the basic model are:

$$
\begin{aligned}
d[S]/dt &= (k_{1r}+k_2)[SA] - k_{1f}[S][A] \\
d[A]/dt &= k_{1r}[SA] - k_{1f}[S][A] + k_4[XA^*] - k_{10f}[A][B] + k_{10r}[AB] \\
&\quad -k_{11f}[A][B^*] + k_{11r}[AB^*] \\
d[A^*]/dt &= k_2[SA] - k_{3f}[X][A^*] + k_{3r}[XA^*] - k_{7f}[A^*][B] + k_{7r}[A^*B] \\
&\quad +k_8[A^*B] - (k_{9f}[A^*][B^*] - k_{9r}[A^*B^*]) \\
d[B]/dt &= k_6[YB^*] - k_{7f}[A^*][B] + k_{7r}[A^*B] - k_{10f}[A][B] + k_{10r}[AB] \\
d[B^*]/dt &= k_8[A^*B] - k_{5f}[Y][B^*] + k_{5r}[YB^*] - k_{9f}[A^*][B^*] + k_{9r}[A^*B^*] \\
&\quad -k_{11f}[A][B^*] + k_{11r}[AB^*] \\
d[X]/dt &= (k_{3r}+k_4)[XA^*] - k_{3f}[X][A^*] \\
d[Y]/dt &= (k_{5r}+k_6)[YB^*] - k_{5f}[Y][B^*] \\
d[SA]/dt &= k_{1f}[S][A] - (k_{1r}+k_2)[SA] \\
d[XA^*]/dt &= k_{3f}[X][A^*] - (k_{3r}+k_4)[XA^*] \\
d[YB^*]/dt &= k_{5f}[Y][B^*] - (k_{5r}+k_6)[YB^*] \\
d[A^*B]/dt &= k_{7f}[A^*][B] - (k_{7r}+k_8)[A^*B] \\
d[A^*B^*]/dt &= k_{9f}[A^*][B^*] - k_{9r}[A^*B^*] \\
d[AB]/dt &= k_{10f}[A][B] - k_{10r}[AB] \\
d[AB^*]/dt &= k_{11f}[A][B^*] - k_{11r}[AB^*] \qquad (4.1)
\end{aligned}
$$

The dynamics of the additional interactions are seen in the kinetics of the formation of the complexes A*B* (product inhibition), AB (inactive enzyme interference), and AB* (inactive enzyme and modified substrate) in the final three equations. Our goal will be to examine the effects of these interactions on the the dynamics of the system. This will be done by focussing first on the effects of these additional interactions in isolation from one another (by setting the rate constants controlling the other interactions to zero). Subsequently, we will study the combined effects of these interactions.

In order to extend the scope of our investigation, and examine the generality of our results, we also consider two variations of the basic model described above. The first variation of the model involves situation where the enzyme leads to the double modification of the substrate, B, producing the modified forms B* and B**. Multiple modification of a sub-

strate by a single enzyme is seen in many contexts, such as phosphorylation Cohen (2000) and ubiquitylation Sun and Chen (2004). Depending on the details of the mechanism and reaction kinetics, these systems may be capable of ultrasensitivity Gunawardena (2005) and multistability Thomson and Gunawardena (2009), and may be useful for regulating the timing of events K et al. (2010); Salazar et al. (2010); Seaton and Krishnan (2011b). The model we use is similar to the basic model, but with an additional reaction from B* to B**. This reaction is catalysed by A*, while the reverse reaction is catalysed by Y. This model corresponds to a sequential and distributive model of multisite modification of substrate, as has been studied in the case of protein phosphorylation Gunawardena (2005); Thomson and Gunawardena (2009). "Distributive" means that each distinct modification requires a distinct enzyme binding event, as opposed to a "processive" mechanism in which multiple modifications can take place during a single enzyme binding event. "Sequential" means that the modifications occur in a particular order, with modification at the first site necessary before modification at the second site can take place. While more complex examples of the multiple modification of proteins exist, this model captures some of the essential features of these cases. The mass action model of this scenario is obtained from a kinetic description of all the elementary steps similar to the previous case and is given below.

$$
\begin{aligned}
d[S]/dt &= (k_{1r}+k_2)[SA] - k_{1f}[S][A] \\
d[A]/dt &= k_4[XA^*] - k_{1f}[S][A] + k_{1r}[SA] - k_{10f}[A][B] + k_{10r}[AB]) \\
&\quad -k_{10f}[A][B^*] + k_{10r}[AB^*] - k_{11r}[AB^{**}] + k_{11f}[A][B^{**}] \\
d[A^*]/dt &= k_2[SA] - k_{3f}[X][A^*] + k_{3r}[XA^*] - k_{7f}[A^*][B] + k_{7r}[A^*B] \\
&\quad +k_8[A^*B] - k_{9f}[A^*][B^*] + k_{9r}[A^*][B^*] \\
d[B]/dt &= k_6[YB^*] - k_{7f}[A^*][B] + k_{7r}[A^*B] - k_{10f}[A][B] + k_{10r}[AB] \\
d[B^*]/dt &= k_8[A^*B] - k_{5f}[Y][B^*] + k_{5r}[YB^*] - k_{9f}[A^*][B^*] + k_{9r}[A^*][B^*] \\
&\quad -k_{10f}[A][B^*] + k_{10r}[AB^*] \\
d[B^{**}]/dt &= k_8[A^*B^*] - k_{5f}[Y][B^{**}] + k_{5r}[YB^{**}] - k_{9f}[A^*][B^{**}] + k_{9r}[A^*][B^{**}] \\
&\quad -k_{11f}[A][B^{**}] + k_{11r}[AB^{**}] \\
d[X]/dt &= (k_{3r}+k_4)[XA^*] - k_{3f}[X][A^*] \\
d[Y]/dt &= (k_{5r}+k_6)[YB^*] - k_{5f}[Y][B^*] + (k_{5r}+k_6)[YB^{**}] - k_{5f}[Y][B^{**}] \\
d[SA]/dt &= k_{1f}[S][A] - (k_{1r}+k_2)[SA] \\
d[XA^*]/dt &= k_{3f}[X][A^*] - (k_{3r}+k_4)[XA^*] \\
d[YB^*]/dt &= k_{5f}[Y][B^*] - (k_{5r}+k_6)[YB^*] \\
d[YB^{**}]/dt &= k_{5f}[Y][B^{**}] - (k_{5r}+k_6)[YB^{**}] \\
d[A^*B]/dt &= k_{7f}[A^*][B] - (k_{7r}+k_8)[A^*B] \\
d[A^*B^*]/dt &= k_{7f}[A^*][B^*] - (k_{7r}+k_8)[A^*B^*] \\
d[A^*B^{**}]/dt &= k_{9f}[A^*][B^{**}] - k_{9r}[A^*][B^{**}] \\
d[AB]/dt &= k_{10f}[A][B] - k_{10r}[AB] \\
d[AB^*]/dt &= k_{10f}[A][B^*] - k_{10r}[AB^*] \\
d[AB^{**}]/dt &= k_{11f}[A][B^{**}] - k_{11r}[AB^{**}]
\end{aligned}
\tag{4.2}
$$

The introduction of an additional modification step leads to several new species, corresponding to B^{**} and the complexes it forms. The additional interactions which we examine in this case correspond to product inhibition and inactive enzyme interference. The interaction between the active enzyme, A*, and the doubly modified substrate, B**, corresponds to product inhibition (note that A* already interacts with B* in order to convert it to B**),

and the dynamics of this interaction are seen in the kinetics of the formation of the complex A^*B^{**}. The interaction between inactive enzyme, A, and either the unmodified or singly modified substrate (B and B^*), corresponds to inactive enzyme interference, resulting in the complexes AB and AB^*. We also include the interaction between inactive enzyme and double modified substrate. It should be noted that in our model we do not incorporate potentially different binding sites for multiple modifications.

The second variation of the model involves the scaffold-mediated modification of B by A*. Scaffolds are ubiquitous in cell signalling - they provide a structure for both substrate and enzyme to bind to through the interaction of scaffold domains with binding domains present on the substrate and enzyme. These binding domains are typically distinct from both the substrate domain to be modified and the enzyme domain responsible for its enzymatic activity. In our model, the reactions which occur are the same, but a scaffold, C, is required to bind to the active enzyme, A^*, and the unmodified substrate, B, in order for the modification of B to occur. The binding of A^* and B to the scaffold are assumed to be independent of one another i.e. there is no allostery or cooperative binding present.

We consider this model to be the simplest model that captures the essential characteristics of scaffold-mediated signalling signalling, similar to a recent investigation Yang and Hlavacek (2011). Other possible models of scaffold signalling might involve cooperative binding, or have more species involved, as in the yeast pheromone sensing pathway in which three species bind to the scaffold Chapman and Asthagiri (2009); Good et al. (2011); Levchenko et al. (2000); Locasale et al. (2007); Thalhauser and Komarova (2010). In constructing each of these models, assumptions must be made concerning issues such as whether enzyme being bound to the scaffold prevents its deactivation, or whether substrate binding prevents removal of its modifications. The range of models of scaffolding highlights the potential complexity of the protein-protein interactions. Given these factors, and keeping the focus on the main issue of interest, we make use of what we consider to be the simplest model that captures the essential characteristics of scaffold-mediated signalling. The ODE model is developed in an analogous way to the previous models, and the equations are given below.

$$
\begin{aligned}
d[S]/dt &= (k1r + k_2)[SA] - k_{1f}[S][A] \\
d[A]/dt &= k_4[XA^*] - k_{1f}[S][A] + k1r[SA]) - k_{10f}[A][C] + k_{10r}[AC] \\
&\quad -k_{10f}[A][B^*C] + k_{10r}[AB^*C] - k_{10f}[A][BC] + k_{10r}[ABC]) \\
d[A^*]/dt &= k_2[SA] - k_{3f}[X][A^*] + k_{3r}[XA^*] - k_{7f}[A^*][C] + k_{7r}[A^*C]) \\
&\quad -k_{7f}[A^*][B^*C] + k_{7r}[A^*B^*C] - (k_{7f}[A^*][BC] + k_{7r}[A^*BC] \\
d[B]/dt &= k_6[YB^*] - k_{8f}[B][C] + k_{8r}[BC] - k_{8f}[B][A^*C] + k_{8r}[A^*BC]) \\
&\quad -k_{8f}[B][AC] + k_{8r}[ABC] \\
d[B^*]/dt &= k_{5r}[YB^*] - k_{5f}[Y][B^*] - k_{9f}[B^*][C] + k_{9r}[B^*C] \\
&\quad -k_{9f}[B^*][A^*C] + k_{9r}[A^*B^*C] - k_{9f}[B^*][AC] + k_{9r}[AB^*C] \\
d[X]/dt &= (k_{3r} + k_4)[XA^*] - k_{3f}[X][A^*] \\
d[Y]/dt &= (k_{5r} + k_6)[YB^*] - k_{5f}[Y][B^*] \\
d[SA]/dt &= k_{1f}[S][A] - (k1r + k_2)[SA] \\
d[XA^*]/dt &= k_{3f}[X][A^*] - (k_{3r} + k_4)[XA^*] \\
d[YB^*]/dt &= k_{5f}[Y][B^*] - (k_{5r} + k_6)[YB^*] \\
d[C]/dt &= k_{7r}[A^*C] - k_{7f}[A^*][C] - k_{10f}[A][C] \\
&\quad +k_{10r}[AC] - k_{8f}[B][C] + k_{8r}[BC] \\
&\quad -k_{9f}[B^*][C] + k_{9r}[B^*C]) \\
d[A^*C]/dt &= k_{7f}[A^*][C] - k_{7r}[A^*C] - k_{8f}[B][A^*C] \\
&\quad +k_{8r}[A^*BC] - k_{9f}[B^*][A^*C] + k_{9r}[A^*B^*C]) \\
d[AC]/dt &= k_{10f}[A][C] - k_{10r}[AC] - k_{8f}[B][AC] \\
&\quad +k_{8r}[ABC] - k_{9f}[B^*][AC] + k_{9r}[AB^*C] \\
d[B^*C]/dt &= k_{9f}[B^*][C] - k_{9r}[B^*C] - k_{7f}[A^*][B^*C] + k_{7r}[A^*B^*C] \\
&\quad -k_{10f}[A][B^*C] + k_{10r}[AB^*C] \\
d[BC]/dt &= k_{8f}[B][C] - k_{8r}[BC] - k_{7f}[A^*][BC] + k_{7r}[A^*BC] \\
&\quad -k_{10f}[A][BC] + k_{10r}[ABC] \\
d[A^*B^*C]/dt &= k_{7f}[A^*][B^*C] - k_{7r}[A^*B^*C] + k_{9f}[B^*][A^*C] \\
&\quad -k_{9r}[A^*B^*C] + k_{11}[A^*BC] \\
d[AB^*C]/dt &= k_{10f}[A][B^*C] - k_{10r}[AB^*C] + k_{9f}[B^*][AC] - k_{9r}[AB^*C] \\
d[A^*BC]/dt &= k_{7f}[A^*][BC] - k_{7r}[A^*BC] + k_{8f}[B][A^*C] - k_{8r}[A^*BC] \\
&\quad -k_{11}[A^*BC] \\
d[ABC]/dt &= k_{10f}[A][BC] - k_{10r}[ABC] + k_{8f}[B][AC] - k_{8r}[ABC]
\end{aligned}
\tag{4.3}
$$

In contrast to a model in which cooperative binding occurs, the dynamics of association of the scaffold with a particular species are described with the same kinetics regardless of the state of the scaffold. So, for example, the active enzyme, A^*, binds to C,BC, and B^*C with identical kinetics. Again, interactions which are analogous to product inhibition and inactive enzyme interference are included in this model, but they occur through the binding of species to the scaffold. In particular, product inhibition is the result of B* binding to C, while inactive enzyme interference is the result of A binding to C. Again, there are additional complexes which might form in some situations but which we do not consider in this model (e.g. ternary complexes between S, A, and C, or between C, B, and Y). Therefore the model does not allow A to be activated, A^* to be deactivated, or B^* to be demodified while they are bound to the scaffold.

We now comment on the choice of parameters and initial conditions (which set the total quantities of all species), and the way in which we investigate the models. We make use of two sets of parameters and initial conditions: a "basal" set of parameters, which is used for most simulations, and an "alternative" set of parameters, which is used to help establish the generality of our conclusions. The basal set of parameters corresponds to an enzymatic cascade in which the enzymes X and Y are acting relatively close to saturation (as in Goldbeter and Koshland (1981)), and in which the interaction between A^* and B is relatively high affinity (see below). These parameters give a more-or-less switch-like input-output response at steady state similar to that seen in many contexts (e.g. the MAPK cascade Ferrell (1996)). In contrast, the alternative parameter set corresponds to a cascade in which both X and Y are unsaturated. This parameter set gives a graded response at steady state, rather than a switch-like response. The affinities and concentrations used in the model are appropriately scaled to one another and are therefore dimensionless.

In both sets of parameters, the affinity of the essential interaction (between A* and B) is the same (with a dissociation constant $K_d = 0.1$), as are the total concentrations of A and B ($[A_T] = 3$, $[B_T] = 1$). These concentrations and affinities correspond to a scenario in which the ratios of enzyme and substrate concentrations to the dissociation constant (i.e. $[A_T]/K_d$ and $[B_T]/K_d$) are of order 10. For signalling cascades with concentrations of components in the 100 nM to 1 μM range (as is typical in such systems Chung et al. (2011); O'Shaughnessy et al. (2011)), this corresponds to K_ds in the 10 to 100 nM range. A wide variety of parameters have been used in similar models in the literature Ferrell (1996); Levchenko et al. (2000); O'Shaughnessy et al. (2011), and examples of models with similarly high affinity interactions are found in Kholodenko et al. (2010);

Kim and Ferrell (2007); Markevich et al. (2004); Thalhauser and Komarova (2010). While many experimentally determined enzyme-substrate signalling interactions have K_d in the μM range, examples of signalling enzyme-substrate interactions with affinities in the nM range are also readily available Bae et al. (2009); Bardwell et al. (1996); Huynh et al. (2009). High affinity interactions have also been noted between enzyme-substrate docking domains Gordus et al. (2009); Jones et al. (2006); Kohn et al. (2007); Lee et al. (2010); Wolf-Yadlin et al. (2009). We note that the model parameters chosen could also be relevant to enzyme-substrate interactions with a K_d in the μM range in cases where the local concentrations have been increased to the μM range through compartmentalisation effects or similar effects. In order to establish the generality of the conclusions reached, simulations in different ranges of concentrations and affinities are performed, and we show some mathematical analysis of the model under some simplifying assumptions. All simulations are performed in MATLAB, using the ode15s solver. The code used to obtain all results presented here is provided as part of the digital appendices, documented in Appendix E.0.3. Parameter values are provided with the code, and are also provided in Appendix B.

Our investigations will focus on how the additional interactions considered affect the signal processing properties of these systems. This will be done, to start with, by analysing the effects of each additional interaction in isolation. Thus the basal parameter set will be kept fixed, and the parameter determining the strength of the additional interaction under consideration will be varied, with the other additional interactions not occurring. The strengths of the interactions are varied within a range from zero (no additional interaction) to the strength of the interaction between A* for B (the essential interaction). This approach allows the elucidation of the effects of the additional interaction. Once the effects of these interactions have been studied separately, the combined effects of the extra interactions are also investigated. For completeness, in the basic model we examine the effect of these interactions together alongside a further interaction involving inactive enzyme binding to active substrate.

4.3 Results

We present the results as follows. We start with the basic model, and examine the roles of product inhibition and inactive enzyme interference in isolation from one another. We examine both steady state and dynamic behaviour. We then examine the combined effects of these interactions. We also examine the interaction between the inactive enzyme and

modified substrate. Subsequently, we examine the role of additional interactions in variations of our basic model. The results we present are based on simulation and analysis of the models.

4.3.1 Product Inhibition

Steady state response

We begin with the case of product inhibition. As mentioned, we regard the total signal concentration, $[S_T]$, as the input and the concentration of free modified substrate, $[B^*]$, as the output. In the case of product inhibition, we observe that at steady state there is a biphasic response to the signal - the output initially increases with the input signal and reaches a maximum, before decreasing to a steady value above zero (see Fig. 4.2). This is in contrast to the monotonic response observed without product inhibition. A similar change in behaviour as a result of product inhibition is observed with the alternative parameter set (see Fig. 4.3). Biphasic behaviour has previously been identified in systems containing incoherent feedforward loops Kaplan et al. (2008); Kim et al. (2008). It is interesting that in this case there is no explicit incoherent feedforward loop - the behaviour is the result of the combination of the essential catalytic interaction between A* and B, and the product inhibition of A* by B*. With these two interactions present, a change occurs in the primary role of the activated enzyme, A*, as signal levels increase. At low signalling levels, A* is primarily involved in the modification of B, while at high signalling levels it is primarily involved in uptake of B*. At low $[S_T]$, both $[A^*]$ and $[B]$ are low, so changes in $[A^*]$ primarily result in increasing $[B^*]$ through formation of the catalysis-competent complex A*B. This is illustrated by the initial increase in $[A^*B]$ with $[S_T]$ in Fig. 4.2. Product inhibition is not important at low $[S_T]$, since both $[A^*]$ and $[B^*]$ are low. As $[S_T]$ increases, however, A*B levels saturate, and A* begins to uptake significant quantities of B*. This is seen by the increase in $[A^*B^*]$ with $[S_T]$ at higher signal levels in Fig. 4.2b). Under these conditions, changes in A* primarily result in reducing the free B* available to act as output, rather than generating more B*. The result is a decrease in $[B^*]$, and a biphasic response. Of course, if the complex A*B*, rather than only free B*, is able to contribute to the output, the effect of B* uptake on the output is lost (results not shown). We note that in Salazar and Hofer (2006), all forms of modified substrate (A*B*, B*, and YB*) are used together as output. While this may be the relevant variable in some situations, we argue

that the free concentration is the most natural output variable (a similar choice was made in Buchler and Louis (2008)).

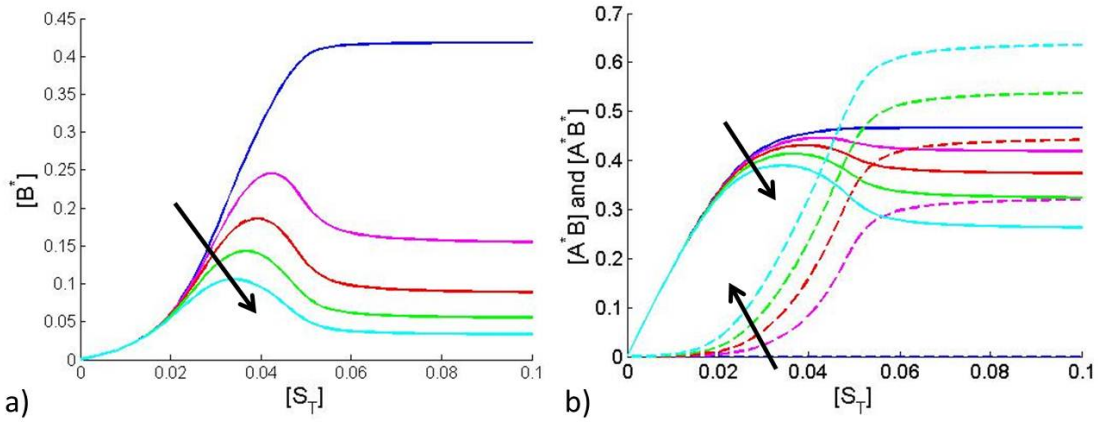

Figure 4.2: The modified behaviour of the pathway in the presence of product inhibition is shown. a) shows the steady-state input-output response curve of the concentration of free modified substrate, B*, to the total concentration of signal, S, for five different strengths of product inhibition (ranging from zero to the strength of the essential interaction between A* and B). b) shows how the quantity of A*B (solid lines) and A*B* (dashed lines) change with the signal, demonstrating the switch in the primary role of A* with increasing levels of S. Increasing strength of product inhibition (i.e. increasing k_{9f}) is indicated by the black arrows.

We can further demonstrate how the behaviour observed in simulations can be understood through analysis of the model. We note at the outset that the model has a relatively large number of parameters and is rather cumbersome to analyse, and therefore we will make appropriate simplifications to demonstrate the results and analyse the origin of the particular behaviour. We thus aim to obtain transparency in the analysis in each case, rather than an overall exhaustive study of the model.

We will focus on the steady state. A basic analysis of the model equations for the complexes AS, XA^* and YB^* (see Eq. 4.1), incorporating the conservation of total S, X and Y results in:

$$\begin{aligned}
[SA] &= \frac{k_{1f}[A]}{k_{1r}+k_2}.\frac{[S_T]}{1+k_{1f}[A]/(k_{1r}+k_2)} \\
[XA^*] &= \frac{k_{3f}[A^*]}{(k_{3r}+k_4)}.\frac{[X_T]}{1+k_{3f}[A^*]/(k_{3r}+k_4)} \\
[YB^*] &= \frac{k_{5f}[B]}{(k_{5r}+k_6)}.\frac{[Y_T]}{1+k_{5f}[B^*]/(k_{5r}+k_6)}
\end{aligned} \tag{4.4}$$

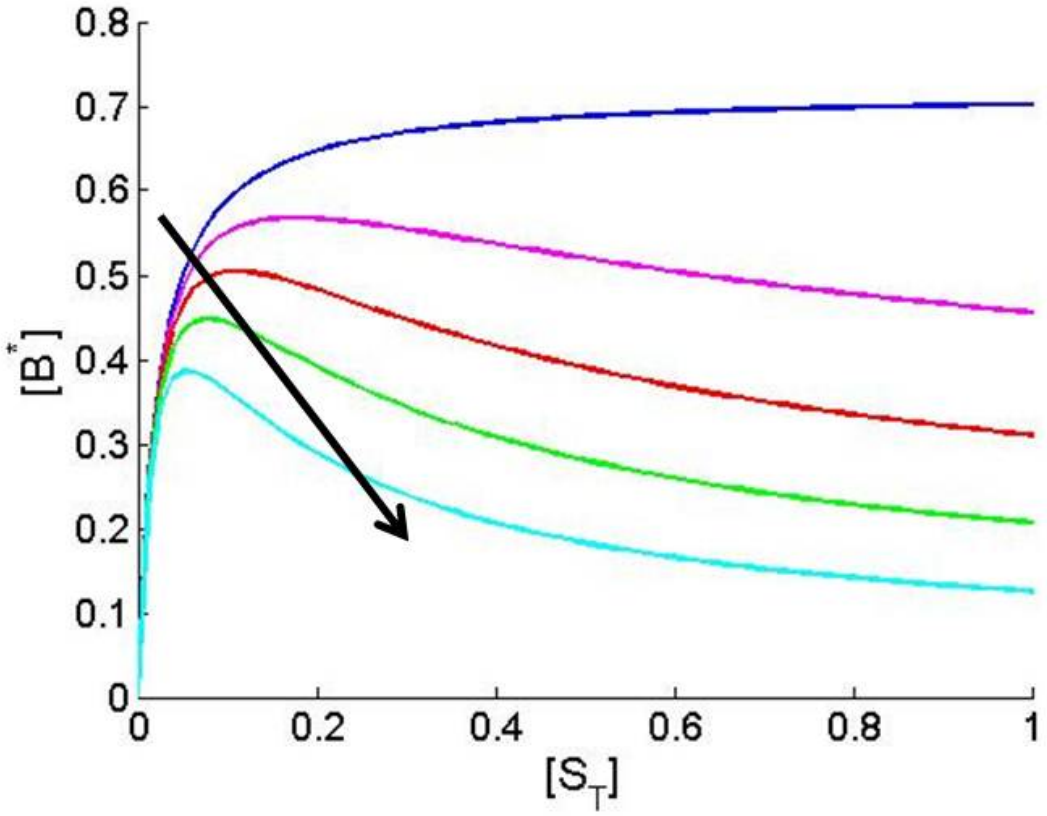

Figure 4.3: The response to different strengths of product inhibition for the basic model with the alternative parameter set is shown, demonstrating the similarity of the effects in this different parameter regime. This shows the steady-state input-output response curve of the concentration of free modified substrate, B*, to the total concentration of signal, S, for five different strengths of product inhibition (ranging from zero to the strength of the essential interaction between A* and B). Increasing strength of product inhibition (i.e. increasing k_{9f}) is indicated by the black arrows.

In all our analysis, we will assume that the concentrations of the complexes XA^* and YB^* (denoted $[XA^*]$ and $[YB^*]$ are small), for instance due to relatively large (forward) dissociation rates. This is done for simplicity and transparency. In particular, this means that practically all X and Y are present in free form. In analysing the case of product inhibition, we also consider the concentration of the complex SA (denoted $[SA]$) to be negligible, since we are interested in understanding just the interaction between A^* and B^*.

In this case the steady state equations for the network results in

$$\begin{aligned}
\frac{[A^*]}{[A]} &= \frac{k_{1f}[S_T]}{k_{3f}[X_T]} \\
[A^*B] &= \frac{k_{5f}[Y_T][B^*]}{k_8} \\
[B] &= \frac{(k_{7r}+k_8)k_{5f}[Y_T][B^*]}{[A^*]k_{7f}k_8} \\
[A^*B^*] &= \frac{k_{9f}}{k_{9r}}[A^*][B^*] \\
[A]+[A^*]+[A^*B]+[A^*B^*] &= [A_T] \\
[B]+[B^*]+[A^*B]+[A^*B^*] &= [B_T]
\end{aligned}$$

This results in the following equations:

$$\begin{aligned}
[A^*] &= \frac{[A_T]-q[B^*]}{1+k_{3f}[X_T]/(k_{1f}[S_T])+k_{9f}[B^*]/k_{9r}} \\
[B^*] &= \frac{[B_T]}{1+k_{5f}[Y_T]/k_8+k_{5f}/(k_{7f}[A^*])+k_{9f}[A^*]/k_{9r}}
\end{aligned} \tag{4.5}$$

Note that the above equation reflects two terms involving opposite effects of A^* in B^*. In the above equation $q = k_{5f}[Y_T]/k_8$. These equations can be differentiated with respect to

$[S_T]$ to yield

$$\begin{aligned}\frac{d[A^*]}{d[S_T]} &= -\frac{([A_T]-q[B^*])\left((k_{9f}/k_{9r})(d[B^*]/d[S_T])-k_{3f}/(k_{1f}[S_T]^2)\right)}{(1+k_{3f}[X_T]/(k_{1f}[S_T])+k_{9f}[B^*]/k_{9r})^2} \\ &\quad -\frac{q(d[B^*]/d[S_T])}{1+k_{3f}[X_T]/(k_{1f}[S_T])+k_{9f}[B^*]/k_{9r}} \\ \frac{d[B^*]}{d[S_T]} &= -\frac{[B_T](d[A^*]/d[S_T])\left((k_{9f}/k_{9r})-k_{5f}/(k_{7f}[A^*]^2)\right)}{(1+k_{5f}[Y_T]/k_8+k_{5f}/(k_{7f}[A^*])+k_{9f}[A^*]/k_{9r})^2}\end{aligned} \tag{4.6}$$

From the above equations, looking at the expression for $d[B^*]/d[S_T]$, we find that it can indeed become zero at some finite S, owing to the competition of the two terms in the numerator (incidentally, we notice from the above equations that $d[B^*]/d[S_T]$ cannot be zero because $d[A^*]/d[S_T]$ is zero: the equation for $d[A^*]/d[S_T]$ shows that both $d[A^*]/d[S_T]$ and $d[B^*]/d[S_T]$ cannot both be zero together. This is immediately seen by noting that $[A_T]-q[B^*]$ (the total A not in the complex AB^*) is non-zero and hence if $d[B^*]/d[S_T]=0$ then $d[A^*]/d[S_T]$ is non-zero. Thus we see that the response $[B^*]$ can indeed exhibit a biphasic response to $[S_T]$ while $[A^*]$ remains monophasic (at least locally in that range of signal). This response depends on some key parameters, notably the ratios k_{5f}/k_{7f} and k_{9f}/k_{9r}. We immediately see that if the A^*B^* binding is very weak, then $d[B^*]/d[S_T]$ can never become zero: this is because $[A^*]$ is bounded above by the value of $[A_T]$, and the numerator can never become zero. Thus the analysis reveals that a critical strength of binding between A^* and B^* is required for a biphasic response to occur. On the other hand if the binding reaction is extremely strong, and if the total amount of B is greater than the total amount of A, we see that all A^* is bound to B^* (this can be obtained also by an asymptotic analysis) and this prevents a biphasic response. Thus conditions which facilitate a biphasic response generally are an intermediate strength of binding of A^* and B^* and an excess of (total) A when compared to B.

We can further expand on this analysis by considering what happens to the behaviour of the system when the total quantities of enzyme and substrate (i.e. $[A_T]$ and $[B_T]$) change. Fig. 4.4 shows what happens in the case of full product inhibition (i.e. when the interaction between A* and B* is as strong as the interaction between A* and B). It is observed that, for a range of values of $[S_T]$, a biphasic response to $[A_T]$ is obtained. The same is true for the response to $[S_T]$ for a broad range of values of $[A_T]$. This is a result of the uptake of B* at high $[A_T]$ and $[S_T]$ - low levels of either result in insufficient levels of A* to significantly

uptake of B*, and so a biphasic response is not possible. This also means that the biphasic response to $[S_T]$ becomes more pronounced at high $[A_T]$, and vice versa (see Fig. 4.4).

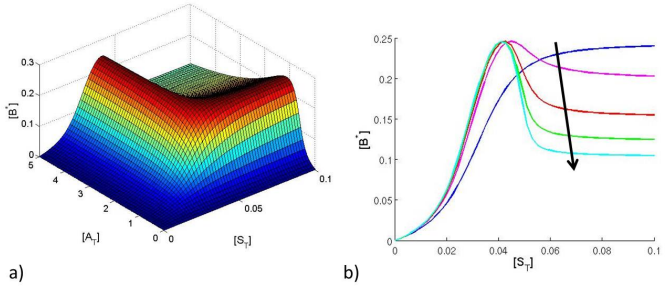

Figure 4.4: The response of the system to changes in $[A_T]$ and $[S_T]$ is shown in a). The system is capable of responding in a biphasic manner to $[A_T]$ at sufficient levels of $[S_T]$, and vice versa. b) shows how the biphasic response to $[S_T]$ becomes more pronounced at higher $[A_T]$. In b), the black arrow denotes the direction of increasing $[A_T]$.

The modulation of $[B_T]$ has less dramatic consequences on the properties of the signalling pathway, as increasing $[B_T]$ leads to a steady linear increase in the levels at all appreciable levels of $[S_T]$ (results not shown). This means that, while the biphasic behaviour is not lost at high $[B_T]$, it is relatively less pronounced since there is a fixed offset between peak $[B^*]$ and its asymptotic value. This offset is the result of the fixed quantity of A available in the system to suppress B*. Finally, as expected from the mechanism described here, we note that increasing the affinity of the essential interaction makes the biphasic response more pronounced, while it is less pronounced at lower affinities (see Fig. 4.5).

Dynamic response

In the dynamic case, a stepwise increase in signal can result in a single-pulse response which mirrors the steady state response - it first increases, before decreasing to its steady state value (see Fig. 4.6a)). Again, we can explain this by a change in the primary role of A*, from modification of B at early times, to suppressor of free B* at later times. The pulse-like behaviour is not a result of slow uptake of any component, since increasing the timescale separation between the binding interactions and the catalytic reactions produced the same results. A point worth emphasizing about the response is that its existence depends upon the size of the step change (for fixed network parameters): if the step change is insufficient to bring the system into the regime where there is sufficient A* to suppress

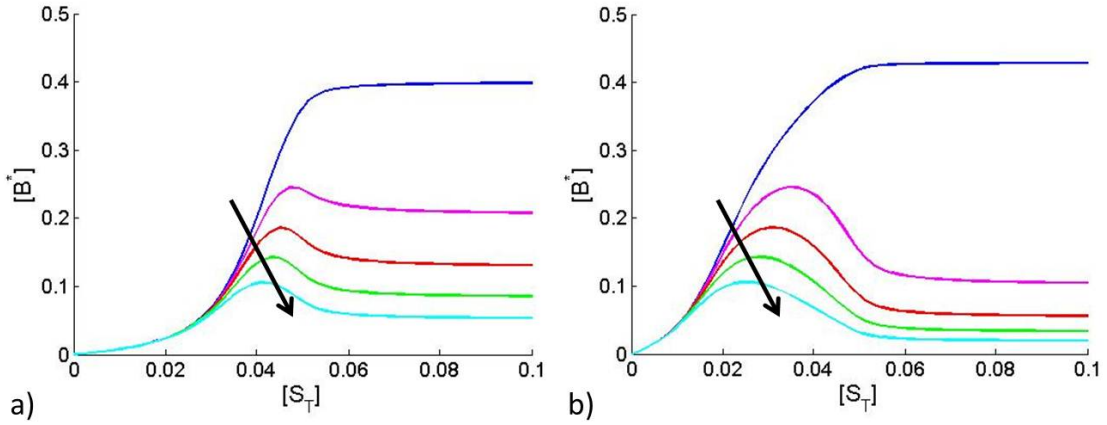

Figure 4.5: The change in behaviour induced by increasing strengths of product inhibition is shown for cases where the enzyme-substrate affinity (determined by k_{9f}) is a) half the basal value, and b) twice the basal value. There is a diminished response at lower affinities, compared to higher affinities. The range of product inhibition strengths investigated has been rescaled to vary between zero and the maximal strength of the essential interaction. Increasing strength of product inhibition (i.e. increasing k_{9f}) is indicated by the black arrows.

B*, no pulse-like behaviour is observed (see Fig. 4.6b)). This is an important difference between the behaviour observed here and similar behaviour in other systems. In particular, we note that adaptive signalling networks produce pulse-like responses to small input signals, but may saturate at high input levels Krishnan (2011). This is in contrast to the situation considered here. No active adaptive mechanism is present in the system studied here, and pulse-like responses are only observed to changes from low to high signal.

As in the steady state response, the range of accessible output values decreases with the strength of product inhibition. However, it is also clear that the peak in output is attained more rapidly in systems with product inhibition. This is because, while the upswing in B* levels is the same for different strengths of product inhibition, the suppression of free B* levels by uptake of B* occurs earlier in cases of stronger product inhibition. This is confirmed by direct comparison of the times of peak response and the size of those peaks as the strength of product inhibition is changed (see Fig. 4.6c)). Therefore, a trade-off appears to exist between the range of output values attainable by the signalling pathway and the time to the peak.

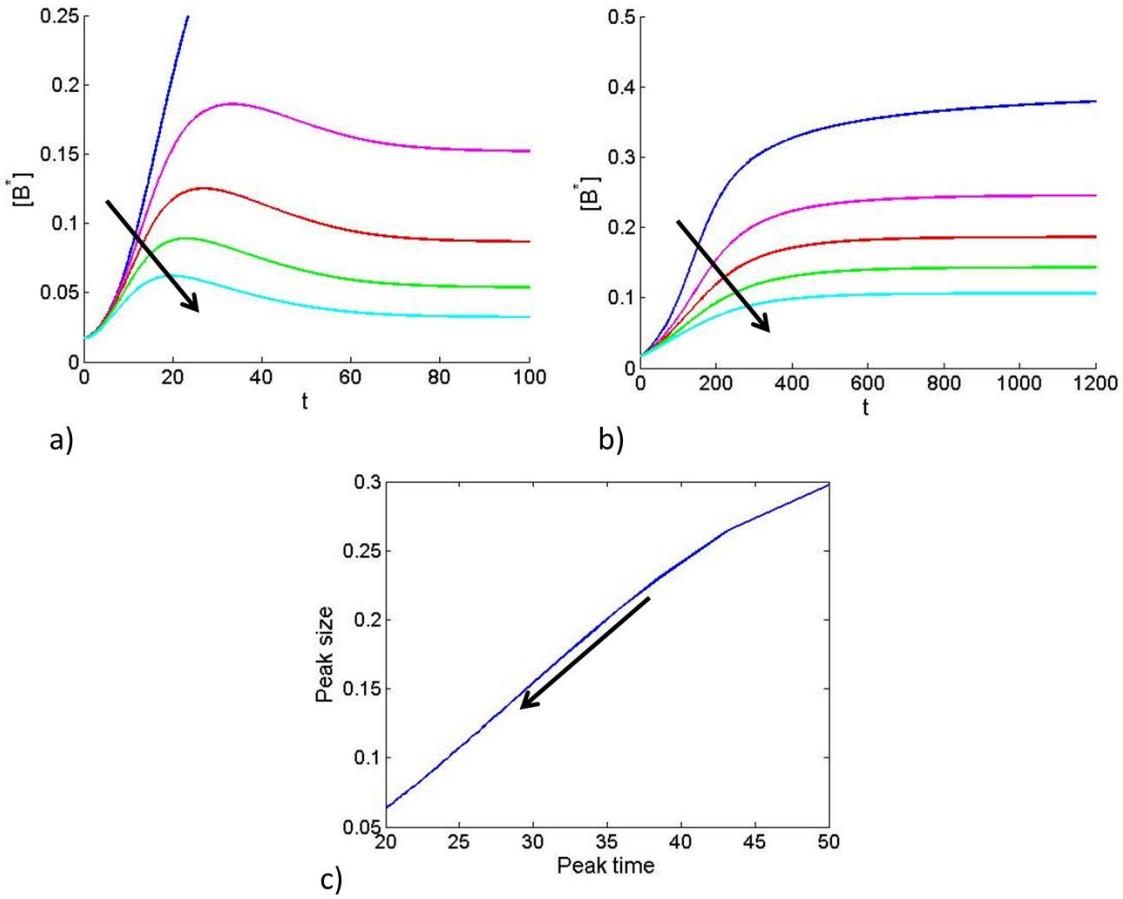

Figure 4.6: The potential dynamics of the system with product inhibition are shown. a) demonstrates the possibility of pulse-like behaviour in response to a step change in signal, while b) shows that a pulse-like response is not observed if the step change is not sufficiently large. The step changes in signal applied in b) are all significantly smaller than those applied in a). c) illustrates the trade-off between the size of the peak in the response and the speed of the response. The black arrows in a) and c) denote increasing strength of product inhibition (i.e. increasing k_{9f}), while the black arrow in b) denotes decreasing size of step change in input, $[S_T]$.

4.3.2 Inactive Enzyme Interference

Steady state response

At steady state, the qualitative "ultrasensitive" or threshold-like behaviour of the pathway is not changed by the introduction of inactive enzyme interference (see Fig. 4.7 a)). However, there is a clear change in the quantitative characteristics of the ultrasensitivity. The maximum relative sensitivity (defined by $R = d(ln[B^*])/d(ln[S_T])$) of the output to changes in input is larger, and occurs at higher input levels in the presence of inactive enzyme interference (see Fig. 4.7 b)). An increase in sensitivity is also seen using the alternative parameter set, although the response remains essentially graded in character (see Fig. 4.8). It is possible, however, to convert a graded response to an ultrasensitive response by increasing the strength of inactive enzyme interference, as shown in Fig. 4.9 for a different set of parameters (see Appendix B for parameter values). The increased sensitivity observed in these cases is a result of the signal having an additional mechanism through which it can modulate the output. This new mechanism, introduced by inactive enzyme interference, is the molecular titration of the unmodified substrate, B, by the inactive enzyme, A (the competition between A and A^* for B), since A is present at higher levels than B. Similar effects have been noted previously in other systems, notably multiphosphorylation switches Legewie et al. (2007), and genetic circuits Buchler and Cross (2009); Buchler and Louis (2008).

We can investigate the origins of this effect analytically, beginning by simplifying the model description. We expect that ultrasensitive and threshold like responses result from kinetics being far from the mass-action: in other words we would expect significant concentrations of some complexes. Thus, in this case, we do not neglect the concentration of the complex SA. We perform basic analysis in the case where the A and B binding is very strong. i.e. $k_{10r}/k_{10f} = \epsilon \ll 1$, for instance through high k_{10f}. Now since both A and B can exist under basal conditions even without any stimulus, we would expect a high degree of binding between A and B. For a fixed signal S, we can expand all variables perturbatively

in the small parameter ϵ. Thus we employ an expansion

$$\begin{aligned} [A] &= A_0 + \epsilon A_1 + ... \\ [B] &= B_0 + \epsilon B_1 + ... \\ [A^*] &= A_0^* + \epsilon A_1^* + ... \\ [B^*] &= B_0^* + \epsilon B_1^* + ... \end{aligned} \tag{4.7}$$

and similarly for other complexes. This results in the leading order behaviour for A and B governed by the equation $A_0 B_0 = 0$, where A_0, B_0 are the leading order terms in the concentrations of A and B respectively. This intuitive result simply indicates that if there is a very strong degree of binding of A and B, then for a fixed signal (or no signal) either the concentration of A or B has to be zero. In other words the species present in less total amount is completely taken up and bound to the species present in greater total amount. The concentrations of the other entities in the network can be inferred from this equation.

We are now able to examine the scenario above, in which the upstream component is present in excess concentration compared to the downstream component (i.e. $[B_T] > [A_T]$). From the perturbation analysis, we see that practically all B is bound to A, with A in excess. This now implies that the concentration of free B is $O(\epsilon)$. Now we notice from the steady state equations that

$$[A^*B] = \frac{k_{7f}}{(k_{7r} + k_8)}[A^*][B] \tag{4.8}$$

From the chain of equations above, we see that if free B is negligible, then so is $[A^*B]$ (note that A^*B is needed to produce B^*). In asymptotic terms the concentration of B at steady state is $O(\epsilon)$. The only way to produce a finite $O(1)$ level of free B (and hence response) is to increase $[A^*]$ to a high level to make it of the order of $1/\epsilon$ (note that the earlier perturbation result assumed all other rate constants rate constants and $[S_T]$ of O(1)). We see that for significant concentrations of A^*B, a high concentration of A^* is needed, which directly translates to a high degree of signal (and high availability of A). Thus we see here how a threshold emerges just due to the strong A-B interaction. Here the signal must generate enough A^* to compete with B's strong affinity for binding with A.

As before, we are able to investigate how the behaviour of this system changes when the total quantity of intermediate species available (i.e. $[A_T]$ and $[B_T]$) is altered. This allows

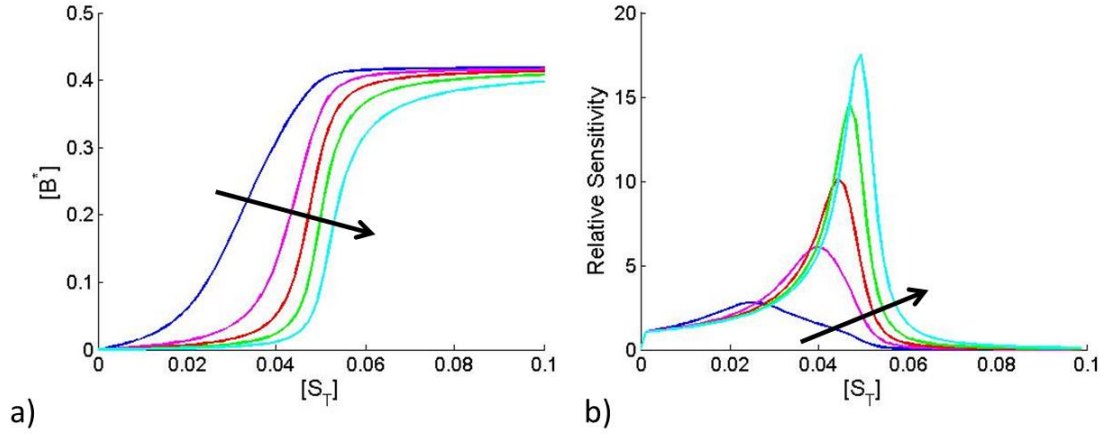

Figure 4.7: The modified behaviour of the pathway in the presence of inactive enzyme interference is shown. a) shows the steady-state input-output response curve of the concentration of free modified substrate, B*, to the total concentration of signal, S, for five different strengths of inactive enzyme interference (ranging from zero to the strength of the essential interaction between A* and B). b) shows the relative sensitivity of the output to changes in the input in the same cases, demonstrating that inactive enzyme interference leads to increased sensitivity. Increasing strength of inactive enzyme interference (i.e. increasing k_{10f}) is indicated by the black arrows.

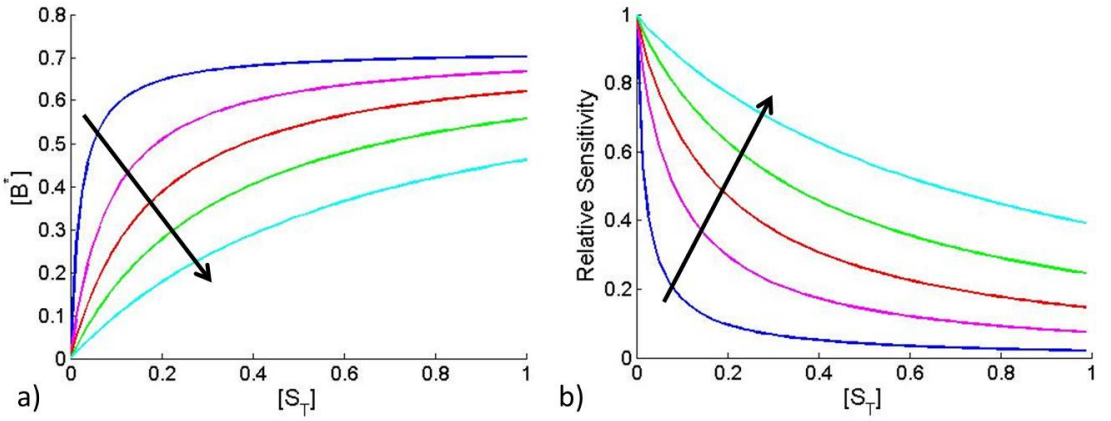

Figure 4.8: The modified behaviour of the pathway in the presence of inactive enzyme interference is shown for the alternative parameter set. a) shows the steady-state input-output response curve of the concentration of free modified substrate, B*, to the total concentration of signal, S, for five different strengths of inactive enzyme interference (ranging from zero to the strength of the essential interaction between A* and B). The qualitative graded nature of the response does not change significantly, but b) shows that relative sensitivity of the output to changes in the input is increased for cases with stronger inactive enzyme interference. Increasing strength of inactive enzyme interference (i.e. increasing k_{10f}) is indicated by the black arrows.

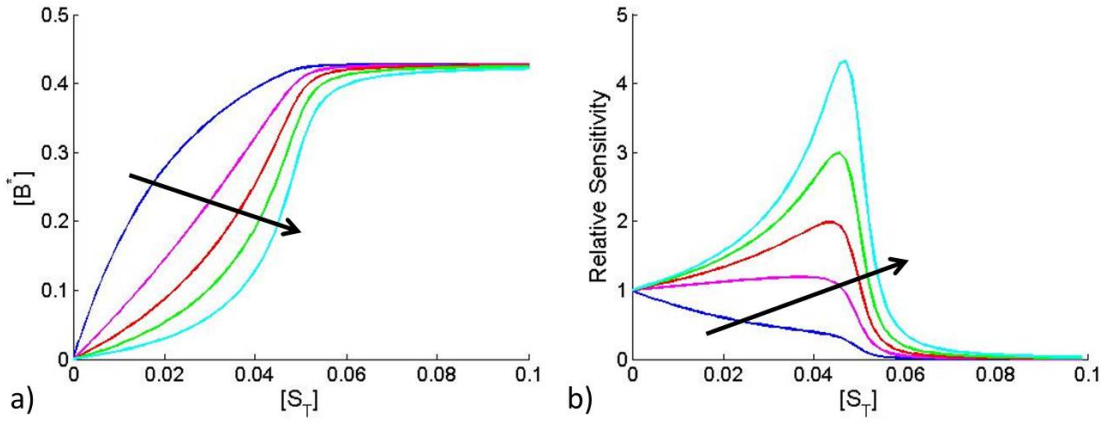

Figure 4.9: The conversion of a graded response to a threshold response by increasing the strength of inactive enzyme interference is shown. a) shows the steady-state input-output response curve of the concentration of free modified substrate, B*, to the total concentration of signal, S, for five different strengths of inactive enzyme interference (ranging from zero to the strength of the essential interaction between A* and B). It is clear that the graded response becomes increasingly switch-like with increasing strength of inactive enzyme interference. This is confirmed by b), which shows the relative sensitivity of the output to changes in the input in the same cases, demonstrating that inactive enzyme interference leads to increased sensitivity. Increasing strength of inactive enzyme interference (i.e. increasing k_{10f}) is indicated by the black arrows.

us identify mechanisms by which ultrasensitivity can arise in this system. In particular, if we consider a case in which $[A_T] < [B_T]$ (the reverse of the cases considered above, in which $[A_T] > [B_T]$), we observe a similar threshold effect and a similar increase in sensitivity with increasing strength of inactive enzyme interference (see Fig. 4.10). Since B is relatively abundant, this effect is not due to competition between A and A* for B. Instead, it is a result of competition between S and B for A. The increased sensitivity observed in free B* is therefore the result of the increased sensitivity observed in A*. A comparison of the response of A* in the two cases analysed is shown in Fig. 4.11, demonstrating very little change in $[A^*]$ with increasing strength of the additional interaction for a case where $[A_T] > [B_T]$ (Fig. 4.11a), while substantial changes in $[A^*]$, in particular increased sensitivity of the response of $[A^*]$, is observed in a case where $[B_T] > [A_T]$ (Fig. 4.11b).

Again, we are able to demonstrate the basis of this behaviour analytically. Here, with $[B_T] > [A_T]$, we find that if the A-B binding is very strong then almost all A is bound to B, leaving negligible A^* and hence negligible B^*. We notice from the steady state equations

that

$$\begin{aligned}
[SA] &= \frac{k_{1f}[A]}{k_{1r}+k_2)}\frac{[S_T]}{1+k_{1f}[A]/(k_{1r}+k_2)} \\
[A^*] &= \frac{k_2[SA]}{k_{3f}[X_T]} \\
[A^*B] &= \frac{k_{7f}}{(k_{7r}+k_8)}[A^*][B]
\end{aligned} \tag{4.9}$$

From the chain of equations above, we see that if free A is negligible, then so are $[SA]$, $[A^*]$ and $[A^*B]$ (A^*B is needed to produce B^*). In asymptotic terms the concentration of A at steady state is $O(\epsilon)$. The only way to produce a finite $O(1)$ level of free A (and hence response) is to increase $[S_T]$ to a high level to make it of the order of $1/\epsilon$ (note that the earlier perturbation result assumed all other rate constants rate constants and $[S_T]$ of O(1)). Intuitively what this says is that the extremely strong binding affinity of A with B has to be compensated by a sufficiently high level of signal to pull part of A into a complex with the stimulus and eventually convert it to A^*B and hence produce B^*. This reveals how a certain threshold of signal is needed for a non trivial response. As S becomes comparable with $1/\epsilon$ non-trivial binding of A with S is to be expected leading to non-trivial output. Thus we see here that the role of strong binding of A and B causes a threshold effect in the response, essentially through molecular titration (the essential feature is similar to the case studied in Chapter 3, with A being shared between B and S, and the non-shared component S being modulated).

Such effects, whereby the interaction of an enzyme with its substrate modulates its own pattern of activity, may be important in the coordination of signalling through different pathways when a signalling enzyme has multiple substrates Rape et al. (2006); Seaton and Krishnan (2011b). Note that the situation with $[B_T] \approx [A_T]$ results in increased sensitivity through a combination of both mechanisms considered here (results not shown).

Finally, we consider how the situation changes with different affinities of interaction between A and B. Simulations in which this affinity is halved and doubled in magnitude are shown in Fig. 4.12. This demonstrates that the change in behaviour resulting from the additional interaction is reduced when the affinity is halved, but there remains a significant effect. Further, the change in behaviour becomes more pronounced at double affinity, as expected.

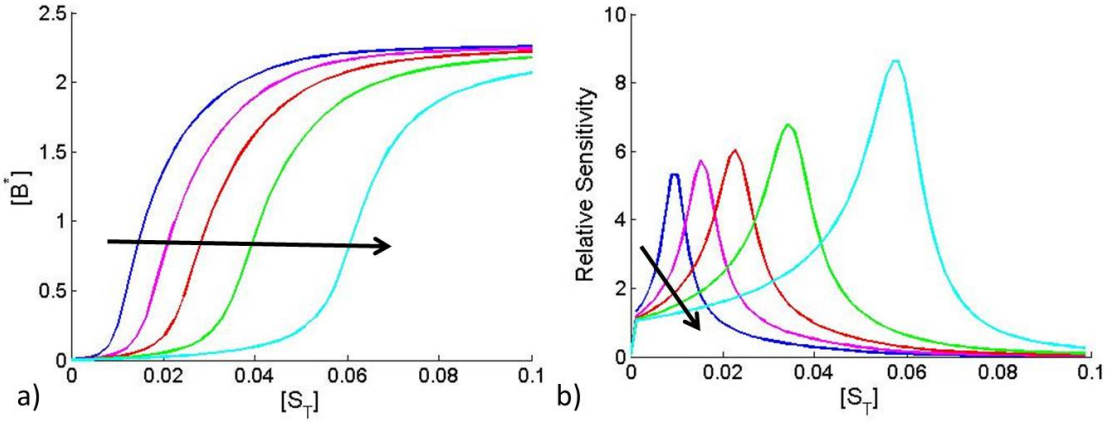

Figure 4.10: The increased sensitivity for a case in which $[B_T] > [A_T]$ is shown, demonstrating the generality of the observation. a) shows the steady-state input-output response curve of the concentration of free modified substrate, B*, to the total concentration of signal, S, for five different strengths of inactive enzyme interference(ranging from zero to the strength of the essential interaction between A* and B). b) shows the relative sensitivity of the output to changes in the input in the same cases, demonstrating that inactive enzyme interference leads to increased sensitivity. Increasing strength of inactive enzyme interference (i.e. increasing k_{10f}) is indicated by the black arrows.

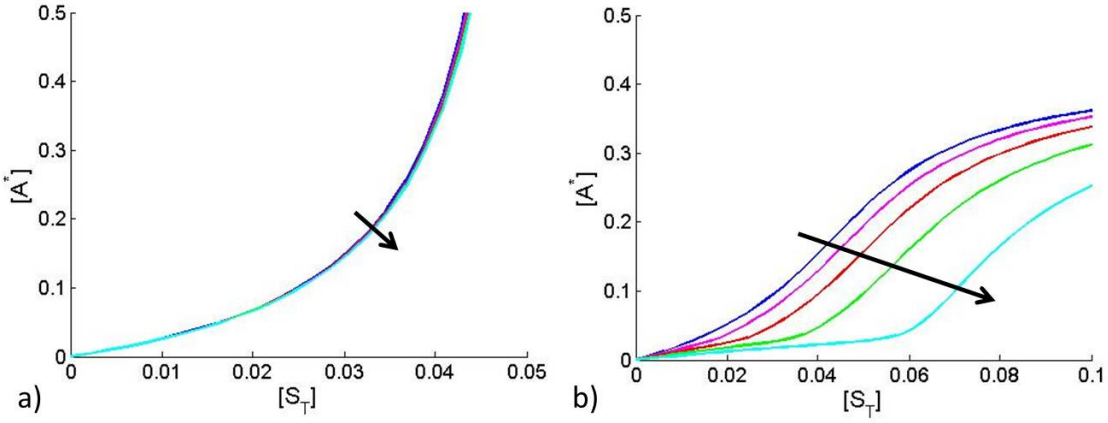

Figure 4.11: The changes in free concentration of upstream enzyme, A*, with the strength of inactive enzyme interference, are shown for the basal case in a), in which $[A_T] > [B_T]$. A situation in which $[B_T] > [A_T]$ is shown in b). It is clear that the presence of inactive enzyme interference significantly alters the response in the case where $[B_T] > [A_T]$, introducing a threshold in the concentration of A*. Increasing strength of inactive enzyme interference (i.e. increasing k_{10f}) is indicated by the black arrows.

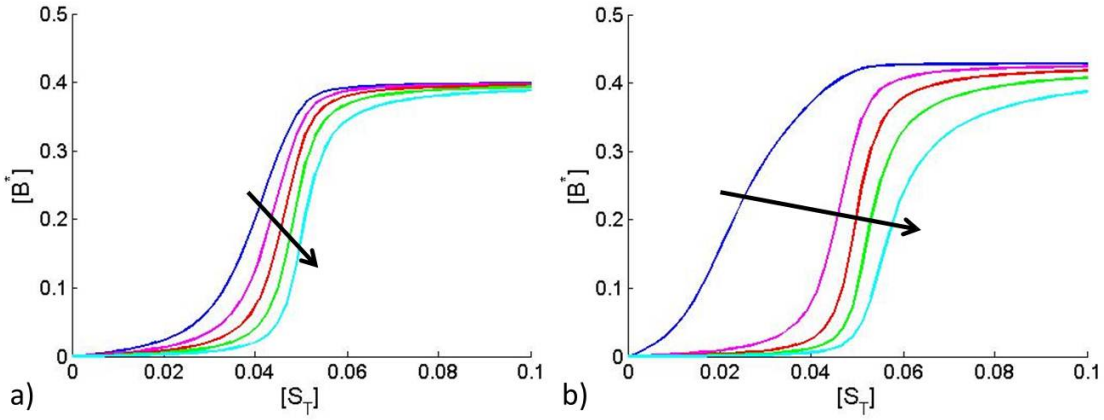

Figure 4.12: The change in behaviour induced by increasing strengths of inactive enzyme interference is shown for cases where the enzyme-substrate affinity (determined by k_{10f}) is a) half the basal value, and b) twice the basal value. There is a diminished response at lower affinities, compared to higher affinities. Increasing strength of inactive enzyme interference (i.e. increasing k_{10f}) is indicated by the black arrows.

Dynamic response

In the dynamic case, a stepwise increase in signal results in a monotonic increase in the output (see 4.13a)). The response time, defined as the time taken for the output to reach half its maximum level, clearly increases with increasing strength of inactive enzyme interference. This is a result of the inactive enzyme A sequestering B, and consequently slowing its conversion to B*. Again, by increasing the timescale separation between the binding interactions and the catalytic reactions, we confirm that the observed effects are the result of the underlying reaction kinetics, rather than the dynamics of substrate uptake and release. From the relationship observed between the strength of inactive enzyme interference and both ultrasensitivity and response times, we conclude that there is a trade-off between the ultrasensitivity attainable in the pathway through this mechanism, and the speed of its response (see Fig. 4.13b)).

4.3.3 The interaction between inactive enzyme and modified substrate

The final enzyme-substrate interaction which remains to be considered is the interaction between inactive enzyme, A, and modified substrate, B*. This interaction is pehaps relatively less likely to occur in isolation from the other interactions, as it suggests that the inactive enzyme may bind strongly to modified substrate.. This is in contrast to the other additional interactions, which can be thought of as arising from a lack of special regulation

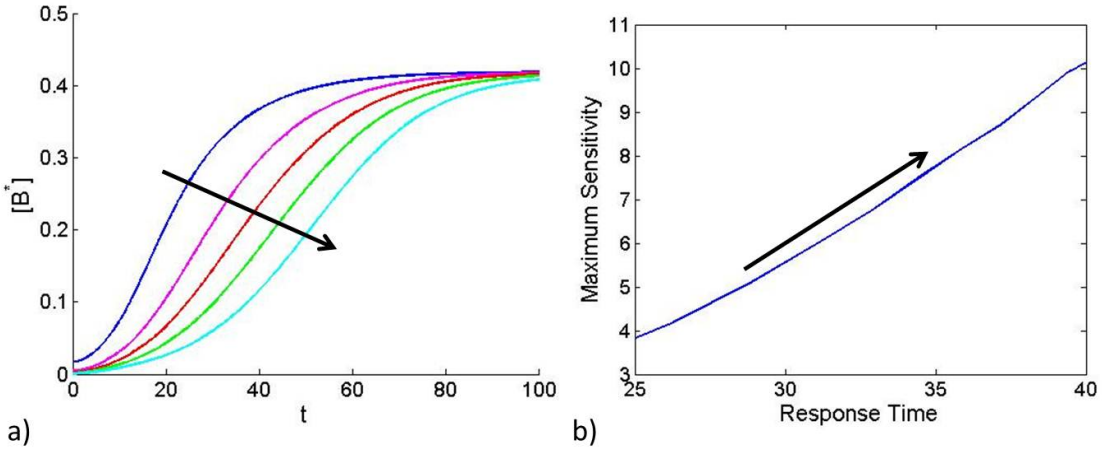

Figure 4.13: The slow down in signalling dynamics with increasing inactive enzyme interference is shown. This is clear from the dynamics of the output shown in a). The trade-off between the maximum relative sensitivity obtained and the response time (defined as the time taken to reach half the maximal output) is illustrated in b). Increasing strength of inactive enzyme interference (i.e. increasing k_{10f}) is indicated by the black arrows.

(e.g. in the case of product inhibition, the additional interaction arises from active enzyme lacking specificity for unmodified substrate as opposed to modified substrate). However, it remains instructive to include this interaction in the model to examine what this particular interaction results in and to understand the case where all possible combinations of interaction occur (see next section). We note that this interaction on its own produces behaviour similar to that of inactive enzyme interference, modulating the sensitivity through a threshold effect (see Fig. 4.14).

Perturbation analysis is again able to provide analytical insight into the underlying mechanism of increased sensitivity in this case. Again, we analyse this by examining the limiting case of very strong binding between A and B^*. By expanding the steady state concentrations in a perturbation series in k_{11r}/k_{11f} (a small parameter, due to for instance large k_{11f}) we find that, exactly as before, to leading order: $A_0 B_0^* = 0$. What this says is that, due to strong binding, either the concentration of free B^* (the output) is zero or the concentration of free A is zero. Thus the only way to obtain a non-negligible output is to practically deplete all free A , which in turn needs a sufficiently high signal. The basic mechanism at play here is similar to what was observed previously. Again, while this analysis is obtained in the limiting case, similar trends are observed for moderate levels of binding of A and B^*.

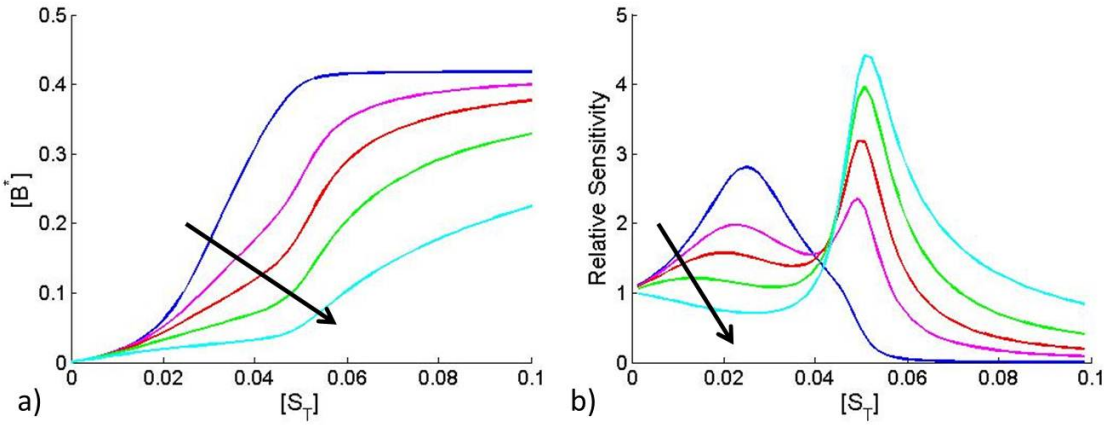

Figure 4.14: The change in behaviour with the strength of interaction between inactive enzyme and modified substrate is shown. This interaction introduces a threshold-like response similar to that observed for inactive enzyme interference. Increasing strength of the additional interaction (i.e. increasing k_{11f}) is indicated by the black arrows.

4.3.4 Combinations of additional interactions

It is natural to consider how product inhibition and inactive enzyme interference affect signalling when both are included at the same time. The consequence of combining both interactions is illustrated in Fig. 4.15, in which the strengths of both interactions are modulated in unison. It is clear that at low strengths of additional interactions, the combination of both interactions gives a response that is a combination of the two cases: there is a biphasic response as a result of product inhibition, and sensitivity is increased within a certain range as a result of the inactive enzyme interference. However, the biphasic response observed here is very much less pronounced than it is in the case when only product inhibition is considered, and the range of accessible outputs is substantially reduced compared to when only inactive enzyme interference is considered. This is especially clear when the additional interactions are of comparable strength to the essential interaction.

The scenario in which both additional interactions occur simultaneously, and at comparable strengths to the main interaction, corresponds to a signalling cascade in which the interaction between enzyme and substrate is mostly unregulated - the modification of substrate doesn't prevent it from binding to active enzyme, and the inactivation of enzyme doesn't prevent it from binding to unmodified substrate. It is also natural, then, to include the final possible interaction between enzyme and substrate, between inactive enzyme and modified substrate (i.e. A and B*). Including all possible interactions between enzyme

and substrate corresponds to the complete deregulation of the interaction between enzyme and substrate, since they bind to one another regardless of their activation or modification states. Fig. 4.15 shows how the response in this case is merely extremely damped, with no biphasic response or increased sensitivity. This is a result of the uptake of B* by any form of A under any signalling conditions.

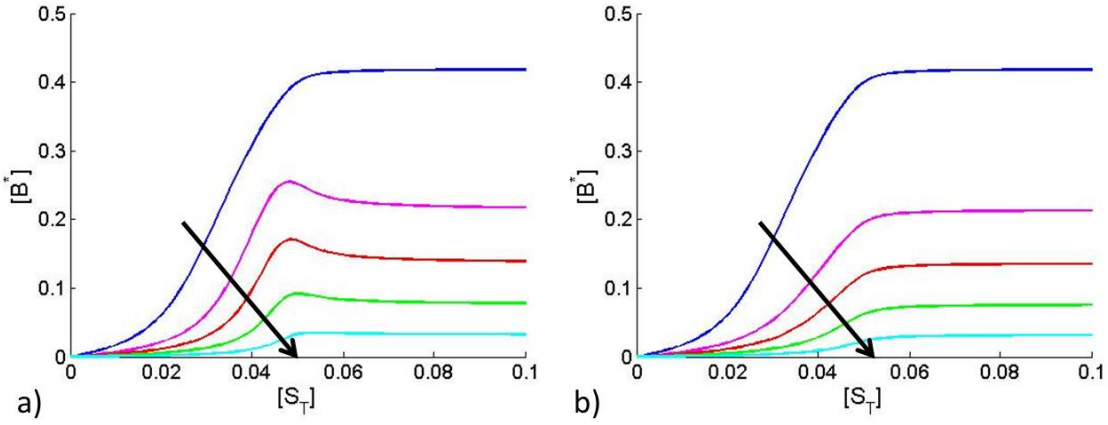

Figure 4.15: The steady state response of the system under different strengths of the combined interactions are shown. a) shows the response with the two additional interactions at increasing strengths, and b) shows the response with all possible interactions between enzyme and substrate. The black arrows denote the direction of increasing strength of additional interactions (i.e. increasing k_{9f} and k_{10f} in a), and in addition k_{11f} in b)), but with all additional interaction strengths equal to one another in each case shown.

We conclude from this that the complete deregulation of the interaction between enzyme and substrate, which leads to multiple additional interactions occurring at once, eliminates or dampens out the changes in behaviour observed when a single interaction is introduced. This is a consequence of the signal being unable to differentially regulate the uptake of substrate by enzyme in cases where all forms of enzyme and substrate bind to one another equally well.

4.3.5 Double Modification of Substrate

We now move on to consider simple variations of the basic model, beginning with the double modification of the downstream substrate. As discussed above, the model used here assumes that the two modifications are made distributively and sequentially, as discussed in Thomson and Gunawardena (2009). This is the simplest relevant model of multiple modification of substrate. Note that the model assumes that the active enzyme bound to

the singly modified substrate necessarily has the capability of converting into the doubly modified form. Further, we do not consider situations in which the enzyme may bind at different sites on the substrate to orchestrate the different modifications. Fig. 4.16 shows how additional interactions can affect signalling in this case. The outputs of interest are the free concentrations of singly- and doubly-modified substrate (denoted $[B^*]$ and $[B^{**}]$, respectively), and the sum of the two. This is because different forms of the substrate may be involved in different interactions downstream.

To begin with, we briefly examine the case without any of the additional interactions. This case has already been well studied in the literature Gunawardena (2005); Thomson and Gunawardena (2009), and so we only make two observations here. First, we see that $[B^{**}]$, and the sum of both $[B^*]$ and $[B^{**}]$, can exhibit ultrasensitivity (threshold effects) at steady state, as expected. Second, we see that the response of $[B^*]$ alone to the signal is biphasic. This is in agreement with our results above, since the uptake of B* by A* is a form of product inhibition, the only difference being that A* is then able to convert B* to B**. In fact, the biphasic response in this case is more pronounced than that observed in the case of simple product inhibition. This is the result of A* being able to suppress B* both by uptaking it, and by converting it to B** (which releases A*).

We can now consider the effects of product inhibition on this system, introducing an interaction between A* and B**. We see in Fig. 4.16 that the effects of product inhibition are largely the same as in the case of the basic model. The main point here is that, because of the pronounced biphasic response of $[B^*]$ to $[S_T]$ even without this additional interaction, the biphasic response of both $[B^*]$ and $[B^{**}]$ together is more pronounced than in the case of the basic model. The situation is similar in the case of inactive enzyme interference, with both $[B^{**}]$ and the sum of $[B^*]$ and $[B^{**}]$ responding with increased ultrasensitivity to $[S_T]$. The biphasic response of $[B^*]$ to $[S_T]$, by way of contrast, is strongly diminished under inactive enzyme interference. This is simply the result of strong uptake of B* by A.

In summary, we have seen that this variation of the basic model, involving an additional modification of the substrate, leads us to similar conclusions to those already drawn. It also provides additional insights into the interplay between multiple steps of substrate modification and the interactions we have studied.

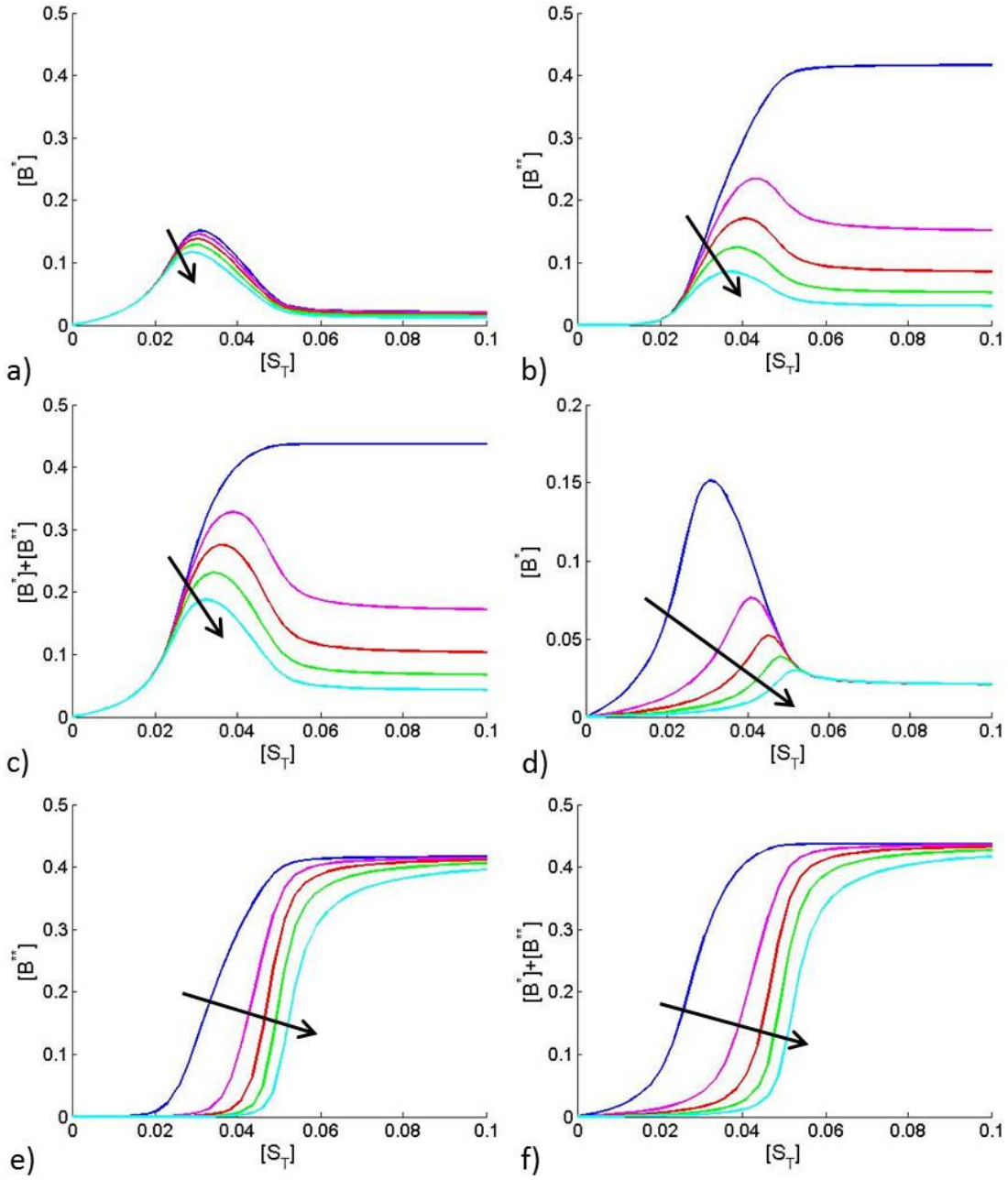

Figure 4.16: The effects of product inhibition (in a), b), and c)) and inactive enzyme interference (in d), e), and f)) on the concentration of singly-modified substrate, B*, (in a) and d)), doubly-modified substrate, B**, (in b) and e)), and both forms together (in c) and f)) are shown. Product inhibition leads to a pronounced biphasic response in $[B^{**}]$ and the sum of $[B^{*}]$ and $[B^{**}]$, while inactive enzyme interference leads to pronounced ultrasenstivity in $[B^{**}]$. The black arrow denotes the direction of increasing strength of the additional interaction under consideration (i.e. increasing k_{9f} and k_{10f}, respectively).

4.3.6 Scaffold-mediated modification

In our second variation of the basic model, we consider what happens when a scaffold mediates the interaction between enzyme and substrate. This is common in signalling cascades, a particularly well-studied example being MAPK cascades Ferrell (1996). We can investigate how the presence of a scaffold might change the effects of two additional interactions we have been considering - product inhibition through binding of B* to the scaffold, C, and inactive enzyme interference through binding of A to C. Fig. 4.17 shows how the steady state response is altered by the additional interactions. Interestingly, the basal response without additional interactions has become substantially less ultrasensitive than in the basic model, where the scaffold was not present. This is a result of the strong binding between the scaffold, enzyme, and substrate, as discussed in Thalhauser and Komarova (2010). At higher scaffold concentrations, the response becomes even less sensitive.

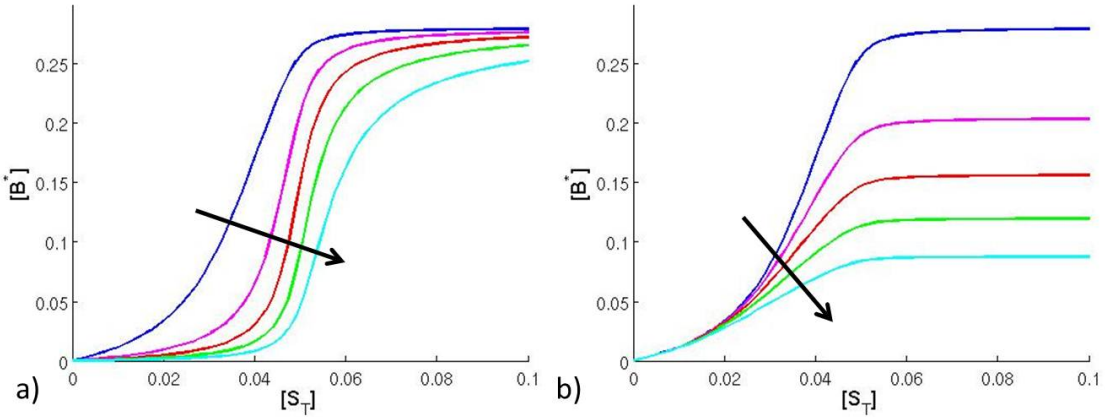

Figure 4.17: The effects of a) inactive enzyme interference and b) product inhibition on scaffold-mediated signalling are shown. Inactive enzyme interference is capable of increasing the sensitivity of the switch, while product inhibition decreases the accessible range of signalling. The black arrow denotes the direction of increasing strength of the additional interaction under consideration.

In Fig. 4.17, we see that increasing the strength of product inhibition only suppresses the output, and does not lead to any biphasic response to $[S_T]$. This is because the binding of B* to the scaffold C does not depend upon C already being bound to A* and so A* is not able to influence uptake of B*. The only effect the product inhibition has, then, is to cause uptake of B* by C, an effect which decreases the free B* available at each signalling level. In this way, C is acting as a buffer between A* and B, preventing A* from regulating B as it does in the case where the scaffold is not present. While the model considered

here assumes independent binding of A and B to C, the situation is likely to be different when cooperative binding is present. In this situation, the scaffold's buffering properties are likely to be diminished.

Also shown in Fig. 4.17 is the effect of inactive enzyme interference on scaffold mediated signalling, where the response becomes progressively more ultrasensitive and switch-like. Again, this is the result of the competition in binding between A and A*, although in this case they are competing for binding to the scaffold rather than the substrate. Interestingly, this additional mechanism of producing ultrasensitivity means that an ultrasensitive response becomes possible even with high-affinity binding to the scaffold, as long as scaffold-binding isn't dependent on the activation state of the upstream enzyme.

4.4 Conclusions

A basic element of signalling in protein networks is the enzyme-catalysed modification of a substrate protein. While this may be understood in terms of an interaction between active enzyme and unmodified substrate, additional enzyme-substrate interactions are possible. From the perspective of cellular signal processing, we can examine the interaction of enzyme and substrate as the interaction between two two-state networks of inactive/active enzyme and unmodified/modified substrate. While the essential interaction in these networks is between the active enzyme and unmodified substrate, we focussed on the effects of additional interactions, in particular those between modified substrate and active enzyme (product inhibition) and inactive enzyme and unmodified substrate (inactive enzyme interference). Our goal was to examine how these interactions modulate signal processing in this basic unit of signal transmission. The effects of the additional interactions were examined one at a time to start with, then in combination. We further examined the roles of these interactions in two related situations: one in which the enzyme multiply modifies the substrate and one in which the enzyme-substrate interaction was mediated by a scaffold/adapator protein.

The results presented demonstrate some of the interesting new signalling behaviours available to these simple systems if additional enzyme-substrate interactions occur. In the case of product inhibition, we have seen that the qualitative nature of the behaviour can change from a monotonic response to a biphasic response. Biphasic responses allow the network to respond specifically to signal strength in an intermediate range, where the signal is not too high or low. Similar responses are commonly seen in incoherent feedforward

circuits Kaplan et al. (2008); Kim et al. (2008), and have been suggested to play roles in the regulation of signalling crosstalk de Ronde et al. (2011). We have further seen that product inhibition is capable of resulting in pulse-like responses to a change in the input signal. By considering the effects of uptake of substrate by enzyme, these results complement other work analysing the consequences of product inhibition in similar systems Ortega et al. (2002); Salazar and Hofer (2006). The biphasic behaviour is exaggerated when multiple modifications of the substrate occur. In contrast to the basic and multiple modification models, however, biphasic and pulse-like responses are not seen in the scaffold model. Thus, in this situation, the scaffold acts as a buffer to prevent this behaviour.

In the case of inactive enzyme interference, we have seen that the additional interaction is capable of emphasising threshold-type responses to signals, and that this may be understood in terms of molecular titration effects in a variety of conditions. Such thresholds are important in allowing cells to trigger all-or-none responses to extracellular stimuli Ferrell (1996). A trade-off was identified between the speed of the dynamic response and the degree of sensitivity observed in the steady state response, depending on the strength of the additional interaction. These conclusions also hold when multiple modifications of the substrate occur. Interestingly, the inactive enzyme interference effect can increase sensitivity even in the case of scaffold-mediated interactions between enzyme and substrate.

When the product inhibition and inactive enzyme interference interactions are present side-by-side, a combination of their effects could be observed. However, when multiple strong additional interactions are present, the qualitative differences in the response are lost. This is a result of the signal being unable to differentially regulate binding between the enzyme and substrate. These results show how some regulation of the binding properties of enzyme and substrate is required in order for the observed signalling properties to occur.

We have shown how the tuning of individual protein-protein interactions can be used to create new signalling behaviours. The details of the interactions between two proteins in a network, and how they depend on the modification state of those proteins, can substantially alter the network's global signal processing properties, both at steady state and dynamically. Information transmission in cellular pathways involves more complex networks than those considered here, wherein a protein may interact with a number of other proteins to form a variety of different complexes under changing conditions. Thus the results and insights presented here and extensions thereof are particularly relevant when one examines the natural complexity of signalling networks and the modular structure of protein-protein interactions in conjunction with one another. Parallels with recent work include analysis

of a case where both kinases and phosphatases simulataneously bind to a substrate (motivated by observations in phosphopinositide signalling) Szomolay and Shahrezaei (2012), and the observation that the introduction of an interaction between an inactive enzyme and its substrate can lead to bistability in a simple feedback circuit Ciliberto et al. (2007). While additional interactions beyond those typically considered are included in the models studied, it was still necessary, in the interests of simplicity, to make assumptions about some interactions not occurring. The consequences of the relaxation of these assumptions is a topic for future work.

Our findings have relevance for both signal processing in natural cellular and synthetic cellular networks as well as the understanding of biological signal transduction processes. Importantly, we have demonstrated some ways in which signalling behaviours such as thresholds or biphasic responses can be generated purely from local interactions between two components in a network, rather than involving extra entities or pathways. This indicates that an extra layer of robustness in these behaviours may be built into a network by combining these local features with global network features such as feedforward and feedback signalling pathways (e.g. multiple threshold effects in a cascade may provide a more robust threshold effect to the cascade as a whole). It is also possible that some complex behaviours may have their origins largely or entirely in local interactions in a signalling network, and therefore that such behaviour may sometimes be misattributed to additional (or missing) pathways, perhaps based on inspection of the topology of the signalling network. This, in turn, can lead to a mistaken understanding of signalling in the network. Furthermore, the presence of strongly nonlinear signalling processing as examined above in multiple enzyme-substrate interactions in a network can have very nontrivial effect on the network dynamics as a whole. Finally, we note that the rules governing enzyme-substrate interactions are likely to be important in the design of synthetic signalling systems. This is particularly important for cases in which signalling complexes are designed by combining multiple modular domains, as in these cases the relationship between the activation/modification state of a protein and its binding properties are likely to be unknown. Of course, given sufficient knowledge, it should also be possible to generate different signalling behaviours in synthetic circuits by modulating or engineering the type and strength of interactions which are allowed to occur.

In summary, the investigations presented constitute a systematic examination of the role of additional protein-protein interactions in affecting signal transmission in a simple unit of signal transduction. It suggests that the nature of the protein interactions can signifi-

cantly distort the signal transduction in chemical networks and that part of the complexity and nature of signal transmission in reaction networks may be traced to the complexity of interactions occurring between individual proteins. The modulation of protein-protein interactions in networks such as these therefore represents an important aspect of signalling in these systems, tunable by evolution and synthetic approaches alike to produce new signalling behaviours.

Chapter 5

A modular systems approach to understanding the interaction of adaptive, monostable, and bistable threshold processes

5.1 Introduction

In the preceding chapters, we have considered how simple biochemical motifs can produce a variety of interesting signalling behaviours. In this chapter, we extend this approach by considering how modules with different, well-defined signalling behaviours may interact with one another. In order to do this in a general way, we take advantage of the observation that some aspects of signalling recur from system to system Tyson et al. (2003).

One example of a dynamic characteristic which occurs in different kinds of signal transduction is adaptation. This loosely means that following the application of a stimulus, a transient response is observed which eventually recovers (exactly or approximately) to the original basal pre-stimulus state Drengstig et al. (2008); Ma et al. (2009). Such signals are particularly common in stress responses El-Samad et al. (2005); Muzzey et al. (2009); Ni et al. (2009); Zhang and Andersen (2007), and also occur in sensory systems Friedlander and Brenner (2009); Wark et al. (2007) and chemotactic systems Levchenko and Iglesias (2002); Yi et al. (2000). We also note that these adaptive responses may occur across a wide range of network scales - from a single receptor (e.g. adaptation to chemoattractant

concentration Yi et al. (2000)), to several pathways at once (e.g. adaptation to changes in inorganic ion concentration Ni et al. (2009)). Ultimately, adaptive signal transduction involves the conversion (through the underlying chemical circuits) of a persistent signal into a transient signal, which carries the relevant information to downstream targets.

Another dynamic characteristic which is present in different cellular contexts is that of thresholds or switch-like behaviour Ferrell (1996); Huang and Ferrell (1996). This implies that, following an activating signal, the downstream response is activated only when the upstream signal exceeds a particular (threshold) value. This prevents the unnecessary activation and production of downstream second messengers. In cells, thresholds can be realized in many different biochemical ways, but these can be separated into two essentially different categories based on the number of stable steady states present. In the first place, there are ultrasensitive systems which have a single stable steady state for any value of parameters, which we refer to as monostable switches Ferrell (1996); Goldbeter and Koshland (1981); Huang and Ferrell (1996). In the second place, there are systems which have two stable steady states for a range of parameters, which we refer to as bistable switches Angeli et al. (2004); Bagowski and Ferrell (2001); Ramakrishnan and Bhalla (2008). The presence of two stable steady states in bistable elements manifests itself in their steady state response in the form of hysteresis. Thus, while both of these signalling elements exhibit a sharply elevated steady state response when the threshold is crossed, there are important qualitative differences in their behaviour. Both monostable and bistable elements are frequently encountered in signal transduction.

In this chapter we use a modular systems approach to try to achieve an understanding of the ways in which adaptive signalling interacts with threshold processes (a schematic is shown in figure 5.1). This is important for various reasons. The first, already discussed above, is the fact that both of these processes are very common in biological signal transduction, and have been seen in a variety of biological networks. Thus such interactions may generically be expected in signalling networks, and may have important functional roles. Secondly, the activation of switches by transient signals is quite different from the activation of switches by static signals. Since the outputs of adaptive modules are pulse-like signals, this systems approach also sheds light on the ways in which pulsatile signals interact with threshold processes. Such an understanding also has relevance to the manipulation of particular pathways through transient signals. In fact, a modular approach with an explicit biochemical description of adaptive processes is the first step towards understanding the role of adaptive signal transduction and transient signal propagation in the context

of complex signal transduction networks. A systems approach entails viewing the adaptive and threshold processes as individual signal processing entities and examining the qualitatively essentially different ways in which these entities interact. This involves analyzing and distilling the signal processing characteristics and capabilities from different interactions/interconnections of these modules. A systems-based understanding would provide insights into the behaviour of different systems which involve these modules and their interaction. Specific biological examples of the interaction of transient signals with bistable signalling modules are found in Bhalla and Iyengar (1999); Hayer and Bhalla (2005). Similarly, the network involved in osmotic stress response in yeast shows adaptive responses of components such as Hog1 Klipp et al. (2005); Muzzey et al. (2009). Hog1 plays an important role in triggering gene expression, where threshold effects may be expected.

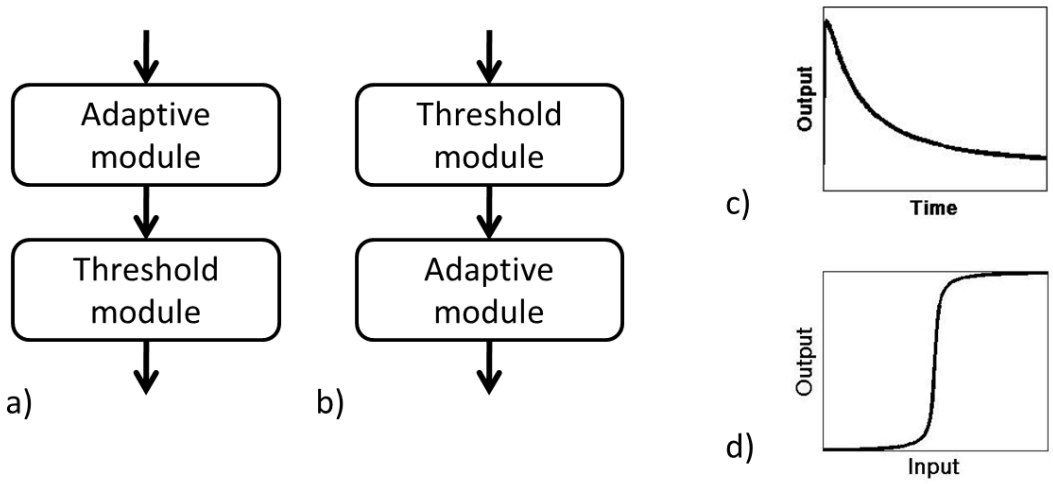

Figure 5.1: A schematic of the interaction of the adaptive and threshold (monostable/bistable) modules is shown. In (a) the adaptive module is upstream of the threshold module while in (b) the order is reversed. Schematics of the modules input-output behaviour are shown in (c) (a transient pulse in response to a step-change in input), and (d) (the steady state response curve).

Since our goal is to try to achieve a systems understanding of the interaction of adaptive and threshold modules, rather than focus on various specific details of a single biological process/system (which would obscure rather than illuminate some of the issues under consideration), we isolate representative modules of adaptation and monostable and bistable switching behaviour. The modules chosen are compact representations which possess the essential characteristics of the relevant signal processing. In each case we examine more than one representative module to check if our analysis depends in any essential way on the

particular choice of module. Simplified models are also employed to shed direct light on key aspects of our analysis. In all cases we use a combination of analytical results as well as numerical simulations and bifurcation analysis to elucidate key aspects of the interaction. Some of the questions we address are: what are the ways in which adaptive and threshold processes can interact and how does this depend on their time scales? Can a transient signal lead to the permanent activation of a switch and what factors does that depend on? What kinds of signal processing may be generated from the interaction of these processes? Overall a dynamical-systems approach underpins the way in which we organize our analysis of these modules and their interaction.

This chapter is organized as follows. In the next section we present and discuss the different modules which we employ. In the following sections we carefully analyse the interaction of adaptive signals with monostable and bistable threshold modules. We then examine the processing of multiple pulse signals by these threshold modules. We then analyse some issues relating to the interaction of adaptive signal processing and bistability. We also study the response of the combined system to time varying signals. Following this, we examine alternate interconnections of these modules, and conclude with a summary of our results.

5.2 Models

In this section, we discuss the representative modules of adaptation, monostable threshold and bistable threshold modules which we use in our study, and how they interact. Schematic diagrams depicting the interaction topologies of the biochemical models used are given in Fig. 5.2. MATLAB code used to simulate these models in their various combinations is provided in the digital appendices, documented in Appendix E.0.4. Parameter values are detailed in Appendix C.

5.2.1 Modules of adaptation

Adaptive modules convert a sustained steady change in input to a transient change in output. Different models of adaptation in signal transduction exist in the literature, some of which have been developed in the context of specific biological processes. Some of these models lead to exact adaptation Drengstig et al. (2008); Sontag (2010); Yi et al. (2000) while others display approximate (inexact) adaptation Behar et al. (2007); Ma et al. (2009).

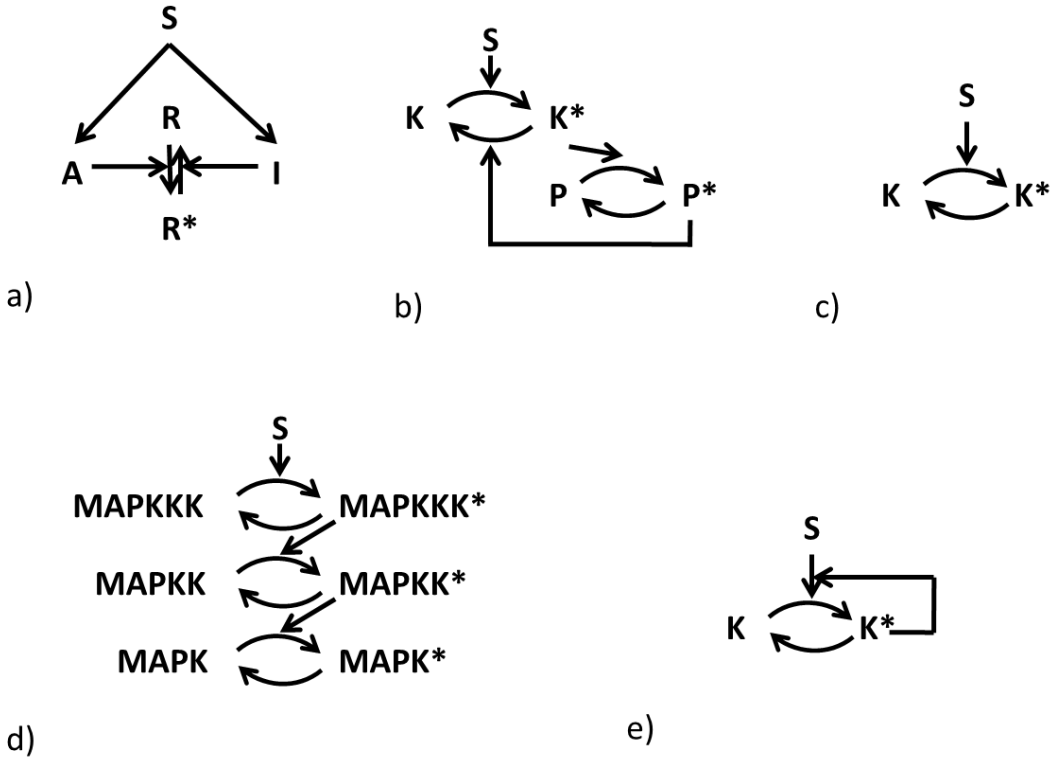

Figure 5.2: This figure shows the interaction topologies of the biochemical models of adaptation and thresholds which were used. (a) depicts the excitation/inhibition model of adaptation, where R^* is the output. (b) depicts the Behar model of adaptation, where $K*$ is the output, (c) depicts the Goldbeter-Koshland switch, where K^* is the output (denoted by u in the text, after normalization of the concentration). (d) depicts the MAPK cascade, where $MAPK^*$ is the output (denoted by x_3 in the text, after normalization of concentrations). (e) depicts the bistable switch with saturated degradation, where K^* is the output (denoted by u in the text, after normalization of concentrations).

Further, of the models which display exact adaptation, some models display exact adaptation without fine tuning parameters in the model. This feature is called robust exact adaptation. A detailed parametric analysis of three node networks leading to adaptation Ma et al. (2009) suggests that two common ways in which adaptation may be achieved are incoherent feedforward and negative feedback regulation.

In this chapter we employ two representative models of adaptation. The first is a generic feedforward adaptive model involving a response element (the output of the module) being regulated by two opposing pathways, an activator and an inhibitor, each of which is regulated by an input signal. This model was suggested and qualitatively analysed in the biological literature by Koshland Koshland (1977), and has been subsequently expanded and mathematically modelled to explain adaptation and spatial sensing Levchenko and Iglesias (2002). For our purposes, we employ the temporal adaptation network here without concerning ourselves with spatial sensing. The model equations are

$$\begin{aligned} dA/dt &= k_a S - k_{-a} A \\ dI/dt &= k_i S - k_{-i} I \\ dR/dt &= -k_f AR + k_r IR^* \\ dR^*/dt &= k_f AR - k_r IR^* \end{aligned} \tag{5.1}$$

The equations are non-dimensionalized so that $R + R^* = 1$ initially(note that the total amount is conserved) and so the last two equations can be collapsed to

$$dR^*/dt = k_f A(1 - R^*) - k_r IR^* \tag{5.2}$$

This module displays robust exact adaptation, as has been noted earlier. The steady state for R^* (the module output), depends on the ratio A/I, which is independent of the upstream signal S. Thus a step change in signal will cause the system to recover to basal levels. Earlier analysis reveals that such parallel regulation of opposite pathways places restrictions on the dynamic range of the output of this system Krishnan (2009).

A second representative module which we use is the adaptation model developed by Behar and co-workers, henceforth called the Behar model Behar et al. (2007). The key elements are two proteins, a kinase and a phosphatase, each of which can exist in active and inactive forms. The input signal (denoted by S) activates the kinase, which activates the phosphatase. The latter in turn negatively regulates the kinase. This is thus an example

of adaptation resulting from negative feedback. Denoting the active form of the kinase by K^* (the output of the module) and that of the phosphatase by P^*, the equations for this model are

$$\begin{aligned} dK^*/dt &= \frac{k_1 S(1-K^*)}{k_{1m}+(1-K^*)} - \frac{V_2 K^*}{k_{2m}+K^*} - \frac{k_3 P^* K^*}{k_{3m}+K^*} \\ dP^*/dt &= \frac{k_4 K^*(1-P^*)}{k_{4m}+(1-P^*)} - \frac{V_5 P^*}{k_{5m}+P^*} \end{aligned} \tag{5.3}$$

These equations describe the reactions using Michaelis-Menten kinetics. The equations are normalized so that $K + K^* = P + P^* = 1$ and that is implicit in the above description (see (Behar et al., 2007)). The Behar model exhibits adaptation which is not strictly exact. However, the deviation from exact adaptation is very small for a wide range of signals. While the results in this chapter are shown for the activator/inhibitor module, qualitatively very similar results were obtained with the Behar module, unless otherwise mentioned. We note that both these models capture the key essential dynamic and input-output behaviour of adaptive signalling: a transient change in response to stimuli followed by a monotonic recovery to the basal state (with no damped oscillations). Since it is the input-output signal processing behaviour which is important for our study here (rather than any structural characteristics of the network), these models serve as good representatives of adaptive signalling.

Finally, while we employ the above modules as representative modules of adaptive signalling, at various points in the chapter we also employ idealized pulse-like signals (square pulses, pulse signals representing sharp jumps with exponential decay) to obtain analytical insight into how pulse-like signals (such as the output of an adaptive module) interact with threshold modules.

5.2.2 Modules of monostable thresholds

Monostable threshold modules possess only one stable steady state output for each input, and the steady state input-output response shows a sharp increase when the input crosses the threshold value. In this chapter we employ two representative modules of monostable threshold modules. The first is a simplified version of a single-stage model of zero-order ultrasensitivity which was introduced by Goldbeter and Koshland (Goldbeter and Koshland, 1981) and may be regarded as a benchmark model of a monostable threshold. This model

involves the reversible conversion of a species from its inactive to active form. The enzymes that regulate the forward and reverse reactions act close to saturation. This combined effect results in a steady state response which is a sharp sigmoidal function of the input, and provides the characteristic of a monostable switch. The Goldbeter-Koshland model involves the description of the activation of a protein by an input signal S. The concentration of the active form of the species (the output of the module) is denoted by u. Both forward and backward reactions involve Michaelis-Menten kinetics. The equation for the concentration of active form of the species is

$$du/dt = S.\frac{V_1(1-u)}{K_{m1}+(1-u)} - \frac{V_2 u}{K_{m2}+u} \tag{5.4}$$

The various constants denote the relevant Michaelis-Menten parameters, S denotes the regulating signal and u is the output. The sigmoidal steady state response of this model in response to the signal is depicted in figure 5.3 d).

A second representative module of a monostable switch which we employ is a model of a MAP kinase cascade. MAPK cascades are a well-known example of systems which exhibit switch-like behaviour and models of MAPK cascades have been developed over the years by a number of researchers (for e.g. see(Huang and Ferrell, 1996; Kholodenko, 2000)). The model which we will use is based on the paper (Huang and Ferrell, 1996). The MAPK module involves a cascade of reactions with the output of the upstream reaction regulating the reaction in the cascade immediately below it. The enzymatic reactions are all modelled using Michaelis-Menten equations. The essence of this model is that, while each stage in the cascade has only a weakly sigmoidal input-output response, the compound effect is a very sharp, switch-like input-output response. The equations for the MAPK cascade are given below (parameter values are provided in Appendix C.

$$\begin{aligned} dx_1/dt &= S.\frac{V_1(1-x_1)}{K_{m1}+(1-x_1)} - \frac{V_2 x_1}{K_{m2}+x_1} \\ dx_2/dt &= x_1.\frac{V_3(1-x_2)}{K_{m3}+(1-x_2)} - \frac{V_4 x_2}{K_{m4}+x_2} \\ dx_3/dt &= x_2.\frac{V_5(1-x_3)}{K_{m5}+(1-x_3)} - \frac{V_6 x_3}{K_{m6}+x_3} \end{aligned} \tag{5.5}$$

where x_3 is the output. In addition to these modules, a simple model which captures the signal processing essence of a monostable switch was also used to clarify the analysis and

provide analytical insight, especially related to the response of such modules to transient signals. This model is given by

$$du/dt \;=\; K(H(S - S_t) - u) \tag{5.6}$$

where H denotes the Heaviside function and u is the output. This is a simple module which indicates the presence of a switch with respect to the upstream signal S at the value S_t. The timescale of the response depends on the constant K.

An important issue which immediately arises while considering the interaction of adaptive modules with the biochemical threshold modules, is exactly how the signal from the upstream module regulates or interacts with the downstream module. In both the biochemical modules above the integration with the upstream signal is clear: the output of the upstream module acts as the activating signal for the threshold module. A couple of points are worth mentioning. Firstly, the upstream modules chosen are scaled so that their output is between 0 and 1. Clearly, the effect of the absolute concentration of output of the upstream module can be absorbed in the kinetic constant accompanying this signal in its regulation of the downstream module. Secondly, by introducing another additive constant where this signal appears in the downstream module it is possible to alter the range of regulation of the downstream module by the upstream signal. This also has a natural interpretation, of simply altering the basal value of the output of the downstream module in the absence of upstream signal.

5.2.3 Modules of bistable thresholds

Bistable threshold modules, in contrast to monostable threshold modules, possess two stable steady states for a range of inputs and parameters. They also exhibit switch-like behaviour, but embody very different dynamical characteristics than are seen in the monostable case. Bistable behaviour has been observed in various contexts in cell biology and different models underlie these various processes. However, a common feature for generating bistability in signalling is positive feedback (or double negative feedback). Different simple models using positive feedback have been shown to generate bistable behaviour. Some of these models involve strongly co-operative feedback with high Hill coefficients. We examined and analysed a number of representative modules of bistability. The one which we use to present computations is a module of saturated degradation, along with

positive feedback (Ferrell, 2002). The upstream signal plays a role in catalysing this positive feedback pathway (either exclusively or along with the some other existing enzyme). This model describes the variation in concentration of the active form of a protein u by activation and deactivation reactions, with a positive feedback loop acting to further activate inactive protein. Here, again, the total concentration of the protein is normalized to be 1. The governing equations are

$$du/dt = \frac{V_1(1-u)}{K_{m1}+(1-u)} + S.k_{fb}u(1-u) - \frac{V_2 u}{K_{m2}+u} \tag{5.7}$$

Here the various constants are Michaelis-Menten parameters, S is the upstream input signal, k_{fb} is a kinetic parameter which parametrizes the feedback strength, and u is the output of the module. Some basic analysis of this module is seen by examining the steady state response in this module to the signal S. This is presented in the bifurcation diagram in Fig. 5.4. We clearly see that there are regions of monostability and a finite range of parameter values corresponding to bistability.

One important aspect of our study here is to understand the response of such bistable threshold modules to transient signals. In general owing to both the non-linearity of the modules and the transient nature of the signal, it is difficult to obtain analytical insight into how transient signals are processed by such modules. Thus, we also examine a simple model which possesses the essential characteristics of bistable modules, but is more tractable analytically. This model, which displays the familiar z-shaped nullcline, is given by

$$\begin{aligned} dz/dt &= -\alpha z, S < 0 \\ dz/dt &= \alpha z(1-z)(z-1+S), 0 < S < 1 \\ dz/dt &= \alpha(1-z), S > 1 \end{aligned} \tag{5.8}$$

In the above equations, z is the output variable and S is the regulating input signal. It is clear that for $0 < S < 1$ we have bistable dynamics, with three steady states for z: $z = 0, 1-S, 1$, of which $z = 0$ and $z = 1$ are both stable. Outside this region there is only one steady state.

It is worth pointing out again an important aspect of the interaction of the upstream signal with the bistable module. The basal value of the upstream signal is a non-zero value which lies either in the monostable or bistable region of the bifurcation diagram for the

bistable module. The upstream signal can vary in a finite region and so, for a particular choice of parameters, the upstream signal can regulate the bistable module so that it can be either in both monostable and bistable regions, or only in the bistable region (the case where bistability is never encountered is not of interest). It is also worth pointing out that for the case $S = 0$, the module may in general be either monostable or bistable. In considering the interaction of an adaptive module with a bistable module, the basal steady state conditions for both modules usually correspond to a nonzero value of S, and for the bistable module this state is different from the one corresponding to $S = 0$ (i.e. zero upstream signal). In general, the location of the basal signal value on the bifurcation diagram depends on the various kinetic parameters of the bistable module (including parameters embodying the possible presence of positive feedback in the absence of an upstream signal).

5.2.4 Example equations for interconnected modules

We present example equations for the combined systems of interconnected modules - one example for each order of interconnection. The excitation/inhibition model of adaptation and the saturated degradation model of bistability are used here. The interconnection of other modules is similar, with the output of the upstream module feeding into the input of the downstream module.

Adaptive module upstream of bistable threshold module

$$\begin{aligned} dA/dt &= k_a S - k_{-a} A \\ dI/dt &= k_i S - k_{-i} I \\ dR^*/dt &= k_f A(1 - R^*) - k_r I R^* \\ du/dt &= \frac{V_1(1-u)}{K_{m1} + (1-u)} + R^*.k_{fb} u(1-u) - \frac{V_2 u}{K_{m2} + u} \end{aligned} \tag{5.9}$$

Bistable threshold module upstream of the adaptive module

$$\begin{aligned} du/dt &= \frac{V_1(1-u)}{K_{m1}+(1-u)} + S.k_{fb}u(1-u) - \frac{V_2 u}{K_{m2}+u} \\ dA/dt &= k_a u - k_{-a}A \\ dI/dt &= k_i u - k_{-i}I \\ dR^*/dt &= k_f A(1-R^*) - k_r I R^* \end{aligned} \tag{5.10}$$

5.3 Results

5.3.1 Interaction of adaptive and monostable threshold modules

We investigate the interaction of adaptive modules and monostable threshold modules. This is done as follows. The adaptive module is regulated by an external signal and the output of the adaptive module in each case is an input to the threshold modules as outlined in the previous section (see Fig. 5.1 (a)). We analyse the interaction of modules in general using both simulations and analytical work. We first start by subjecting the composite system to a step change in input. The response of the adaptive module to this change in input is shown in Fig. 5.3 (a). If the response of the adaptive module is always below the threshold, effectively no output is seen. On the other hand, if the output of the adaptive module transiently exceeds the threshold then an output may be seen, depending on the relative speed of dynamics of the adaptive and monostable threshold modules. We consider two different cases, concentrating for the time being on the Goldbeter-Koshland model. In the first case (shown in Fig. 5.3(b)), the adaptive module dynamics are slower than that of the threshold module, and so an output is seen once the threshold is crossed. This output eventually decays back to zero, and the decay starts once the threshold is crossed in the reverse direction. In the second case, if the adaptive dynamics are much faster than that of the threshold module, a negligible output response is obtained.

Similarly, we examined the interaction between adaptive signalling and the MAPK cascade model of a monostable threshold. Fig 5.3(c) shows the behaviour of the output as a function of cascade length. We see that the output of the one step reaction cascade actually has a higher amplitude than that of the three-stage cascade. While the three step cascade acts as a sharper switch, this comes at the cost of slowing down of the dynamics, and thus the less sensitive switch acts as a better transient amplifier in this case for such adaptive

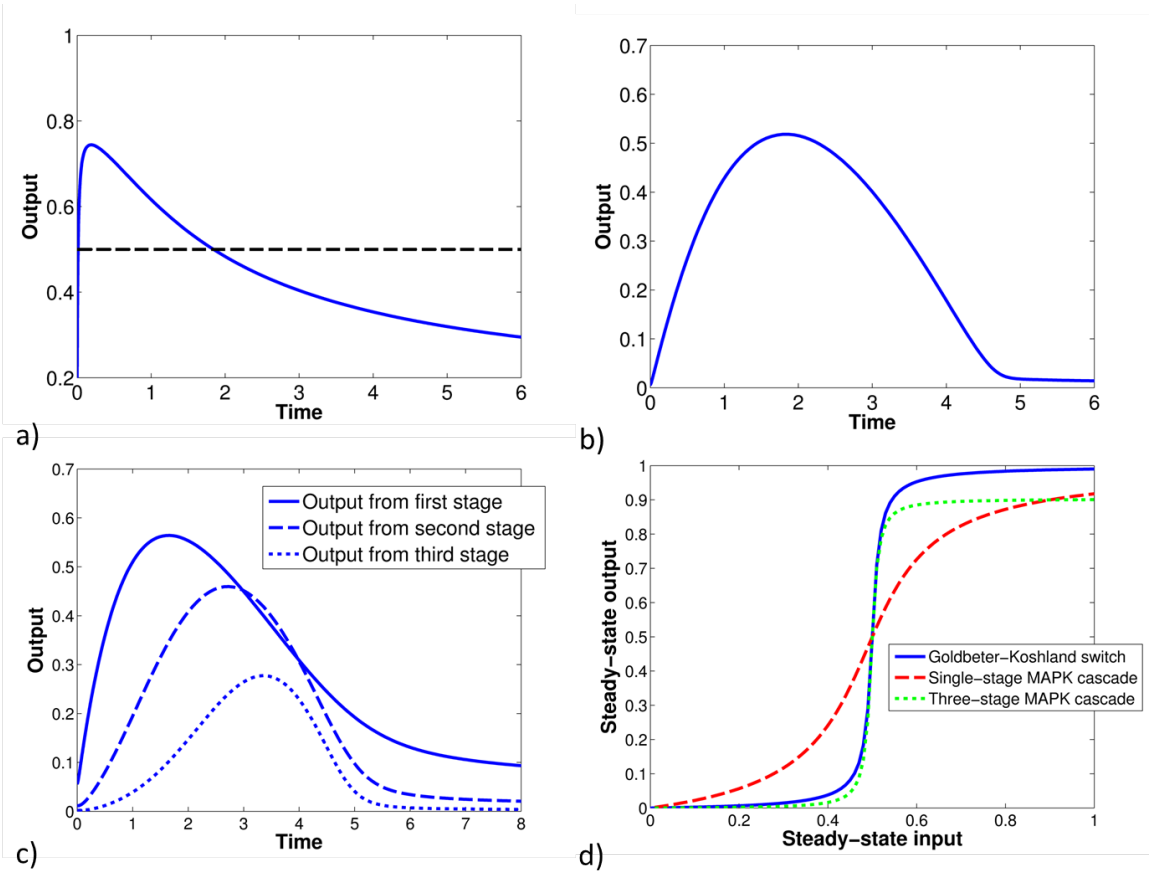

Figure 5.3: **Interaction of the adaptive module with monostable threshold module** (a) The response of the adaptive module to a step-change in input (at t=0) is shown. This output of this module is then the input to the downstream monostable threshold modules. The location of the threshold is marked by the dashed line. (b) The response of the downstream monostable threshold module for the case of the Goldbeter-Koshland switch is shown. (c) The responses of single- and multiple- stage MAPK cascades are shown, indicating a decreased amplitude of pulse with increasing cascade length. (d) The steady state characteristics of the Goldbeter-Koshland switch, and one- and three-stage MAPK cascades, are shown. Note the very similar steady state characteristics of the Goldbeter-Koshland and three-stage MAPK cascades.

signals. We note further that, in contrast to the Goldbeter-Koshland threshold, there is a delay before the MAPK cascade output begins to decrease, after the input decreases below the threshold. This is because, in the MAPK cascade, several switch-like stages must be successively switched off before the output will begin to decrease. We note that the differences observed between the behaviour of the Goldbeter-Koshland model and MAPK cascade cannot be the result of differences in the steady-state signal processing, as these are very similar for the parameter values used (see Fig. 5.3(d)).

Analytical work provides additional understanding of the signal transduction above. This is done for two cases, one the Goldbeter-Koshland model, and another the simplified model describing the switch by a Heaviside function described previously. For the Goldbeter-Koshland model, the amplitude of the response depends on the time T during which the upstream signal is above the threshold. We note that, for the duration that the signal is above the threshold and the output satisfies $u \ll 1$, Eq. 5.4 can be simplified to:

$$du/dt \;=\; S.V_1 - \frac{V_2}{K_{m2}} \tag{5.11}$$

Thus, once the threshold is crossed, the Goldbeter-Koshland module exhibits linear-in-time dynamics for a particular input signal value. This is true only when the module operates away from complete conversion. This means that, for a square-pulse input, the amplitude of the response is given by $A = (S.V_1 - V_2/K_{m2})T$, up to the maximal output of the Goldbeter-Koshland threshold. In contrast, the simplified model with a Heaviside function results in an amplitude given by $A = 1 - exp(-KT)$, as is found from an analytical solution for this model. We see that in this case the dependence of amplitude on time is different from that of the Goldbeter-Koshland model. This feature is important when we re-examine the response of these modules to multiple pulse signals.

5.3.2 Interaction of adaptive and bistable threshold modules

In this subsection we analyse the interaction of the adaptive and bistable modules. Fig. 5.4 shows three cases depicting this interaction. In each case, the adaptive module is subjected to a step change in input, and an adapting output is produced on three different timescales, corresponding to different pulse durations (Fig. 5.4(a)). In the first case, where the step change in input produces a short pulse from the adaptive module, the output from the

bistable module also adapts (Fig. 5.4(b)). In the second case, where an intermediate pulse is produced by the adaptive module, the output of the bistable module again adapts, but there is a prolonged excursion before the system recovers to the basal state (Fig. 5.4(b)). In the third case, where the adaptive module produces a long pulse, there is a qualitative difference – the output of the bistable module does not adapt, and instead asymptotes to a new value (Fig. 5.4(c)).

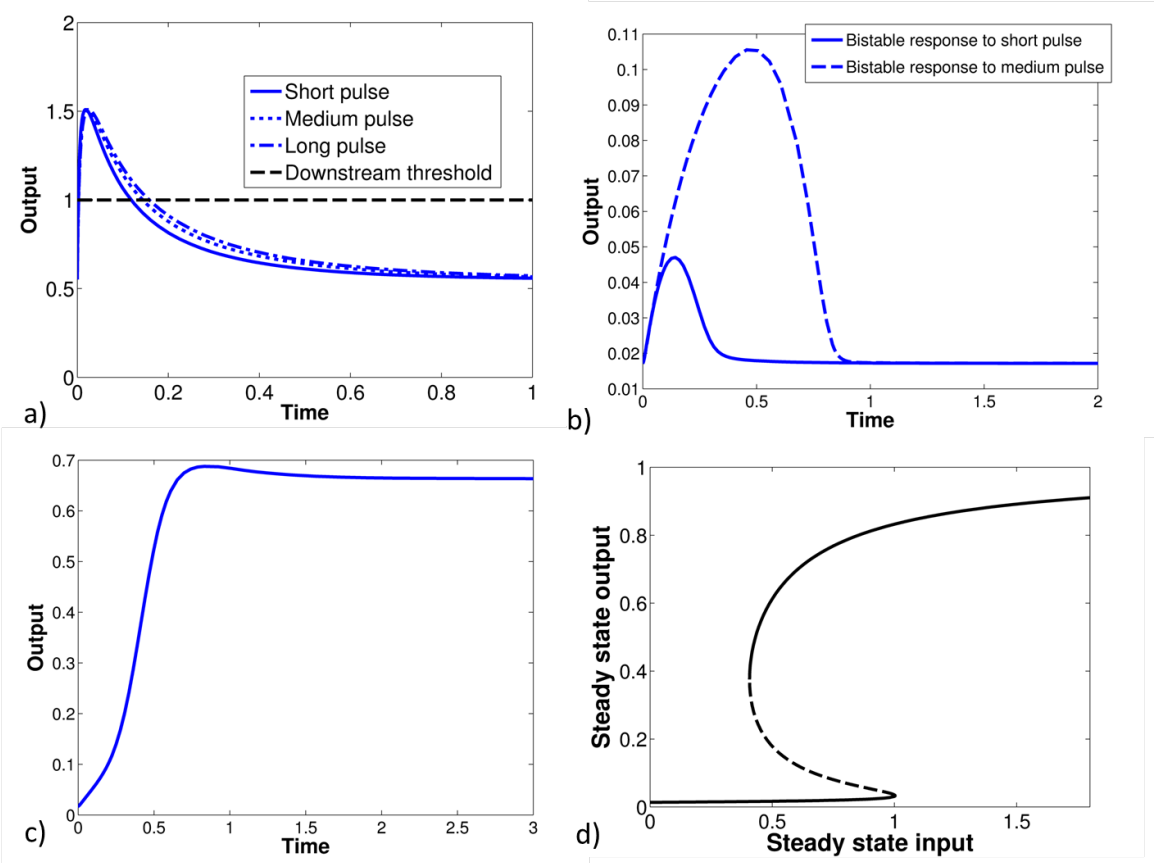

Figure 5.4: **Interaction of the adaptive module with the bistable threshold module**(a) The response of the adaptive module to a step change in input (at t = 0) for different rates of adaptation, resulting in pulses which we call short, medium and long. (b) The response of the downstream bistable module to short and medium pulses is shown. Switching does not occur. (c) The response of the downstream bistable module to a long pulse is shown, in which switching occurs. (d) The bifurcation diagram for the bistable switch is shown. The solid lines represent stable steady states, and the dashed line represents unstable steady states.

This behaviour can be understood intuitively as follows. In the last case, the output of the adaptive module causes the regulation of the bistable module into a regime where it is monostable. Further, this leads to the variables in the bistable module increasing in value in the monostable region. In the time taken for the output of the adaptive module to

essentially reach its basal value, the output of the bistable module (now back in the bistable region) is now in the basin of attraction of the upper stable steady state and eventually reaches this upper steady state. This behaviour can be systematically examined in greater depth. Intuitively, looking at the dynamics of the two modules, we recognize that the mere regulation of the output of the adaptive module into a regime where it corresponds to the monostable regime of the downstream module is not sufficient to induce this switching of steady states. For example, if the adaptive dynamics were much faster than the threshold dynamics, the switching behaviour would not be observed. Thus we expect that not only crossing into the monostable regime, but also spending sufficient time in the monostable regime, is needed for this switching to happen (for e.g. also see (Bhalla and Iyengar, 1999)).

The critical case which acts as a boundary between recovery to the basal steady state and switching to the elevated steady state corresponds to a special situation where the system asymptotes to the intermediate unstable steady state. We can now explore the critical amplitude or time duration of a pulse of a particular profile to result in switching. This is shown in a plot of critical pulse amplitude versus pulse duration for switching for different specific pulse profiles (Fig. 5.5). One specific case was that of a square pulse (Fig. 5.5 (a)). The second profile, which more closely resembles the output of an adaptive module, corresponds to a sharp increase followed by an exponential decay to basal levels. This is shown in Fig. 5.5(b). For a pulse (of a fixed rate of decay) whose amplitude is greater than the critical threshold shown in Fig.4(b), the output of the bistable module will result in switching. This critical curve was obtained using two methods. One was using simulations, varying the pulse amplitude systematically for each decay rate, analysing the asymptotic state and hence estimating the critical amplitude. A second way of estimating this curve was from the dynamic equations, by starting at the intermediate unstable steady state (at basal parameter values) and performing backwards time integration for the parameter variation (away from the basal value). The location (i.e. parameter value) at which the state variable reaches the basal prestimulus value provides an estimate for the critical amplitude. These two methods yielded indistinguishable results. The critical curve is plotted in Fig. 5.5(b). Also plotted in this figure is a conservative estimate for the amplitude of a pulse required to induce switching (see below): this is a sufficient condition for the amplitude of the pulse to result in switching, which can in certain cases be estimated analytically.

In general, it is difficult to analytically describe the signal processing and dynamics resulting from a transient signal interacting with a bistable system. In order to obtain some analytical insight into the interaction of adaptive signals with bistable switch-like modules,

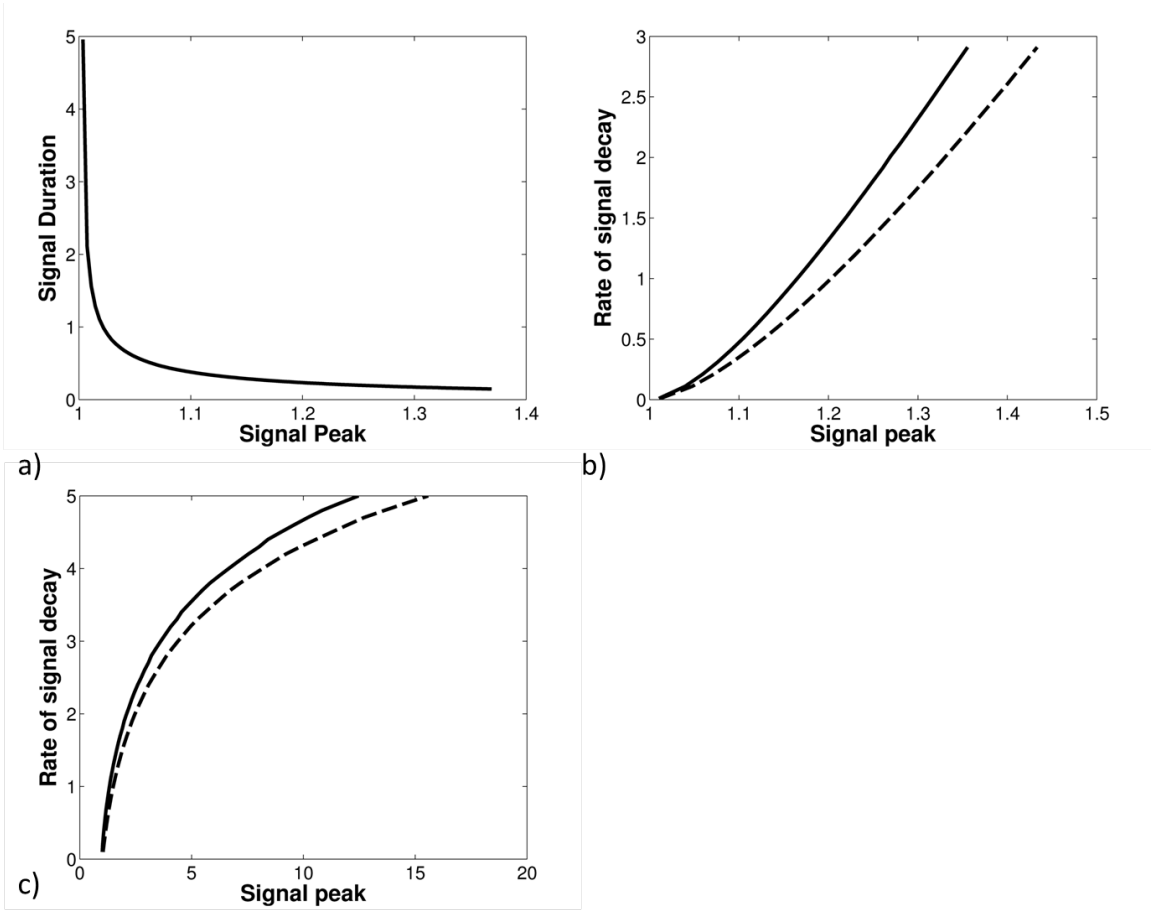

Figure 5.5: (a) We see the effect of pulse duration and amplitude to induce switching for a square pulse. The switching threshold is located at an input value of 1. We see that the critical duration needed becomes larger as the amplitude gets smaller as the bistable switch location is approached. (b) shows the critical curve for an exponential pulse, in terms of the amplitude and signal decay rate (solid curve). Also shown is the sufficient condition (dashed curve) needed to induce switching (see text). (c) A similar plot as (b), for the toy bistable switch.

we examine the simplified model of bistability discussed earlier.

Basic insight into the interaction of adaptive signals with this module can be obtained by varying S in a pulse-like manner starting from $S = S_0$ (and $z = 0$), where $0 < S_0 < 1$. We examine different pulse-like profiles for the temporal variation of the input S. The first is a square-pulse profile, where the input is changed to $S = S_1$ ($S_1 > 1$) for a time interval τ, and then immediately brought back to the basal value. Since, for this time interval, z is in the monostable regime and evolves according to the above equations, it immediately follows that at the end of this interval

$$z \;=\; 1 - exp(-\alpha\tau) \tag{5.12}$$

We immediately see that the condition for the upper steady state to be (asymptotically) reached is that, when the input is returned to basal values, z must be in the "basin of attraction" of the upper steady state (the "basin of attraction" of a stable steady state is defined as the set of states which asymptotically approach that steady state as time progresses), and so must be greater than the unstable intermediate state $(1 - S_0)$. Thus we must have

$$exp(-\alpha\tau) \;<\; S_0 \tag{5.13}$$

for switching, with equality in the above equation being the critical condition for switching. Clearly for any τ greater than the critical value switching will occur. Notice that for this model of bistability and for a square pulse, the condition for switching does not depend on the amplitude of the pulse. Equation 5.13 shows explicitly that a critical time duration for the activating signal to push the bistable module into a monostable regime is needed to activate the switch.

We now examine a profile similar to that examined above: the parameter is given an instantaneous jump to a value S_1 after which it decreases to its basal level at an exponential rate γ. Clearly, for a fixed amplitude a lower value of γ will work towards switching between steady states. This is seen in Fig. 5.5(c) where a plot of critical amplitude versus critical decay rate is shown. While it is difficult to estimate this curve analytically, for any particular decay rate it is possible to get a bound on the amplitude. This is done as follows. From the discussion above we note that a condition for the variable z to switch steady states is that it ends up in the basin of attraction of the upper steady state - it must attain a value greater than the intermediate steady state when S has essentially recovered to basal

value. Estimating the behaviour of z explicitly as a function of time in the bistable regime is difficult. However, a sufficient condition for the variable to end up eventually in the upper steady state is that when the parameter returns to the bistable regime ($S = 1$), the variable value is already above that of the intermediate unsteady state of the basal parameter value. This will guarantee switching to the elevated steady state. Note that for exponential decay, the time spent in the monostable region is

$$\tau = (1/\gamma)ln(S_1) \tag{5.14}$$

Therefore a sufficient condition for switching is $(1/\alpha)ln(1/S_0) < (1/\gamma)ln(S_1)$. This provides a bound on the critical amplitude and any S_1 above this value will result in switching.

The above analysis is easily generalised to any arbitrary variation of $S(t)$. If T is the time spent by the parameter in the monostable regime, then a sufficient condition for switching is

$$exp(-\alpha T) \quad < \quad S_0 \tag{5.15}$$

Note that this sufficient condition coincides with the necessary condition for switching for a square pulse signal.

5.3.3 Consequences of under- and overadaptation

While we have been concerned with analysis of exact adaptation, there exist a broad class of systems which exhibit only partial, or inexact, adaptation. In these systems, when the input is changed, there is a transient response in the output before it comes back to a new steady state, different from its initial steady state. In underadaptation this final steady state is above (below) the initial steady state after a transient increase (decrease), while in overadaptation the final steady state is below (above) the initial steady state after a transient increase (decrease). We note that the classification of a system as partially adapting, as opposed to simply being a system which overshoots its ultimate steady state, is an arbitrary one, but a reasonable distinction can be made based on the relative magnitude and duration of the overshooting (see Ma et al. (2009) for an example). Thus under- and overadapting systems possess two signalling processing abilities - steady state signal transduction, and pulse generation in response to rapid changes in input.

In this section we analyse the effects of under- and overadaptation for the two alternate

interconnections of adaptive and threshold modules - first with adaptation occurring upstream of the threshold, then with adaptation occurring downstream of the threshold. We pay particular attention to the differences between these systems and exactly adapting ones.

Adaptation upstream of the threshold

If the adaptive output begins below the threshold (so the switch is off), and the adaptive module is then subjected to a signal, there are two possible outcomes. As in the main text, similar results hold for the reversed case, where the adaptive output begins above the threshold (so the switch is on), and the adaptive module is then subjected to a decreased signal.

In the first case, the new steady state of the adaptive module may be located above the threshold. In this case switching will occur for both monostable and bistable threhsolds, whatever the timescale of changes in the input signal. This differs from the situation with an exactly adapting module, where switching depends on the characteristics of the pulse, and thus on the timescale of changes in the input signal. Here, no pulse is required - the switching is the result of the steady state signal transduction. We note further that, in the case of overadaptation, this provides a way for a decrease in the input to activate the switch. This happens because, while a decrease in the input will produce a negative pulse, the ultimate steady state lies above the original steady state, which may lie above the threshold and thus lead to activation.

In the second case, the new steady state of the adaptive module may remain below the threshold. Where the threshold is monostable, the system output will be very similar to that obtained with exact adaptation - pulses or no response, depending on the timescales involved (see Fig. 5.12). Where it is bistable, the adaptation to a new steady state may affect the duration and magnitude of the pulse required to achieve switching. This can be seen by analysing the response of bistable thresholds to square pulses with different initial and final states (square pulses are chosen because the location of the final steady state can be modified separately from the rest of the dynamics of the system). Fig. 5.6 shows a comparison of the bistable module responding to an exactly adapting step pulse (no switching occurs) and an underadapting one (switching does occur). This is due to the change in location of the unstable steady state before and after the pulse for underadaptation as opposed to exact adaptation - it comes down, rather than remaining the same. Thus during the pulse the system with exact adaptation cannot rise above its final unstable steady

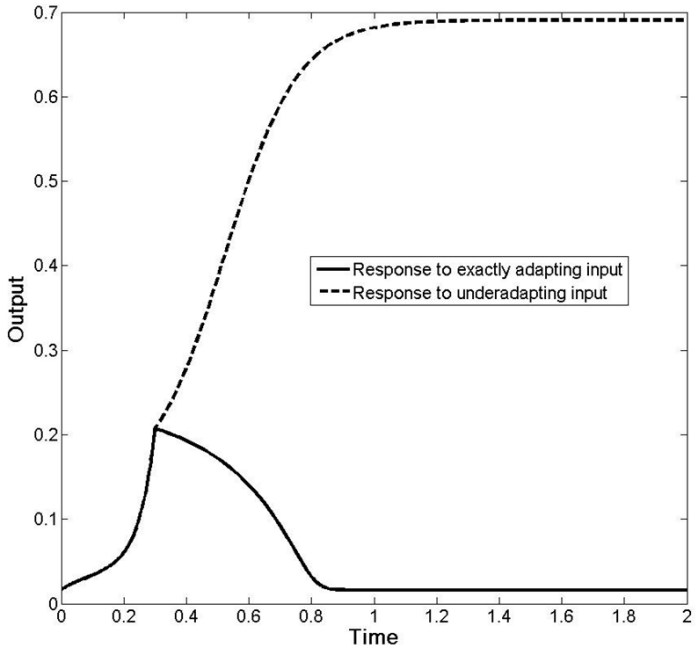

Figure 5.6: This figure shows how the output from an underadapting module may switch a downstream bistable module where an exactly adapting module will not.

state, while the system with underadaptation, with its new, lower unstable steady state, is able to rise above it. This can be seen by a simple modification of the expression for critical pulse duration (equation 5.13) for the toy model of bistability given by equation 5.8:

$$\tau > \alpha \ln (1/S_f) \tag{5.16}$$

In this case, S_f is the final steady state, replacing S_0 in the original expression (S_0 there represented both the initial and final steady states, but here the initial steady state is irrelevant because all lower stable steady states have the same location). This result shows how the duration of the pulse required for switching decreases for underadaptation, and increases for overadaptation. We note that these results depend not only on the properties of the bistable switch and, in particular, on the variation of the location of its stable and unstable steady states with the input.

Adaptation downstream of the threshold

When inexact adaptation occurs downstream of the threshold, the results are similar to those found for exact adaptation. The only difference is that inexact adaptation provides a mechanism for information on the current state of the threshold (on or off) to be propagated downstream of the adaptive module.

5.3.4 The processing of multiple-pulse (pulse train) signals by threshold modules

The analysis of the previous sections essentially focussed on the interaction of a pulse-like signal (output of the adaptive module) with threshold modules. In this section, we extend the analysis of the previous section by examining the response of these threshold modules to multiple-pulse (pulse train) signals, since this is also relevant to how threshold modules process transient input signals.

Processing of multiple-pulse signals by monostable threshold modules

We first examine how multiple-pulse signals are processed by monostable threshold modules. To do this we examine square pulse signals where the signal period is T, and a fraction of this period α corresponds to the pulse, where the signal strength is S_1; the signal strength

is the basal level S_0 for the remaining time. The systematic variation of the parameter α allows us to examine the effect of different signal pofiles, ranging from narrow pulses (small α) to broad pulses (α closer to 1). The monostable threshold responds to narrow pulse inputs with periodic, small increases from the lower steady state, and responds to broad pulses with periodic, small decreases from the upper steady state. Examples of these two situations are seen in Fig. 5.7 in the case of the Goldbeter-Koshland switch. We note that $\alpha = 1$ corresponds to permanent elevation of the signal.

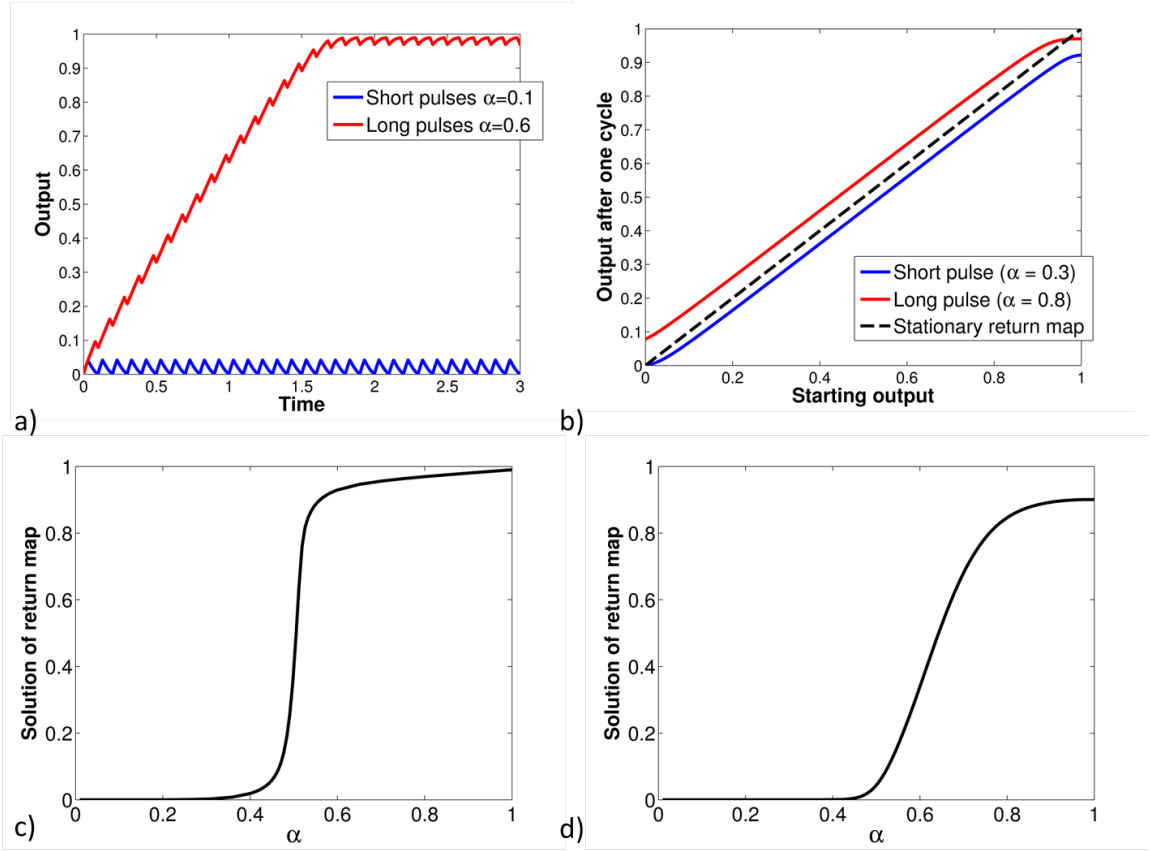

Figure 5.7: This figure shows how the monostable Goldbeter-Koshland switch responds to multiple-pulse inputs. (a) shows how the output may oscillate about either extreme state, depending on the duration of the pulses. (b) shows the corresponding return map. The linearity of this return map across a wide range of states outside the extreme states explains the observation of (a). (c) shows the location of the stable periodic output as a function of α. (d) shows a plot analogous to (c) but for the MAPK model. We see that in contract to (c), this curve as a function of α is less sharp.

Simulations were also performed with intermediate values of α. Two cases are observed regarding the periodic solutions centred around intermediate values of the output for intermediate values of α, depending on the model of the monostable threshold used.

In the case of the Goldbeter-Koshland model of the monostable threshold, such solutions are rarely found. This is shown in the bifurcation diagram shown in Fig. 5.7(c), where, interestingly, the periodic solutions tend to be centered around the upper and lower steady states.

We studied this further by examining the result of time integration of the module for a time equal to the period of the pulse train (y_1) and how it depended on the starting point (y_0). We note that if the result of integration for this period equals the initial value, then this implies that the trajectory is a periodic trajectory of the forced dynamical system.

The result is plotted in Fig. 5.7(b) for two different α values. Plotted on the y-axis is the variable value after one time period as a function of its starting level. This result can in fact be estimated analytically for a whole range of y-values. Due to the behaviour of the Goldbeter-Koshland model, the dynamics of the variable on either side of the switch threshold is linear. This results in a plot of this function (i.e. the final value as a function of the initial value) which is in fact linear for a range of y-values. Thus for $\alpha = 0.3$, we see a linear plot for a wide range of y-values which does not intersect the line $y = x$. This line is curved near the extremities, and intersects this line very close to $(x, y) = (0, 0)$. This in turn corresponds to a periodic solution which represents relatively small amplitude perturbations about the base (zero) state. An exactly analogous result may be seen for high values of $\alpha = 0.8$ where the intersection is close to $(x, y) = (1, 1)$. Examining an intermediate value $\alpha = 0.6$ shows however that the intersection is still quite close to the upper extremity. In fact, owing to the shape of the function under consideration and that it is linear for a wide range (and parallel to $y = x$), we may expect intersections relatively close to the extremities. The function above may also be explicitly written analytically when y_0 is far away from the extremities (under which conditions dy/dt is practically constant). In fact, for the case of a periodic signal between $S = 0$ and $S = 1$ (chosen for simplicity) we find that

$$y_1 \;=\; y_0 + (V_1 - V_2)\alpha T - V_2(T - \alpha T) \tag{5.17}$$

We see here that the second term on the right hand side corresponds to the increase for the fraction of the time the signal is above the threshold and the third term corresponds to the decrease for the fraction of the time the signal is at basal levels (below the threshold). The main point is that irrespective of α and T, this curve is a straight line parallel to $y = x$. Thus for y_0 values away from the extremities (where this analysis holds) this curve will not

exhibit any fixed point (i.e. cross the line $y = x$), and so no periodic solutions away from the extremities may be observed. This is clearly seen in Fig. 5.7(c), showing the location of the stable periodic output (as the solution of the fixed point of the return map $y_1 = y_0$) as a function of α.

In the case of the MAPK and Heaviside function models of monostable thresholds, periodic solutions centred around intermediate values of the output are observed. This is seen for the MAPK cascade in the bifurcation diagram shown in Fig. 5.7(d), and we further note that increasing the number of stages in the cascade leads to a considerable reduction in the amplitude of the response (as in Fig. 5.3c)). For the Heaviside function model, the intermediate periodic solution may be obtained explicitly by analysis of the return map (which is a plot of the result of integration of the module, for one time period, as a function of the starting point). This results in

$$y_1 \quad = \quad exp(-kT(1-\alpha)) - (1-y_0)exp(-kT) \tag{5.18}$$

where y_1 represents the output integration for one time period, starting from $y = y_0$. The above equation reveals that a nontrivial fixed-point of the return map ($y_1 = y_0$) –which corresponds to a periodic response–may be obtained explicitly. The fact that this fixed point exhibits intermediate values between 0 and 1 as the parameters are varied provides a direct indication that a periodic output whose maximum and minimum lie between 0 and 1 is the result.

Processing of multiple-pulse signals by bistable threshold modules

We now examine the analogous situation in the context of the bistable module. Fig.5.8(a) shows two situations. In the first case, for relatively small α we have (relatively small amplitude) periodic perturbations about the basal state, these being induced by periods in the monostable regime. In Fig.5.8(a) we also see the response of the system to broader pulses, and we see that after a few periods the system evolves to a periodic solution which is based about the upper steady state. A few things must be pointed out in this context. Firstly, this periodic pulse-like signal in effect induces switching. Thus even if the pulse signals were subsequently switched off, the system would end up in the upper steady state. Secondly, this switching occurs in response to this multiple-pulse input even though it did not occur in response to a single pulse of the same amplitude and duration as one of these

pulses. This is an example of switching induced by a finite number of pulses, and indicates another aspect of the interaction of pulse-like signals and bistable modules.

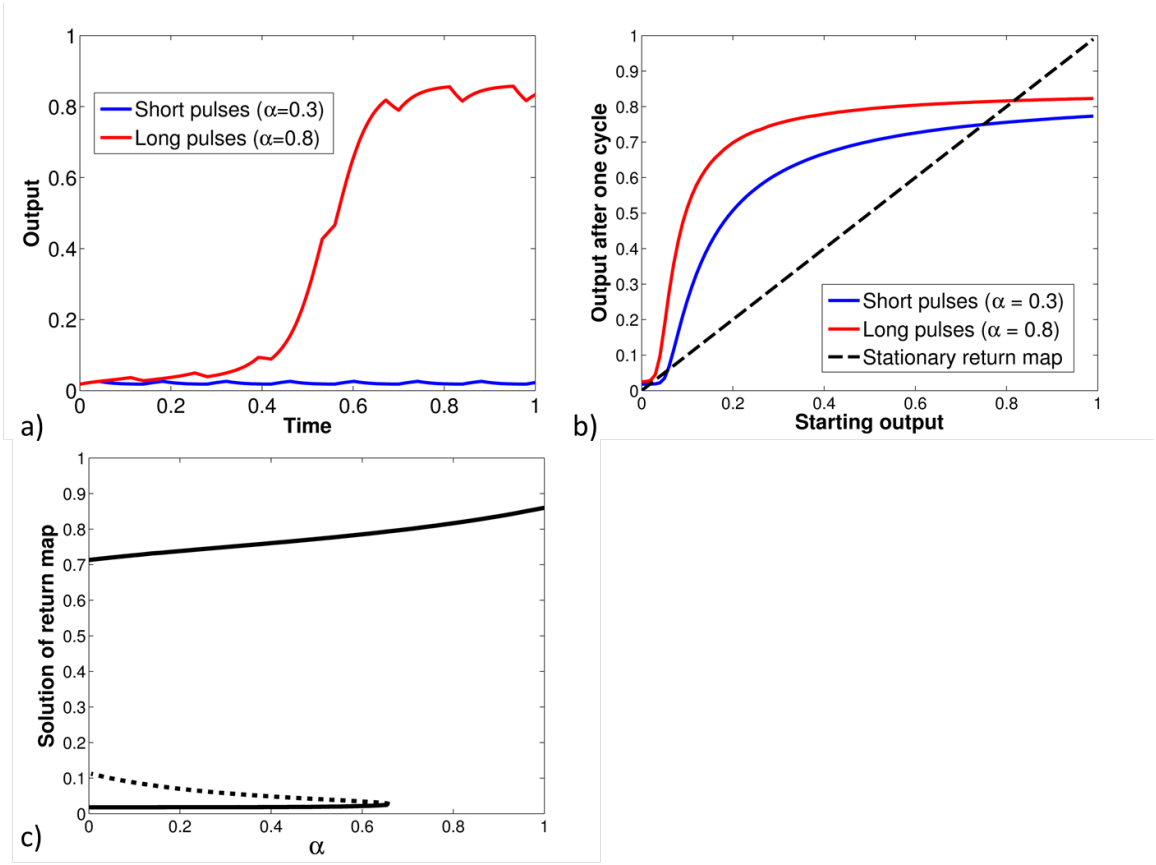

Figure 5.8: (a) We see the effect of two different multiple pulse inputs to the bistable module $\alpha = 0.3$ and $\alpha = 0.8$ –the latter induces switching while the former doesn't. This is explained by the return map (b), indicating two stable fixed points for $\alpha = 0.3$ and one for $\alpha = 0.8$. (c) displays the solution of the return map as a function of α. The solid curves correspond to points in attracting periodic solutions, while the dashed curve corresponds to points in repelling periodic solutions.

Further insight into the response of this bistable module can be obtained by examining the return map constructed numerically by evaluating the output at the end of a single pulse period. Fig. 5.8(b) shows the return map for two different values of α. We notice here that for low α there are three intersections of the return map with the line $y = x$. Thus we have two periodic solutions roughly based about the stable steady states, but also another intermediate periodic solution. This intermediate solution is in fact unstable. Thus this is not observed in simulations. Gradually increasing the α value results in this intermediate periodic solution getting extinguished in a saddle-node bifurcation at a critical value of α. For higher values of α only the periodic solution based about the upper branch exists. This

is seen in the bifurcation diagram shown in Fig. 5.8(c). For low values of α, the return map suggests that any finite number of pulses (of this amplitude) will not result in the other stable steady to be reached. On the other hand for higher values of α, as noted above, the return map has only one fixed point. Here a finite number of pulses can indeed guarantee that the upper steady state is reached eventually.

To summarize, the analysis of the return map complements the analysis performed for the monostable situation. In contrast to that case, the bistable threshold module exhibits two stable periodic solutions and an intermediate unstable periodic solution. As the parameter α is increased, a saddle node bifurcation results in only one stable periodic solution. Thus, there is a sharp transition leading to qualitatively different periodic output.

5.3.5 Inducing switching in bistable networks

The previous sections highlighted many aspects of the interaction of adaptive signal transduction and threshold processes, both monostable and bistable. We analyzed this interaction by means of specific representative modules of adaptation and bistability. In particular, this entailed postulating specific regulation of a bistable process. In the case we considered, the adaptive signal was able to activate a bistable switch by pushing the system into the monostable regime transiently. Bistable switches (in response to steady signals) also rely typically on a signal pushing them into a monostable regime. In taking a systems approach to the interaction of adaptive signals and bistable networks, other questions arise. Do other interconnections of adaptive signals and bistable networks result in switching of steady states? Does the switching necessarily occur through an essentially similar scenario? Is it possible for bistable networks to be induced to switch steady states without ever transiently leaving the bistable regime?

We will examine whether a transient upstream signal (such as that arising from an upstream adaptive module) can result in switching of steady states in a bistable network without ever pushing this network into a monostable regime. To obtain some insight into these systems questions, rather than build specific examples of bistable networks, we will work with simplified models which distil the dynamical systems essence of the problem. A bistable network is typically some system involving one or more variables which is governed by an underlying dynamical system (governing the kinetics of the reactions of the network). This network, by assumption, has two stable steady states. Furthermore, an adaptive signal regulates this network by modulating or affecting one or more reaction rates

(enzymatic regulation). This is done so that the network never leaves the bistable regime. This means that at any instant, the instantaneous value of the parameter is one which results in bistability.The variables of the network respond dynamically to the change in network dynamics induced by this signal.

We describe the bistable network dynamics in the simplest possible way by means of a bistable model. From our point of view, we work with a single variable model, which has three steady states, two of which are stable. Since we anticipate that the location of the roots plays an important role we choose a simple explicit form for the model:

$$du/dt \;=\; -a(u-u_1(S))(u-u_2(S))(u-u_3(S)) \tag{5.19}$$

The variable u represents a typical variable of the network which responds under its dynamics. Its dynamics is modulated by some upstream signal S. This upstream signal may regulate the location of the roots u_1, u_2, u_3 (we assume that $u_1 < u_2 < u_3$), and we will assume that it will do so in an adaptive way. Thus these parameters will display adaptive dynamics and recover to basal values exactly. The variable u will be assumed to be initially at the stable steady state $u1$, but all the essential insights carry through when starting at the other stable steady state, u_3.

This setting allows us to examine a few issues in a more general manner. The signal could regulate each of these parameters in an independent and very different way. We start by considering the case where the system starts at the lower steady state $u = u_1$ and u_1, u_2, u_3 are all subject to a transient increase before reaching their basal state. This describes the dynamics of a bistable system with a particular class of adaptive modulation.

Using this model, we can immediately make some quite general conclusions. Firstly, if the adaptive dynamics are much faster than the intrinsic dynamics of the bistable network (parametrized by a), the system barely registers the change and the system remains very close to the basal state. The other extreme case, where the adaptive dynamics are much slower than the intrinsic dynamics of the bistable network, is also worth examining. In this case, u_1, u_2, u_3 are slowly varying and so the system instantaneously adjusts to these slowly varying parameters. Since the system starts out at $u = u_1$, it ends up tracking the slow variation of this steady state. Thus, neither of these extreme cases will lead to switching of steady states. We then look at the intermediate case, where the dynamics of the two modules are of comparable timescales. The resulting behaviour is shown in Fig. 5.9. In this case, we see that the bistable network variable, u, starts to decrease to basal

values after an initial increase (this corresponds geometrically to the root u_1 crossing below the trajectory of u). However, as it decreases, the root u_2 also crosses the trajectory of u, and thus the system is in the basin of attraction of the upper steady state u_3, and eventually reaches this steady state. This is an example of steady state switching induced by the adaptive modulation of a bistable network without the system ever leaving the bistable regime. An examination of this case reveals the core underlying factors responsible: the system evolves in such a way that it ends up in a region which belongs to the basin of attraction of a different steady state at basal conditions.

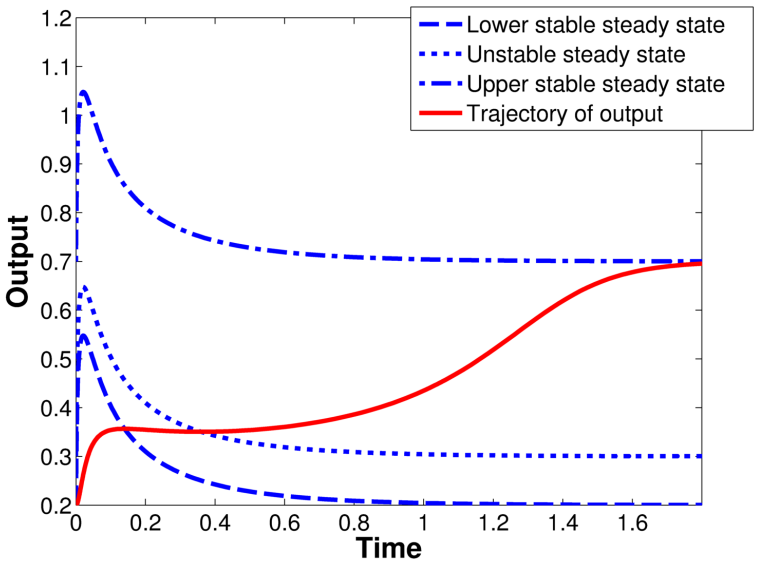

Figure 5.9: We see the effect of adaptive module of the features of the simple model and how switching of steady states can be induced by a transient signal without every leaving the bistable regime. Depicted are the adaptive dynamics of the parameters u_1, u_2, u_3 (dashed lines) and the system response (dark line).

Other scenarios can similarly be examined. For instance, in the above example, a very similar situation can be observed if all the roots decrease to a point such that the system ends up in the basin of attraction of the upper steady state and remains there in the subsequent recovery to basal conditions. This suggests the key elements involved in switching steady states through adaptive signalling. There are two possibilities. In one case the location of the roots initially changes rapidly, so that the system is in the basin of attraction of a different steady state. This is followed by a slow recovery of the roots to their basal values, ensuring that for all subsequent instants the system is in the basin of attraction of the new steady state. In the second case the location of the roots initially changes slowly, with the

system tracking the root at which it started out. This is followed by a rapid recovery of the roots to their basal values, putting the system in the basin of attraction of a different steady state. These represent non-trivial insights into how transient signals can induce switching in bistable networks without the networks ever transiently becoming monostable.

The above examples all dealt with cases of roots increasing or decreasing together. Obviously this is not necessary, as the main point is that this behaviour pushes the system into the basin of attraction of a different steady state. Clearly, different examples with different variations of the three roots can be analyzed which give rise to the same switching. Finally, another point to be emphasized is that while our discussion above was based on one-dimensional systems, all the relevant points essentially generalize to multiple dimensional systems. Again, transient signals may regulate the relevant steady state locations and basins of attraction (corresponding to the instantaneous value of the signal) and possibly orchestrate a transition between steady states similar to that discussed above.

While our discussion of transitions between steady states in the bistable regime was discussed in terms of movement of the location of steady states of a simple model, it is worth asking if there are biochemical systems which exhibit such behaviour. We have not identified such a system, and the simple biochemical models considered here do not seem to allow for this behaviour, but it will be interesting to see whether some of the more complex bistable networks postulated in the literature (e.g. (Bhalla and Iyengar, 1999; Thomson and Gunawardena, 2009)) are capable of being controlled in this manner.

In summary, our studies suggest that it is possible for transient signals to induce switching between steady states in bistable networks (which always remain bistable) under certain conditions. In essence, our analysis reveals a few points. The modulation of the bistable network must neither be too fast nor too slow (relative to its intrinsic timescale) for this to happen. In fact, two parallel scenarios have been demonstrated. In the first, the modulation of the bistable network involves a fast change followed by a slow recovery to basal values. In the second, the modulation involves a slow change followed by a relatively fast recovery. Thus we notice that a concatenation of slow and fast modulation can induce switching in this bistable network even though neither fast modulation nor slow modulation by themselves can achieve this.

5.3.6 Analysis of the processing of time-varying signals

Thus far, we have only examined the response of the combined system of adaptive and threshold modules to step changes in input. In this section, we examine the nature of signal processing of the same connection of modules to complex temporal signals. This is important for several reasons. Firstly, it expands our understanding of signal transduction through this composite module. Secondly, in understanding the role of adaptive signal transduction in complex cellular systems, a key point is to understand how upstream time-varying signals are received and processed into pulse-like signals. Thirdly, adaptation is often postulated as a key element in gradient sensing (either temporal or spatial) and it has been suggested that downstream amplification may occur through some threshold processes. Finally, understanding how the upstream adaptive module deals with temporal signals will provide insight into how the adaptive module deals with inputs when it is the downstream module (see following section). With these points in mind we analyze the response of the modules to inputs which vary with time.

We begin by noting that it can be shown analytically for the model of adaptation investigated here that the output adapts to a constant linear temporal gradient (see (Seaton and Krishnan, 2011a) for details). With this as a basis we can understand the output of the combined modules in response to a constant temporal gradient. If the gradient is very weak, then hardly any change from the basal state is observed. This is because for practically all the time evolution, A and I are essentially proportional and slowly varying, and hence the adaptive module produces a very small deviation from basal conditions. When the gradient is strong then a non-trivial response is observed. We first examine the response of the adaptive module connected to a monostable threshold module. In this case we find that a transient output is obtained provided the output of the adaptive module crosses the threshold of the downstream module. Thus if the gradient is weak no output response is observed (results not shown). Another point to be noted is that if a negative gradient were given (for a finite time), no output would be observed either, simply because the output of the adaptive module moves further away from the threshold. In the case of a bistable module, two kinds of non-trivial behaviour may be observed. If the gradient is not too strong, then the output may result in a transient change before a recovery to the basal state. On the other hand if the gradient is strong, it may be possible for the system to asymptote to the other stable state purely in response to the gradient. These scenarios are depicted in Fig. 5.10. This response indicates that gradient sensing can lead to switching steady states, provided that the

gradient is steep enough. This is of importance with regard to how a system may process further time varying signals. While the analysis of adaptation to linear gradients above is based on the activator-inhibitor model, very similar behaviour is obtained for other adaptation models in sensory transduction like the well-known Barkai-Leibler model (Barkai and Leibler, 1997) of bacterial chemotaxis. We also note that some temporal adaptive modules may display a response where a non-adaptive response dependent on the gradient strength may be obtained.

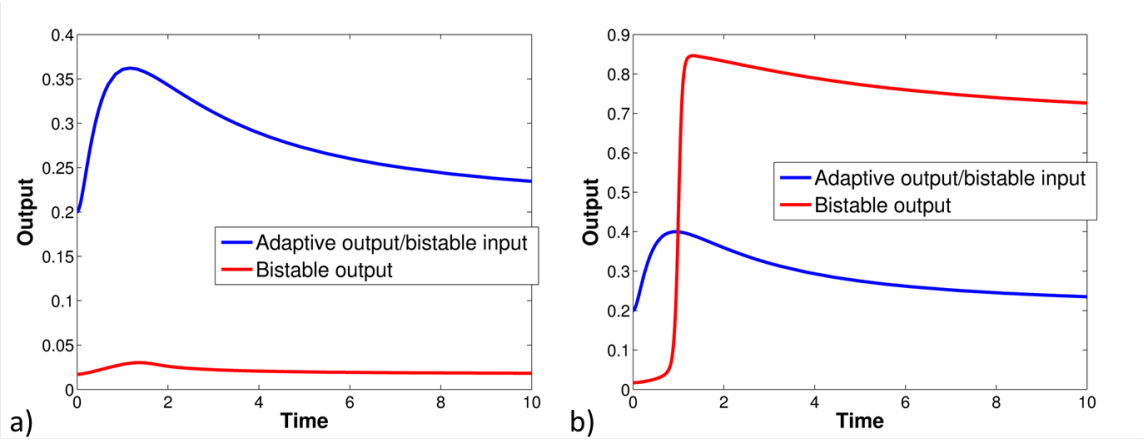

Figure 5.10: The effect of two different ramp signals is shown here.(a) When the signal is increased from $S = 1$ to $S = 10$ in 3 time units, the output from the bistable module adapts. (b) When the same increase is effected over 2 time units, the output of the bistable module indicates switching. Thus the steepness of the gradient could have a substantial effect on downstream response.

Taken together, we can make a few conclusions about the gradient response of the combined modules. The output of the adaptive module considered to a constant gradient is in fact adaptive. Thus a monostable module will provide a transient response, acting as a simple threshold filter. Furthermore, negative gradients are not registered by this combination of modules, at least in the case considered, where the threshold module begins in the lower state. In the bistable case, a gradient could also induce switching of steady states, if the gradient is strong enough. Overall this analysis points to the possible qualitative changes in signal propagation in adaptive signalling pathways in response to gradients, in particular when interacting with downstream thresholds.

5.3.7 Alternate interconnection of modules

Another aspect which directly relates to the interaction of adaptive and threshold modules is the order in which they are connected. In all the cases considered so far the adaptive module was upstream of the threshold module. In this subsection, we will analyze the opposite case. In order to do this, we consider the case where the external signal regulates the threshold module and the output of the threshold module is the input to the adaptive module. Thus, the adaptive module receives a time-varying signal. We now examine the effect of a step change in input to the threshold module. If the step change in input is still below the threshold of the switch module, the response from the threshold module is, at best, very weak and the output of the adaptive module is negligible. This is true for both the monostable and bistable threshold modules. If the step change in input results in the threshold being exceeded, the threshold module reaches a markedly elevated steady state. The response of the downstream adaptive module then depends on the relative timescales of the adaptive and threshold modules. If the adaptive module is much slower than the threshold module, the response will be a transient increase followed by recovery to basal levels (see Fig. 5.11). The amplitude of the transient jump is related to the magnitude of the switch, and the speed of switching. We observe from Fig. 5.11 that if the upstream switch is effected quickly, the output of the downstream module is a sharp robust pulse. This robustness is the result of the fast transition between the two states of the switch being processed as a step change by the adaptive module. On the other hand, if the switch is effected relatively gradually, a much smaller pulse is seen from the downstream module. If the adaptive module dynamics are much faster than the threshold module, then even a switch will elicit very little response.

Exactly the same kinds of conclusions can be reached regarding the response of modules to step decreases. In this case, the monostable module will register a decrease, and the response of the adaptive module is to cause a transient decrease. In the case of the bistable threshold module, if the system is originally in the upper branch of steady states, then a step decrease can lead to the system ending up in the lower branch of steady states, and in this case the adaptive module (if slower than the threshold module) will convert this signal into a transient decrease.

In summary the presence of the adaptive module downstream of threshold modules has a completely different effect when compared to being upstream of the threshold module. The adaptive module converts switch-like signals to transient pulse like signals and also

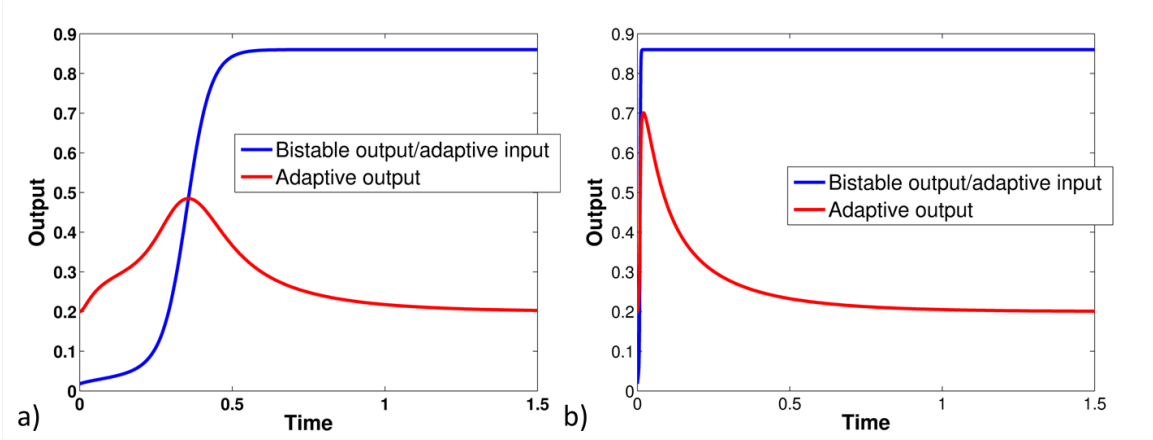

Figure 5.11: The response of the system in this alternate interconnection of modules is shown, when subject to a step change in input at $t = 0$. (a)We see that the output is a pulse-like signal which registers when the upstream threshold is crossed (b) If the threshold module is relatively slow, a smaller amplitude pulse is seen.

encodes information about the direction of the switch. Thus this interconnection could be a way to generate robust pulse-like signals. When the adaptive module has slower dynamics, the output of this system is essentially a binary pulse. A summary of the interaction of adaptive and threshold modules is presented in Fig. 5.12.

5.4 Conclusions

In this chapter we performed an investigation of the interaction of adaptive and threshold processes from a modular systems perspective (see Fig. 5.12). Given the ubiquitous presence of adaptive as well as threshold processes and their importance in signal transduction in reaction networks, this is a natural systems investigation from the perspective of signal transduction. Our aim was to understand the essential ways in which adaptive and threshold modules interacted from the perspective of signal processing, and to distill some basic insights which may be broadly applicable in biological signal transduction. To analyze the interaction of adaptive and threshold modules, we chose representative modules for each case.

In general, while we made specific choices for our modules, our insights are more general than the context in which they were obtained. A dynamical systems approach is implicit in the choice of modules and simplified models, the kinds of analysis performed, and it is the insights from such an approach which suggest that many of these conclusions are generalizable to more complex networks.

Timescale of...		Function
Adaptive module relative to input	**Threshold module relative to adaptive module**	
Fast	Slow or fast	No signal processing
Slow	Fast	Possible switching (if the threshold is bistable) or pulse generation with filtering
Slow	Slow	No signal processing

a)

Timescale of adaptive module relative to threshold module	Function
Slow	Robust pulse generation
Fast	No signal processing

b)

Figure 5.12: This figure shows how the functionality of the system depends on the interconnection of system modules and on their relative timescales, in some limiting cases. Other cases, in which timescales of the different modules are comparable, are less clear-cut. Note that the input in all cases is considered to be a simple step - inputs such as ramp or oscillatory inputs are not considered here and the amplitude of the input signal is assumed to be sufficient to activate downstream processes. Very small inputs, whatever their timescale, will not produce any response.

Both threshold modules acted as filters for the transient, pulse-like signals. In contrast to the monostable module, the bistable module was able to result in switching even from transient signals, and we analysed how this switching depends on the characteristics of the transient signal. This suggests that altering some basic, even apparently minor, characteristics of the signalling which generates the pulse-like signal can cause a fundamentally different downstream response. An examination of multiple-pulse regulation of threshold modules revealed similar characteristics; in addition, it was shown that a finite number of pulses may induce switching where a single pulse did not. These insights are broadly relevant to the triggering of switches by transient signals.

While our analysis of bistable modules revealed that steady state switching could be induced by transient signals by regulation to a monostable regime, we also investigated a broader issue – whether steady state switching could be induced in bistable systems by transient signals without the bistable network ever transiently leaving the region of bistability. The analysis was performed on a simplified generic model, and revealed that such steady state switching could indeed be induced by transient signals without leaving the bistable regime. It was found that if the dynamics of the modulating adaptive signal were either too fast or too slow compared to the bistable module such switching would never occur. Switching induced by the adaptive module could be induced under certain circumstances via a combination of slow and fast signals. The additional significance of this point is that, while bistable modules/networks in cells may work as switches in response to some signals in the usual way, other signals could modulate these networks to induce switching without the system leaving a bistable regime. The above analyses thus reveal different aspects of the interaction of pulse-like signals with bistable networks.

Further to our analysis of the response of the combined modules to step changes in input, our investigation of the response to a temporal gradient revealed that the output was adaptive in some cases, whereas switching could be induced in other cases if the downstream threshold module was bistable. It should be pointed out that, for certain adaptive modules, a gradient may not always lead to adaptation. Finally, we investigated the effect of having a threshold module upstream of an adaptive module. This configuration was shown to produce pulsatile signals when the threshold is crossed. We have also suggested that such a configuration could be a mechanism for robust pulse generation in signal transduction.

It is worth examining what kinds of signal processing capabilities are generated by both of the sequential interconnections of modules that we have analyzed, and what possible advantages each configuration may have. Adaptive and threshold modules represent opposites

from a steady state signalling perspective. In general it is worth asking what the presence of the downstream module brings to the upstream module. If the upstream module is an adaptive module then a downstream threshold module acts as a filter; more importantly, a downstream bistable threshold module may lead to switching and non-adaptive dynamics. Further, this switching is triggered by sufficiently fast varying input signals, of sufficient amplitude. On the other hand, if the adaptive module is downstream of the threshold module, then this allows for the possibility of counteracting the permanent elevation of signals and masking certain downstream targets from this. In each case the presence of the downstream module brings a very distinct mode of signal processing, which is very different from alternative (essentially) linear modules. It is possible that both these modules may be present as downstream pathways in addition to (essentially) linear modules, thus offering differing modes of signal propagation.

In conclusion, we have demonstrated a range of complex behaviours that may be generated by the combination of two simple and ubiquitously seen components of cellular signalling networks - adaptive and threshold modules. This chapter has provided insights which may be relevant in a number of biological contexts. It shows how monostable and bistable switches respond to transient signals, and how these may have a permanent effect. It also provides insights into how these threshold modules may amplify signals in the context of specific biological processes, such as gradient sensing.

Chapter 6

Principles of dynamic regulation of the budding yeast cell cycle

6.1 Introduction

The cell cycle is the process by which cells alternate replication of their DNA with cell division. As a central process in the life of a cell, it is subject to multiple forms of regulation. These range from hormonal and growth factor signals in higher organisms, down to nutrient and temperature signals in micro-organisms. Together, these combined regulations dictate not only the lifetime of a single cell, but the distribution of cell cycle progression across a population of cells, whether in culture or in tissue. While there has been progress in understanding the mechanisms driving cell cycle progression, and identification of some signalling pathways responsible for the modulation of this progression, a system-level understanding of how signals regulate the progression of the cell cycle has been lacking. In this chapter, a framework is developed and applied to the investigation of the dynamic response of the cell cycle to perturbations. In particular the coordination of external conditions with the cell cycle of a particular model organism - the budding yeast *Saccharomyces cerevisiae* - with cell growth and environmental conditions is investigated through a detailed sensitivity analysis of multiple mathematical models of the process, taken from the literature.

The progression of the cell cycle in eukaryotic cells can be divided into four phases: G1, S, G2, and M phase. Cells are born in G1 phase, and remain in G1 phase until DNA synthesis is initiated. This event marks the beginning of S phase. Upon completion of DNA

replication, the cell enters G2 phase, until progressing through mitosis in M phase. The G1 and G2 ("gap") phases then mark the pauses between the essential processes of DNA duplication and separation. A wide variety of checkpoint mechanisms regulate progression through the cell cycle. These checkpoints act to ensure that progression through the cell cycle occurs only when the cell is in a suitable environment, and has adequately completed the previous stages of the cell cycle. For example, cells in G1 (with unreplicated DNA) must pass a checkpoint to go into S phase and begin synthesising DNA. This checkpoint is regulated by factors such as nutrient availability, growth rate, and the size of the cell (Ferrezuelo et al., 2012; Jorgensen and Tyers, 2004). Similarly, cells in the G2 phase must pass through checkpoints to enter mitosis (one such checkpoint requires that the DNA has been duplicated), and checkpoints exist at different stages of mitosis (e.g. the spindle alignment checkpoint).

The prevailing view of the cell cycle mechanism is one of interlocking positive and negative feedback loops which trigger this cascade of transitions (Tyson and Novak, 2008). One of the central components in the cell cycle network is cyclin-dependent kinase (CDK). A pre-requisite for the kinase activity of Cdk1 during the cell cycle is the presence of cyclins. Different cyclins are expressed in different phases of the cell cycle and lend specificity to the CDK-cyclin complex, allowing regulation of many transcription factors and other processes (Csikasz-Nagy et al., 2009). These cyclins may be broadly divided into Starter cyclins, responsible for the transition from G1 into S phase, and Mitotic cyclins, responsible for the transition from G2 into M phase. The abundance of cyclins is heavily regulated at the levels of transcription, translation, and degradation. In addition, the CDK-cyclin complex may be rendered inactive by phosphorylation, or inhibited by binding to stoichiometric inhibitors such as Far1 and Sic1. These additional regulatory factors also form feedback loops, and as a result their levels also oscillate with the cell cycle progression. The cell cycle is completed by an increase in the activity of the Anaphase Promoting Complex (APC), which degrades cyclins, allowing the cell to progress through anaphase and cytokinesis. The basic progression through the cell cycle is then guided by these oscillations, and is shown in figure 6.1. As shown, the cell is born with low but increasing levels of Starter cyclins. When the level of Starter cyclin reaches a threshold, S-phase is initiated. Levels of Starter cyclins then decrease, with a complementary increase in Mitotic cyclins maintaining Cdk activity. After sufficient time for progression through mitosis and the satisfaction of additional checkpoints, CDK inhibitors and components responsible for cyclin degradation (such as the APC) become active. This rapidly depletes CDK activity,

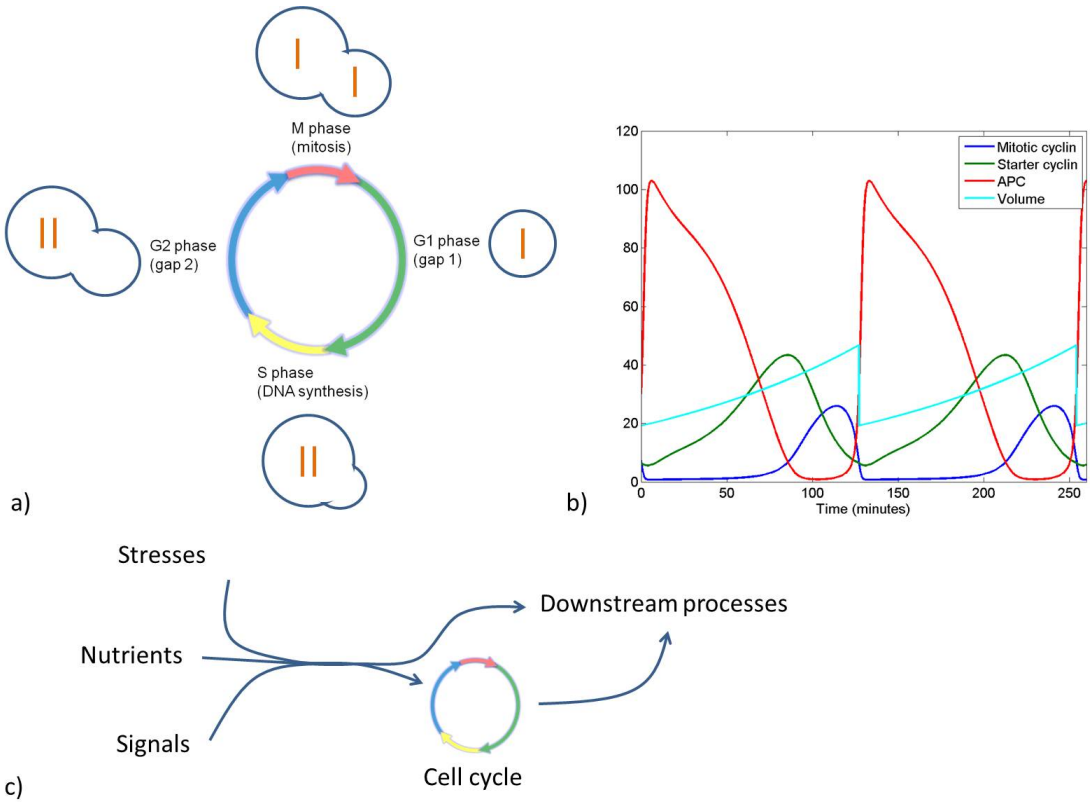

Figure 6.1: a) A schematic of the essential characteristics of the budding yeast cell cycle is shown, illustrating the coordination between cell cycle progression and changes in cell morphology (i.e. budding). b) The dynamics of some key cell cycle components are shown, along with the changes in cell volume, across two cycles. The discontinuous change in volume marks the point of cell division. c) A schematic of the essential signalling structure is shown, emphasising the centrality of the cell cycle as a complex process capable of processing information in sophisticated ways.

allowing cytokinesis to occur and a new cell to be produced.

Cell cycle progression is a complex and highly regulated process. This is a result of the importance of the processes it coordinates, and of the flexibility of response required in changing conditions. Extracellular signals such as nutrients and osmotic stress change the rate of progression through different phases. Cell cycle progression is also regulated by other complex intracellular processes - for example, a gating effect of circadian rhythms on the cell cycle has been observed in cyanobacteria (Yang et al., 2010). In higher organisms cell division is regulated by signals such as growth factors (Schwank and Basler, 2010; Ulloa and Briscoe, 2007) and cell-extracellular matrix interactions (Streuli, 2009), allowing patterning and control over properties such as organ size. In addition to these levels of complexity in regulation of the cell cycle in normally proliferating cells, there is also the

role the cell cycle plays in allowing differentiation to other cell types or modes of development. A striking example of this is the switch to meiotic cycles, in which two rounds of division are performed without an intervening round of DNA replication. In some species, including yeast, this switch precedes sporulation. Another clear example is the (reversible) switch from proliferation to quiescence. In summary, the diversity of regulation of the cell cycle, and its plasticity across species, cell types, and environments, demonstrates the complexity which must be dealt with in studying this process.

The complexity inherent in cell cycle regulation has been addressed, in part, by experimental investigation of cell cycle progression in model organisms such as the budding yeast, *Saccharomyces cerevisiae*, which is the particular case studied here. The budding yeast cell cycle follows a simple pattern of growth and division, as depicted in figure 6.1. After birth, the cell grows isotropically during the G1 phase. The duration of this phase is strongly correlated with the size of the cell as a result of a "cell size checkpoint". Beyond this checkpoint, the cell is allowed to pass into S phase. Upon entry to S phase, DNA replication begins and a bud forms. Cell growth continues, but now all new growth is directed into the bud. The cell then passes through the G2 and M phases and begins the process of cytokinesis. This results in the bud splitting from the mother cell, producing a new daughter cell. The size of this daughter is generally smaller than the mother cell, and under some conditions it is much smaller than the mother cell. The fraction of cell mass passed on to the daughter cell depends in a simple way on the durations of the cell cycle phases post- and pre- budding (see following sections, and (Charvin et al., 2009)).

The distinct morphology of budding yeast - in particular the correspondence between the initiation of S-phase and the appearance of the bud - mean that it has been a useful model organism for the study of the cell cycle. The budding yeast cell cycle has been observed to respond to a wide variety of changes in external conditions. For example, addition of glucose to cells growing in ethanol elicits changes in both the average size of the cells at bud initiation, and the duration of the cell cycle. The cell cycle is also regulated by changes in other nutrient signals (Broach, 2012; Cai and Tu, 2012; Zaman et al., 2008, 2009), osmotic stress (Hohmann, 2002), and temperature (Spriggs et al., 2010). In addition, it has long been known that under certain conditions the cell cycles of a population of budding yeast cells can spontaneously exhibit partial synchronisation with an oxidative metabolic cycle (Tu et al., 2005). Finally, manipulation of cell cycle controls to make cyclin production inducible by an externally controlled signal has demonstrated the feasibility of mode locking the cell cycle to a periodic stimulus (Charvin et al., 2009).

Despite the rapid accumulation of knowledge of the molecular details of the cell cycle mechanism and its regulation, such are the number of pathways and the complexity of the cell cycle engine that it is difficult to predict *a priori* how the cell cycle will respond to changes in conditions. As a result, it is also difficult to evaluate the significance of experimental observations and determine whether an observed phenomenon can be accounted for by the known regulatory mechanisms. To this end, mathematical modelling approaches are useful to investigate hypotheses about regulation of the cell cycle. Models describing the dynamics of essential cell cycle components have been around for some time, and have reached high levels of complexity in the past decade (Barik et al., 2010; Chen et al., 2000, 2004). In this chapter, a systems framework is developed for the investigation of the dynamic regulatory capabilities of cell cycle models, and by extension the cell cycle. In this chapter we develop an input-output systems framework to understand the interaction and co-ordination between size, growth and growth landmarks and the cell cycle, and their regulation by extracellular signals. This is developed in the concrete case of budding yeast, to understand the interaction of external signals, the cell cycle, size and budding. Working within this framework, we examine how the cell cycle might respond to changes in conditions, both dynamic and sustained and employ a selection of models for this purpose. In this investigation, particular focus is placed on analysis of the most recent model of the Tyson group (Barik et al., 2010). However, by performing this analysis on all parameters in several models, behaviours and characteristics displayed by multiple models can be identified. This allows several key questions about cell cycle regulation to be addressed. For example: to what extent can key cell cycle characteristics such as period and size at division be regulated independently? What qualitative behaviours can be observed in the response of the cell cycle to a sudden change in conditions? How flexible can this dynamic response be for a given eventual change in behaviour?

6.2 Models of the cell cycle

In this section, a basic mathematical description of the budding yeast cell cycle is given. This describes the phenomenology of cell cycle progression, rather than the biochemical details. Specifically, under some simple assumptions about the growth of the cell, it is possible to interrelate macroscopic cell cycle properties such as daughter cell size, cell cycle duration, and cell size at budding. This mathematical description then provides a basic framework for understanding the detailed models that follow. These detailed models

are ODE models of the cell cycle, including both budding-yeast specific models and general models adapted here for use with budding yeast. The nature of the alterations made here to the cell cycle models, amounting merely to the setting of thresholds for the occurrence of budding at appropriate times during the cell cycle, is also discussed.

6.2.1 Basic mathematical description of the cell cycle

All of the models considered share the same essential behaviour, alternating between division and budding. The volume of the cell at these points, and their relative timing, constitute a simple description of the dynamics. This model incorporates the assumptions that growth is exponential (Di Talia et al., 2007) (growing at an exponential rate μ), that all growth after budding is localised to the bud, and that the daughter cell receives all of the mass of the bud. The variables of interest are the cell cycle period (i.e. the time from birth to division, denoted T_{div}), the time from birth to budding (denoted T_{bud}), the size of the cell at division (denoted V_{div}), at budding (denoted V_{bud}), the size of the daughter cell (also the size of the cell at birth, denoted V_{dau}), and the fraction of the cell volume given to the daughter cell after division (denoted f). At constant growth rate, these variables are interrelated according to the following expressions:

$$\begin{aligned} V_{div} &= V_{dau} e^{\mu T_{div}} \\ V_{bud} &= V_{dau} e^{\mu T_{bud}} \\ f &= V_{dau}/V_{div} \end{aligned} \tag{6.1}$$

All models considered here give a pattern of behaviour that can be related directly to this simple description, after slight alteration to include a budding event where appropriate. The differences between the models of the budding yeast cell cycle then come from the quantitative details of their parameters and their dynamic response.

6.2.2 Selection of suitable models to investigate

In this section, the models analysed are described, concentrating on the intended purpose of the models, and their level of detail. The number of variables and parameters used in each model are also given. For more complete descriptions, schematics, model equations,

and basal parameter values, reference should be made to the appropriate papers. The three models of the Tyson group are listed first, in chronological order, followed by two simpler, less mechanistic models, from Sriram et al (Sriram et al., 2007) and Pfeuty and Kaneko (Pfeuty and Kaneko, 2007). The models of the Tyson group are chosen so that they span approximately five-year intervals in the development of the models. This automatically introduces variation in the model structures, allowing evaluation of which model properties are generic and which are specific to a particular model. The most recent detailed of the Tyson group appears in (Barik et al., 2010), and it is that model on which many example analyses are performed. Examples of other types of models of the budding yeast cell cycle in the literature include Boolean and stochastic models . The ODE formalism of models is chosen for several reasons. First, several models have been developed using this formalism. Second, it provides a level of detail that allows the investigation of how incremental changes in parameters change the system behaviour. Such investigation is not possible with Boolean network models. Third, a useful and straightforward framework exists for the calculation and interpretation of sensitivity analysis. Such analysis is necessarily more complex in the stochastic case. It should further be noted that models that just consider particular phases of the cell cycle (e.g. models of the G1-S transition (Adrover et al., 2011; Barberis et al., 2007) or mitosis are not suitable for investigation here, since they cannot be run across multiple cycles. The code used to simulate and analyse all models is provided in the digital appendices, as documented in Appendix E.0.5.

The Chen model

The first detailed model of the budding yeast cell cycle considered is that of Chen et al (Chen et al., 2000) (more specifically, the moderately reduced version of this model considered in (Battogtokh and Tyson, 2004)), referred to here simply as the Chen model. This model brought together a large quantity of literature data to give a molecular cell cycle model that displayed the correct pattern of behaviour in the wild type, and in a large number of cell cycle mutants.

This model contains multiple "hybrid" aspects, in which multiple events are controlled by concentrations of cell cycle components passing through specified checkpoints, at which point a rule is applied. These aspects make the original Chen model substantially different from the other models considered here. However, a simplification of the Chen model is derived by Battogtokh et al (Battogtokh and Tyson, 2004) for the purpose of bifurcation

analysis. Multiple simplifications of the Chen model are derived in (Battogtokh and Tyson, 2004) - the most complex variation is used here in order to represent the Chen model.

The Csikasz-Nagy model

The Ciskasz-Nagy model of the cell cycle (Csikasz-Nagy et al., 2006) was developed in a modular form to establish the manner in which the same model structure can describe the cell cycle of different eukaryotes simply by changing the choice of parameters and the selection of modules. The parameter set used here, therefore, is the parameter set identified in (Csikasz-Nagy et al., 2006) as being capable of representing the dynamics of the budding yeast cell cycle.

The Barik model

The Barik model of the cell cycle was based upon the previous models of the Tyson group, with several modifications. The model contains pure mass-action kinetics. This was done so that stochastic simulations of the model could be performed to relate the noise characteristics of the model's performance to experimental observations. The model contains the main cell cycle mechanisms, such as the positive feedback between starter cyclins and Whi5. While it is a complex model, and contains many unknown parameters constrained by a relatively small quantity of experimental data, it contains multiple simplifications of known biology. These include the lumping of many species considered to have partially redundant roles (such as Cln1/2, the cyclins involved in S phase initiation, and Bck2, which is partially redundant with Cln3). Further, some cell cycle regulatory elements are missing completely from this model, even if they were present in previous models (e.g. the Cdk inhibitor Sic1).

The Sriram model

The Sriram model of the cell cycle consists of parallel negative and positive feedback loops. The negative feedback loop consists of a three species joined by three negative regulatory interactions (a so-called "repressilator" structure), representing the post-translational mechanisms of regulation between the Cln-Cdk, Clb-Cdk, and Sic1. The positive feedback loop consists of three species joined by three positive regulatory interactions, representing the transcriptional regulation of the cell cycle .

This model is only an abstract representation of the cell cycle mechanisms. This is clear from the symmetry of the model structure, the abstract nature of the species (the components are not assigned to specific cell cycle components), and the symmetry of the parameter choices (which are the same for many of the regulatory interactions). Nonetheless, it is useful to include in the present investigation since it captures much of the essential behaviour of the cell cycle. Therefore, it provides some idea of what features of the cell cycle are specific to the series of models developed by the Tyson group, and which are more general, and may be features of many other models of the cell cycle with the same basic behaviour.

The Pfeuty model

The Pfeuty model is the simplest model considered here, and was developed as a generic model of the eukaryotic cell cycle in order to study the coordination of growth with cell cycle progression (Pfeuty and Kaneko, 2007). In this case, there are three variables: one representing the mass of the cell, and two variables representing cell cycle components, in a negative feedback. In this case, one variable represents components involved in the transition into S-phase, whose activity is suppressed by a component responsible for instigating mitosis and, eventually, cytokinesis, as represented by the second variable.

This model is included in this investigation in order to give an idea of which cell cycle features identified in complex models can be captured by very simple models such as this one.

6.2.3 Adapting models to include the effects of budding

One of the key aspects of the budding yeast cell cycle is the asymmetric division of the cells. As discussed above, growth following budding is localised to the bud, meaning that the duration of the budded phase determines the size of the daughter cell. The daughter cell will then, in general, be different in size to its mother. This asymmetry has important implications for the regulation of cell size and period in different conditions. For example, the extent of asymmetry decreases with increasing growth rate (Charvin et al., 2009). However, in the models listed, asymmetry was either not taken into account, or the asymmetry was fixed.

In order to capture the relevant behaviour, it is necessary to modify the models so that

asymmetric division occurs, and so that the extent of asymmetry depends on the dynamics of the cell cycle. Given the role of the cyclins Cln1,2 in regulating the initiation of budding, it is natural to include a threshold mechanism whereby budding is initiated when Cln1,2 increase beyond a critical concentration. By recording the size of the cell at budding and comparing it to the size at division, it is then possible to simulate the regulation of asymmetric division. The species chosen as initiating budding, and the value of the thresholds, are listed in table.

The values of the thresholds were chosen such that the mass fraction of the cell given to the daughter was in the biological range (taken to be 0.35-0.45) for the growth rates chosen. An additional constraint on this choice was the dynamics of the species responsible for initiating budding - it needs to pass through an appreciable threshold at an appropriate time during the cycle.

6.3 Steady state sensitivity analysis

As a first step towards understanding how the cell cycle may respond to signals, a parametric sensitivity analysis of the cell cycle models is performed. This allows identification of the types of control that may be exerted on the cell cycle through modulation of particular parameters. In order to be confident of the generality of the results, it is important to find patterns in the sensitivity which can be observed for multiple parameters and models, rather than analysing the consequences of one model's sensitivity to changes in one parameter.

We begin by analysing the sensitivity of the cell cycle at steady state. Here, the term "steady state sensitivity analysis" is used to refer to the situation in which parameters are constant with time and the oscillations have converged to a consistent, well-defined oscillatory behaviour (recognising the distinction with a scenario in which a system as converged to a fixed point). In contrast, "dynamic sensitivity analysis" refers to the response of the system as parameters are varied dynamically (see section 6.4 for details). The sensitivity analysis is done locally, using the basal set of parameters originally used in the development of each model, as published. The extent to which the models respond linearly to changes in parameters is evaluated by comparing the accuracy of first- and second-order approximations of behaviour. It is then shown that cell cycle characteristics such as the cell cycle period and size at division can be controlled in identical ways by many different combinations of parameters.

Given the asymmetric division of budding yeast, the generation-on-generation increase

in size of mother cells, and the consequent diversity of cells in a real population, it is necessary to define precisely what is meant by the "steady state" conditions at which the sensitivity analysis is performed. Simulations of asymmetrically dividing cells must necessarily choose one cell lineage to track as the basal case, as the alternative is to simulate all cells in a population. This is infeasible for models of the complexity considered here. As mentioned, in this case, the mother cell retains whatever mass it creates before budding with each generation, meaning that its size at the beginning of each new cycle increases steadily. A lineage of mother cells is then clearly unsuitable as the basal state, as the size/state of the cells at birth diverge over time. On the other hand, a lineage of daughters-of-daughters do converge to a constant state at birth for all models considered, making this the natural state to consider as the basal state. Other choices might include daughters of an alternating sequence of mothers and daughters, but such choices are less natural. Of course, the fraction of cells that are the progeny of first daughters going back several generations is likely to be very small in any population.

The sensitivity of an observable quantity, Q, to relative changes in a parameter, k_i, is defined by:

$$C_{k_i}^{Q} = k_i \frac{dQ}{dk_i} \tag{6.2}$$

Here, Q can be any of several observable quantities, such as the relative phases of the peaks of different cyclins, the magnitude of the peak level of cyclin inhibitors, or the timing of cell cycle events such as kinetochore attachment. Such a general approach has been taken in the analysis of circadian rhythms (Rand et al., 2004). However, in the case of *Saccharomyces cerevisiae*, as discussed above, most experiments on the behaviour of the cell cycle have concentrated on the changes in the timing of budding and division and their coordination with the cell's size. This is also true of the theoretical investigations. For the purposes of simplicity, therefore, these are the characteristics investigated here.

In order to perform sensitivity analysis for a sustained change in parameters, the models are first simulated from given initial conditions over multiple cycles until the state of the cell at the beginning of the cell cycle had converged. At this point, the parameter is changed in a step-wise fashion and the simulation continued, again until convergence of the state at the beginning of one cycle. For the step change, the parameter under consideration was multiplied by a factor of 1.001, corresponding to a 0.1% change in the parameter. This was found to be a large enough change to make the sensitivity measurements unaffected by

numerical errors in the ODE solver, but small enough to give an accurate measure of the first-derivative of the observables to changes in the parameter. The solver used was ode15s, in MATLAB, run with absolute and relative tolerances of 10^{-10}. Repeating the analysis with tolerances of 10^{-13} had no significant effect on the results. The code used to perform this analysis is provided in the digital appendices, as documented in Appendix E.0.5.

Having simulated cell cycle behaviour with the basal and perturbed sets of parameters, it is possible to calculate the sensitivity of the observables to changes in the parameter in question according to:

$$C_{k_i}^{Q} \approx k_i \frac{\Delta Q}{\Delta k_i} \tag{6.3}$$

Where $\Delta Q = Q_{perturbed} - Q_{basal}$ and $\Delta k_i / k_i = 0.001$. For a given parameter perturbation, this sensitivity gives a first-order estimate of the change in behaviour:

$$\Delta Q_{1^{st}} = \frac{\Delta k_i}{k_i} . C_{k_i}^{Q} \tag{6.4}$$

The second derivative of an observable quantity with respect to a parameter change, labelled $D_{k_i}^{Q}$, can be approximated numerically as follows:

$$D_{k_i}^{Q} = \frac{k_i^2 (Q_{perturbed,2} - 2Q_{perturbed,1} + Q_{basal})}{2\Delta k_i^2} \tag{6.5}$$

Here, $Q_{perturbed,1}$ and $Q_{perturbed,2}$ denotes the behaviour after parameter changes of Δk_i and $2\Delta k_i$, respectively. When combined with the sensitivity, $C_{k_i}^{Q}$, this provides a second-order estimate of the change in behaviour:

$$\Delta Q_{2^{nd}} = \frac{\Delta k_i}{k_i} . C_{k_i}^{Q} + \frac{\Delta k_i^2}{k_i^2} . D_{k_i}^{Q} \tag{6.6}$$

Comparisons of the predictions produced using first- and second-order approximations to the sensitivity of the cell cycle period (denoted T_{div}) are shown in figure 6.3 for several parameters. The difference in magnitude of $\Delta T_{div,2^{nd}}$ compared to $\Delta T_{div,1^{st}}$ gives an idea the extent to which the linear approximation is useful. It is possible to calculate the relative change in a parameter required to produce a given relative difference between the first- and second-order approximations (labelled "x" below) as follows:

$$\begin{aligned}
\frac{\Delta T_{div,1^{st}} - \Delta T_{div,2^{nd}}}{\Delta T_{div,1^{st}}} &= x \\
\Rightarrow (1-x).\frac{\Delta k_i}{k_i}.C^Q_{k_i} &= \frac{\Delta k_i}{k_i}.C^Q_{k_i} + \frac{\Delta k_i^2}{k_i^2}.D^Q_{k_i} \\
\Rightarrow -x.\frac{\Delta k_i}{k_i}.C^Q_{k_i} &= \frac{\Delta k_i^2}{k_i^2}.D^Q_{k_i} \\
\Rightarrow \frac{\Delta k_i}{k_i} &= -x.\frac{C^Q_{k_i}}{D^Q_{k_i}}
\end{aligned} \tag{6.7}$$

The cumulative distribution of parameter perturbations required to give a 10% difference ($x = 0.1$) between $\Delta T_{div,1^{st}}$ and $\Delta T_{div,2^{nd}}$ is shown in figure 6.2. This demonstrates that the model responses to parameter perturbations are significantly nonlinear. For example, a majority of parameters display a greater than 10% difference between $\Delta T_{div,1^{st}}$ and $\Delta T_{div,2^{nd}}$ for a parameter perturbation of 10%. This significant nonlinearity is as expected from the model structures and behaviour. Nevertheless, the application of linear analysis to these models can serve as a first step towards understanding how they work.

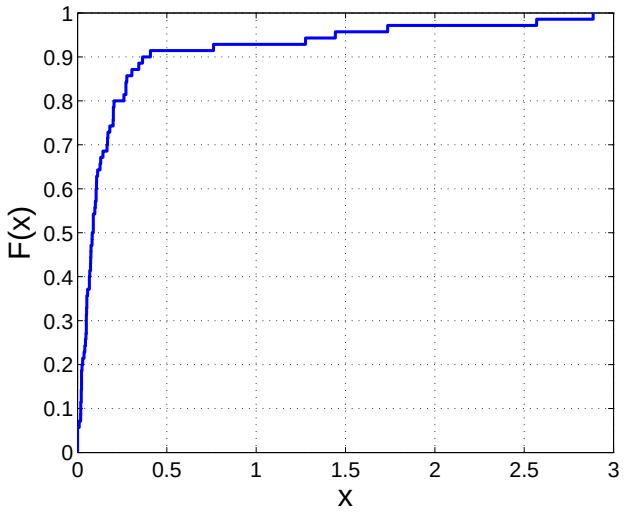

Figure 6.2: The cumulative distribution of the proportion of parameters in the Barik model for which a relative parameter change of less than $x(= \Delta k/k)$ (i.e. $x = 1$ corresponds to a 100% change in the parameter) results in difference in the estimates of less than 10%.

As mentioned above, the variables of interest are the cell cycle period (i.e. the time from birth to division, denoted T_{div}), the time from birth to budding (denoted T_{bud}), the size of

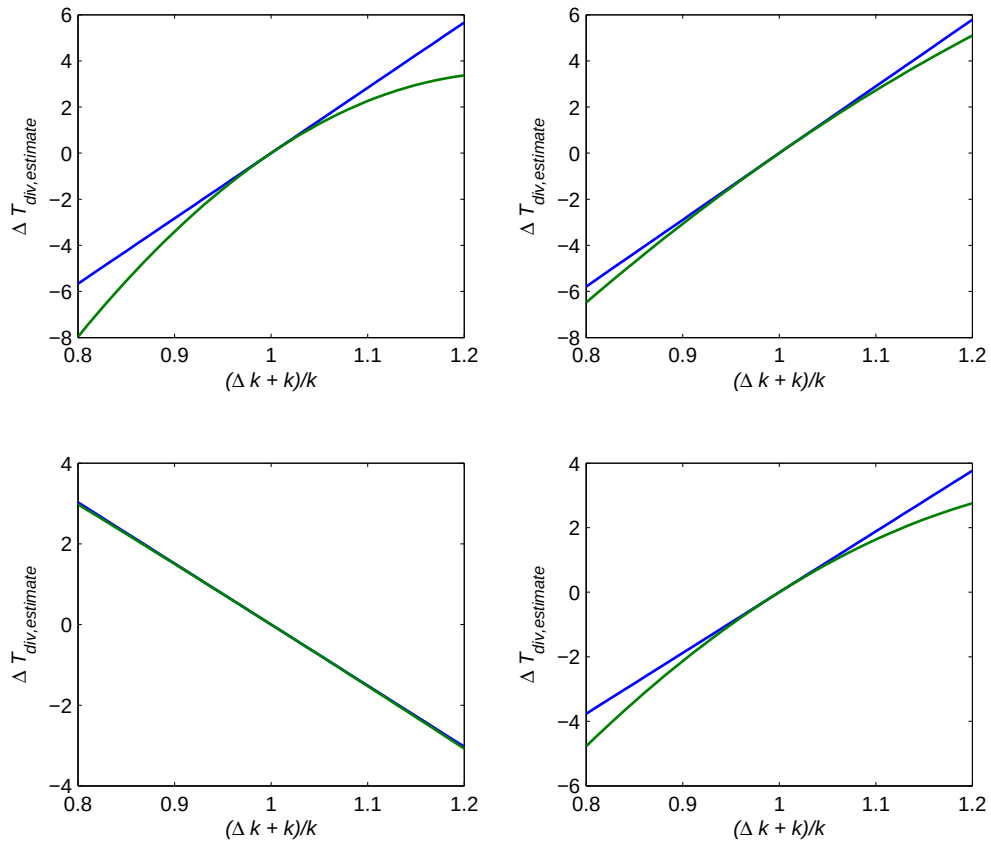

Figure 6.3: Examples of how the first- and second-order estimates diverge for some example parameters are shown. The parameters involved are a) the rate of translation of mitotic cyclin, k_{sbm}, b) the rate of phosphorylation of Whi5 by starter cyclins, k_{pi5p}, c) the rate of Whi5 dephosphorylation by Hi5, k_{di5}, and d) the rate of degradation of Ht1 mRNA g_{dmht1}.

the cell at division (denoted V_{div}), at budding (denoted V_{bud}), the size of the daughter cell (also the size of the cell at birth, denoted V_{dau}), and the fraction of the cell volume given to the daughter cell after division (denoted f). As discussed previously, at constant growth rate, these variables are interrelated according to the following expressions:

$$\begin{aligned} V_{div} &= V_{dau} e^{\mu T_{div}} \\ V_{bud} &= V_{dau} e^{\mu T_{bud}} \\ f &= V_{dau}/V_{div} \end{aligned} \tag{6.8}$$

From equation 6.8 it is clear that these variables are not independent of one another. For example, the budded duration and daughter cell size can be calculated directly from the cell cycle period and division size, according to:

$$\begin{aligned} V_{dau} &= V_{div}e^{-\mu T_{div}} \\ T_{div} - T_{bud} = \frac{ln(V_{dau}/V_{bud})}{\mu} &= \frac{ln(V_{dau}/(V_{div} - V_{dau}))}{\mu} \end{aligned} \tag{6.9}$$

Therefore, there are only two independent variables under constant conditions. This means that the sensitivity of the cell cycle to a perturbation of parameter k_i under constant conditions can be reduced to the sensitivity of V_{div} and T_{div} to this parameter (denoted $C_{k_i}^{V_{div}}$ and $C_{k_i}^{T_{div}}$, respectively). It should be emphasised that the cell cycle "behaviour" in this context is the pattern of phase durations and cell sizes in those phases. Other characteristics, such as the amplitude and phase of the various cell cycle components, will in general be different between perturbations even when the timing and sizes are the same, but the analysis described here can be applied to these other characteristics in a similar way.

The results of performing this sensitivity analysis on all models are shown in figure 6.4. This figure summarises information about how these cell cycle characteristics can be modified under constant conditions by the parameters in each model. In particular, given a perturbation $\delta\eta$ $(= (\delta k_i/k_i, \delta k_j/k_j)^T)$, the resultant change in the cell cycle behaviour is given by:

$$\begin{pmatrix} \delta V_{div} \\ \delta T_{div} \end{pmatrix} = \begin{pmatrix} \delta k_i/k_i \\ \delta k_j/k_j \end{pmatrix} \begin{pmatrix} C_{k_i}^{V_{div}} & C_{k_j}^{V_{div}} \\ C_{k_i}^{T_{div}} & C_{k_j}^{T_{div}} \end{pmatrix} \tag{6.10}$$

In the case where the sensitivities $C_k^{V_{div}}$ and $C_k^{T_{div}}$ are linearly independent for the two parameters, k_i and k_j, it is possible to calculate the perturbation of these two parameters necessary to produce a given change in behaviour (note that there are many parameters which are linearly dependent - this property will be evaluated quantitatively in a subsequent section):

$$\delta\eta = \begin{pmatrix} \delta k_i/k_i \\ \delta k_j/k_j \end{pmatrix} = \begin{pmatrix} C_{k_i}^{V_{div}} & C_{k_j}^{V_{div}} \\ C_{k_i}^{T_{div}} & C_{k_j}^{T_{div}} \end{pmatrix}^{-1} \begin{pmatrix} \delta V_{div} \\ \delta T_{div} \end{pmatrix} \tag{6.11}$$

The solution to this equation is unique - there is only one perturbation of these two

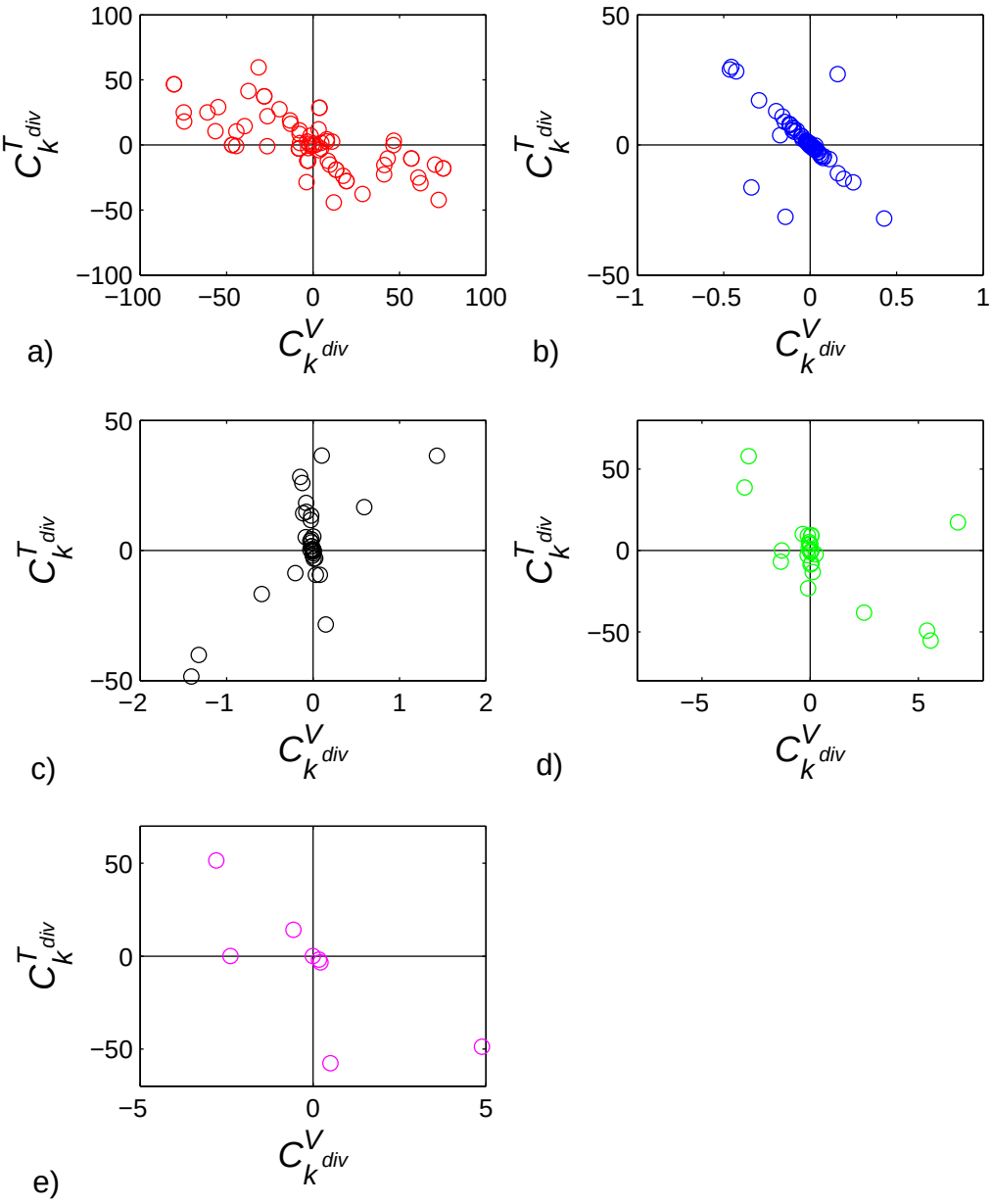

Figure 6.4: The $C_k^{T_{div}}$ and $C_k^{V_{div}}$ for parameters in a) the Barik model, b) the Csikasz-Nagy model, c) the Chen model, d) the Sriram model, and e) the Pfeuty model. The spread of sensitivities, especially in the case of the Barik model, give some indication of the regulatory flexibility available.

parameters which produces the given change in behaviour. If a third parameter, *k*, is introduced, however, a vector of parameter perturbations is obtained through:

$$\delta\eta = \begin{pmatrix} \delta k_i/k_i \\ \delta k_j/k_j \\ \delta k_k/k_k \end{pmatrix} = \begin{pmatrix} C_{k_i}^{V_{div}} & C_{k_j}^{V_{div}} & C_{k_k}^{V_{div}} \\ C_{k_i}^{T_{div}} & C_{k_j}^{T_{div}} & C_{k_k}^{T_{div}} \\ 0 & 0 & 1 \end{pmatrix}^{-1} \begin{pmatrix} \delta V_{div} \\ \delta T_{div} \\ \theta \end{pmatrix} \tag{6.12}$$

In this case, θ parameterises the vector of perturbations which produce the same eventual change in behaviour, such that $\theta = \delta k_k/k_k$. An equivalent representation which makes this explicit is given by:

$$\delta\eta = \begin{pmatrix} \delta k_i/k_i \\ \delta k_j/k_j \end{pmatrix} = \begin{pmatrix} C_{k_i}^{V_{div}} & C_{k_j}^{V_{div}} \\ C_{k_i}^{T_{div}} & C_{k_j}^{T_{div}} \end{pmatrix}^{-1} \left[\begin{pmatrix} \delta V_{div} \\ \delta T_{div} \end{pmatrix} - \theta \begin{pmatrix} C_{k_k}^{V_{div}} \\ C_{k_k}^{T_{div}} \end{pmatrix} \right] \tag{6.13}$$

This equation can be generalised to cases in which more than three parameters are perturbed:

$$\delta\eta = C_{(i,j)}^{-1}(\delta Q - C_{(k_1,k_2,...,k_n)\theta}) \tag{6.14}$$

where $C_{(i,j)}$ is 2×2 matrix of sensitivities of the characteristics Q with respect to the parameters i and j, while $C_{(k_1,k_2,...,k_n)}$ is a $2 \times n$ matrix of sensitivities of the additional parameters $k_1, k_2, ..., k_n$, perturbed by the strengths given in the $n \times 1$ vector θ.

6.4 Dynamic response of the cell cycle to changes in parameters

The previous section considered how the eventual behaviour of the cell cycle model (defined in terms of properties of the size and timing of key cell cycle events) could be modified by changes in model parameters. It is now of interest to consider how the dynamics of the system as the cell cycle behaviour changes from its initial state to the eventual behaviour. This investigation is done in three stages. First, exhaustive dynamic sensitivity analysis is applied to each parameter in each of the models in turn. This allows identification of the basic properties of the dynamic responses, and how they depend on the time at which a perturbation is applied. Since a given perturbation of a particular parameter will result in the same change in the steady state behaviour, the different approaches to this eventual behaviour allow the calculation of quantities such as the phase shift. Second, the fact that multiple combinations of parameters can be chosen to provide the same

change in the steady state behaviour is used to compare sets of parameter perturbations to one another. This allows the significance of the dynamical sensitivity to be evaluated by comparing many different sets of responses to one another. Finally, the effects of a more complex dynamic modulation of parameters - specifically a steady increase or decrease of parameters - on the cell cycle are considered.

6.4.1 Methodology

Dynamic sensitivity analysis of an oscillating system can be performed in a variety of ways, and can provide a variety of different types of information. The objective here is to understand how the cell cycle models respond to step changes in parameters at different times during the cell cycle. This response is characterised by changes in the duration of the cell cycle, and the size of the cell at budding and division, over several generations. Looking at the change in a cell cycle characteristic, Q, in the *j*th subsequent cycle following the application of the step change at time t, the dynamic sensitivity of Q_j to perturbations in parameter *k* is given by:

$$S_k^{Q_j}(t) = k\frac{dQ_j}{dk}(t) \tag{6.15}$$

This applies whether k is a vector of parameters, or a single parameter.

It is also possible to represent the same information in the form of a sensitivity to perturbations of infinitesimal duration at time t, as given by:

$$Z_k^{Q_j}(t) = \frac{dS_k^{Q_j}(t)}{dt} \tag{6.16}$$

This gives an idea of how the function $S_k^{Q_j}(t)$ is changing over time during the cell cycle. The dynamic sensitivities can be related to the sensitivities under constant conditions calculated in the previous section:

$$S_k^{Q_j}(t) \to C_k^Q \; as \; j \; \to \infty \tag{6.17}$$

Numerical approximations to these quantities can be calculated similarly to the sensitivities under constant conditions. First, the initial conditions were found by running the simulation over multiple cell cycles until the state of the cell at the beginning of the cell cycle had converged. The model was then simulated across a single cell cycle under the

basal set of conditions, with the state of the system at each of m equally spaced timepoints (with $m = 60$ here) spanning the period of the cell cycle recorded. Then, simulations were run for each parameter perturbation from each of these initial conditions, with the difference in behaviour across multiple cycles recorded and the resulting sensitivity calculated according to:

$$S_k^{Q_j}(t) \approx \frac{k(\Delta Q_j)}{\Delta k} \tag{6.18}$$

Where $\Delta Q_j = Q_{j,perturbed} - Q_{j,basal}$. As before, absolute and relative tolerances of 10^{-10} in the MATLAB ODE solver ode15s were used. Again, the parameter perturbations $\Delta k_i/k_i$ were 0.001 (equal to 0.1% of the basal parameter value). Alternative methods of calculating the same properties (e.g. simulating responses to pulse-like perturbations and summing) were found to produce the same results. It should be noted that the numerically efficient algorithms which exist for calculating these properties for limit cycle oscillators (e.g. (Rand, 2008)) are not directly applicable to the cases considered here as a result of the discrete state transitions and discontinuous changes in the cell volume.

Furthermore, the eventual difference in timing between division events, as a function of the time at which a perturbation was applied, can be calculated. This quantity is referred to as the "phase shift" of the cell cycle, by analogy with literature on circadian and neural oscillators . In these cases, the change in timing of an event (e.g. the peak in oscillation of a particular species) after a perturbation is referred to as a "phase shift" arising from this perturbation.

Since the eventual period of the cell cycle after a step change in a parameter is in general different from the original period, it is necessary to choose a basal case against which to compare the approach to the new conditions. This is taken to be the approach when a step change is applied at $t = 0$. The phase shift is then given by:

$$R_k(t) = \sum_{j=1}^{\infty} \left(S_k^{T_{div,j}}(t) - S_k^{T_{div,j}}(0) \right) \tag{6.19}$$

This sum converges since the eventual value of T_{div} is the same regardless of the time during the cell cycle at which the perturbation was applied. Good approximations of the phase shift only require the summation of these values over at most five generations for the models considered here.

6.4.2 Dynamic sensitivity to changes in individual parameters

The analysis described above provides information on the approach to the steady state behaviour over several generations. Unlike the analysis of behaviour under constant conditions, in which the sensitivities of all of these characteristics can be reduced to, for example, just the sensitivity of V_{div} and T_{div} ($C^{V_{div}}$ and $C^{T_{div}}$, respectively), in this case there are additional degrees of freedom. For the *i*th division:

$$\begin{aligned} V_{div,i} &= V_{dau,i-1}e^{\mu T_{div,i}} \\ V_{bud,i} &= V_{dau,i-1}e^{\mu T_{bud,i}} \\ V_{dau,i} &= V_{div,i} - V_{bud,i} \end{aligned} \tag{6.20}$$

This reduces to the converged constant cycling conditions when $Q_i = Q_{i-1}$ for the various characteristics considered. The consequences of these additional degrees of freedom are precisely what make the investigation of dynamic responses interesting, as they indicate the potential for many alternative dynamic approaches to the same eventual behaviour.

There are a wide variety of ways of visualising the data generated by the application of the analysis to the models considered. The most basic unit of information is that derived from tracking the changes in cell cycle behaviour after modulating a single specific parameter at a specified time during the cell cycle. Some examples of these results are shown in figures 6.5 and 6.6 for two different parameters (the rate of translation of starter cyclins (k_{sn3}) and the rate of translation of mitotic cyclins (k_{sbM}), respectively) modulated at two different times ($t = 83mins$ and $t = 41mins$, respectively) in the Barik model. An important observation from these figures is that the approaches to the new behaviour are not necessarily monotonic down generations. For example, the cell size at division can decrease in the first generation, even if eventually the cells are larger at division, as in figure 6.6. This demonstrates some unintuitive aspects of the underlying dynamics, and also suggests that experiments done on a population of synchronised cells, with a perturbation applied at only one time and with observations made over one subsequent cycle may incorrectly infer the type of regulation that is occurring.

In order to understand the dynamic response of the cell cycle in greater generality, these responses can be plotted as functions of the time at which the perturbation is applied, as shown in figures 6.7 and 6.8, again for the same parameters as were shown in figures

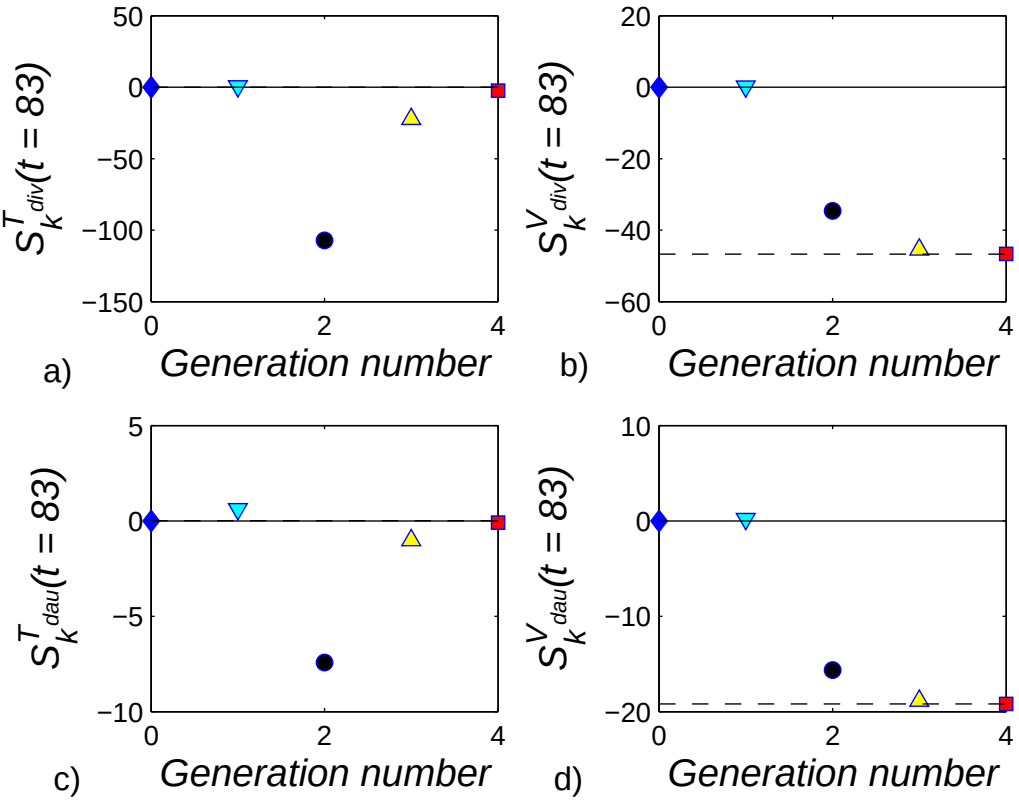

Figure 6.5: The sensitivity of some cell cycle characteristics down generations to a perturbation of the parameter determining the rate of translation of starter cyclins k_{sn3} applied at $t = 83mins$ during the first generation. The dashed black line marks the eventual change in the value of the characteristic. a) The cell cycle duration is decreased over the first two generations, before recovering to its initial value. b) The cell volume at division decreases monotonically down generations, approaching the asymptotic value at a smaller cell size. c) The duration of the budded phase displays similar behaviour to that of the overall cell cycle duration. d) The daughter cell size displays similar behaviour to that of the cell size at division.

6.5 and 6.6, respectively. These display changes in behaviour as a function of the time at which the perturbation is applied (e.g. the functions $S_k^{T_{div,1}}(t)$, $S_k^{T_{div,2}}(t)$, and $S_k^{T_{div,3}}(t)$). From these curves, it is possible to identify some basic patterns in the dynamic sensitivity of the models to changes in parameters, which are valid beyond just the two examples shown. For example, it is clear that the sensitivities of timing of the division events can display biphasic behaviour (e.g. in figure 6.6a)). This means that the same perturbation can either delay or advance a given division event (or, alternatively, increase or decrease the cell size at that event), depending on the time at which the perturbation is applied. This is also true for budding events, and these differences in timing inevitably affect the sizes

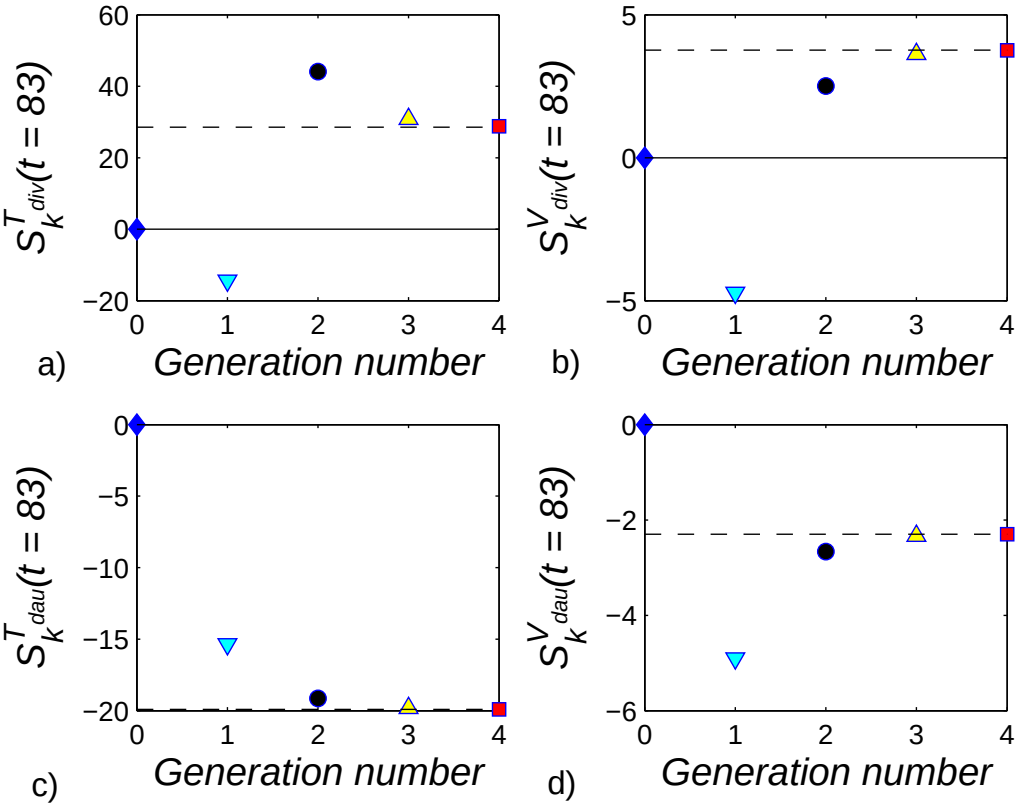

Figure 6.6: The sensitivity of some cell cycle characteristics down generations to a perturbation of the parameter determining the rate of translation of mitotic cyclins k_{sbM} applied at $t = 41mins$ during the first generation. The dashed black line marks the eventual change in the value of the characteristic. a) The cell cycle duration displays nonmonotonic approach to its eventual value, including overshooting this value. b) The cell size at division decreases in the first generation before monotonically increasing to its eventual value, above the initial value. c) The duration of the budded phase monotonically approaches its eventual, shorter duration. d) The daughter cell size overshoots in its approach to its eventual, smaller value.

at which budding and division occur. This biphasic property of the sensitivity curves is observed in many biological oscillators, including neural (Brown et al., 2004) and circadian oscillators (Pfeuty et al., 2011). Furthermore, a relationship between the timing of budding and division is evident from these curves - a delay in budding is often accompanied by a delay in division, and vice versa (compare figures 6.6a) and e)). This implies that there is an inherent inflexibility to the system, whereby the timing of different events cannot be arbitrarily modulated by parameters.

Of particular interest is the dependence of the phase shift of the cell cycle on the timing of the perturbations, some examples of which are shown in figure 6.9. As with the dynamic sensitivities, these curves display biphasic characteristics. Interestingly, there also appears to be a strong correspondence between the relative phase shift and the mass fraction donated to the daughter cell. In particular, stronger phase advances (i.e. negative phase shifts) appear to be correlated with a higher fraction of mass being donated to the daughter cell. Note that the phase responses in figure 6.9 are not comparable to one another as the eventual changes in behaviour (i.e. the converged state of the cell cycle) will be different. Sensible comparisons can only be made between phase shifts at different points in the cell cycle for the same perturbation. For example, it is clear from figure 6.9 that the parameter perturbation marked in blue leads to stronger phase delays when the perturbation is applied late in the cell cycle, and that this correlates with the time at which the mass fraction donated to the daughter cell is higher.

These results can be understood in a general setting by a cell cycle which initially has a period T_0, a size at division $V_{div,0}$, and a daughter size $V_{dau,0}$, meaning the resulting fraction of volume given to the daughter cell is $f_0 = V_{dau,0}/V_{div,0}$. Two perturbations are applied which result in changes in these characteristics down generations. The first set of characteristics are labelled $T_1, T_2, T_3, ..., V_{Div,1}, V_{div,2}, V_{div,3}, ..., V_{dau,1}, V_{dau,2}, V_{dau,3}, ...$, giving daughter fractions $f_1, f_2, f_3, ...$, while the second are labelled $\tau_1, \tau_2, \tau_3, ..., \nu_{div,1}, \nu_{div,2}, \nu_{div,3}, ...$, and $\nu_{dau,1}, \nu_{dau,2}, \nu_{dau,3}, ...$, giving daughter fractions $\rho_1, \rho_2, \rho_3, ...$ These two perturbations result in the same eventual behaviour, such that, for sufficiently large n:

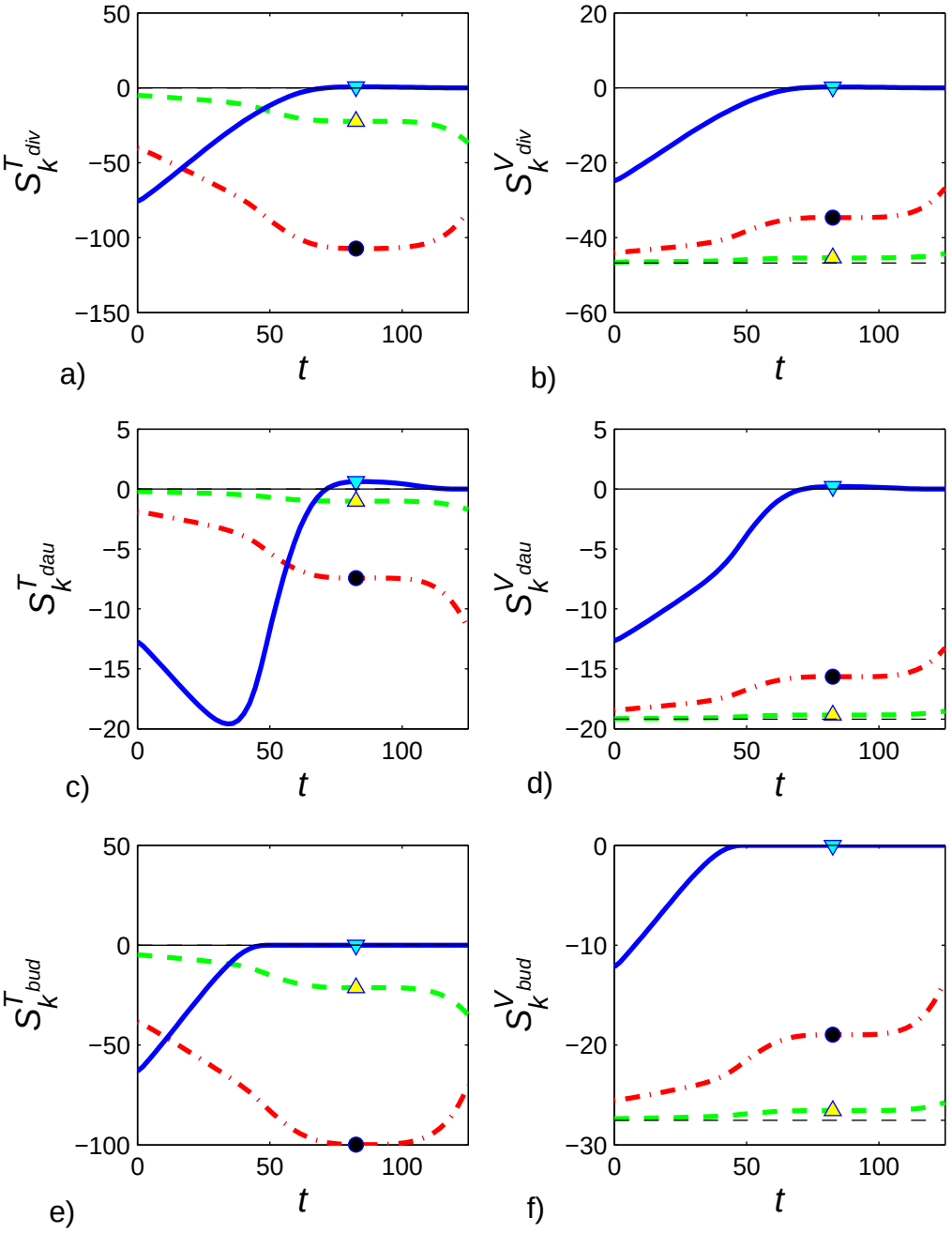

Figure 6.7: The sensitivity of some cell cycle characteristics down generations to a perturbation of the parameter determining the rate of translation of starter cyclins k_{sbM}, as a function of the cell cycle time at which it is applied. The dashed black line marks the eventual change in the characteristics. The shapes mark the generations for the case shown in figure 6.5. The basic behaviour observed in this figure is seen to hold for the same perturbation applied over a wide range of times. Specifically, there is a nonmonotonic approach to the eventual values of cell cycle period and timing of other cell cycle events, and a monotonic approach of the cell size at these events to their eventual values.

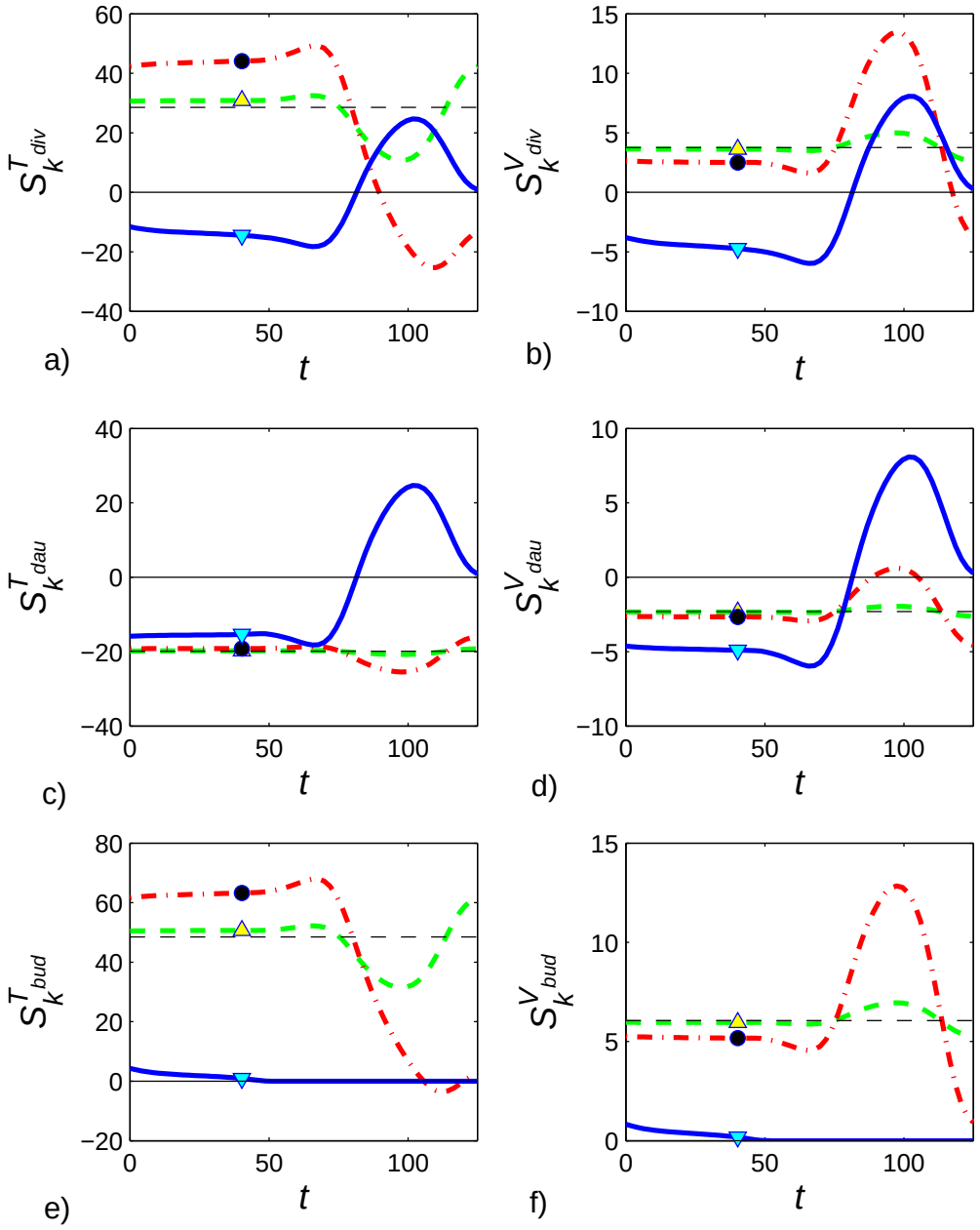

Figure 6.8: The sensitivity of some cell cycle characteristics down generations to a perturbation of the parameter determining the rate of translation of starter cyclins k_{sn3}, as a function of the cell cycle time at which it is applied. The dashed black line marks the eventual change in the characteristics. The shapes mark the generations for the case shown in figure 6.6. In this case, the correspondence between the observations made in figure 6.6 do not hold over a wide range of cell cycle times, with the dynamics down generations of characteristics displaying a myriad of different patterns of approach to their eventual values.

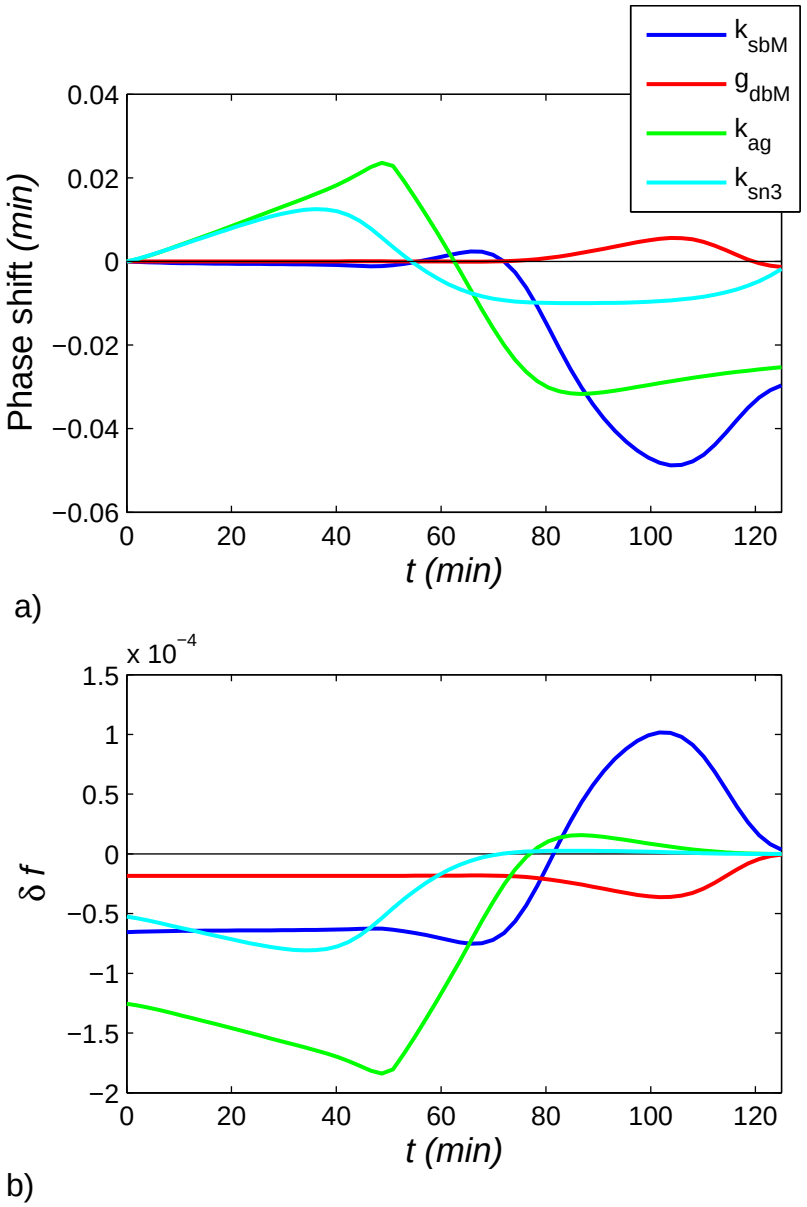

Figure 6.9: a) The phase response curves ($R_k(t)$) are shown for four different parameters in the Barik model. Note that these curves are not directly comparable to one another, since the eventual behaviour of the cell cycle in response to these perturbations is different. (b) The change in mass fraction donated to the first daughter cell after the perturbation is applied is shown as a function of the time at which that perturbation is applied.

$$T_n \approx \tau_n \tag{6.21}$$

$$V_{dau,n} \approx \nu_{dau,n} \tag{6.22}$$

$$V_{div,n} \approx \nu_{div,n} \tag{6.23}$$

$$f_n \approx \rho_n \tag{6.24}$$

Using the equality of daughter sizes after n generations and the basic description of the cell cycle given in equation 6.8:

$$f_n V_{dau,n-1} e^{T_n \mu} = \rho_n \nu_{dau,n-1} e^{\tau_n \mu} \tag{6.25}$$

This assumes a constant growth rate, μ. In general, going back k generations:

$$\left(\prod_{i=0}^{k} f_{n-i} \right) . V_{dau,n-k-1} . e^{\left(\sum_{i=0}^{k} T_{n-i}\right)\mu} = \left(\prod_{i=0}^{k} \rho_{n-i} \right) . \nu_{dau,n-k-1} . e^{\left(\sum_{i=0}^{k} \tau_{n-i}\right)\mu} \tag{6.26}$$

Since $V_{dau,0} = \nu_{dau,0}$, going back $n-1$ generations:

$$\left(\prod_{i=0}^{n-1} f_{n-i} \right) e^{\left(\sum_{i=0}^{n-1} T_{n-i}\right)\mu} = \left(\prod_{i=0}^{n-1} \rho_{n-i} \right) e^{\left(\sum_{i=0}^{n-1} \tau_{n-i}\right)\mu} \tag{6.27}$$

Giving:

$$\mu \sum_{i=1}^{n} (\tau_i - T_i) = ln(\frac{\prod_{i=1}^{n} f_i}{\prod_{i=1}^{n} \rho_i}) \tag{6.28}$$

The quantity on the left hand side is the phase shift. For a phase shift to be observed, the products of the fractions of mass given to the daughter cell must be different. In particular, the perturbation which is phase advanced (i.e. a phase shift with negative value) has a larger product of these mass fractions. One immediate consequence of this is that phase shifts are not possible when cells divide symmetrically, since in that case $f = 0.5$ in all cycles (this will be of particular interest when considering the response of cell populations to signals - see section 6.7). This also explains the distinction between how perturbations which act to rapidly increase the size of daughter cells can result in phase advances, since larger

daughter cells are an immediate consequence of the daughter obtaining a more significant fraction of mass of the cell at division. Similarly, it explains why perturbations that rapidly decrease the size of daughter cells result in phase delays.

Having considered how timing differences in perturbations affect the approach to the new steady state behaviour, it is natural to compare the dynamics of different parameter perturbations. For the individual parameter perturbations considered above, it is not possible to compare the dynamic responses in any meaningful way, since their eventual behaviours are, in general, different. For example, it is unclear how to understand the consequences of differences in the dynamic responses of two parameter perturbations if one leads to a significant change in cell cycle period while the other does not. However, as discussed in the steady state analysis, it is possible to find combinations of parameter perturbations which produce the same change in steady state behaviour, and it is these which are considered next.

6.4.3 Dynamic sensitivity to changes in combinations of parameters

Having established how parameters can be combined to obtain specified changes in behaviour in the cell cycle under constant conditions, it is interesting to ask how to discriminate between alternative sets of parameter changes which produce the same eventual behaviour. This is done by analysis of the dynamic response of the cell cycle to these parameter changes at different times, averaged over the entire cell cycle. This allows us to perform controlled comparisons of the way in which different parameter changes approach this new behaviour. It should be emphasised again that the "behaviour" in this context is the pattern of phase durations and cell sizes in those phases. Other characteristics, such as the amplitude and phase of the various cell cycle components, will in general be different between perturbations even when the timing and sizes are the same, but the analysis described here can be applied to these other characteristics in a similar way.

To begin with, given two parameters with linearly independent sensitivities and a specified change in behaviour, the change in parameters required is given by equation 6.11. As mentioned previously, it is also possible to obtain a range of parameter perturbations applied to a set of three parameters which give a specified change in behaviour by parameterising a set of perturbations by θ, as given in equation 6.12. This provides another way to identify parameter perturbations which produce the same change in behaviour under constant cycling conditions, but which have different dynamic response profiles. This results

in the following expressions for the approach to the new behaviour, for example as a sum of two sustained-perturbation sensitivities:

$$\begin{pmatrix} \delta V_{div,l}(t) \\ \delta T_{div,l}(t) \end{pmatrix} = \begin{pmatrix} \delta k_i/k_i \\ \delta k_j/k_j \end{pmatrix} \begin{pmatrix} S_{k_i}^{V_{div,l}}(t) & S_{k_j}^{V_{div,l}}(t) \\ S_{k_i}^{T_{div,l}}(t) & S_{k_j}^{T_{div,l}}(t) \end{pmatrix} \tag{6.29}$$

The sensitivity profiles obtained describe the approaches of different combinations of parameter perturbation to the same eventual behaviour, as a function of the time at which the perturbation is applied. This gives a set of response curves to the sustained perturbations. As expected when combining two sensitivity curves, there is a greater variety in the shapes of these response curves than was the case in the response curves of single parameters. A particular point of interest in this respect is that the qualitative properties of a combined response needn't be the same as the qualitative properties of the individual responses. This is illustrated in figure 6.10, in which two parameters with monophasic sensitivities counteract one another to produce a response which is biphasic overall.

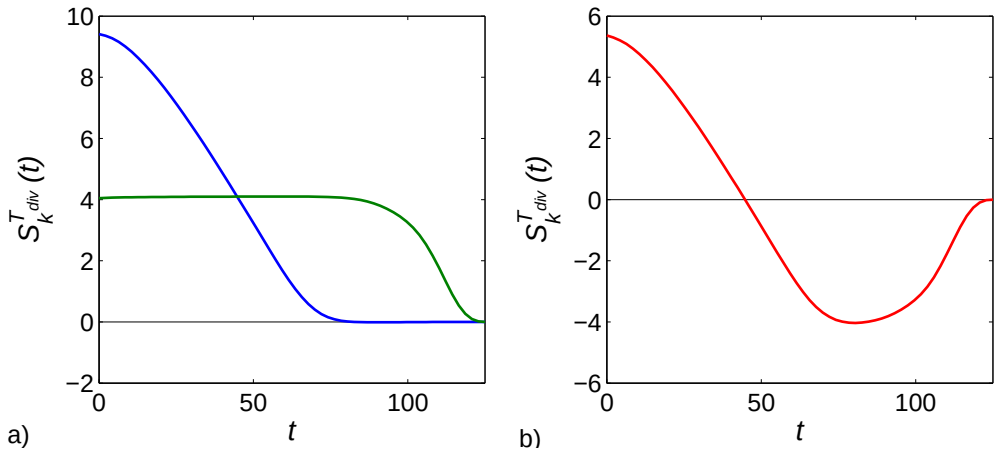

Figure 6.10: The combination of regulation of two parameters (k_{dcm} in blue and k_{dnt} in green) with monophasic sensitivities (as shown in a)) can produce a biphasic response (as shown in b)). These parameters are regulated to counteract one another, with the difference in timing in their sensitivities giving rise to a biphasic response.

As before, it is possible to calculate the phase shift observed between these different combinations of parameters. For the case with three parameters the "basal" case against which the phase shift is measured is taken as $t = 0, \theta = 0$, meaning that the phase shift is given by:

$$R_k(t) = \begin{pmatrix} \delta k_i/k_i, & \delta k_j/k_j, & \delta k_k/k_k \end{pmatrix} . \begin{pmatrix} R_{k_i}(t) \\ R_{k_j}(t) \\ R_{k_k}(t) \end{pmatrix} - \begin{pmatrix} \delta k_i/k_i, & \delta k_j/k_j \end{pmatrix} . \begin{pmatrix} R_{k_i}(0) \\ R_{k_j}(0) \end{pmatrix} \tag{6.30}$$

The significance of these different response curves can be assessed in a number of ways. As an example, we consider three different "metrics" that in some sense summarise the dynamics, and that may be considered biologically relevant. These are: the speed at which the new daughter size is achieved (denoted M_{dau}), the speed with which the new cell cycle period is achieved (denoted M_{period}), and the phase shift of the cell cycle as a whole (denoted M_{phase}). In a biological context it is to be expected that a perturbation may occur at any time during a cell cycle. It is therefore sensible to consider properties of the approach to the new steady state that are averaged over perturbations applied at all points during the cell cycle.

To begin with, the speed of approach to an eventual behaviour given a perturbation applied at a particular time t can be given by the functions $m_{dau}(t)$ and $m_{period}(t)$ for the daughter size and cell cycle period, respectively. These quantities are given by:

$$m_{dau}(t) = \sum_{j=1}^{\infty} \left(\delta V_{dau,j}(t) - \delta V_{dau}\right)^2 \tag{6.31}$$

and:

$$m_{period}(t) = \sum_{j=1}^{\infty} \left(\delta T_{div,j}(t) - \delta T_{div}\right)^2 \tag{6.32}$$

For a given change in behaviour, these functions fulfil the basic property that a perturbation in which the characteristic immediately attains the eventual value will have a lower metric than a perturbation which takes several cell cycles to attain the eventual value.

As mentioned above, it is sensible to average these metrics across perturbations occurring at all times during the cell cycle. This has the advantage of removing the dependence of the metric on the time at which the perturbation is applied. Therefore, the speed with which the eventual daughter size is achieved, measured by the metric M_{dau}, defined by equation 6.33:

$$\begin{aligned} M_{dau} &= \int_{t=0}^{T_{div}} m_{dau}(t)dt \\ &= \sum_{j=1}^{\infty}\left[\int_{t=0}^{T_{div}} \left(\delta V_{dau,j}(t) - \delta V_{dau}\right)^2 dt\right] \end{aligned} \tag{6.33}$$

The speed with which the eventual cell cycle period is achieved is measured by the metric M_{period}, and is defined by equation 6.34:

$$\begin{aligned} M_{period} &= \int_{t=0}^{T_{div}} m_{period}(t)dt \\ &= \sum_{j=1}^{\infty}\left[\int_{t=0}^{T_{div}} \left(\delta T_{div,j}(t) - \delta T_{div}\right)^2 dt\right] \end{aligned} \tag{6.34}$$

These metrics are insensitive to the transformation $\delta k = -\delta k_0$ (which merely results in a change in sign in the vector δQ, and to any combination of parameter perturbations that produce the same eventual change in behaviour. As in equation 6.12, such combinations of parameters can be generated that vary linearly with the auxiliary parameter θ. The resulting linear variation of $\delta Q_j(t)$ with θ (note that the eventual change in behaviour, δQ, remains constant) means that M_{dau} and M_{div} vary quadratically with θ. As a result, it can be shown that there exists values of θ for which M_{dau} or M_{period} are at a minimum.

This generalises in a straightforward way to the case where θ is a vector and more than three parameters are combined. This means that a unique minimum exists for a given set of parameters and a given perturbation of V_{div} and T_{div}. Examples of combined response curves for three parameters which minimise the metric M_{dau} and M_{period} are shown in figures 6.11 and 6.12, respectively. Note that in both cases, the same sets of three parameters are shown, and the speed of their approach to the relevant quantity (δV_{dau} and δT_{div}, respectively) can be observed. Interestingly, all of these curves make use of the biphasic property identified earlier as common in the response of an oscillating system to a change in parameters at different times. The parameter perturbations minimising these two metrics are in general different from one another, but the dynamic responses display some similarities, as shown in figure 6.13, especially compared to randomly chosen examples which do not minimise these metrics. This suggests that rapid response is in some sense a general property,

with certain parameter perturbations achieving rapid responses in several metrics, although locally one metric may be minimised at the expense of another. While the examples shown are all taken from the Barik model, the results of a similar analysis of the Sriram model are given in Appendix D (figures D.1, D.2, and D.3).

The third metric of interest is the phase shift between different combinations of parameter perturbations reaching the same eventual cycling behaviour. As before, this is averaged over a cycle, and is given by equation 6.35.

$$M_{phase} = \int_{t=0}^{T_{div}} R_k(t)dt \tag{6.35}$$

This metric depends on the choice of the basal case, and therefore is used here only to compare different choices of perturbations for a given set of parameters, as given by the chosen value of θ, with the basal case as $t = 0, \theta = 0$. In contrast to M_{dau} and M_{period}, this metric is sensitive to the transformation $\delta k = -\delta k_0$ (since equation 6.35 is linear rather than quadratic).

The difference in how M_{dau} and M_{phase} change with the direction of δk means that there is a balance to be found between controlling the phase advance and controlling the daughter size. This is shown for two separate sets of parameters in figures 6.14 and 6.15.

This agrees with what is expected based on the analysis in the previous section. Specifically, rapid daughter size adjustment requires rapid change of $f = V_{dau}/V_{div}$. When the daughter size is increasing, rapid response means f goes up quickly, and there is a phase advance. However, in the reverse case, f is decreased equally quickly, and there is a phase delay.

The sensitivity analysis considered above allows analysis of the response of the cell cycle to simultaneous step changes in sets of parameters. However, there are several other types of signal which the cell cycle may observe. Analysis of these cases is a first step towards considering how the cell cycle may behave when coupled to a complex signalling network capable of a wide variety of signalling behaviours. Given the number and complexity of signalling pathways leading to the cell cycle, it is also reasonable to investigate how it might respond to more complex signals. The case of a steadily increasing or decreasing signal is a sensible first case to look at.

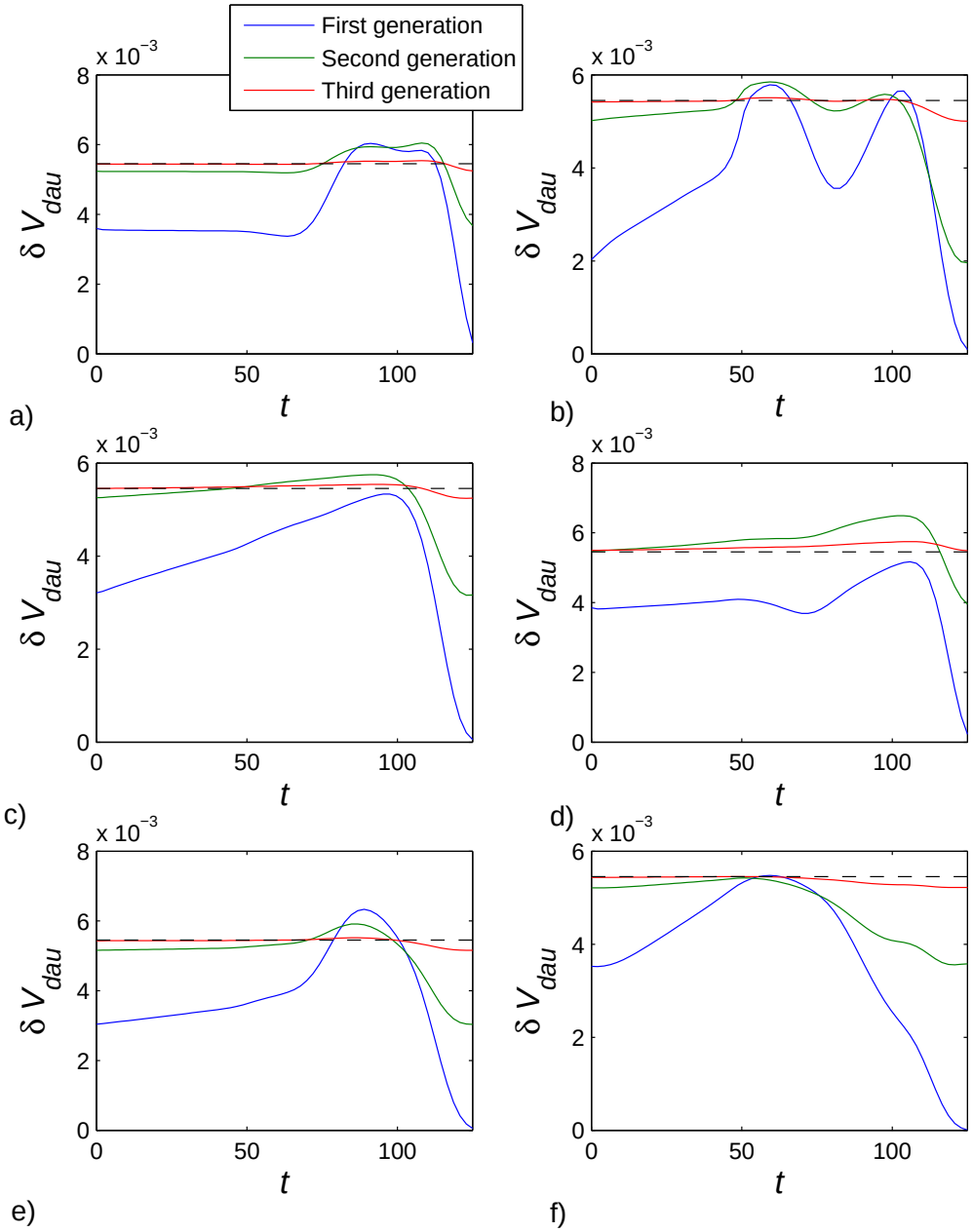

Figure 6.11: Changes in daughter size down three generations for different combinations of different sets of three parameters which achieve the same eventual change in behaviour, and all of which achieve minimal M_{dau} compared to other combinations of those three parameters. The dashed line gives the eventual change of behaviour, which is the same in all examples. The curves approach this behaviour asymptotically though, as noted, not necessarily monotonically. Strikingly, these curves all display some degree of biphasic response.

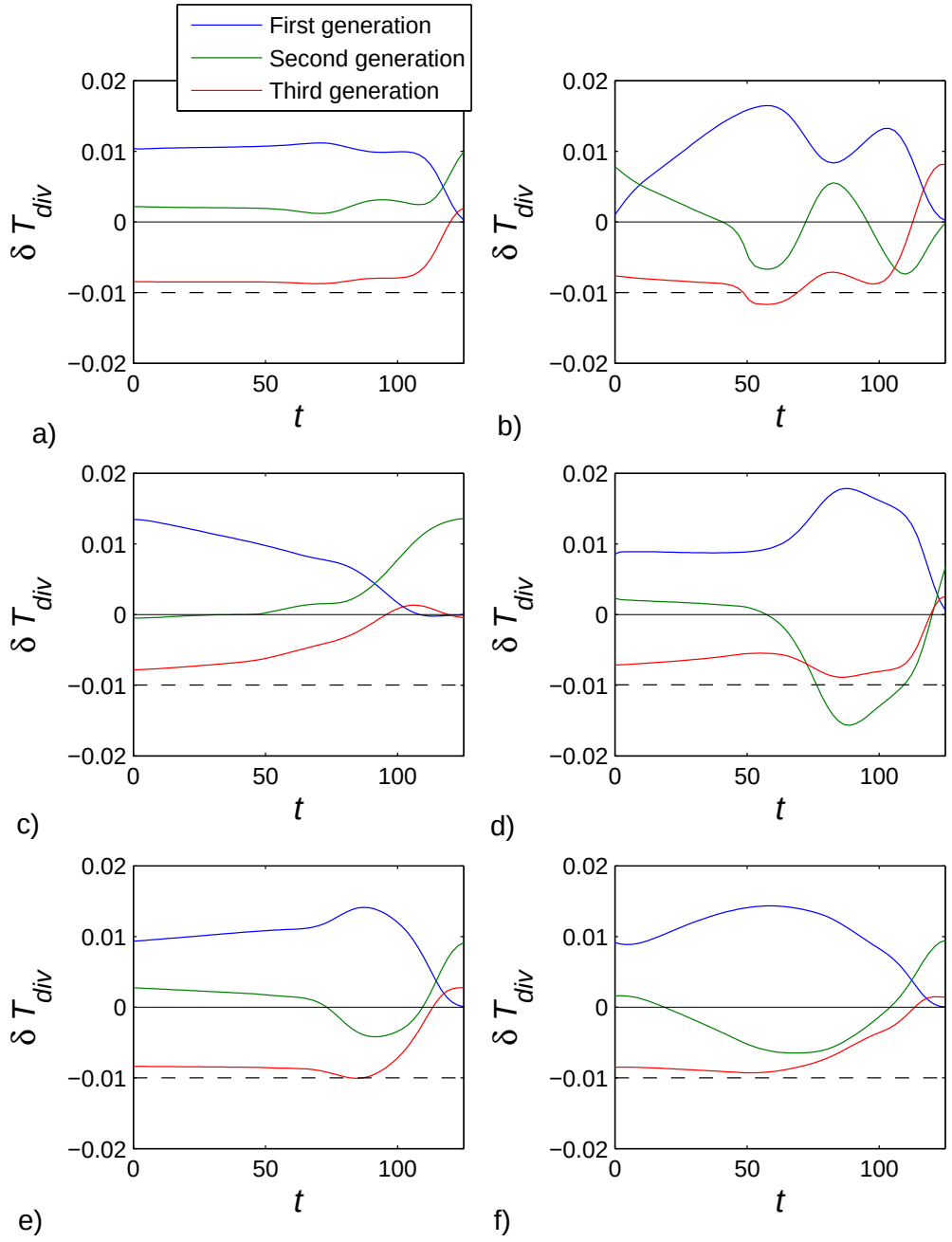

Figure 6.12: Changes in cell cycle period down three generations for different combinations of different sets of three parameters which achieve the same eventual change in behaviour, and all of which achieve minimal M_{period} compared to other combinations of those three parameters. The dashed line gives the eventual change of behaviour, which is the same in all examples. The curves approach this behaviour asymptotically. As in the case for the approach of parameter perturbations exhibiting minimal M_{period}, these curves all display some degree of biphasic response.

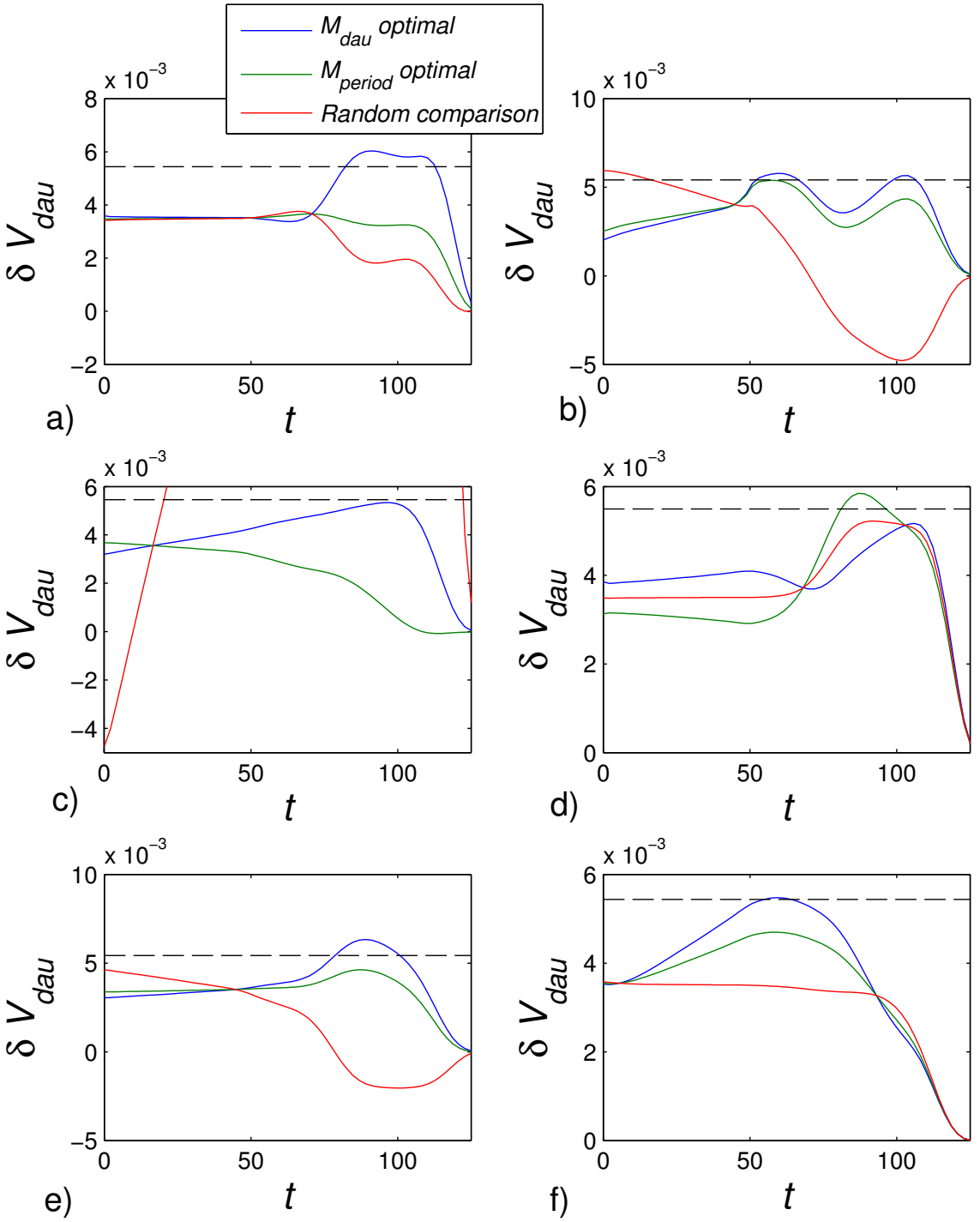

Figure 6.13: The dynamic responses of V_{dau} over the first generation are compared for the examples considered in figures 6.11 and 6.12, minimising M_{dau} (blue) and M_{period} (green), respectively. Examples of responses far from minimising these metrics, chosen at random, are also displayed (red). The similarity in the response curves exhibiting minimal M_{dau} and M_{period} suggests a common principle in the attainment of rapid approach to the eventual change in behaviour of the cell cycle.

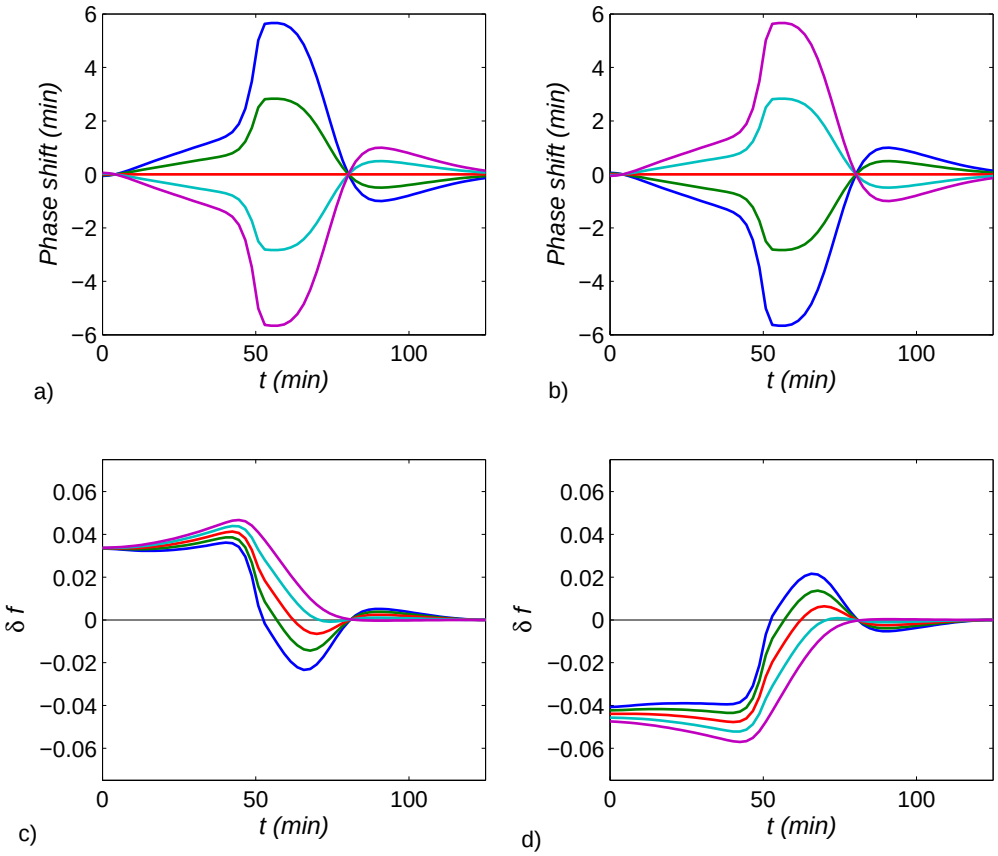

Figure 6.14: The phase responses for different combinations of the three parameters k_{sbS}, k_{pcmp}, and k_{dt1} are plotted alongside the change in the mass fraction donated to the daughter cell in the first generation for cases of increasing and decreasing daughter sizes. The lines of the same colour in the plots are parameter perturbations which are coordinated in the same way with the imposed objective. a) and c) display the case in which the mass fraction donated to the daughter cell is increased, while b) and d) display the case in which the reverse regulation is applied. It is clear that rapid modulation of daughter size leads to phase advance in the case of increasing daughter size, but that the reverse is true for decreasing daughter size. In particular, the regulation providing the most rapid change in f (the purple line, with the rapid regulation seen in c) and d)) leads to the most significant phase advances in one case (shown in a)), but also to the most significant phase delays in the reverse case (shown in b)).

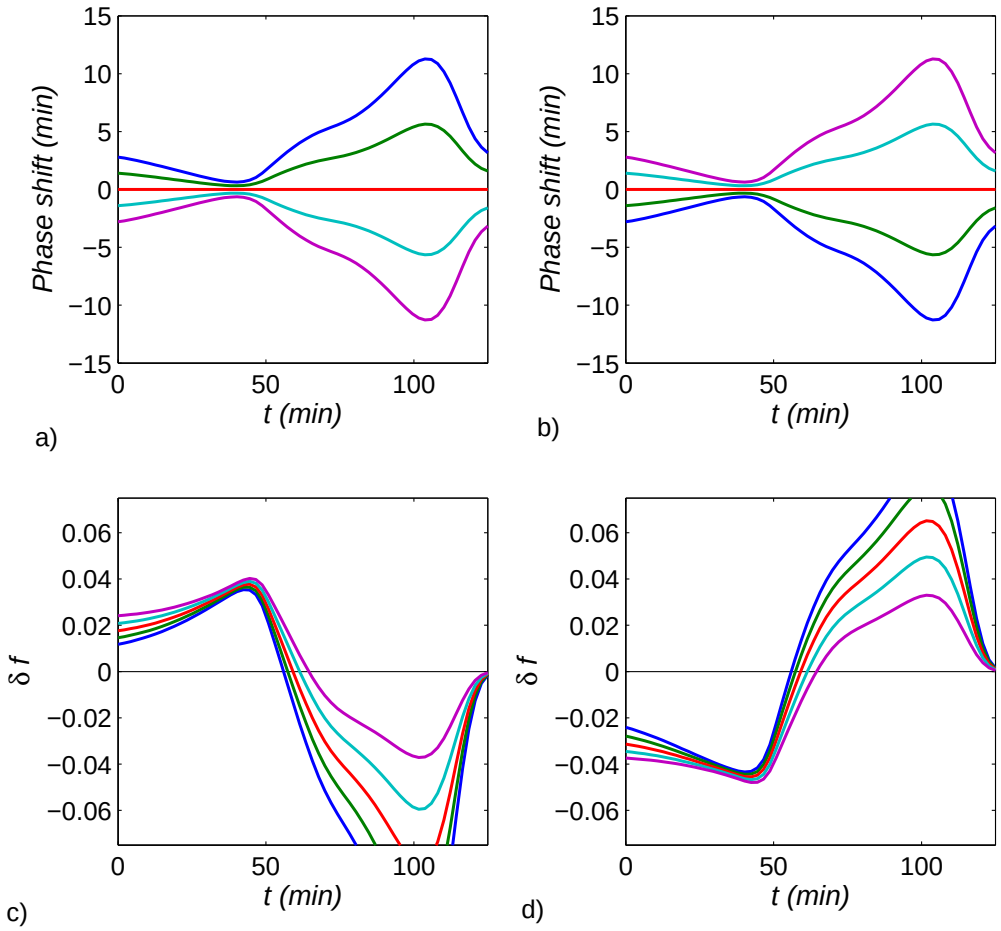

Figure 6.15: Another example of the case plotted in figure 6.14 is shown, for a different choice of three parameters (in this case, k_{dbMi}, k_{pi5p}, and k_{sn3}). Again, the lines of the same colour in the plots are parameter perturbations which are coordinated in the same way with the imposed objective. a) and c) display the case in which the mass fraction donated to the daughter cell is increased, while b) and d) display the case in which the reverse regulation is applied. As was seen in figure 6.14, rapid modulation of daughter size leads to phase advance in the case of increasing daughter size, but that the reverse is true for decreasing daughter size.

6.4.4 Response to steadily increasing or decreasing signals

One important class of dynamic signal which might regulate the cell cycle is a steadily increasing or decreasing signal. This type of signalling can occur in several different scenarios. For example, it may take a signalling network some time to reach its new steady state after a change in the cell's environment, or the environment itself may be undergoing a steady change. This case is particularly interesting since in this case differences in response can be interpreted as differences in how the cell predicts future conditions. In addition to the biological relevance of this particular type of perturbation, it also provides an example for the investigation of the consequences of temporally varying perturbations in general.

Controlled comparisons between different combinations of parameter perturbations which achieve the same eventual response can again be performed, this time for parameter perturbations which are steadily increasing or decreasing with time. For example, the response of a characteristic Q to a parameter change with time with relative gradient of size m ($= \Delta k/(k_0 t) = \Delta\eta/t$).

$$\begin{aligned} \Delta Q &= \int_{t=0}^{T_{div}} \frac{d\eta}{dt}\frac{dQ}{d\eta}dt \\ &= m\int_{t=0}^{T_{div}} \frac{dQ}{d\eta}dt \end{aligned} \tag{6.36}$$

Therefore the sensitivity to gradients (denoted here as $W_k^Q(t)$) can be calculated as:

$$W_k^Q(t) = \frac{dQ}{dm}(t) = \int_{\tau=t}^{T_{div}} S_k^Q(\tau)d\tau$$

When $t = 0$, this is similar to the expression given in 6.33. It can immediately be seen that, if $S_{k_1}^Q(t) > S_{k_2}^Q(t)\forall t$ for the parameter perturbations k_1 and k_2, then also $W_{k_1}^Q(t) > W_{k_2}^Q(t)$, meaning that rapidly responding parameters also respond rapidly to gradually changing conditions. An example of such a comparison is shown in figure 6.16 for perturbations with identical eventual effects, with rapid response to step changes leading to more emphatic responses to gradient changes, regardless of the time at which the steady change in parameters begins, as expected. It should also be noted that the functions $W_k^Q(t)$ have fewer stationary and inflection points than the corresponding $S_k^Q(t)$ - this is simply a result of integration over time.

One interesting interpretation of this observation is that there may exist perturbations

which cause the cell cycle to "anticipate" future conditions by responding rapidly and strongly in the anticipated direction of regulation, while other parameter perturbations exhibit "inertia", whereby the cell cycle maintains its previous behaviour for some time.

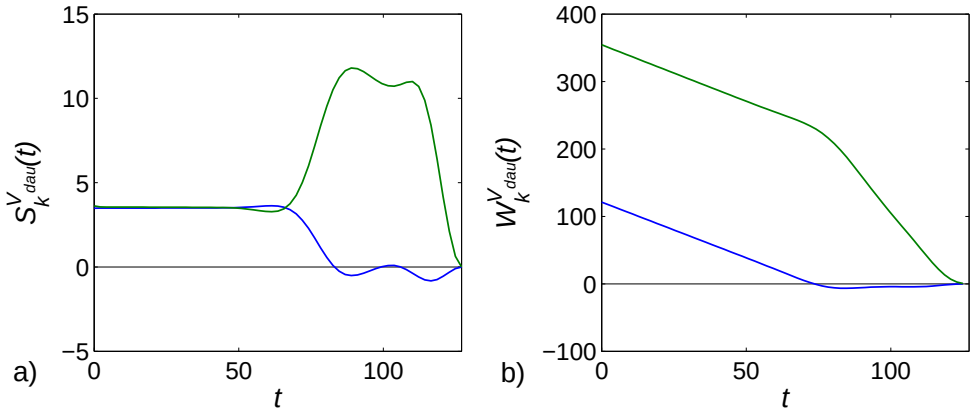

Figure 6.16: The correspondence between the sensitivity to step changes ($S_k^Q(t)$) and the sensitivity to temporally graded perturbations ($W_k^Q(t)$) is shown. As expected, the perturbation with the more pronounced response to step-changes (marked in green) also displays a more pronounced response to temporal gradients. Further, the dependence of $W_k^Q(t)$ on the time integral of $S_k^Q(t)$ results in a more monotonic function. Both of the parameter perturbations applied in this case consist of differently weighted combinations of the parameters g_{dbM}, k_{dh1}, and k_{dh1p}.

As before, the analysis in equation 6.36 and the simulated examples in figure 6.16 apply to the case where the parameter perturbations are small. When looking at step changes in parameters, it was possible to extend this reasoning somewhat to include cases where parameter perturbations were somewhat larger, and still perform controlled comparisons of the different perturbations. In the case of steadily changing parameters, however, this is not possible, since it is inevitable that after some time the parameter change compared to the basal case will be significant. Thus, here the response depends on the nonlinearities in parameter responses, rather than just the shape of the response curves. This means that it is not possible to ascribe differences in the response to differences in the qualitative features of the response curves.

Overall, it is seen that the dynamic sensitivity analysis performed provides an entry point to understanding the consequences of more complex types of regulation on the cell cycle, and that this can connect in a natural way to biological questions. Other biologically motivated investigations, perhaps in context where multiple parameters are perturbed at different times, or change over time in different ways, can be considered in a similar way on a case-by-case basis.

6.5 Case study: Glucose regulation of the cell cycle

A wide range of suggestions have been made for the action of pathways on the cell cycle, very few of which have been characterised quantitatively. Nonetheless, it is important to consider how such suggestions may be evaluated in the context of the preceding analysis. The example chosen here as a case study is the glucose-sensing pathway. While this pathway is itself complex, understanding the interface between elements of this pathways and the cell cycle is a first step towards understanding broader combinatorial regulation. The consideration of a particular case study here also demonstrates some ways in which the preceding sensitivity analysis can be used to interrogate model behaviours.

There are multiple proposed pathways through which glucose can affect the cell cycle, both through direct sensing (Broach, 2012; Busti et al., 2010; Zaman et al., 2008, 2009), and indirect effects via metabolism (Broach, 2012; Cai and Tu, 2012). Here, direct signalling pathways are considered, since these are generally the fastest to respond to changes in conditions. Three particular forms of regulation are considered. The first mechanism of cell cycle regulation by glucose involves the control of translation of Cln3 - a cyclin responsible for inducing G1-S transition. The regulation of Cln3 translation is mediated in part through the direct regulation of the translation initiation factor eIF4E (Danaie et al., 1999), and can also be controlled through the relief of competition for translation initiation factors due to rapid degradation of GAL1 transcripts (Baumgartner et al., 2011). The rate of translation of Cln3 is represented in the Barik model by the parameter $k_{s,n3}$. Secondly, it is known that glucose-sensing pathways lead to repression of Cln2 expression (Flick et al., 1998). In the Barik model, Cln2 falls within the class of starter cyclins, denoted by ClbS. The rate of ClbS transcription is represented by the parameter $k_{s,mbS}$. Finally, it is known that signalling through the TOR kinase complex is capable of modulating the activity of the PP2A phosphatase complex (Castermans et al., 2012; Santhanam et al., 2004). Upon phosphorylation by the TOR1C complex, this phosphatase dephosphorylates a wide range of targets, including Net1. Net1, in turn, is responsible for sequestering the cell-cycle phosphatase Cdc14, which is required for progression through mitosis. The dephosphorylation of Net1 in the Barik model is represented by the constitutive activity of a generic phosphatase, Ht1. The model parameters representing this activity are $k_{d,t1}$ and $k_{d,nt}$, regulating free Net1 and Net1 in the RENT complex, respectively. A natural assumption is that regulation of this pair of parameters is coupled, and therefore that they are modulated proportionally to one another. The above summary of some regulatory mechanisms is by

no means complete, partly as a result of some pathways regulating components not present in this model (e.g. the regulation of Cdk1 phosphorylation by Cdc25 and Swe1 (Enders, 2010)), but it provides a useful illustration.

The above information on regulatory mechanisms can be summarised by the following constraints on the parameter perturbations applied through this pathway (where the "signal", assumed to be proportional in some way to the glucose availability, is represented by X):

$$\begin{aligned} \frac{1}{k_{s,n3}}\frac{dk_{s,n3}}{dX} &> 0 \\ \frac{1}{k_{s,mbS}}\frac{dk_{s,mbS}}{dX} &< 0 \\ \frac{1}{k_{d,t1}}\frac{dk_{d,t1}}{dX} = \frac{1}{k_{d,nt}}\frac{dk_{d,nt}}{dX} &> 0 \end{aligned} \tag{6.37}$$

These constraints imply a certain attainable range of responses in V_{div} and T_{div}, meaning that only particular changes in V_{div} and T_{div} are possible in response to changes in X. In the context of the actual system, the strengths of these regulations are dependent on the structure, dynamics, and sensitivity of the complex, branching signalling pathways linking glucose levels to the cell cycle. In general, given a set of parameters and whether they are up- or down-regulated by a given pathway, the attainable range of responses will be given by any convex combination of those perturbations. In this case, this range is depicted as the shaded region in figure 6.17 b). Here, the regulatory mechanisms suggested are limited to speeding up the cell cycle with increasing glucose levels (i.e. $\delta T_{div}/\delta X < 0$). Additionally, while this form of regulation can freely decrease the cell size without having a significant impact on the cell cycle period, there must be a decrease in periodicity to affect an increase in cell size. This runs contrary to the intuitive notion that increasing the duration of cell growth would result in increased cell sizes, but is a natural result of the combined effects of parameter changes on the size checkpoint and the relative timing of budding. It should be noted that the parameter combinations suggested here are capable of reproducing some of the basic qualitative behaviours of the cell cycle in response to glucose i.e. a shortened period with a larger cell size . Using this observation, the analysis can be honed further to look at combinations of these three parameters which give this qualitative change in behaviour.

Another interesting aspect of the attainable region is that it is bounded by the opposing effects of stimulation of Cln3 translation and inhibition of ClbS transcription. This means that regulation of Net1 dephosphorylation does not affect the range of behaviours that can be bought about through the suggested pathway. However, there are clear changes in the dynamic sensitivity when this parameter is more strongly regulated, as shown in figure 6.17. Here, three cases with various strengths of up-regulation of Net1 dephosphorylation with glucose levels (through k_{dt1} and k_{dnt}) are shown, in which a balance of the counteracting parameters k_{sn3} and k_{smbS} means that the same eventual change in behaviour is attained (as discussed above), namely a specific instance of a shortened period and a larger cell size. Specifically, as the strength of regulation through Net1 increases, the strengths of regulation through Cln3 and ClbS decrease. The resultant changes in the dynamic sensitivity ($S_k^{T_{div}}(t)$) shown in figure 6.17d) are the result of differences in the timing of sensitivity of the cell cycle to the different parameters (see figure 6.17 c) for the individual sensitivity profiles), whereby regulation of Cln2 transcription and Cln3 translation alone is only capable of modulating cell cycle progression around the G1-S transition, while regulation of Net1 dephosphorylation modulates progression through mitosis.

It has been noted previously that glucose levels act predominantly to modulate duration of the G1 phase of the cell cycle (Porro et al., 2003). An important conclusion arising from the work presented here is that this form of regulation does not in any way exclude active regulation of processes occurring during mitosis (or other phases of the cell cycle). Indeed, it suggests that, as long as counteracting pathways can be modulated in tandem, regulation of processes occurring in mitosis may be a useful strategy for dynamic adjustment of cell cycle characteristics after a change in conditions. In the particular example of strong Net1 regulation shown in figure 6.17d), this is seen to lead to much more rapid modulation of cell cycle duration than would be possible if only Cln2 and Cln3 were regulated. Observations of cell populations under constant conditions (e.g. the chemostat experiments in (Brauer et al., 2008; Porro et al., 2003)) are not capable of distinguishing between these strategies of regulation.

Finally, it should be recognised that application of this analysis to particular cases/pathways is made difficult by several factors. First, the models presented here have not been constructed to take into account all forms of regulation a given pathway may exert on the cell cycle (e.g. a regulated component may not be present in any of the models considered here). Development of new models, perhaps including additional components, may be required. Secondly, even when a parameter is present in several of the models, there is often a lack of

even qualitative agreement concerning the regulation exerted by that parameter (see above). Thirdly, experimental data on the response of the cell cycle to changes in a given pathway is not generally available, meaning that reasoning about pathway responses is relatively unconstrained. This is a problem especially given the noted flexibility of regulation of behaviour. While there are prospects for such data becoming available as novel experimental techniques become more widely adopted (e.g. quantitative single-cell imaging technology (Charvin et al., 2008; Spiller et al., 2010)), for the moment it is sufficient to describe in principle how regulatory flexibility might exist in some known signalling pathways. As demonstrated here, this type of understanding can be obtained in a straightforward way by use of the preceding sensitivity analysis.

6.6 Comparison of sensitivities for analogous parameters across models

Up to this point, the analysis has been very general - the analysis has been applicable to all models considered, and general properties of these models have been identified. It is then sensible to ask whether the models also share similarities in the responses of particular parameters that are shared by all models. In many cases it is not possible to identify sets of parameters that should be considered directly comparable between the models considered. For example, only the Csikasz-Nagy model contains the protein Swe1, meaning that parameters in this model relating to the functions of Swe1 are not directly comparable to any parameters in the other models. Despite this, there are some classes of parameters that can be used as examples to investigate these properties: the production of starter and mitotic cyclins (i.e. cyclins responsible for promoting the G1-S transition and G2-M transition, respectively). These components are common to all models considered, and provide a useful basis for direct model comparison.

6.6.1 Starter cyclin production

The starter cyclins, Cln1, Cln2, Clb5, and Clb6, stimulate the transition to the budded phase. The representation of these components differ between models. For example, the Csikasz-Nagy model differentiates between Cln1,2 and Clb5,6, while the Barik model lumps all starter cyclins under the pseudo-component “ClbS”. In all of these models, however, there are parameters responsible for the production of these cyclins. The question

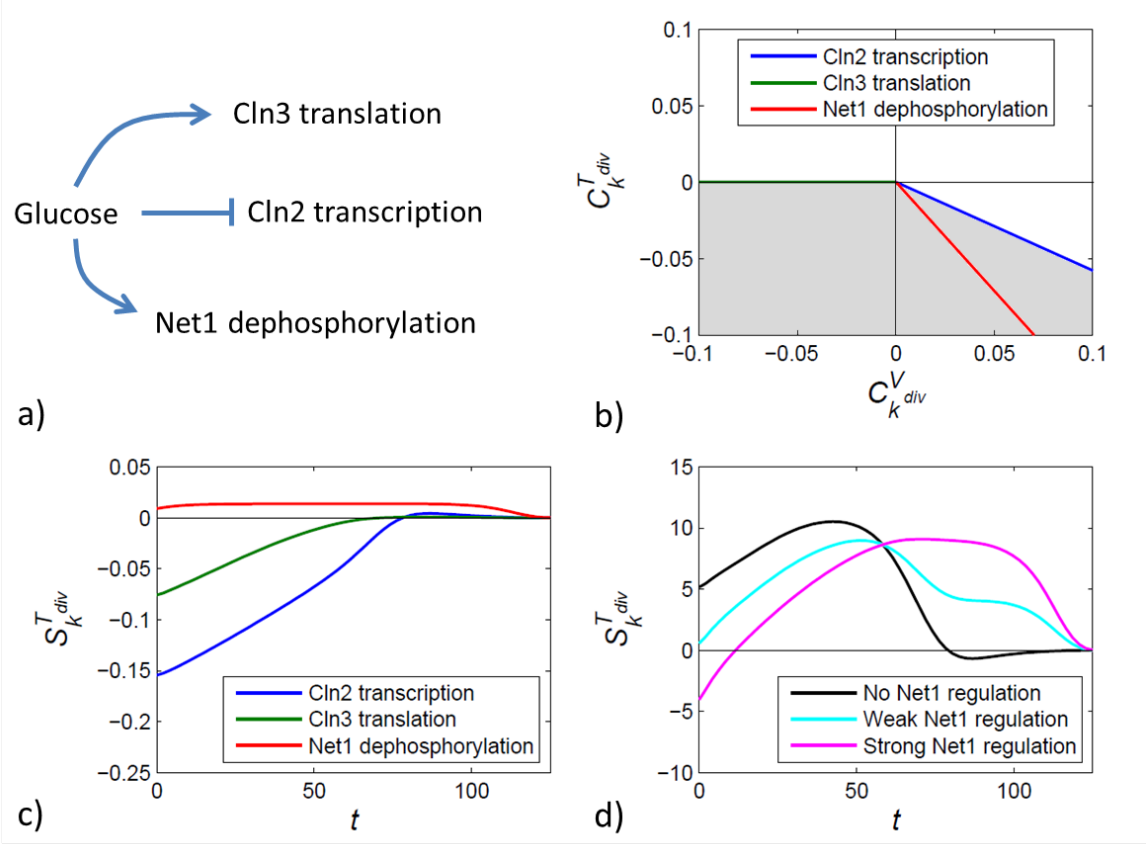

Figure 6.17: a) A schematic of glucose regulation. Glucose is known to act on the cell cycle and many other processes through a diverse range of signalling pathways. b) The feasible region is given by any convex combination of the three regulations, and is marked by the shaded region. This is determined by the intrinsic regulatory capabilities of the parameters, constrained by the direction in which they are known to be regulated by increases in glucose levels. c) The dynamic sensitivities of the pathways are shown (parameter sensitivities are combined as stipulated in equation 6.37. d) The consequences of different balances of these three parameter perturbations are shown, all of which have the same eventual change in behaviour. The inclusion of strong regulation in mitosis (through Net1) allows dynamic response to changes in glucose levels late in the cell cycle.

then arises as to whether the regulation applied by these parameters is consistent between models.

An overview of the steady state and dynamic sensitivities (in terms of $S_k^{V_{dau}}$) for these sets of parameters are shown in figure 6.18. As is clear from figure 6.18a), there is little agreement at even the qualitative level between the sensitivities. While increases in any of these parameters reduce the size of the cell at division, the cell cycle duration may increase or decrease. At the same time, however, there is some agreement between the models on the qualitative properties of the dynamic sensitivity of the timing of the first division event after the perturbation is applied, agreeing with the intuitive notion that stimulating production of starter cyclins should cause earlier division.

6.6.2 Mitotic cyclin production

Like the cyclins associated with the G1-S transition, the cyclins associated with mitosis (namely, Clb1 and Clb2) are present in the Chen, Csikasz-Nagy, Barik, and Sriram models, and an analogously acting component can be identified in the Kaneko model. Similarly, parameters controlling the rate of mitotic cyclin production can be identified in each model. The results of the comparison are shown in figure 6.19. Again, it is clear that there is no qualitative agreement between the different models in the steady state sensitivities. It is interesting to note the biphasic properties of several of the dynamic sensitivity of the timing of the first division event after the perturbation is applied. This fits with the intuitive notion that production of mitotic cyclins is necessary for mitosis, but at the same time rapid degradation of cyclins is required to allow cytokinesis. Stimulation of mitotic cyclin production slows the overall depletion of mitotic cyclins during this late stage of the cell cycle.

In conclusion, in both of the classes of parameters investigated, the models disagree even at the qualitative level in many cases. This suggests that it is difficult to make any conclusions about the responses of the cell cycle to any particular pathway based on agreement across multiple models. On the other hand, it also suggests that qualitative differences in response to sustained perturbations may provide a useful discriminating factor between multiple models.

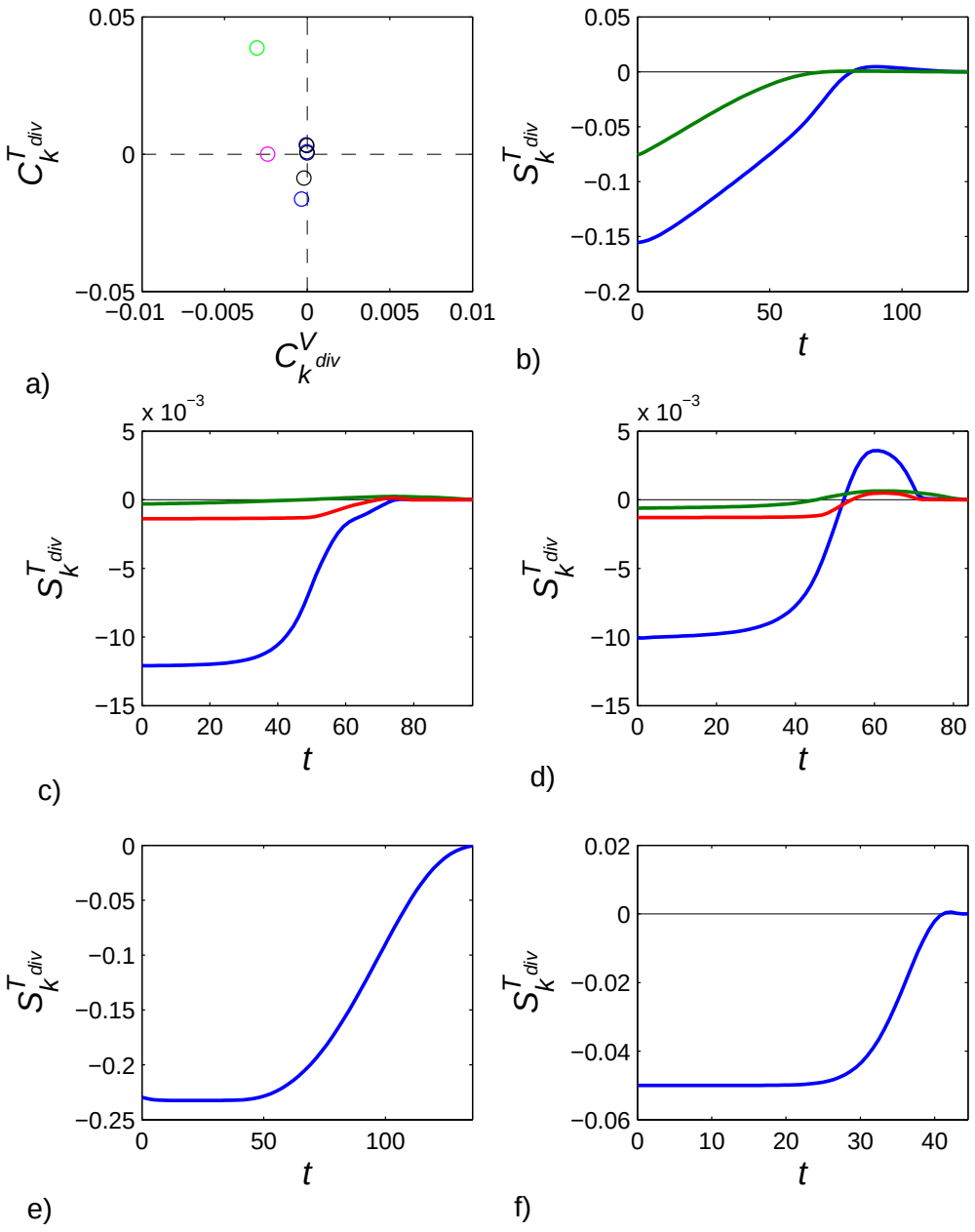

Figure 6.18: Comparison of parameter sensitivities between models - starter cyclin production parameters. The spread of steady state sensitivities is shown in a). The dynamic sensitivities are displayed for b) the Barik model, c) the Chen model, d) the Csikasz-Nagy model, e) the Sriram model, and f) the Kaneko model.

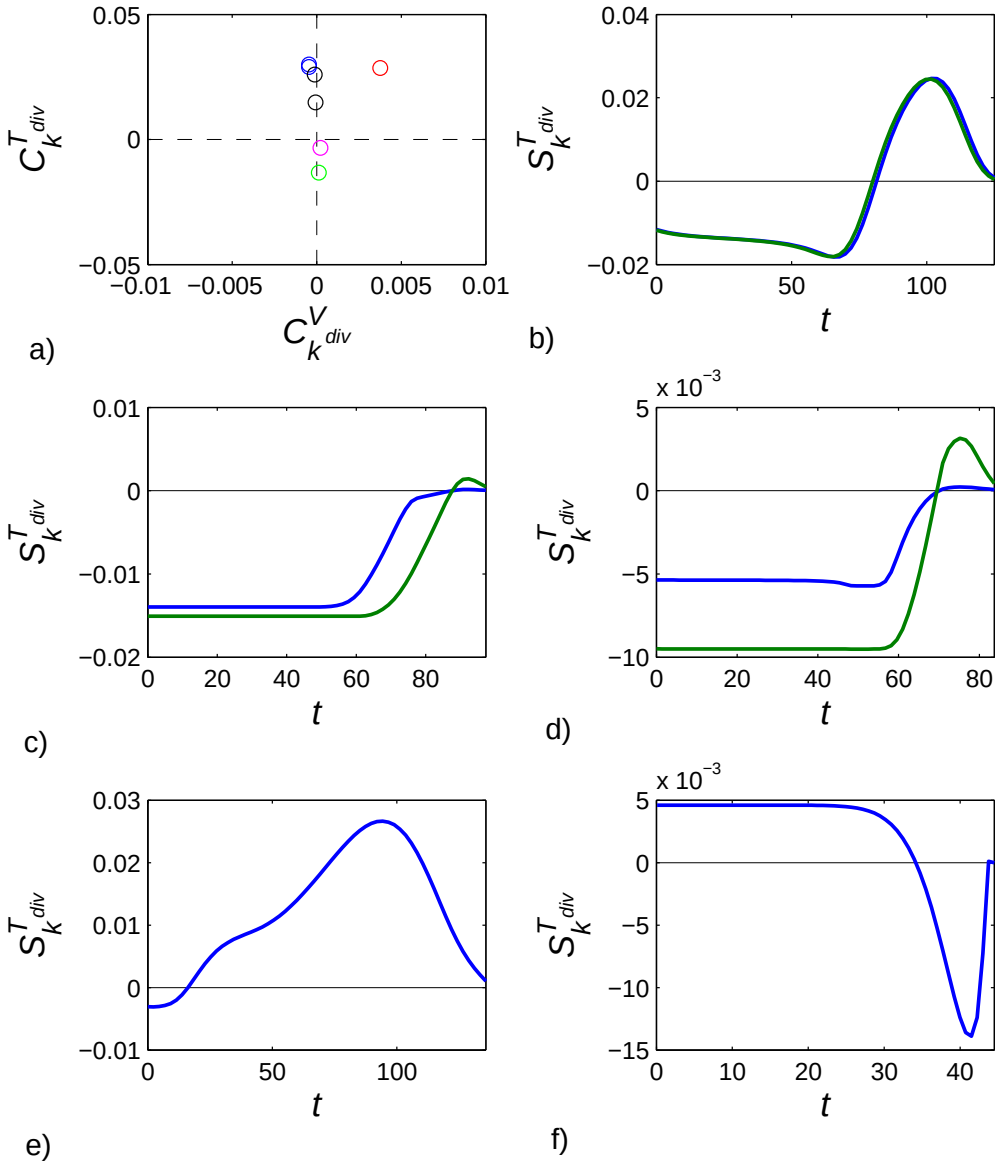

Figure 6.19: Comparison of parameter sensitivities between models - mitotic cyclin production parameters. The spread of steady state sensitivities is shown in a). The dynamic sensitivities are displayed for b) the Barik model, c) the Chen model, d) the Csikasz-Nagy model, e) the Sriram model, and f) the Kaneko model.

6.7 Application of analysis to subpopulations of cells

Many interesting phenomena are observed at the level of cell populations, and the control of cell populations is a topic of relevance to industrial biotechnology. Furthermore, the quantities of biomass required for application of many commonplace experimental techniques (e.g. Western blotting, microarrays, and qRT-PCR) mean that many measurements are made at the level of cell population. It is therefore of interest to examine the consequences of the preceding analysis to the behaviour of populations of cells.

The preceding numerical analysis has been performed on a lineage of daughters-of-daughter cells, meaning that analysis of populations in this context must be limited to populations of such cells. In contrast, the structure of populations of budding yeast consists of a complicated mixture of generations of mother and daughter cells , with different sizes and at different cell cycle stages. As a first step, however, towards understanding the dynamic response of populations of cells, the subpopulation of daughter cells can be examined in terms of the dynamic sensitivity analysis performed above.

Upon application of a step-change in parameters, the relative timing of cell cycle events changes according to the phase shifts given by equation 6.30. These cause a permanent transformation in the distribution of cells across cell cycle stages. The phase shift functions $R_k(phi)$ describe the transformation from one cell cycle stage to another, such that the phase shift of a cell at cell cycle position ϕ subjected to a perturbation Δk is given by the function $h(\phi)$ as follows:

$$h(\phi) = \phi + R_k(\phi).\Delta k \tag{6.38}$$

This expression can be used to numerically evaluate the consequences of perturbations for populations of cells, under the assumption that linear approximations are reasonable. Some examples of the effects of three example perturbations on a uniformly distributed population of daughter cells are shown in figure 6.20. The key observation that can be made is that step-changes in parameters can partially synchronise the population, as seen in the peaks which develop in the distribution (labelled $f(\phi)$) of cell cycle phases. These peaks appear at times in which the slope of the phase shift curve (in figure 6.20 a)) is negative. Intuitively, this is because the cells later are more delayed in their progression than earlier cells, meaning that there is an accumulation of cells around this phase. Similarly, depleted regions in the distribution are the result of a positive slope of the phase shift curve. A

simple corollary of these observations is that it is also possible to partially desynchronise a partially synchronised population of cells if a correctly timed perturbation is applied.

It should be emphasised that the distribution of phases in the population is relative to a reference cell, meaning that the distribution of a population observed at any time will be a phase-shifted version of these distributions. Specifically, this means that the observed distribution of cell cycle phases will match the shape of the given distribution, but that this distribution will be shifted depending on the time at which the observation is made. Even so, different perturbations do, in general, lead to different phases of partially synchronised populations. An example of this is shown in figure 6.20b), in which the perturbation of the parameter k_{ph1p} (displayed in green) partially synchronises the population to a later cell cycle phase than do either of the other perturbations.

This demonstrates clearly that differences in phase shifts observed in cells at different stages of their cell cycles result in compression of cells into particular phases of the cell cycle, and depletion of cells at other phases. This modulation of the population-level behaviour is the key aspect allowing populations of cells to be mode-locked to a periodic external stimulus, as described in (Charvin et al., 2009). Indeed, in (Charvin et al., 2009), it is the daughter cell subpopulation that is mode-locked to periodic stimulation of cyclin production. It is also likely to be significant in the partial synchronisation of yeast cells undergoing metabolic cycling (Tu et al., 2005). Furthermore, it is significant to note that the previous observation that phase shifting of cells is not possible in cell types which divide symmetrically would suggest that attempts to synchronise populations of cells by techniques utilising perturbations of the cell cycle are unlikely to be successful. This is in agreement with previous observations (Cooper, 2004).

Note that while the numerical evaluation of the partial synchronisation of a population of cells can be complemented by analytical results, this is made difficult by the ability of cells to overtake one another in their cell cycle position (i.e. the ordering of cell cycle stages is not preserved upon the application of a step-change in parameters), and is therefore outside the scope of the present investigation.

6.8 System-wide comparisons of models

The preceding analysis has focussed on some examples of ways in which the cell cycle models suggest dynamic regulation of the cell cycle might occur, and the models have been compared to one another in a relatively limited way, in terms of sensitivities of analogous

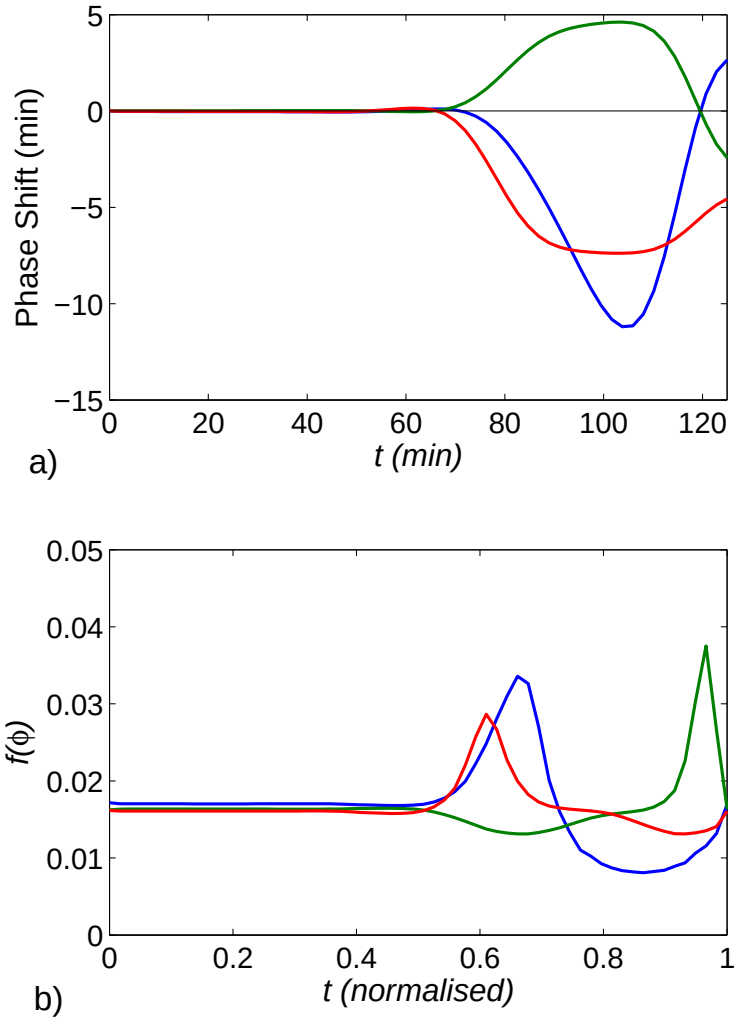

Figure 6.20: (a) The phase responses of the system in response to the three example parameters considered here (g_{dbM} in blue,k_{ph1p} in green, and k_{dh1p} in red). (b) The partial synchronisation of cells that are initially uniformly distributed across cell cycle stages is shown. It is seen that distribution resulting from the perturbation of k_{ph1p} (green) is, on average, phased later in the cell cycle than the other two perturbations. Further, it is clear that perturbation of g_{dbM} (blue) has the strongest overall synchronising effect, as can partly be expected by the greater magnitude of phase shifting occurring in this case (as displayed in a)).

parameters in the models. It is also possible, however, to investigate some more general properties of these models. This is useful for understanding more about what the models have in common in their essential behaviours, irrespective of which particular parameter is being looked at. The properties investigated here are the dynamic flexibility of the models, and the timing of biphasic sensitivity responses.

6.8.1 Comparison of model flexibility

A first step towards making system-wide comparisons between models is to evaluate the dynamic "flexibility" of the models. One way of quantitatively measuring this is to calculate the singular value decomposition (SVD) of a matrix of sensitivities, as described in (Rand et al., 2006). The first step is to define a relationship between observable characteristics Q and the parameter perturbations $\delta\eta$ through a sensitivity matrix A:

$$\delta Q = A\delta\eta \tag{6.39}$$

Where $\delta\eta$ is a vector of relative changes in parameters (so $\delta k = \delta\eta\Delta_k$, where Δ_k is the diagonal matrix $diag(k_1, k_2, ..., k_n)$). The SVD of the matrix A can then be computed easily. How rapidly the relative singular values, σ, of this matrix decrease gives a measure of how flexible the model structure is. If there are many large singular values then this suggests that there are several dimensions which the parameters of the model can regulate independently, and the model is flexible. On the other hand, if the singular values decrease in magnitude rapidly then this suggests that the parameters are not capable of independent regulation of the characteristics Q examined, and the model is inflexible. This method of analysis has previously been applied to evaluate models of circadian oscillators (Rand et al., 2006).

In this case, δQ can be chosen in several different ways. One way is to make it a vector of the changes in cell volume at division and the cell cycle period at the end of one cycle:

$$\delta Q = \begin{pmatrix} \delta V_{div} \\ \delta T_{div} \\ \delta V_{div,1}(t) \\ \delta T_{div,1}(t) \end{pmatrix} \tag{6.40}$$

The relevant sensitivity matrix is then given by:

$$A = \begin{pmatrix} C_{k_1}^{V_{div}} & C_{k_2}^{V_{div}} & ... & C_{k_n}^{V_{div}} \\ C_{k_1}^{T_{div}} & C_{k_2}^{T_{div}} & ... & C_{k_n}^{T_{div}} \\ S_{k_1}^{V_{div},1}(t) & S_{k_2}^{V_{div},1}(t) & ... & S_{k_n}^{V_{div},1}(t) \\ S_{k_1}^{T_{div},1}(t) & S_{k_2}^{T_{div},1}(t) & ... & S_{k_n}^{T_{div},1}(t) \end{pmatrix} \tag{6.41}$$

Here, n gives the number of parameters for the model in question. Since the calculations use discrete values, and dynamic functions have been included in equations 6.40 and 6.41, the functions $S_k^Q(t)$ are replaced by vectors containing 60 values each ($S_k^Q(t_1), S_k^Q(t_2), ...S_k^Q(t_{60})$), equally spaced in time. Having defined the vector of characteristics, it is now possible to describe the specific meaning of the relative magnitude of the singular values of A: they describe how independently the cell size and timing of division can be varied, if any combination of parameters is allowed to be perturbed. It therefore quantifies the intuitive idea that the model behaviour is modulated along fewer dimensions than the dimensions of the parameter space. While the specific meaning of the singular value decomposition in this case is determined by equations 6.40 and 6.41, it should be noted that including additional outputs (e.g. $T_{bud,3}$) does not significantly affect the results of the analysis. This is explained by the fact that the SVD is insensitive to the inclusion of additional data that can be expressed as a linear function of data already present.

The results of applying the above analysis to the models considered (except the Pfeuty model) is shown in figure 6.21. Interestingly, there do not appear to be substantial differences in the flexibility observed in these models, with the exception of the Sriram model, which appears slightly less flexible. This is in broad agreement with the idea that more complex models, with multiple forms of feedback regulation, exhibit greater flexibility (Rand et al., 2006).

Given the qualitative observation made of the steady state sensitivities previously, in which the Csikasz-Nagy model did not appear to have much capacity for independent modulation of V_{div} and T_{div} (i.e. many of the pairs of sensitivities $(C_k^{V_{div}}, C_k^{T_{div}})$ appeared to be linearly dependent), it is somewhat surprising that the Csikasz-Nagy model shows at least as much flexibility in response as the other models considered. This can be explained by the relatively insignificant weight placed in the flexibility analysis on the steady state response. It is not possible to apply the above analysis to just the steady state characteristics, since the singular value decomposition requires that the number of parameters be fewer than the number of characteristics (hence the inclusion of dynamic response functions above). However, the analysis may be adapted by considering the average flexibility of regulation

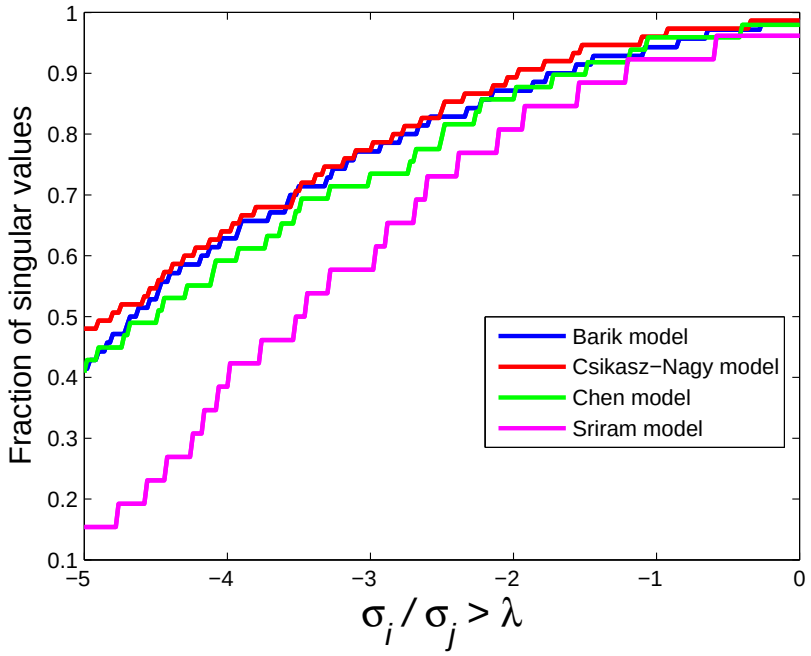

Figure 6.21: The flexibility of the models is plotted according to the fraction of singular values σ_i of the matrix A which obey the relationship $\sigma_i/\sigma_{max} > \lambda$, in which σ_{max} is the maximal singular value of A. The more rapidly this fraction drops off with λ, the more rapidly the singular values decline, and the less flexible the mode is. Thus, it is seen that the Sriram model displays noticeably less flexibility than the other models considered here. This is partially expected as a result of the smaller number of parameters and species in the Sriram model.

Table 6.1: Flexibility of modulation of V_{div} and T_{div}

Model	Average σ_2/σ_1
Barik	0.1762
Csikasz-Nagy	0.0021
Chen	0.0032
Sriram	0.0377
Kaneko	0.0694

of all possible pairs of parameters, so that the quantities in equation 6.39 are defined by:

$$\delta Q = \begin{pmatrix} \delta V_{div} \\ \delta T_{div} \end{pmatrix} \tag{6.42}$$

$$A = \begin{pmatrix} C_{k_1}^{V_{div}} & C_{k_2}^{V_{div}} \\ C_{k_1}^{T_{div}} & C_{k_2}^{T_{div}} \end{pmatrix} \tag{6.43}$$

This provides a pair of singular values (or, equivalently in this case, eigenvalues) for each pair of parameters. The relative magnitude of the smaller singular value (compared to the larger singular value), averaged across all pairs of parameters, is then a measure of how flexible the steady state behaviour is. The results of this analysis are shown in table 6.1.

This gives quantitative backing to the observations made above that the Csikasz-Nagy model has a relatively inflexible steady state response. It further demonstrates that the Pfeuty and Sriram models, included here as examples of more abstract models of the cell cycle, are quite flexible, and that the Barik model is the most flexible in this sense.

6.8.2 Post-G1-phase dynamics as a source of biphasic responses

An observation that can be made from surveying the wealth of sensitivity data available is that the $Z_k^Q(t)$ of parameters associated with species involved in the early stages of the cell cycle (G1 phase, pre-budding) are monophasic, meaning they are strictly positive or negative (and, therefore, that $S_k^Q(t)$ is strictly increasing or decreasing, respectively). In contrast, the dynamic sensitivities of parameters associated with species involved in post-G1 phases often appear to display some degree of biphasic response, where they increase and decrease. This qualitative observation can be made quantitative by dividing the cell cycle into pre- and post-budded stages and asking what fraction of model parameters exhibit biphasicity above a given threshold, γ. Specifically, this asks what fraction of parameters

obey the relationships:

$$\begin{aligned} max(Z_k^Q(t)) &> 0 \\ min(Z_k^Q(t)) &< 0 \\ ||log_2\left(\frac{|max(Z_k^Q(t))|}{|min(Z_k^Q(t))|}\right)||_\infty &< \gamma \end{aligned} \tag{6.44}$$

The first two conditions require that there is a change in the direction of $Z_k^Q(t)$, while the second requires that the fold-change between the peak and trough of $Z_k^Q(t)$ is less than γ. Varying γ varies how strenuous this requirement is. Figure 6.22 displays the variation in these proportions for the Barik, Csikasz-Nagy, Chen, and Sriram models (the Pfeuty model is excluded here since it only makes use of 8 parameters), with the characteristic taken to be $Q = T_{div,1}$.

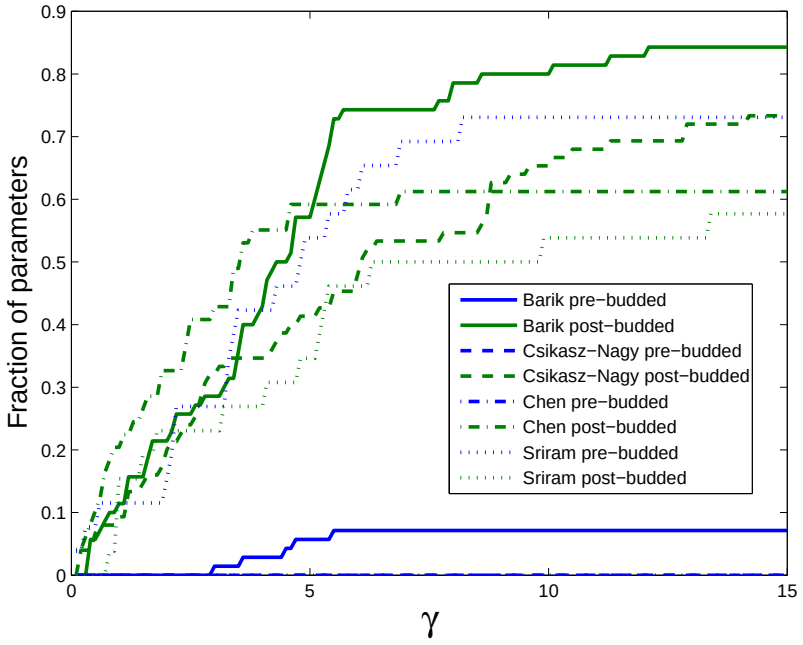

Figure 6.22: Fraction of parameters for each model with a biphasic response below the threshold γ in the post-budded phase (green lines) compared to the fraction with biphasic response in the pre-budded phase (blue lines). In all cases, a significant fraction of parameters are observed to exhibit biphasic responses in the post-budded phase, and in all cases except the Sriram model this fraction is much greater than the fraction of parameters observed to exhibit biphasic responses in the pre-budded phase.

As can be seen, there is a general trend towards parameters being biphasic in the post-budded phase - only in the Sriram model are a greater fraction of parameters biphasic in the pre-budded phase compared to the post-budded phase, and even in this case a significant fraction of sensitivities are biphasic in the post-budded phase. The Chen and Csikasz-Nagy display no biphasic responses in the pre-budded phase whatsoever across the range of γ considered. This observation can be understood at a simplified level as resulting from the dynamic structure of the models, as studied through bifurcation analysis previously .

Bifurcation analysis of all of the models discussed here has shown that their behaviour is characterised by a size threshold. When the cell volume is below this threshold, the cell cycle sits at a stable steady state. Upon passing through a bifurcation at a critical size, the cell cycle leaves this steady state, entering an oscillatory regime. The frequency of these oscillations depends on the parameters. The cell cycle is therefore divided into two regimes - a regime in which a stable steady state dominates the dynamics, and an oscillatory regime. As a simple approximation, these regimes can be identified as the pre- and post-budded stages of the cell cycle, respectively, since the budding threshold is passed during the first "upswing" in starter kinase activity in the oscillatory regime. A detailed analysis of these properties is beyond the scope of this work.

6.9 Conclusions

In this chapter a systems framework was developed and employed to understand dynamic regulation of the cell cycle and growth in budding yeast. The budding yeast is a model organism for the study of the cell cycle, and its progression through the cell cycle is marked by the appearance of a growing bud, which eventually forms the daughter cell after division. The budding event is coordinated by the cell cycle, but also feeds back on it, since the timing of these events has consequences for the size of daughter cells in subsequent generations. The investigation of the connections and coordination between the cell cycle and these developmental events across changing environmental conditions provide the motivation for the application of the analytical framework developed here.

Working within the framework developed, a detailed sensitivity analysis was employed to investigate five different models of the budding yeast cell cycle (two of which are adapted from more general models of the eukaryotic cell cycle). While these models disagree on some of the details of mechanisms, and represent varying levels of abstraction, it has been shown here that there are some common properties between the models which can be taken

advantage of to look at principles of dynamical regulation. While some results are specific to models of the budding yeast cell cycle, it is likely that other results are more general. This is especially true given that some of the models considered (the Sriram and Pfeuty models) were not developed to be specific to the budding yeast cell cycle, but were intended to represent a more general picture of the eukaryotic cell cycle.

In order to develop some basic understanding to the regulation of the cell cycle, linear sensitivity analysis was performed of a set of cell cycle models. Implicitly, this represents a signal regulating the cell cycle as a change in a model parameter. The advantage of linear analysis is that sensitivities of the system to combinations of parameters, or a series of changes, arise automatically from analysis of the individual parameter sensitivities. The sensitivity analysis performed here can be divided into the steady state and dynamic analyses. The steady state analysis investigated the eventual behaviour of the system in response to a sustained change in parameters, while the dynamic analysis investigated the dynamic approach to that eventual behaviour.

In the steady state analysis, it was shown that there exists a capacity for independent modulation of the size and timing of division in budding yeast. This is in part a result of the flexibility of regulation demonstrated by parameters in the model, but relies especially on the asymmetric division of budding yeast, and thus the ability to alter the fraction of mass donated to the daughter cell upon division. In exponentially growing, symmetrically dividing species and cell types, it is clear that under constant conditions the division time must equal the mass doubling time. It is interesting to note, however, that the concept of "asymmetric division" needn't be restricted to asymmetric division of mass, but may also involve other factors that are preferentially donated to one cell after division (for example, sequestration of damaged proteins). The consequences of other sources of asymmetry in other cell types is a subject for future investigation.

Building on the changes in cell cycle behaviour under constant condition, an exhaustive dynamic sensitivity analysis was performed, looking at changes in division and budding times and sizes across multiple generations. Some simple qualitative properties of these sensitivity curves were described, such as biphasicity. This property means the application of a perturbation may either increase or decrease the observable characteristic, depending on the time of application, and is a property common to the phase response of biological oscillators. In addition, the dynamic sensitivity analysis automatically provided information on the phase shift of the cell cycle observed after a perturbation has been applied, and a relationship was identified between daughter size and these phase shifts. In particular, phase

advances are observed when a greater fraction of mass is donated to the daughter cell, while phase delays are observed in the reverse case. Further investigation of the properties of dynamic sensitivity was then performed by building upon the observation of flexibility of regulation of the cell cycle behaviour under constant conditions. In particular, this flexibility allowed multiple sets of parameter perturbations to be chosen that shared the same change in behaviour under constant conditions, but displayed widely varying differences in their dynamic responses. By considering a continuum of particular subsets of parameter perturbations with the same eventual behaviour, it was then possible to ask what characteristics might be shared by parameter perturbations which achieve optimally fast (under a defined metric) approach to this eventual behaviour. An apparent similarity was observed between the "optimal" parameter perturbations under two metrics - optimising the speed of attainment of the change in cell cycle duration, and in daughter cell size. This is interesting in that it suggests an underlying rigidity in regulation. For example, it may not be possible to both rapidly change the cell cycle duration, and slowly modulate the daughter size at the same time. Finally, the dynamic analysis was further extended by considering the effects of a steady, linear change in parameters over time. In such a scenario, it was demonstrated that signalling mechanisms can again be seen as rapidly or slowly adapting to changes in conditions. One interpretation of this is that signalling mechanisms can operate so as to anticipate future changes, or remember previous conditions.

The preceding analysis has demonstrated some interesting principles which may be important for the regulation of the cell cycle. However, given that in most practical cases there will be only one model and one signalling pathway of interest, it was necessary to consider a case study in which aspects of the analysis were applied to a specific example of cell cycle regulation. The example chosen here was the interaction of glucose signalling pathways with the cell cycle - a physiologically important pathway which allows the cell to rapidly respond to changes in nutrient availability.

The evaluation of sensitivities across multiple models allowed confidence that some patterns of behaviour seen (e.g. nonmonotonic relaxation to the eventual cell cycle behaviour) were generic. It was then of interest to perform some systematic comparison of the different model behaviours. This was first done by comparing the sensitivity of different models to changes in sets of parameters that can reasonably be considered to be analogous to one another. The set of parameters chosen was the sets of parameters regulating the production of different cyclins. This showed that there was some agreement between models, but also that there were some serious qualitative differences between models. The comparison of

analogous parameters here was a special case, since most parameters do not exist analogously in all models considered. Therefore, it was necessary to consider more general, system-level properties of the models. The first such comparison made was at the abstract level of evaluating the regulatory flexibility of the models. The models displayed similar dynamic regulatory flexibility, but dissimilar steady state regulatory flexibility, with two models in particular - the Csikasz-Nagy and Chen models - showing a more restricted set of parameters available for independent modulation (see 6.1). The lack of flexibility cannot immediately be explained by differences in the complexities of the models, since the Csikasz-Nagy model is of comparable structural complexity to the other detailed models. Instead, it seems likely that the Csikasz-Nagy model has a reduced dimension of dynamics as a result of a separation of timescales. In addition to this, an evaluation of the timing of the biphasic property of dynamic sensitivities was performed, finding that in most models it is predominantly localised to the budded phase of the cell cycle (the exception is the Sriram model).

There are two key ways in which the work presented here can be built upon in the future - extension of the theoretical results, and application of the results for experimental investigations. In the first case, there are numerous ways in which the results here can be extended. The most obvious extension is to investigate other cell types. While, as discussed, the most information is available to constrain models of *Saccharomyces cerevisiae*, there have also been modelling investigations of *Saccharomyces pombe*, *Xenopus laeviae*, and mammalian cells. This is particular important given the role that asymmetric division had in the preceding analysis here. Another important aspect to be investigated will be the consequences of regulation of population-level behaviour. This is a natural extension given the importance of population-level behaviours in general processes such as colony establishment and organ growth, and the fact that cell cycle progression automatically determines the dynamics of these processes. Finally, it will be interesting to investigate possible consequences of growth patterns which are not strictly exponential. Such patterns have been known for some time in fission yeast (Baumgartner and Tolic-Norrelykke, 2009), and have recently been identified in some cases in budding yeast (Goranov and Amon, 2010), and mammalian cells (Son et al., 2012). Overall the use of systems frameworks, complemented by experiments, to understand the interaction between cell cycle growth and growth landmarks, the environmental regulation and the consideration of population level effects will provide important insights into these issues in multiple systems.

The feasibility of applying the results presented here to interpret experimental results

depends crucially on the current state-of-the art. Recently, an investigation of the interaction between osmotic stress signalling and the G1-S transition has been performed (Adrover et al., 2011) (note that the mathematical model developed in this paper is not suitable for the analysis performed here as it only represents the G1-S transition). While these results are interesting, they make extensive use of population-level measurements, and do not link changes in one cell cycle to subsequent cycles. However, the essential motivation for the work - looking for how different combinations of regulation explain the dynamic regulation at different cell cycle times - is in common with the approach taken here, and it is to be expected that further work along these lines will connect closely with aspects discussed here. An important factor in the success of future investigations along these lines will be the technology available. Here, there are two aspects which should be highlighted: the ability to observe behaviour at the single-cell level, and the ability to precisely control the application of perturbations to cells being observed in this way. Live-cell imaging techniques are becoming widely available (Larson et al., 2009; Locke and Elowitz, 2009; Spiller et al., 2010), and much excellent work has already been performed in budding yeast making use of such technology (Baumgartner et al., 2011; Bean et al., 2006; Charvin et al., 2009, 2008, 2010; Muzzey et al., 2009). Furthermore, advances in microfluidics (Bean et al., 2006; Charvin et al., 2008; Rowat et al., 2009) allow previously infeasible degrees of control to be applied to perturbations of these cells. In summary, the basic experimental techniques are available to probe the questions raised by this analysis, at least at the qualitative level, in a variety of cell types.

The most interesting possibility raised by the advancement of experimental techniques for investigating controlled perturbation of the cell cycle is the potential identification of common properties across the different signalling pathways to the cell cycle. For example, the regulation of the cell cycle by nitrogen- and glucose-sensing signalling pathways, which have both evolved to play similar roles, may be expected to exhibit similarities at the level of dynamic regulation. The evaluation and comparison of such control mechanisms is naturally facilitated by the framework established here.

In conclusion, a systems framework has been developed to understand different aspects of the regulation of the cell cycle and interaction of growth and growth landmarks in budding yeast. This provides various insights into the dynamic regulation of the cell cycle in budding yeast. The development and use of such systems frameworks, complemented by experiments, is expected to be very useful in understanding the interaction between the cell cycle and various other cellular processes, in multiple systems.

Chapter 7

Conclusions and future work

This thesis has presented a range of studies seeking to understand a wide variety of different aspects of cellular signalling. In each case, a specific example system was identified, and exhaustive analysis applied to discover the range of behaviours the system was capable of producing. These example systems spanned a wide range of signalling systems, from the simple to the complex.

Beginning at the level of models of generic signalling systems, Chapter 3 investigated the consequences of coupling between two pathways by the sharing of a common component between these pathways. This simple motif is seen across a wide range of biological systems, in which proteins are often involved in multiple functions at the same time. The analysis of the signalling capabilities of this system are thus of broad interest. As such, interesting behaviours such as ultrasensitive and adaptive behaviours were identified. This analysis was then built upon to include other features common to signalling networks, such as post-translational modification, spatial variation, and allosteric control. These elaborations provided biologically motivated example systems with a richer variety of behaviours, and interesting properties of these systems were identified. For example, it was found that two molecular switches sharing the same modifying enzyme could be robustly coordinated with one another by this coupling.

The identification of interesting behaviours resulting from the combination of protein-protein interactions and enzymatic reactions then motivated the investigation of a series of models of a simple two-stage cascade of post-translational modifications in Chapter 4. These models represent another class of generically seen motifs in biological signalling networks. Here, it was shown that some nontrivial transformations in the signalling behaviour

of these systems could result from the incorporation in these models of some additional protein-protein interactions other than those usually considered in models of these systems. These additional protein-protein interactions include product inhibition, and the interaction of inactive enzyme with its substrate. In particular, product inhibition was found to allow biphasic signalling behaviour, while binding of inactive enzyme to substrate facilitated additional sensitivity of signalling. These results were robust to the choice of parameters, and even to further elaboration of the model structure (e.g. by including multiple modification of substrate by enzyme).

Having established a range of behaviours possible in some systems, it was then of interest to consider the consequences of connecting signalling modules with different behaviours to one another (Chapter 5). In this case, rather than asking what the behaviour is of a particular module, it is assumed from the start that a module exhibits a particular behaviour - in this case either adaptive or threshold responses - and the objective is then to identify the behaviours exhibited by combinations of these modules. In the case of the combination of adaptive and threshold modules considered here, behaviours including switching in response to temporal gradients and robust pulsing of signalling were identified. By casting the interaction of these processes in a modular systems framework, we have taken the first steps towards understanding how these fundamental elements interact. In complex networks additional effects or pathways may further alter the output from each module. The possibility of more complex interaction as well as feedback between these modules points to the possibility of more complex temporal patterns. The study presented here will be used as a basis for further expansion, as well as a systematic exploration of these additional features. It could also provide interesting insights in the emerging area of synthetic biology, especially in the context of circuits which may involve the elements discussed here. More generally, we believe that a modular systems-based approach can provide valuable new insights and the basis of a systematic exploration the possible variety of roles of different elements in cell signalling.

The first three chapters of results were able to establish robust, interesting conclusions by considering representations of signalling behaviours and mechanisms that are ubiquitous in biological systems. In contrast, the final chapter of results (Chapter 6) involves a detailed analysis of a particular process - the budding yeast cell cycle. This is of interest due to the central role played by the cell cycle in the lifetime of cells, and detailed investigation is made possible by the availability of detailed information on the mechanism of progression of the budding yeast cell cycle. This knowledge has been consolidated in the

literature in the form of a variety of mathematical models of the cell cycle. In this chapter, a framework is developed and applied for the investigation of the dynamic response of the cell cycle to external perturbations. This framework involved detailed sensitivity analysis of a selection of cell cycle models taken from the literature. This demonstrated the link between cell size control and cell cycle synchronisation of a population of cells in a changing environment. It also demonstrated a variety of interesting dynamic responses of the cell cycle to changes in conditions. Such dynamics remain to be identified experimentally, but the analysis performed here provides a framework within which such experiments might be performed.

In conclusion, this thesis has, in the first place, utilised a wide range of mathematical modelling and analysis to investigate the essential capabilities of some simple biochemical signalling mechanisms, and the behaviours resulting from the composition of such mechanisms. In the second place, it has established a framework for understanding the regulatory mechanisms underlying the complex process of cell cycle progression. The continued development of approaches along these lines is expected to expedite biological discovery as the discipline fulfils its potential as a fully quantitative science.

Appendix A

Coupling of pathways: Parameter values

The parameter values for the simulations shown in the figures are listed below.

Figure 3.2

Total amounts of A and B were maintained ($[AT] = [BT] = 1$), and the simulations were run to steady state. The affinities used were $K_A = 10^3$, $K_B = 70$.

Figure 3.3

$K_A = 10^3$, $K_B = 70$. All degradation constants were equal: $k_{dx} = k_{da} = k_{db} = k_{dax} = k_{dbx} = 0.01$. Production of A and B was set at the same rate: $k_{pa} = k_{pb} = 0.02$. Initially, no X is produced ($k_{px} = 0$), but at the start of the simulation it is stepped up to $k_{px} = 0.08$. In a) the timescales of both interactions, set by the disassociation rates, are equal: $k_{a2} = 1/\tau_B = k_{b2} = 1/\tau_B = 1$. In b), $k_{a2} = 1/\tau_A = 1$, $k_{b2} = 1/\tau_B = 0.001$. In c), $k_{a2} = 1/\tau_A = 0.001$, $k_{b2} = 1/\tau_B = 1$. In d) $k_{a2} = 1/\tau_A = 0.001$, $k_{b2} = 1/\tau_B = 1$, with 0.5 X being added at $t = 0$.

A.0.1 Figure 3.4

The affinities here are equal, $K_A = K_B = 1$, while the timescales differ: $k_{a2} = 1/\tau_A = 1000, k_{b2} = 1/\tau_B = 0.1$. The production and degradation of all species are initially equal: $k_{dx} = k_{da} = k_{db} = k_{dax} = k_{dbx} = k_{px} = k_{pa} = k_{pb} = 0.01$. The production rate of X is then pulsed up to a peak of 0.11 over a time of 1 (arbitrary units).

Figure 3.5

The affinities used were $K_A = 103$, $K_B = 70$. All degradation constants were equal: $k_{dx} = k_{da} = k_{db} = k_{dax} = k_{dbx} = 0.01$. Production of X was the same: $k_{px} = 0.01$. In a), production of A was stepped up from $k_{pa} = 0$ to $k_{pa} = 0.02$ at $t = 0$, while production of B was maintained at $k_{pb} = 0.02$. In b), production of B was stepped up from $k_{pb} = 0$ to $k_{pb} = 0.02$ at $t = 0$, while production of A was maintained at $k_{pa} = 0.02$.

Figure 3.6

The parameters were identical as those for figure 3.5, except that here the production of both A and B was stepped up from $k_{pa} = k_{pb} = 0$ to $k_{pa} = k_{pb} = 0.02$ at $t = 0$.

Figure 3.8

In part a), $K_{A1} = 5$, $K_{A2} = 20$, $K_B = 10$. In part b), $K_{A1} = 20$, $K_{A2} = 20$, $K_B = 10$. In c), just A, X, and Y were considered, and $K_{A1} = 20$, $K_{A2} = 20$ was taken for both mechanisms, allowing comparisons to be drawn. In d), $K_{A1} = 1$, $K_{A2} = 1$, $K_B = 10$, $\alpha = 100$.

Figures 3.9 and 3.10

Here, the kinetics of the two switches differ only in the rate of association between enzyme and substrate. The complete parameters are: $k_{a1} = 100$, $k_{a2} = 1$, $k_{a3} = 10$, $k_{a4} = 1$, $K_{ma4} = 0.01$, $k_{b1} = 10$, $k_{b2} = 1$, $k_{b3} = 10$, $k_{b4} = 1$, $K_{mb4} = 0.01$. There is no production and degradation of proteins involved, since we look at the steady state response.

Figure 3.11

The parameters used for the multiphosphorylation (activating A) are identical to those given in Markevich et al Markevich et al. (2004). These are: $k_1 = 0.02$, $k_{-1} = 1$, $k_2 = 0.01$, $k_3 = 0.032$, $k_{-3} = 1$, $k_4 = 15$, $h_1 = 0.045$, $h_{-1} =$, $h_2 = 0.092$, $h_3 = 1$, $h_{-3} = 0.01$, $h_4 = 0.01$, $h_{-4} = 1$, $h_5 = 0.5$, $h_6 = 0.086$, $h_{-6} = 0.0011$. The parameters for the monophosphorylation (activating B) are $k_{b1} = 0.02$, $k_{b2} = 1$, $k_{b3} = 0.4$, $k_{b4} = 1$, $K_{mb4} = 0.1$.

Figures 3.12 and 3.13

Here, the interactions are all equal affinities and timescales, $K_A = K_B = 70$. The degradation rates for all components, and production rates of A and B, are equal: $k_{dx} = k_{da} = k_{db} = k_{dax} = k_{dbx} = k_{pa} = k_{pb} = 0.01$. Non diffusible components had $D = 0$, while diffusible components had $D = 100$. Production of X was varied as indicated. A Gaussian production term was used for localised production, with a standard deviation of 5% of the domain size.

Figure 3.14

Here, the conditions are as in figures 3.12 and 3.13, except for the affinities, which are varied. Here the low affinity component had $K = 5$, while the high affinity component had $K = 50$. Where affinities are equal, they are each set to $K = 5$. Production of X was maintained constant at, $kpx = 0.001$.

Appendix B

Multiple enzyme-substrate interactions: Parameter values

Basic model

The basic model uses mass action kinetics to model the interactions and reactions between a signal, S, an enzyme, A, its substrate, B, and two proteins, X and Y, responsible for deactivation of A and demodification of B, respectively. We have chosen a basal set of parameters for use with the model, corresponding to an enzymatic cascade with X and Y acting close to saturation. In addition, we look at an alternative parameter set with X and Y far from saturation. All concentrations and dissociation constants (the reciprocal of affinities) are made dimensionless by being scaled to one another. The dissociation constants are given by $K_d = k_r/k_f$, where the parameter subscripts "*f*" and "*r*" denote binding and unbinding rates, respectively. Here, we use concentrations of A and B of dimensionless order 1 (see below), with the dissociation constant of their interaction of order 0.1. This corresponds to an interaction between A and B where their overall concentrations are 100 nM and the dissociation constant is 10 nM, as discussed in the text. Catalytic reaction rates are dimensionless, the key point being that the interactions are on a faster timescale than the catalytic reactions (the degree of timescale separation was one of the factors investigated, and found to have little effect on the results).

For the basal parameter set, the initial conditions determine the quantities of S, A, B, X, and Y available during the simulations. In particular, the basal conditions were $[A_T] = 3$, $[B_T] = 1$, $[X_T] = 0.05$, $[Y_T] = 0.1$. In the dynamic case, the initial conditions before the step change in $[S_T]$ were set by allowing the system to reach its steady state at low

signal levels $[S_T] = 0.01$, before applying a step change (to $[S_T] = 0.5$, except in the case of figure 4b), where the step change, following the direction of the black arrow, is made to $[S_T] = 0.05, 0.043, 0.04, 0.037, 0.035$). The basal parameters used were as follows (given in the order: association reactions, dissociation reactions, and catalytic reactions): $k_{1f} = 10$, $k_{3f} = 10$, $k_{5f} = 50$, $k_{7f} = 10$, $k_{9f} = 0$, $k_{10f} = 0$, $k_{11f} = 0$, $k_{1r} = 1$, $k_{3r} = 1$, $k_{5r} = 1$, $k_{7r} = 1$, $k_{9f} = 1$, $k_{10f} = 1$, $k_{11f} = 1$, $k_2 = 0.1$, $k_4 = 0.1$, $k_6 = 0.5$, and $k_8 = 0.1$.

In order to show the effects of the additional interactions (as shown in figures 4.2, 4.3, 4.4, 4.5, 4.6, 4.7, 4.8, 4.9, 4.10, 4.11, 4.12, 4.13, and 4.15) the parameters responsible for these interactions were varied in a set way. In the case of product inhibition, inactive enzyme interference, and the interaction of inactive enzyme with modified substrate, the parameters k_{9f}, k_{10f}, and k_{11f}, respectively, took the values 0, 1, 2.5, 5, and 10. In order to show the effects of changing $[A_T]$ (in figures 4.4 and 4.10), $[A_T]$ was varied in the range from 1 to 5. For figures 4.5 and 4.12, which illustrate the effects of affinity variation, the high and low affinity cases were examined by uniformly doubling and halving (respectively) the values of k_{9f} (for product inhibition) and k_{10f} (for inactive enzyme interference). For figure 4.11, illustrating the case of inactive enzyme interference with $[B_T] > [A_T]$, the basal parameter set was used, but with $[A_T] = 1$ and $[B_T] = 3$. In the investigation of the effects of the variation of the relative timescales of catalysis and complex formation, simulations with different relative timescales were performed by uniform fold-changes in the catalytic rates (i.e. k_2,k_4,k_6, and k_8).

The alternative basal conditions (used for figures 4.3 and 4.8) were $[A_T] = 3$, $[B_T] = 1$, $[X_T] = 1$, $[Y_T] = 1$. This is the same as for the basal case, except for $[X_T]$ and $[Y_T]$, which are substantially higher. The alternative parameter set was $k_{1f} = 0.1$, $k_{3f} = 0.1$, $k_{5f} = 0.1$, $k_{7f} = 10$, $k_{9f} = 0$, $k_{10f} = 0$, $k_{11f} = 0$, $k_{1r} = 1$, $k_{3r} = 1$, $k_{5r} = 1$, $k_{7r} = 1$, $k_{9f} = 1$, $k_{10f} = 1$, $k_{11f} = 1$, $k_2 = 0.05$, $k_4 = 0.1$, $k_6 = 0.5$, and $k_8 = 0.1$. This is the same as the basal set, except for k_{1f}, k_{3f}, k_{5f}, and k_2.

The graded response shown being modulated by inactive enzyme interference in figure 4.9 was obtained using parameters identical to the basal parameter set, except for the kinetics of demodification of B ($k_{5f} = 1$, $k_{5r} = 1$,$k_6 = 0.1$), and with the total quantity of the enzyme responsible for that reaction changed (so $[Y_T] = 1$). This corresponds to a situation in which Y is much less saturated than in the basal case.

Double modification of substrate

The parameter values and component concentrations used in the double modification of substrate model (figure 4.16) were identical to the basal set of parameters described above (only one set was used in this case) - the additional reaction has the same kinetics as the original reaction, and so no additional parameters are required. In figure 9, for the cases of product inhibition and inactive enzyme interference, the parameters k_{9f} and k_{10f}, respectively, took the values 0, 1, 2.5, 5, and 10 (as was the case for the analogous study in the basic model).

Scaffold-mediated signalling

The concentrations of the components used for the scaffold-mediated signalling model were the same as those used in the basic model (simulation results shown in figure 4.17). The new component, C, is present in concentration $[C_T]$ = 1. The parameters used (again, given in order of type), were: $k_{1f} = 10$, $k_{3f} = 10$, $k_{5f} = 50$, $k_{7f} = 10$, $k_{8f} = 10$, $k_{9f} = 0$, $k_{10f} = 0$, $k_{1r} = 1$, $k_{3r} = 1$, $k_{5r} = 1$, $k_{7r} = 1$, $k_{9r} = 1$, $k_{10r} = 1$, $k_2 = 0.1$, $k_4 = 0.1$, $k_6 = 0.5$, and $k_{11} = 0.1$. In figure 10, for the cases of product inhibition and inactive enzyme interference, the parameters k_{9f} and k_{10f}, respectively, took the values 0, 1, 2.5, 5, and 10 (as was the case for the analogous study in the basic model).

Appendix C

Interaction of modules: Parameter values

We briefly present the parameter values which are used in this study, module by module. We note that these parameters are dimensionless, as only their relative values are important. The initial conditions in each simulation were the steady state of the system under the initial value of the input signal, S.

Adaptive module The parameter values used were: $k_a = 1$, $k_{-a} = 1$, $k_i = 0.2$, $k_{-i} = 0.05$, $k_f = 1000$, $k_r = 1000$. The initial input signal was $S = 0.1$. This was stepped up to $S = 10$ at $t = 0$. This set of parameter values was used for all simulations, with scaling parameters κ (multiplying all kinetic parameters) and λ (multiplying the output, R^*) used to scale the timescale and amplitude of the pulse, respectively. This allowed the effects of signal duration and magnitude on the downstream module to be analysed independently of changes in the shape of the pulse. For the results shown in figure 5.3, $\kappa = 3$ and $\lambda = 1$. In figure 5.4 the short pulse was obtained by taking $\kappa = 80$, the medium pulse was obtained by taking $\kappa = 66$, and the long pulse was obtained by taking $\kappa = 66$ (all with $\lambda = 2.8$). In figure 5.9 and 5.11, $\kappa = 10$ and $\lambda = 2.8$.

Goldbeter-Koshland switch The parameters used for the Goldbeter-Koshland switch were $V_1 = 2$, $V_2 = 1$, $K_{m1} = 0.01$, and $K_{m2} = 0.01$.

MAPK cascade The equations for each stage of the MAPK cascade involve standard Michaelis-Menten kinetics. The parameters used for each stage of the MAPK cascade were all chosen to be the same: $V_1 = 2$, $V_2 = 1$, $K_{m1} = 0.1$, and $K_{m2} = 0.1$.

Bistable switch with saturated degradation The parameters used for the bistable

switch were $V_1 = 250$, $V_2 = 4.25$, $K_{m1} = 100$, $K_{m2} = 0.01$, and $k_{fb} = 27.1$. In the case of figure 5.11(b), where it is desired to show how an adaptive module responds to a very fast switch, the dynamics of the bistable switch are sped up by multiplying the kinetic parameters V_1, V_2, and k_{fb} by a factor of 40.

Toy bistable switches For the toy model of bistability given by equation 5.8 and used in Fig. 5.5c, $\alpha = 1$. For the toy model of bistability given by equation 5.19 and used in Fig. 5.9, $\alpha = 40$ and the basal states of the roots are $u_1 = 0$, $u_2 = 0.5$, and $u_3 = 1$. The adaptive pulse output in this case is added onto the location of the roots directly.

Parameter values for square and exponential pulses The basal states of the input pulses used to obtain figures 5.5a,b and c were held at S_b = 0.63, S_b = 0.55, and S_b = 0.5, respectively. Note that figure 5.5a was obtained for a square pulse input, while figures 5.5b and c were obtained for the exponential pulse input.

Response of bistable module to multiple pulses The square pulses used to obtain figure 5.8 had period, T = 0.14, basal state, S_b = 0.63, and peak value, S_p = 1.18.

Response of monostable module to multiple pulses The square pulses used to obtain figure 5.7 had period, T = 0.1, basal state, S_b = 0, and peak value, S_p = 1.

Alternate interconnection of modules Simulations were performed for the alternate order of interconnection of modules. The modules (described in the main text) have a clear input and output. Thus when the adaptive module is connected upstream of the threshold module, the output of the adaptive module is the input to the threshold module (and the input to the composite module is the input to the adaptive module). This is used to solve the (now coupled) differential equations.

Appendix D

Cell cycle: additional plots

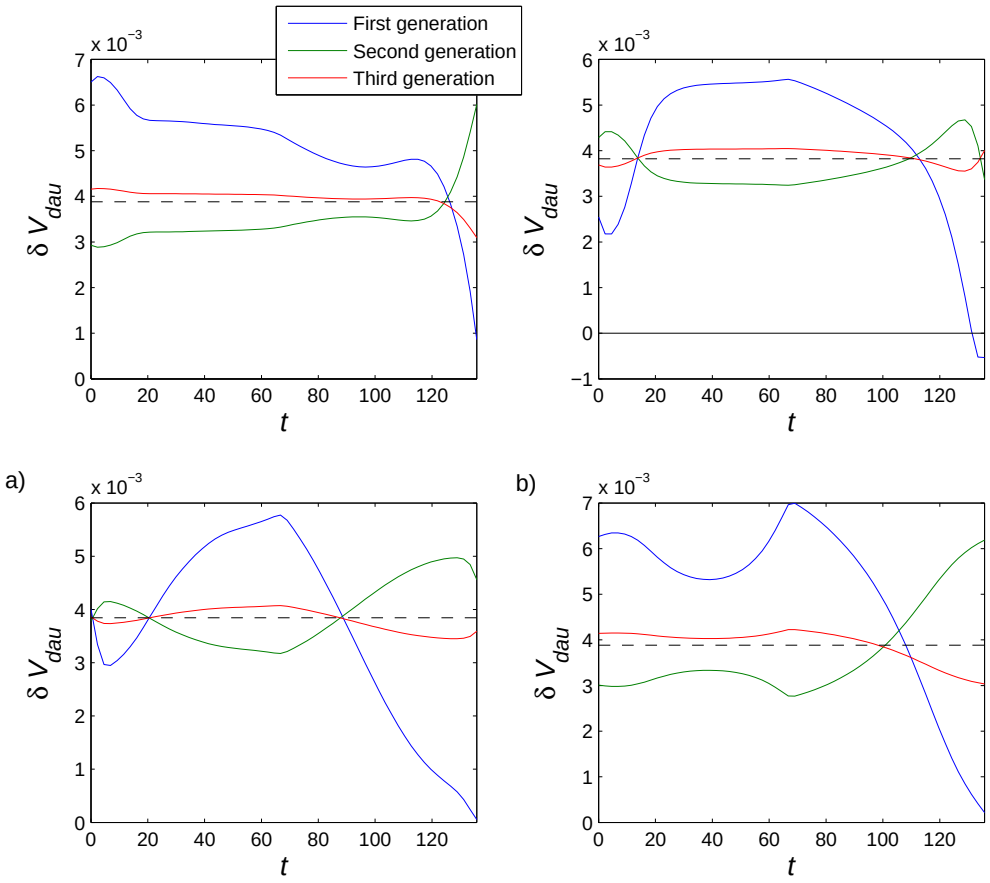

Figure D.1: Changes in daughter size down three generations for different combinations of different sets of three parameters (from the Sriram model) which achieve the same eventual change in behaviour, and all of which achieve minimal M_{dau} compared to other combinations of those three parameters. The dashed line gives the eventual change of behaviour, which is the same in all examples. The curves approach this behaviour asymptotically though, as noted, not necessarily monotonically. As is the case in the examples shown for the Barik model, these curves all display some degree of biphasic response.

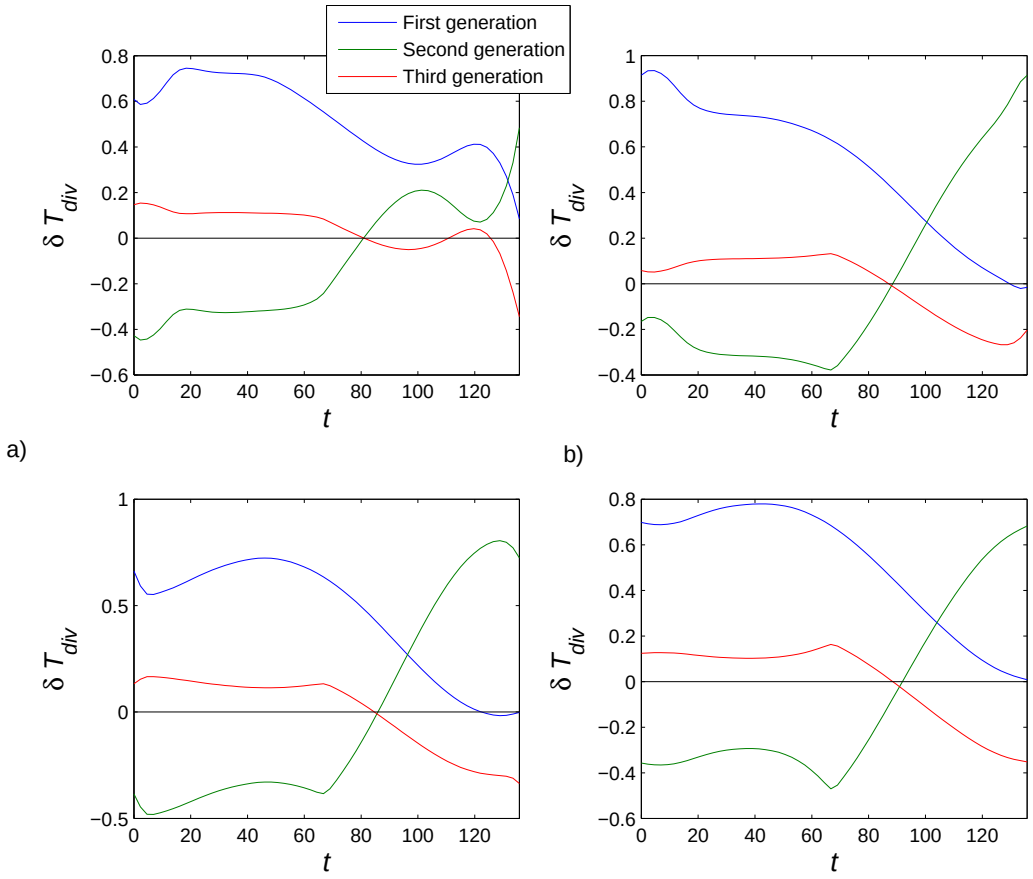

Figure D.2: Changes in cell cycle period down three generations for different combinations of different sets of three parameters (from the Sriram model) which achieve the same eventual change in behaviour, and all of which achieve minimal M_{period} compared to other combinations of those three parameters. The dashed line gives the eventual change of behaviour, which is the same in all examples. The curves approach this behaviour asymptotically. Again, and similarly to the case with the Barik model, these curves all display some degree of biphasic response.

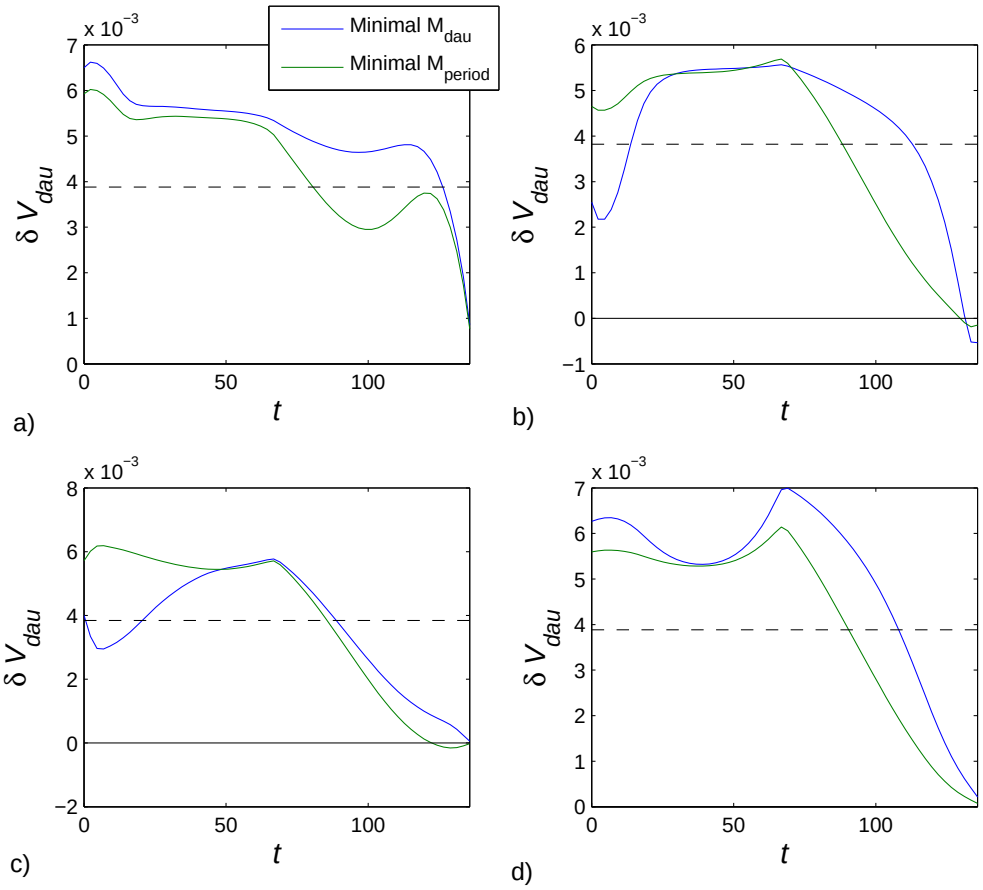

Figure D.3: The dynamic responses of V_{dau} over the first generation in the Sriram model are compared for the examples considered in figures D.1 and D.2, minimising M_{dau} (blue) and M_{period} (green), respectively. The similarity in the response curves exhibiting minimal M_{dau} and M_{period} suggests a common principle in the attainment of rapid approach to the eventual change in behaviour of the cell cycle.

Appendix E

Description of digital appendices - MATLAB simulation code

This Appendix lists simulation code for each chapter, and the figures which they were used to generate (where relevant).

E.0.2 Chapter 3: Coupling of pathways and processes through shared components

Basic interactions

The basic model of X interacting with A and B is simulated (Eq. 3.3) (see Fig. 3.1 for the model schematic). Used for Fig. 3.2.

Combinatorial signalling

The three model variants of combinatorial signalling (depicted in Fig. 3.7) are simulated. Used for Fig. 3.8.

Dynamic response to pulsatile change in X production

Simulates the response of the basic model to a temporary step up in the rate of production of X. Used for Fig. 3.4.

Multiple switching (bistable)

Simulates the interaction between the double phosphorylation and single phosphorylation models described in Sections 3.2.2 and 3.2.2, respectively. Used for Fig. 3.11.

Multiple switching (monostable)

Simulates the interaction between two single phosphorylation modules, as described in Section 3.2.2 in order to demonstrate how enzyme competition may improve signalling specificity. Used for Fig. 3.9.

Simple membrane complex formation

Simulates complex formation on a membrane with different combinations of diffusion rates, affinities, and spatial distributions of species synthesis. Used for Figs. 3.12, 3.13, and 3.14.

Temporal ordering of switching

Simulates the interaction between two single phosphorylation modules, as described in Section 3.2.2 in order to demonstrate the robust ordering of activation. Used for Fig. 3.10.

Temporal response to a step-change

Simulates the response of the basic model to step-changes in production of X, A, and B. Used for Figs. 3.3, 3.5, and 3.6.

E.0.3 Chapter 4:Effects of multiple enzyme-substrate interactions in basic units of cellular signal processing

Note that, throughout this directory, scripts with the prefixes “PI” and “IEI” perform simulations of product inhibition and inactive enzyme interference, respectively.

Basic model

The model dynamics for the model of two single-modification cycles described by Eq. 4.1 are described in `GK_GK_dynamics.m`. Used for Figs. 4.2, 4.3, 4.4, 4.5, 4.6, 4.7, 4.8, 4.9, 4.10, 4.11, 4.12, 4.13, and 4.15.

Multisite modification model

The model dynamics for the model of a single-modification cycle upstream of a double-modification cycle described by Eq. 4.2 are described in `GK_MP_dynamics.m`. Used for Fig. 4.16.

Scaffold model

The model dynamics for the model of scaffold-mediated signalling described by Eq. 4.3 are described in `scaffold_dynamics.m`. Used for Fig. 4.17.

E.0.4 Chapter 5: A modular systems approach to understanding the interaction of adaptive, monostable, and bistable threshold processes

The different modules and combinations of modules are provided in folders according to the key provided below. Model dynamics are supplied as function files with the name of the module, followed by the postfix "`_dynamics.m`", with model parameters supplied as scripts with the postfix "`_parameters.m`".

Adaptive modules

- **AIR** – Adaptive module, with incoherent feedforward look (Activator, Inhibitor, Response)
- **BEHAR** – Adaptive module, with negative feedback

Threshold modules

- **CAS** – Cascade of post-translational modifications
- **ZOU** – Zero-order ultrasensitivity module (i.e. a Goldbeter-Koshland switch)

- **BISD** – Bistable module, with positive feedback
- **Z** – Toy model of bistability (steady states are chosen parameters)

Input types

- **EXP** – Exponentially decaying pulse input signal
- **STEP** – Step change in input
- **VI** – Time varying input (linear gradient)

E.0.5 Chapter 6: Principles of dynamic regulation of the budding yeast cell cycle

Model structure

Each of the five models investigated ((Barik et al., 2010) labelled "barik", (Csikasz-Nagy et al., 2006) (labelled "generic"),(Pfeuty and Kaneko, 2007) (labelled "kaneko"), (Sriram et al., 2007) (labelled "sriram"), and (Battogtokh and Tyson, 2004) (labelled "chen")) is described by a combination of four files:

- **`model_cc.m`** This function takes as input the cell state and returns a vector of time derivatives of all species (as required by the MATLAB ODE solvers).
- **`events_cc.m`** This function takes as input the state of the cell cycle and checks whether key cell cycle events (i.e. budding and division) have occurred.
- **`reset_rule.m`** This function takes as input the cell state at division and the mass fraction to be taken by the new daughter cell, and returns initial conditions for simulations of the daughter cell's cell cycle.
- **`solver.m`** This function takes as input initial conditions, time interval of simulation, and model parameters, and outputs the cell state at the final time (along with information of any events that occurred during the simulation). This function makes use of the above functions, and provides the common interface between all models and the systematic model analysis functions (see below).

Systematic model analysis

- **`ss_sensitivity.m`** This function takes as input a cell cycle solver function (see above) and returns the steady state sensitivities of cell division and budding sizes and times of all parameters, as described in Section 6.3.

- **`step_sensitivity.m`** This function takes as input a cell cycle solver function (see above) and returns the dynamic sensitivities of cell division and budding sizes and times of all parameters at all cell cycle times, as described in Section 6.4.

- **`temporal_sensitivity.m`** This function takes as input a cell cycle solver function (see above) and returns the sensitivities of cell division and budding sizes and times of all parameters to temporary changes in parameters at all cell cycle times, as described in Section 6.4. Used to verify correctness of `step_sensitivity.m`.

References

Miquel ?ngel Adrover, Zhike Zi, Alba Duch, Jorg Schaber, Alberto Gonzalez-Novo, Javier Jimenez, Mariona Nadal-Ribelles, Josep Clotet, Edda Klipp, and Francesc Posas. Time-dependent quantitative multicomponent control of the g?-s network by the stress-activated protein kinase hog1 upon osmostress. *Sci Signal*, 4(192):ra63, Sep 2011. doi: 10.1126/scisignal.2002204. URL http://dx.doi.org/10.1126/scisignal.2002204.

Grigoris D. Amoutzias, David L. Robertson, Yves Van de Peer, and Stephen G. Oliver. Choose your partners: dimerization in eukaryotic transcription factors. *Trends Biochem Sci*, 33(5):220–229, May 2008. doi: 10.1016/j.tibs.2008.02.002. URL http://dx.doi.org/10.1016/j.tibs.2008.02.002.

David Angeli, James E Ferrell, Jr, and Eduardo D. Sontag. Detection of multistability, bifurcations, and hysteresis in a large class of biological positive-feedback systems. *Proc Natl Acad Sci U S A*, 101(7):1822–1827, Feb 2004. doi: 10.1073/pnas.0308265100. URL http://dx.doi.org/10.1073/pnas.0308265100.

Jae Hyun Bae, Erin Denise Lew, Satoru Yuzawa, Francisco Tome, Irit Lax, and Joseph Schlessinger. The selectivity of receptor tyrosine kinase signaling is controlled by a secondary sh2 domain binding site. *Cell*, 138(3):514–524, Aug 2009. doi: 10.1016/j.cell.2009.05.028. URL http://dx.doi.org/10.1016/j.cell.2009.05.028.

C. P. Bagowski and JE Ferrell, Jr. Bistability in the jnk cascade. *Curr Biol*, 11(15):1176–1182, Aug 2001.

Christoph P. Bagowski, Jaya Besser, Christian R. Frey, and James E Ferrell, Jr. The jnk cascade as a biochemical switch in mammalian cells: ultrasensitive and all-or-none responses. *Curr Biol*, 13(4):315–320, Feb 2003.

Albert-Laszlo Barabasi and Zoltan N. Oltvai. Network biology: understanding the cell's functional organization. *Nat Rev Genet*, 5(2):101–113, Feb 2004. doi: 10.1038/nrg1272. URL http://dx.doi.org/10.1038/nrg1272.

Matteo Barberis, Edda Klipp, Marco Vanoni, and Lilia Alberghina. Cell size at s phase initiation: an emergent property of the g1/s network. *PLoS Comput Biol*, 3(4):e64, Apr 2007. doi: 10.1371/journal.pcbi.0030064. URL http://dx.doi.org/10.1371/journal.pcbi.0030064.

L. Bardwell. Mechanisms of mapk signalling specificity. *Biochem Soc Trans*, 34(Pt 5):837–841, Nov 2006. doi: 10.1042/BST0340837. URL http://dx.doi.org/10.1042/BST0340837.

L Bardwell, J G Cook, E C Chang, B R Cairns, J Thorner, L E E Bardwell, Jeanette G Cook, Ernie C Chang, and Bradley R Cairns. Signaling in the yeast pheromone response pathway : specific and high-affinity interaction of the mitogen-activated protein (map) kinases kss1 and fus3 with the upstream map kinase kinase ste7. *Molecular and cellular biology*, 16:3637–50, 1996.

Lee Bardwell, Xiufen Zou, Qing Nie, and Natalia L. Komarova. Mathematical models of specificity in cell signaling. *Biophys J*, 92(10):3425–3441, May 2007. doi: 10.1529/biophysj.106.090084. URL http://dx.doi.org/10.1529/biophysj.106.090084.

Debashis Barik, William T Baumann, Mark R Paul, Bela Novak, and John J Tyson. A model of yeast cell-cycle regulation based on multisite phosphorylation. *Mol Syst Biol*, 6:405, Aug 2010. doi: 10.1038/msb.2010.55. URL http://dx.doi.org/10.1038/msb.2010.55.

N. Barkai and S. Leibler. Robustness in simple biochemical networks. *Nature*, 387(6636):913–917, Jun 1997. doi: 10.1038/43199. URL http://dx.doi.org/10.1038/43199.

Eric Batchelor, Alexander Loewer, and Galit Lahav. The ups and downs of p53: understanding protein dynamics in single cells. *Nat Rev Cancer*, 9(5):371–377, May 2009. doi: 10.1038/nrc2604. URL http://dx.doi.org/10.1038/nrc2604.

Dorjsuren Battogtokh and John J. Tyson. Bifurcation analysis of a model of the budding yeast cell cycle. *Chaos*, 14(3):653–661, Sep 2004. doi: 10.1063/1.1780011. URL http://dx.doi.org/10.1063/1.1780011.

Bridget L Baumgartner, Matthew R Bennett, Michael Ferry, Tracy L Johnson, Lev S Tsimring, and Jeff Hasty. Antagonistic gene transcripts regulate adaptation to new growth environments. *Proc Natl Acad Sci U S A*, 108(52):21087–21092, Dec 2011. doi: 10.1073/pnas.1111408109. URL http://dx.doi.org/10.1073/pnas.1111408109.

Stephan Baumgartner and Iva M. Tolic-Norrelykke. Growth pattern of single fission yeast cells is bilinear and depends on temperature and dna synthesis. *Biophys J*, 96(10):4336–4347, May 2009. doi: 10.1016/j.bpj.2009.02.051. URL http://dx.doi.org/10.1016/j.bpj.2009.02.051.

James M. Bean, Eric D. Siggia, and Frederick R. Cross. Coherence and timing of cell cycle start examined at single-cell resolution. *Mol Cell*, 21(1):3–14, Jan 2006. doi: 10.1016/j.molcel.2005.10.035. URL http://dx.doi.org/10.1016/j.molcel.2005.10.035.

Darren L. Beene and John D. Scott. A-kinase anchoring proteins take shape. *Curr Opin Cell Biol*, 19(2):192–198, Apr 2007. doi: 10.1016/j.ceb.2007.02.011. URL http://dx.doi.org/10.1016/j.ceb.2007.02.011.

Marcelo Behar, Nan Hao, Henrik G. Dohlman, and Timothy C. Elston. Mathematical and computational analysis of adaptation via feedback inhibition in signal transduction pathways. *Biophys J*, 93(3):806–821, Aug 2007. doi: 10.1529/biophysj.107.107516. URL http://dx.doi.org/10.1529/biophysj.107.107516.

U. S. Bhalla and R. Iyengar. Emergent properties of networks of biological signaling pathways. *Science*, 283(5400):381–387, Jan 1999.

Roby P Bhattacharyya, Attila Remenyi, Brian J Yeh, and Wendell A Lim. Domains, motifs, and scaffolds: the role of modular interactions in the evolution and wiring of cell signaling circuits. *Annu Rev Biochem*, 75:655–680, 2006. doi: 10.1146/annurev.biochem.75.103004.142710. URL http://dx.doi.org/10.1146/annurev.biochem.75.103004.142710.

Joanna Bloom and Frederick R. Cross. Multiple levels of cyclin specificity in cell-cycle control. *Nat Rev Mol Cell Biol*, 8(2):149–160, Feb 2007. doi: 10.1038/nrm2105. URL http://dx.doi.org/10.1038/nrm2105.

J. A. Borghans, R. J. de Boer, and L. A. Segel. Extending the quasi-steady state approximation by changing variables. *Bull Math Biol*, 58(1):43–63, Jan 1996.

Matthew J. Brauer, Curtis Huttenhower, Edoardo M. Airoldi, Rachel Rosenstein, John C. Matese, David Gresham, Viktor M. Boer, Olga G. Troyanskaya, and David Botstein. Coordination of growth rate, cell cycle, stress response, and metabolic activity in yeast. *Mol Biol Cell*, 19(1):352–367, Jan 2008. doi: 10.1091/mbc.E07-08-0779. URL http://dx.doi.org/10.1091/mbc.E07-08-0779.

James R. Broach. Nutritional control of growth and development in yeast. *Genetics*, 192 (1):73–105, Sep 2012. doi: 10.1534/genetics.111.135731. URL http://dx.doi.org/10.1534/genetics.111.135731.

Eric Brown, Jeff Moehlis, and Philip Holmes. On the phase reduction and response dynamics of neural oscillator populations. *Neural Comput*, 16(4):673–715, Apr 2004. doi: 10.1162/089976604322860668. URL http://dx.doi.org/10.1162/089976604322860668.

Nicolas E. Buchler and Frederick R. Cross. Protein sequestration generates a flexible ultrasensitive response in a genetic network. *Mol Syst Biol*, 5:272, 2009. doi: 10.1038/msb.2009.30. URL http://dx.doi.org/10.1038/msb.2009.30.

Nicolas E. Buchler and Matthieu Louis. Molecular titration and ultrasensitivity in regulatory networks. *J Mol Biol*, 384(5):1106–1119, Dec 2008. doi: 10.1016/j.jmb.2008.09.079. URL http://dx.doi.org/10.1016/j.jmb.2008.09.079.

Stefano Busti, Paola Coccetti, Lilia Alberghina, and Marco Vanoni. Glucose signaling-mediated coordination of cell growth and cell cycle in saccharomyces cerevisiae. *Sensors (Basel)*, 10(6):6195–6240, 2010. doi: 10.3390/s100606195. URL http://dx.doi.org/10.3390/s100606195.

Ling Cai and Benjamin P. Tu. Driving the cell cycle through metabolism. *Annu Rev Cell Dev Biol*, 28:59–87, Nov 2012. doi: 10.1146/annurev-cellbio-092910-154010. URL http://dx.doi.org/10.1146/annurev-cellbio-092910-154010.

Meritxell Canals, Patrick M. Sexton, and Arthur Christopoulos. Allostery in gpcrs: 'mwc' revisited. *Trends Biochem Sci*, 36(12):663–672, Dec 2011. doi: 10.1016/j.tibs.2011.08.005. URL http://dx.doi.org/10.1016/j.tibs.2011.08.005.

Dries Castermans, Ils Somers, Johan Kriel, Wendy Louwet, Stefaan Wera, Matthias Versele, Veerle Janssens, and Johan M. Thevelein. Glucose-induced posttranslational

activation of protein phosphatases pp2a and pp1 in yeast. *Cell Res*, 22(6):1058–1077, Jun 2012. doi: 10.1038/cr.2012.20. URL http://dx.doi.org/10.1038/cr.2012.20.

Stephen A. Chapman and Anand R. Asthagiri. Quantitative effect of scaffold abundance on signal propagation. *Mol Syst Biol*, 5:313, 2009. doi: 10.1038/msb.2009.73. URL http://dx.doi.org/10.1038/msb.2009.73.

G. Charvin, F. R. Cross, and E. D. Siggia. Forced periodic expression of g1 cyclins phase-locks the budding yeast cell cycle. *Proc Natl Acad Sci U S A*, 106(16):6632–6637, Apr 2009. doi: 10.1073/pnas.0809227106. URL http://dx.doi.org/10.1073/pnas.0809227106.

Gilles Charvin, Frederick R. Cross, and Eric D. Siggia. A microfluidic device for temporally controlled gene expression and long-term fluorescent imaging in unperturbed dividing yeast cells. *PLoS One*, 3(1):e1468, 2008. doi: 10.1371/journal.pone.0001468. URL http://dx.doi.org/10.1371/journal.pone.0001468.

Gilles Charvin, Catherine Oikonomou, Eric D. Siggia, and Frederick R. Cross. Origin of irreversibility of cell cycle start in budding yeast. *PLoS Biol*, 8(1):e1000284, Jan 2010. doi: 10.1371/journal.pbio.1000284. URL http://dx.doi.org/10.1371/journal.pbio.1000284.

Chen Chen, Timothy J. Nott, Jing Jin, and Tony Pawson. Deciphering arginine methylation: Tudor tells the tale. *Nat Rev Mol Cell Biol*, 12(10):629–642, Oct 2011. doi: 10.1038/nrm3185. URL http://dx.doi.org/10.1038/nrm3185.

K. C. Chen, A. Csikasz-Nagy, B. Gyorffy, J. Val, B. Novak, and J. J. Tyson. Kinetic analysis of a molecular model of the budding yeast cell cycle. *Mol Biol Cell*, 11(1):369–391, Jan 2000.

Katherine C. Chen, Laurence Calzone, Attila Csikasz-Nagy, Frederick R. Cross, Bela Novak, and John J. Tyson. Integrative analysis of cell cycle control in budding yeast. *Mol Biol Cell*, 15(8):3841–3862, Aug 2004. doi: 10.1091/mbc.E03-11-0794. URL http://dx.doi.org/10.1091/mbc.E03-11-0794.

Chunaram Choudhary, Chanchal Kumar, Florian Gnad, Michael L. Nielsen, Michael Rehman, Tobias C. Walther, Jesper V. Olsen, and Matthias Mann. Lysine acetylation

targets protein complexes and co-regulates major cellular functions. *Science*, 325(5942): 834–840, Aug 2009. doi: 10.1126/science.1175371. URL http://dx.doi.org/10.1126/science.1175371.

Yi-Da Chung, Michael D. Sinzinger, Petra Bovee-Geurts, Marina Krause, Sip Dinkla, Irma Joosten, Werner J. Koopman, Merel J W. Adjobo-Hermans, and Roland Brock. Analyzing the homeostasis of signaling proteins by a combination of western blot and fluorescence correlation spectroscopy. *Biophys J*, 101(11):2807–2815, Dec 2011. doi: 10.1016/j.bpj.2011.09.058. URL http://dx.doi.org/10.1016/j.bpj.2011.09.058.

Andrea Ciliberto, Fabrizio Capuani, and John J Tyson. Modeling networks of coupled enzymatic reactions using the total quasi-steady state approximation. *PLoS Comput Biol*, 3(3):e45, Mar 2007. doi: 10.1371/journal.pcbi.0030045. URL http://dx.doi.org/10.1371/journal.pcbi.0030045.

Ami Citri and Yosef Yarden. Egf-erbb signalling: towards the systems level. *Nat Rev Mol Cell Biol*, 7(7):505–516, Jul 2006. doi: 10.1038/nrm1962. URL http://dx.doi.org/10.1038/nrm1962.

P. Cohen. The regulation of protein function by multisite phosphorylation–a 25 year update. *Trends Biochem Sci*, 25(12):596–601, Dec 2000.

Stephen Cooper. Rejoinder: whole-culture synchronization cannot, and does not, synchronize cells. *Trends Biotechnol*, 22(6):274–276, Jun 2004. doi: 10.1016/j.tibtech.2004.04.011. URL http://dx.doi.org/10.1016/j.tibtech.2004.04.011.

Shelley D. Copley. Enzymes with extra talents: moonlighting functions and catalytic promiscuity. *Curr Opin Chem Biol*, 7(2):265–272, Apr 2003.

Frederick R. Cross, Vincent Archambault, Mary Miller, and Martha Klovstad. Testing a mathematical model of the yeast cell cycle. *Mol Biol Cell*, 13(1):52–70, Jan 2002. doi: 10.1091/mbc.01-05-0265. URL http://dx.doi.org/10.1091/mbc.01-05-0265.

Sean Crosson, Patrick T. McGrath, Craig Stephens, Harley H. McAdams, and Lucy Shapiro. Conserved modular design of an oxygen sensory/signaling network with species-specific output. *Proc Natl Acad Sci U S A*, 102(22):8018–8023, May 2005. doi: 10.1073/pnas.0503022102. URL http://dx.doi.org/10.1073/pnas.0503022102.

Attila Csikasz-Nagy, Dorjsuren Battogtokh, Katherine C. Chen, Bela Novak, and John J. Tyson. Analysis of a generic model of eukaryotic cell-cycle regulation. *Biophys J*, 90 (12):4361–4379, Jun 2006. doi: 10.1529/biophysj.106.081240. URL http://dx.doi.org/10.1529/biophysj.106.081240.

Attila Csikasz-Nagy, Orsolya Kapuy, Attila Toth, Csaba Pal, Lars Juhl Jensen, Frank Uhlmann, John J Tyson, and Bela Novak. Cell cycle regulation by feed-forward loops coupling transcription and phosphorylation. *Mol Syst Biol*, 5:236, 2009. doi: 10.1038/msb.2008.73. URL http://dx.doi.org/10.1038/msb.2008.73.

P. Danaie, M. Altmann, M. N. Hall, H. Trachsel, and S. B. Helliwell. Cln3 expression is sufficient to restore g1-to-s-phase progression in saccharomyces cerevisiae mutants defective in translation initiation factor eif4e. *Biochem J*, 340 (Pt 1):135–141, May 1999.

Eric H. Davidson. Emerging properties of animal gene regulatory networks. *Nature*, 468 (7326):911–920, Dec 2010. doi: 10.1038/nature09645. URL http://dx.doi.org/10.1038/nature09645.

Wiet de Ronde, Filipe Tostevin, and Pieter Rein ten Wolde. Multiplexing biochemical signals. *Phys Rev Lett*, 107(4):048101, Jul 2011.

Antonio Del Sol, Marcos J. Arauzo-Bravo, Dolors Amoros, and Ruth Nussinov. Modular architecture of protein structures and allosteric communications: potential implications for signaling proteins and regulatory linkages. *Genome Biol*, 8(5):R92, 2007. doi: 10.1186/gb-2007-8-5-r92. URL http://dx.doi.org/10.1186/gb-2007-8-5-r92.

Domitilla Del Vecchio, Alexander J. Ninfa, and Eduardo D. Sontag. Modular cell biology: retroactivity and insulation. *Mol Syst Biol*, 4:161, 2008. doi: 10.1038/msb4100204. URL http://dx.doi.org/10.1038/msb4100204.

D. N. Dhanasekaran, K. Kashef, C. M. Lee, H. Xu, and E. P. Reddy. Scaffold proteins of map-kinase modules. *Oncogene*, 26(22):3185–3202, May 2007. doi: 10.1038/sj.onc.1210411. URL http://dx.doi.org/10.1038/sj.onc.1210411.

Stefano Di Talia, Jan M. Skotheim, James M. Bean, Eric D. Siggia, and Frederick R. Cross. The effects of molecular noise and size control on variability in the budding yeast cell

cycle. *Nature*, 448(7156):947–951, Aug 2007. doi: 10.1038/nature06072. URL http://dx.doi.org/10.1038/nature06072.

Tormod Drengstig, Hiroki R. Ueda, and Peter Ruoff. Predicting perfect adaptation motifs in reaction kinetic networks. *J Phys Chem B*, 112(51):16752–16758, Dec 2008. doi: 10.1021/jp806818c. URL http://dx.doi.org/10.1021/jp806818c.

John E. Dueber, Ethan A. Mirsky, and Wendell A. Lim. Engineering synthetic signaling proteins with ultrasensitive input/output control. *Nat Biotechnol*, 25(6):660–662, Jun 2007. doi: 10.1038/nbt1308. URL http://dx.doi.org/10.1038/nbt1308.

Geneviève Dupont and Huguette Croisier. Spatiotemporal organization of ca dynamics: a modeling-based approach. *HFSP J*, 4(2):43–51, Apr 2010. doi: 10.2976/1.3385660. URL http://dx.doi.org/10.2976/1.3385660.

H. El-Samad, H. Kurata, J. C. Doyle, C. A. Gross, and M. Khammash. Surviving heat shock: control strategies for robustness and performance. *Proc Natl Acad Sci U S A*, 102 (8):2736–2741, Feb 2005. doi: 10.1073/pnas.0403510102. URL http://dx.doi.org/10.1073/pnas.0403510102.

M. B. Elowitz and S. Leibler. A synthetic oscillatory network of transcriptional regulators. *Nature*, 403(6767):335–338, Jan 2000. doi: 10.1038/35002125. URL http://dx.doi.org/10.1038/35002125.

Greg H. Enders. Gauchos and ochos: a wee1-cdk tango regulating mitotic entry. *Cell Div*, 5:12, 2010. doi: 10.1186/1747-1028-5-12. URL http://dx.doi.org/10.1186/1747-1028-5-12.

Jane A. Endicott, Martin E M. Noble, and Louise N. Johnson. The structural basis for control of eukaryotic protein kinases. *Annu Rev Biochem*, 81:1–27, Apr 2012. doi: 10.1146/annurev-biochem-052410-090317. URL http://dx.doi.org/10.1146/annurev-biochem-052410-090317.

Marc Robert Fabian, Nahum Sonenberg, and Witold Filipowicz. Regulation of mrna translation and stability by micrornas. *Annu Rev Biochem*, 79:351–379, 2010. doi: 10.1146/annurev-biochem-060308-103103. URL http://dx.doi.org/10.1146/annurev-biochem-060308-103103.

J. E. Ferrell. Tripping the switch fantastic: how a protein kinase cascade can convert graded inputs into switch-like outputs. *Trends Biochem Sci*, 21(12):460–466, Dec 1996.

James E Ferrell, Jr. Self-perpetuating states in signal transduction: positive feedback, double-negative feedback and bistability. *Curr Opin Cell Biol*, 14(2):140–148, Apr 2002.

Francisco Ferrezuelo, Neus Colomina, Alida Palmisano, Eloi Gari, Carme Gallego, Attila Csikasz-Nagy, and Marti Aldea. The critical size is set at a single-cell level by growth rate to attain homeostasis and adaptation. *Nat Commun*, 3:1012, 2012. doi: 10.1038/ncomms2015. URL http://dx.doi.org/10.1038/ncomms2015.

Mariana Figuera-Losada and Philip V. LoGrasso. Enzyme kinetics and interaction studies for human jnk1?1 and substrates activating transcription factor 2 (atf2) and c-jun n-terminal kinase (c-jun). *J Biol Chem*, 287(16):13291–13302, Apr 2012. doi: 10.1074/jbc.M111.323766. URL http://dx.doi.org/10.1074/jbc.M111.323766.

K. Flick, D. Chapman-Shimshoni, D. Stuart, M. Guaderrama, and C. Wittenberg. Regulation of cell size by glucose is exerted via repression of the cln1 promoter. *Mol Cell Biol*, 18(5):2492–2501, May 1998.

Tamar Friedlander and Naama Brenner. Adaptive response by state-dependent inactivation. *Proc Natl Acad Sci U S A*, 106(52):22558–22563, Dec 2009. doi: 10.1073/pnas.0902146106. URL http://dx.doi.org/10.1073/pnas.0902146106.

Eileen Fung, Wilson W. Wong, Jason K. Suen, Thomas Bulter, Sun-gu Lee, and James C. Liao. A synthetic gene-metabolic oscillator. *Nature*, 435(7038):118–122, May 2005. doi: 10.1038/nature03508. URL http://dx.doi.org/10.1038/nature03508.

Anne-Claude Gavin, Patrick Aloy, Paola Grandi, Roland Krause, Markus Boesche, Martina Marzioch, Christina Rau, Lars Juhl Jensen, Sonja Bastuck, Birgit Dumpelfeld, Angela Edelmann, Marie-Anne Heurtier, Verena Hoffman, Christian Hoefert, Karin Klein, Manuela Hudak, Anne-Marie Michon, Malgorzata Schelder, Markus Schirle, Marita Remor, Tatjana Rudi, Sean Hooper, Andreas Bauer, Tewis Bouwmeester, Georg Casari, Gerard Drewes, Gitte Neubauer, Jens M. Rick, Bernhard Kuster, Peer Bork, Robert B. Russell, and Giulio Superti-Furga. Proteome survey reveals modularity of the yeast cell machinery. *Nature*, 440(7084):631–636, Mar 2006. doi: 10.1038/nature04532. URL http://dx.doi.org/10.1038/nature04532.

Ann B. Georgi, P Todd Stukenberg, and Marc W. Kirschner. Timing of events in mitosis. *Curr Biol*, 12(2):105–114, Jan 2002.

Florian Gnad, Lyris M F. de Godoy, Jurgen Cox, Nadin Neuhauser, Shubin Ren, Jesper V. Olsen, and Matthias Mann. High-accuracy identification and bioinformatic analysis of in vivo protein phosphorylation sites in yeast. *Proteomics*, 9(20):4642–4652, Oct 2009. doi: 10.1002/pmic.200900144. URL http://dx.doi.org/10.1002/pmic.200900144.

A. Goldbeter and DE Koshland, Jr. An amplified sensitivity arising from covalent modification in biological systems. *Proc Natl Acad Sci U S A*, 78(11):6840–6844, Nov 1981.

A. Goldbeter, C. Gérard, D. Gonze, J-C. Leloup, and G. Dupont. Systems biology of cellular rhythms. *FEBS Lett*, 586(18):2955–2965, Aug 2012. doi: 10.1016/j.febslet.2012.07.041. URL http://dx.doi.org/10.1016/j.febslet.2012.07.041.

Elizabeth J. Goldsmith, Radha Akella, Xiaoshan Min, Tianjun Zhou, and John M. Humphreys. Substrate and docking interactions in serine/threonine protein kinases. *Chem Rev*, 107(11):5065–5081, Nov 2007. doi: 10.1021/cr068221w. URL http://dx.doi.org/10.1021/cr068221w.

Matthew C. Good, Jesse G. Zalatan, and Wendell A. Lim. Scaffold proteins: hubs for controlling the flow of cellular information. *Science*, 332(6030):680–686, May 2011. doi: 10.1126/science.1198701. URL http://dx.doi.org/10.1126/science.1198701.

Nina M. Goodey and Stephen J. Benkovic. Allosteric regulation and catalysis emerge via a common route. *Nat Chem Biol*, 4(8):474–482, Aug 2008. doi: 10.1038/nchembio.98. URL http://dx.doi.org/10.1038/nchembio.98.

Alexi I. Goranov and Angelika Amon. Growth and division–not a one-way road. *Curr Opin Cell Biol*, 22(6):795–800, Dec 2010. doi: 10.1016/j.ceb.2010.06.004. URL http://dx.doi.org/10.1016/j.ceb.2010.06.004.

Andrew Gordus, Jordan A. Krall, Elsa M. Beyer, Alexis Kaushansky, Alejandro Wolf-Yadlin, Mark Sevecka, Bryan H. Chang, John Rush, and Gavin MacBeath. Linear combinations of docking affinities explain quantitative differences in rtk signaling. *Mol Syst Biol*, 5:235, 2009. doi: 10.1038/msb.2008.72. URL http://dx.doi.org/10.1038/msb.2008.72.

Jeremy Gunawardena. Multisite protein phosphorylation makes a good threshold but can be a poor switch. *Proc Natl Acad Sci U S A*, 102(41):14617–14622, Oct 2005. doi: 10.1073/pnas.0507322102. URL http://dx.doi.org/10.1073/pnas.0507322102.

Seth Haney, Lee Bardwell, and Qing Nie. Ultrasensitive responses and specificity in cell signaling. *BMC Syst Biol*, 4:119, 2010. doi: 10.1186/1752-0509-4-119. URL http://dx.doi.org/10.1186/1752-0509-4-119.

Arnold Hayer and Upinder S. Bhalla. Molecular switches at the synapse emerge from receptor and kinase traffic. *PLoS Comput Biol*, 1(2):137–154, Jul 2005. doi: 10.1371/journal.pcbi.0010020. URL http://dx.doi.org/10.1371/journal.pcbi.0010020.

Enuo He, Orsolya Kapuy, Raquel A Oliveira, Frank Uhlmann, John J Tyson, and Bela Novak. System-level feedbacks make the anaphase switch irreversible. *Proc Natl Acad Sci U S A*, 108(24):10016–10021, Jun 2011. doi: 10.1073/pnas.1102106108. URL http://dx.doi.org/10.1073/pnas.1102106108.

Stefan Hohmann. Osmotic stress signaling and osmoadaptation in yeasts. *Microbiol Mol Biol Rev*, 66(2):300–372, Jun 2002.

C. Y. Huang and JE Ferrell, Jr. Ultrasensitivity in the mitogen-activated protein kinase cascade. *Proc Natl Acad Sci U S A*, 93(19):10078–10083, Sep 1996.

Won-Ki Huh, James V. Falvo, Luke C. Gerke, Adam S. Carroll, Russell W. Howson, Jonathan S. Weissman, and Erin K. O'Shea. Global analysis of protein localization in budding yeast. *Nature*, 425(6959):686–691, Oct 2003. doi: 10.1038/nature02026. URL http://dx.doi.org/10.1038/nature02026.

Karl Hult and Per Berglund. Enzyme promiscuity: mechanism and applications. *Trends Biotechnol*, 25(5):231–238, May 2007. doi: 10.1016/j.tibtech.2007.03.002. URL http://dx.doi.org/10.1016/j.tibtech.2007.03.002.

Tony Hunter. The age of crosstalk: phosphorylation, ubiquitination, and beyond. *Mol Cell*, 28(5):730–738, Dec 2007. doi: 10.1016/j.molcel.2007.11.019. URL http://dx.doi.org/10.1016/j.molcel.2007.11.019.

Nhat Huynh, Chen-Ting Ma, Ngoc Giang, Jonathan Hagopian, Jacky Ngo, Joseph Adams, and Gourisankar Ghosh. Allosteric interactions direct binding and phosphorylation

of asf/sf2 by srpk1. *Biochemistry*, 48(48):11432–11440, Dec 2009. doi: 10.1021/bi901107q. URL http://dx.doi.org/10.1021/bi901107q.

Q Khai Huynh and Timothy A. McKinsey. Protein kinase d directly phosphorylates histone deacetylase 5 via a random sequential kinetic mechanism. *Arch Biochem Biophys*, 450 (2):141–148, Jun 2006. doi: 10.1016/j.abb.2006.02.014. URL http://dx.doi.org/10.1016/j.abb.2006.02.014.

Q. Khai Huynh and Nikos Pagratis. Kinetic mechanisms of Ca++/calmodulin dependent protein kinases. *Arch Biochem Biophys*, 506(2):130–136, Feb 2011. doi: 10.1016/j.abb.2010.11.008. URL http://dx.doi.org/10.1016/j.abb.2010.11.008.

Richard B. Jones, Andrew Gordus, Jordan A. Krall, and Gavin MacBeath. A quantitative protein interaction network for the erbb receptors using protein microarrays. *Nature*, 439 (7073):168–174, Jan 2006. doi: 10.1038/nature04177. URL http://dx.doi.org/10.1038/nature04177.

Paul Jorgensen and Mike Tyers. How cells coordinate growth and division. *Curr Biol*, 14 (23):R1014–R1027, Dec 2004. doi: 10.1016/j.cub.2004.11.027. URL http://dx.doi.org/10.1016/j.cub.2004.11.027.

S. Marjan Varedi K, Alejandra C Ventura, Sofia D Merajver, and Xiaoxia Nina Lin. Multisite phosphorylation provides an effective and flexible mechanism for switch-like protein degradation. *PLoS One*, 5(12):e14029, 2010. doi: 10.1371/journal.pone.0014029. URL http://dx.doi.org/10.1371/journal.pone.0014029.

S. Kalir, J. McClure, K. Pabbaraju, C. Southward, M. Ronen, S. Leibler, M. G. Surette, and U. Alon. Ordering genes in a flagella pathway by analysis of expression kinetics from living bacteria. *Science*, 292(5524):2080–2083, Jun 2001. doi: 10.1126/science.1058758. URL http://dx.doi.org/10.1126/science.1058758.

Shai Kaplan, Anat Bren, Erez Dekel, and Uri Alon. The incoherent feed-forward loop can generate non-monotonic input functions for genes. *Mol Syst Biol*, 4:203, 2008. doi: 10.1038/msb.2008.43. URL http://dx.doi.org/10.1038/msb.2008.43.

Jonathan R. Karr, Jayodita C. Sanghvi, Derek N. Macklin, Miriam V. Gutschow, Jared M. Jacobs, Benjamin Bolival, Jr, Nacyra Assad-Garcia, John I. Glass, and Markus W.

Covert. A whole-cell computational model predicts phenotype from genotype. *Cell*, 150(2):389–401, Jul 2012. doi: 10.1016/j.cell.2012.05.044. URL http://dx.doi.org/10.1016/j.cell.2012.05.044.

B. N. Kholodenko. Negative feedback and ultrasensitivity can bring about oscillations in the mitogen-activated protein kinase cascades. *Eur J Biochem*, 267(6):1583–1588, Mar 2000.

Boris N. Kholodenko, John F. Hancock, and Walter Kolch. Signalling ballet in space and time. *Nat Rev Mol Cell Biol*, 11(6):414–426, Jun 2010. doi: 10.1038/nrm2901. URL http://dx.doi.org/10.1038/nrm2901.

Dongsan Kim, Yung-Keun Kwon, and Kwang-Hyun Cho. The biphasic behavior of incoherent feed-forward loops in biomolecular regulatory networks. *Bioessays*, 30(11-12):1204–1211, Nov 2008. doi: 10.1002/bies.20839. URL http://dx.doi.org/10.1002/bies.20839.

Sun Young Kim and James E Ferrell, Jr. Substrate competition as a source of ultrasensitivity in the inactivation of wee1. *Cell*, 128(6):1133–1145, Mar 2007. doi: 10.1016/j.cell.2007.01.039. URL http://dx.doi.org/10.1016/j.cell.2007.01.039.

Yoosik Kim, Mathieu Coppey, Rona Grossman, Leiore Ajuria, Gerardo Jimenez, Ze'ev Paroush, and Stanislav Y Shvartsman. Mapk substrate competition integrates patterning signals in the drosophila embryo. *Curr Biol*, 20(5):446–451, Mar 2010. doi: 10.1016/j.cub.2010.01.019. URL http://dx.doi.org/10.1016/j.cub.2010.01.019.

Yoosik Kim, Ze'ev Paroush, Knud Nairz, Ernst Hafen, Gerardo Jimenez, and Stanislav Y. Shvartsman. Substrate-dependent control of mapk phosphorylation in vivo. *Mol Syst Biol*, 7:467, Feb 2011. doi: 10.1038/msb.2010.121. URL http://dx.doi.org/10.1038/msb.2010.121.

Hiroaki Kitano. Biological robustness. *Nat Rev Genet*, 5(11):826–837, Nov 2004. doi: 10.1038/nrg1471. URL http://dx.doi.org/10.1038/nrg1471.

Edda Klipp, Bodil Nordlander, Roland Kruger, Peter Gennemark, and Stefan Hohmann. Integrative model of the response of yeast to osmotic shock. *Nat Biotechnol*, 23(8):975–982, Aug 2005. doi: 10.1038/nbt1114. URL http://dx.doi.org/10.1038/nbt1114.

Maja Kohn, Marta Gutierrez-Rodriguez, Pascal Jonkheijm, Stefan Wetzel, Ron Wacker, Hendrik Schroeder, Heino Prinz, Christof M. Niemeyer, Rolf Breinbauer, Stefan E. Szedlacsek, and Herbert Waldmann. A microarray strategy for mapping the substrate specificity of protein tyrosine phosphatase. *Angew Chem Int Ed Engl*, 46(40):7700–7703, 2007. doi: 10.1002/anie.200701601. URL http://dx.doi.org/10.1002/anie.200701601.

Alexandr P. Kornev, Nina M. Haste, Susan S. Taylor, and Lynn F Ten Eyck. Surface comparison of active and inactive protein kinases identifies a conserved activation mechanism. *Proc Natl Acad Sci U S A*, 103(47):17783–17788, Nov 2006. doi: 10.1073/pnas.0607656103. URL http://dx.doi.org/10.1073/pnas.0607656103.

DE Koshland, Jr. A response regulator model in a simple sensory system. *Science*, 196 (4294):1055–1063, Jun 1977.

J. Krishnan. Signal processing through a generalized module of adaptation and spatial sensing. *J Theor Biol*, 259(1):31–43, Jul 2009. doi: 10.1016/j.jtbi.2009.02.015. URL http://dx.doi.org/10.1016/j.jtbi.2009.02.015.

J. Krishnan. Effects of saturation and enzyme limitation in feedforward adaptive signal transduction. *IET Syst Biol*, 5(3):208–219, May 2011. doi: 10.1049/iet-syb.2010.0048. URL http://dx.doi.org/10.1049/iet-syb.2010.0048.

Daniel R. Larson, Robert H. Singer, and Daniel Zenklusen. A single molecule view of gene expression. *Trends Cell Biol*, 19(11):630–637, Nov 2009. doi: 10.1016/j.tcb.2009.08.008. URL http://dx.doi.org/10.1016/j.tcb.2009.08.008.

M. F. Lavin and N. Gueven. The complexity of p53 stabilization and activation. *Cell Death Differ*, 13(6):941–950, Jun 2006. doi: 10.1038/sj.cdd.4401925. URL http://dx.doi.org/10.1038/sj.cdd.4401925.

Chul Won Lee, Josephine C. Ferreon, Allan Chris M. Ferreon, Munehito Arai, and Peter E. Wright. Graded enhancement of p53 binding to creb-binding protein (cbp) by multisite phosphorylation. *Proc Natl Acad Sci U S A*, 107(45):19290–19295, Nov 2010. doi: 10.1073/pnas.1013078107. URL http://dx.doi.org/10.1073/pnas.1013078107.

Stefan Legewie, Birgit Schoeberl, Nils Blüthgen, and Hanspeter Herzel. Competing docking interactions can bring about bistability in the MAPK cascade. *Biophys J*, 93(7):

2279–2288, Oct 2007. doi: 10.1529/biophysj.107.109132. URL http://dx.doi.org/10.1529/biophysj.107.109132.

A. Levchenko, J. Bruck, and P. W. Sternberg. Scaffold proteins may biphasically affect the levels of mitogen-activated protein kinase signaling and reduce its threshold properties. *Proc Natl Acad Sci U S A*, 97(11):5818–5823, May 2000.

Andre Levchenko and Pablo A. Iglesias. Models of eukaryotic gradient sensing: application to chemotaxis of amoebae and neutrophils. *Biophys J*, 82(1 Pt 1):50–63, Jan 2002. doi: 10.1016/S0006-3495(02)75373-3. URL http://dx.doi.org/10.1016/S0006-3495(02)75373-3.

Laura Lin, Robert Czerwinski, Kerry Kelleher, Marshall M. Siegel, Paul Wu, Ron Kriz, Ann Aulabaugh, and Mark Stahl. Activation loop phosphorylation modulates bruton's tyrosine kinase (btk) kinase domain activity. *Biochemistry*, 48(9):2021–2032, Mar 2009. doi: 10.1021/bi8019756. URL http://dx.doi.org/10.1021/bi8019756.

Xinfeng Liu, Lee Bardwell, and Qing Nie. A combination of multisite phosphorylation and substrate sequestration produces switchlike responses. *Biophys J*, 98(8):1396–1407, Apr 2010. doi: 10.1016/j.bpj.2009.12.4307. URL http://dx.doi.org/10.1016/j.bpj.2009.12.4307.

Jason W. Locasale, Andrey S. Shaw, and Arup K. Chakraborty. Scaffold proteins confer diverse regulatory properties to protein kinase cascades. *Proc Natl Acad Sci U S A*, 104(33):13307–13312, Aug 2007. doi: 10.1073/pnas.0706311104. URL http://dx.doi.org/10.1073/pnas.0706311104.

James C W. Locke and Michael B. Elowitz. Using movies to analyse gene circuit dynamics in single cells. *Nat Rev Microbiol*, 7(5):383–392, May 2009. doi: 10.1038/nrmicro2056. URL http://dx.doi.org/10.1038/nrmicro2056.

Feng Luo, Yunfeng Yang, Chin-Fu Chen, Roger Chang, Jizhong Zhou, and Richard H. Scheuermann. Modular organization of protein interaction networks. *Bioinformatics*, 23(2):207–214, Jan 2007. doi: 10.1093/bioinformatics/btl562. URL http://dx.doi.org/10.1093/bioinformatics/btl562.

Michael Lynch. The evolution of genetic networks by non-adaptive processes. *Nat Rev Genet*, 8(10):803–813, Oct 2007. doi: 10.1038/nrg2192. URL http://dx.doi.org/10.1038/nrg2192.

Wenzhe Ma, Ala Trusina, Hana El-Samad, Wendell A. Lim, and Chao Tang. Defining network topologies that can achieve biochemical adaptation. *Cell*, 138(4):760–773, Aug 2009. doi: 10.1016/j.cell.2009.06.013. URL http://dx.doi.org/10.1016/j.cell.2009.06.013.

Kyle L MacQuarrie, Abraham P Fong, Randall H Morse, and Stephen J Tapscott. Genome-wide transcription factor binding: beyond direct target regulation. *Trends Genet*, 27(4):141–148, Apr 2011. doi: 10.1016/j.tig.2011.01.001. URL http://dx.doi.org/10.1016/j.tig.2011.01.001.

S. Mangan and U. Alon. Structure and function of the feed-forward loop network motif. *Proc Natl Acad Sci U S A*, 100(21):11980–11985, Oct 2003. doi: 10.1073/pnas.2133841100. URL http://dx.doi.org/10.1073/pnas.2133841100.

Nick I. Markevich, Jan B. Hoek, and Boris N. Kholodenko. Signaling switches and bistability arising from multisite phosphorylation in protein kinase cascades. *J Cell Biol*, 164(3):353–359, Feb 2004. doi: 10.1083/jcb.200308060. URL http://dx.doi.org/10.1083/jcb.200308060.

Viveka Mayya, Deborah H. Lundgren, Sun-Il Hwang, Karim Rezaul, Linfeng Wu, Jimmy K. Eng, Vladimir Rodionov, and David K. Han. Quantitative phosphoproteomic analysis of t cell receptor signaling reveals system-wide modulation of protein-protein interactions. *Sci Signal*, 2(84):ra46, 2009. doi: 10.1126/scisignal.2000007. URL http://dx.doi.org/10.1126/scisignal.2000007.

George McConnachie, Lorene K. Langeberg, and John D. Scott. Akap signaling complexes: getting to the heart of the matter. *Trends Mol Med*, 12(7):317–323, Jul 2006. doi: 10.1016/j.molmed.2006.05.008. URL http://dx.doi.org/10.1016/j.molmed.2006.05.008.

Dale Muzzey, Carlos A. Gomez-Uribe, Jerome T. Mettetal, and Alexander van Oudenaarden. A systems-level analysis of perfect adaptation in yeast osmoregulation. *Cell*, 138(1):160–171, Jul 2009. doi: 10.1016/j.cell.2009.04.047. URL http://dx.doi.org/10.1016/j.cell.2009.04.047.

Arjun Narayanan and Matthew P. Jacobson. Computational studies of protein regulation by post-translational phosphorylation. *Curr Opin Struct Biol*, 19(2):156–163, Apr 2009. doi: 10.1016/j.sbi.2009.02.007. URL http://dx.doi.org/10.1016/j.sbi.2009.02.007.

Xiao Yu Ni, Tormod Drengstig, and Peter Ruoff. The control of the controller: molecular mechanisms for robust perfect adaptation and temperature compensation. *Biophys J*, 97 (5):1244–1253, Sep 2009. doi: 10.1016/j.bpj.2009.06.030. URL http://dx.doi.org/10.1016/j.bpj.2009.06.030.

Irene Nobeli, Angelo D. Favia, and Janet M. Thornton. Protein promiscuity and its implications for biotechnology. *Nat Biotechnol*, 27(2):157–167, Feb 2009. doi: 10.1038/nbt1519. URL http://dx.doi.org/10.1038/nbt1519.

Bela Novak and John J Tyson. Design principles of biochemical oscillators. *Nat Rev Mol Cell Biol*, 9(12):981–991, Dec 2008. doi: 10.1038/nrm2530. URL http://dx.doi.org/10.1038/nrm2530.

Andrew C. Oates, Luis G. Morelli, and Sadzl Ares. Patterning embryos with oscillations: structure, function and dynamics of the vertebrate segmentation clock. *Development*, 139(4):625–639, Feb 2012. doi: 10.1242/dev.063735. URL http://dx.doi.org/10.1242/dev.063735.

Richard Oberdorf and Tanja Kortemme. Complex topology rather than complex membership is a determinant of protein dosage sensitivity. *Mol Syst Biol*, 5:253, 2009. doi: 10.1038/msb.2009.9. URL http://dx.doi.org/10.1038/msb.2009.9.

Fernando Ortega, Luis Acerenza, Hans V Westerhoff, Francesc Mas, and Marta Cascante. Product dependence and bifunctionality compromise the ultrasensitivity of signal transduction cascades. *Proc Natl Acad Sci U S A*, 99(3):1170–1175, Feb 2002. doi: 10.1073/pnas.022267399. URL http://dx.doi.org/10.1073/pnas.022267399.

Ellen C. O'Shaughnessy, Santhosh Palani, James J. Collins, and Casim A. Sarkar. Tunable signal processing in synthetic MAP kinase cascades. *Cell*, 144(1):119–131, Jan 2011. doi: 10.1016/j.cell.2010.12.014. URL http://dx.doi.org/10.1016/j.cell.2010.12.014.

Shae B. Padrick and Michael K. Rosen. Physical mechanisms of signal integration by wasp family proteins. *Annu Rev Biochem*, 79:707–735, 2010. doi: 10.1146/

annurev.biochem.77.060407.135452. URL http://dx.doi.org/10.1146/annurev.biochem.77.060407.135452.

Tony Pawson and Michael Kofler. Kinome signaling through regulated protein-protein interactions in normal and cancer cells. *Curr Opin Cell Biol*, 21(2):147–153, Apr 2009. doi: 10.1016/j.ceb.2009.02.005. URL http://dx.doi.org/10.1016/j.ceb.2009.02.005.

M. F. Perutz. Stereochemistry of cooperative effects in haemoglobin. *Nature*, 228(5273): 726–739, Nov 1970.

Jan-Michael Peters. The anaphase promoting complex/cyclosome: a machine designed to destroy. *Nat Rev Mol Cell Biol*, 7(9):644–656, Sep 2006. doi: 10.1038/nrm1988. URL http://dx.doi.org/10.1038/nrm1988.

Benjamin Pfeuty and Kunihiko Kaneko. Minimal requirements for robust cell size control in eukaryotic cells. *Phys Biol*, 4(3):194–204, Sep 2007. doi: 10.1088/1478-3975/4/3/006. URL http://dx.doi.org/10.1088/1478-3975/4/3/006.

Benjamin Pfeuty, Quentin Thommen, and Marc Lefranc. Robust entrainment of circadian oscillators requires specific phase response curves. *Biophys J*, 100(11):2557–2565, Jun 2011. doi: 10.1016/j.bpj.2011.04.043. URL http://dx.doi.org/10.1016/j.bpj.2011.04.043.

Finly Philip, Ganesh Kadamur, Rosa Gonzalez Silos, Jimmy Woodson, and Elliott M. Ross. Synergistic activation of phospholipase c-beta3 by galpha(q) and gbetagamma describes a simple two-state coincidence detector. *Curr Biol*, 20(15):1327–1335, Aug 2010. doi: 10.1016/j.cub.2010.06.013. URL http://dx.doi.org/10.1016/j.cub.2010.06.013.

Danilo Porro, Luca Brambilla, and Lilia Alberghina. Glucose metabolism and cell size in continuous cultures of saccharomyces cerevisiae. *FEMS Microbiol Lett*, 229(2):165–171, Dec 2003.

Kenneth E. Prehoda and Wendell A. Lim. How signaling proteins integrate multiple inputs: a comparison of n-wasp and cdk2. *Curr Opin Cell Biol*, 14(2):149–154, Apr 2002.

Mark Ptashne. Principles of a switch. *Nat Chem Biol*, 7(8):484–487, Aug 2011. doi: 10.1038/nchembio.611. URL http://dx.doi.org/10.1038/nchembio.611.

Matthias Rabiller, Matthaus Getlik, Sabine Kluter, Andre Richters, Sandra Tuckmantel, Jeffrey R. Simard, and Daniel Rauh. Proteus in the world of proteins: conformational changes in protein kinases. *Arch Pharm (Weinheim)*, 343(4):193–206, Apr 2010. doi: 10.1002/ardp.201000028. URL http://dx.doi.org/10.1002/ardp.201000028.

Naren Ramakrishnan and Upinder S. Bhalla. Memory switches in chemical reaction space. *PLoS Comput Biol*, 4(7):e1000122, 2008. doi: 10.1371/journal.pcbi.1000122. URL http://dx.doi.org/10.1371/journal.pcbi.1000122.

D. A. Rand. Mapping global sensitivity of cellular network dynamics: sensitivity heat maps and a global summation law. *J R Soc Interface*, 5 Suppl 1:S59–S69, Aug 2008. doi: 10.1098/rsif.2008.0084.focus. URL http://dx.doi.org/10.1098/rsif.2008.0084.focus.

D. A. Rand, B. V. Shulgin, D. Salazar, and A. J. Millar. Design principles underlying circadian clocks. *J R Soc Interface*, 1(1):119–130, Nov 2004. doi: 10.1098/rsif.2004.0014. URL http://dx.doi.org/10.1098/rsif.2004.0014.

D. A. Rand, B. V. Shulgin, J. D. Salazar, and A. J. Millar. Uncovering the design principles of circadian clocks: mathematical analysis of flexibility and evolutionary goals. *J Theor Biol*, 238(3):616–635, Feb 2006. doi: 10.1016/j.jtbi.2005.06.026. URL http://dx.doi.org/10.1016/j.jtbi.2005.06.026.

Michael Rape, Sashank K. Reddy, and Marc W. Kirschner. The processivity of multiubiquitination by the apc determines the order of substrate degradation. *Cell*, 124(1):89–103, Jan 2006. doi: 10.1016/j.cell.2005.10.032. URL http://dx.doi.org/10.1016/j.cell.2005.10.032.

Daniel M. Rosenbaum, S?ren G F. Rasmussen, and Brian K. Kobilka. The structure and function of g-protein-coupled receptors. *Nature*, 459(7245):356–363, May 2009. doi: 10.1038/nature08144. URL http://dx.doi.org/10.1038/nature08144.

Amy C. Rowat, James C. Bird, Jeremy J. Agresti, Oliver J. Rando, and David A. Weitz. Tracking lineages of single cells in lines using a microfluidic device. *Proc Natl Acad Sci U S A*, 106(43):18149–18154, Oct 2009. doi: 10.1073/pnas.0903163106. URL http://dx.doi.org/10.1073/pnas.0903163106.

Mohsen Sabouri-Ghomi, Andrea Ciliberto, Sandip Kar, Bela Novak, and John J Tyson. Antagonism and bistability in protein interaction networks. *J Theor Biol*, 250(1):209–218, Jan 2008. doi: 10.1016/j.jtbi.2007.09.001. URL http://dx.doi.org/10.1016/j.jtbi.2007.09.001.

Carlos Salazar and Thomas Hofer. Kinetic models of phosphorylation cycles: a systematic approach using the rapid-equilibrium approximation for protein-protein interactions. *Biosystems*, 83(2-3):195–206, 2006. doi: 10.1016/j.biosystems.2005.05.015. URL http://dx.doi.org/10.1016/j.biosystems.2005.05.015.

Carlos Salazar, Anneke Brummer, Lilia Alberghina, and Thomas Höfer. Timing control in regulatory networks by multisite protein modifications. *Trends Cell Biol*, 20(11):634–641, Nov 2010. doi: 10.1016/j.tcb.2010.08.012. URL http://dx.doi.org/10.1016/j.tcb.2010.08.012.

William A. Sands and Timothy M. Palmer. Regulating gene transcription in response to cyclic amp elevation. *Cell Signal*, 20(3):460–466, Mar 2008. doi: 10.1016/j.cellsig.2007.10.005. URL http://dx.doi.org/10.1016/j.cellsig.2007.10.005.

Arti Santhanam, Alan Hartley, Katrin Duvel, James R. Broach, and Stephen Garrett. Pp2a phosphatase activity is required for stress and tor kinase regulation of yeast stress response factor msn2p. *Eukaryot Cell*, 3(5):1261–1271, Oct 2004. doi: 10.1128/EC.3.5.1261-1271.2004. URL http://dx.doi.org/10.1128/EC.3.5.1261-1271.2004.

John F. Schindler, Andrew Godbey, William F. Hood, Suzanne L. Bolten, Richard M. Broadus, Thomas P. Kasten, Aaron J. Cassely, Jeffery L. Hirsch, Michelle A. Merwood, Mark A. Nagy, Kam F. Fok, Matthew J. Saabye, Heidi M. Morgan, Robert P. Compton, Robert J. Mourey, Arthur J. Wittwer, and Joseph B. Monahan. Examination of the kinetic mechanism of mitogen-activated protein kinase activated protein kinase-2. *Biochim Biophys Acta*, 1598(1-2):88–97, Jul 2002.

Gerald Schwank and Konrad Basler. Regulation of organ growth by morphogen gradients. *Cold Spring Harb Perspect Biol*, 2(1):a001669, Jan 2010. doi: 10.1101/cshperspect.a001669. URL http://dx.doi.org/10.1101/cshperspect.a001669.

D. Seaton and J. Krishnan. Modular systems approach to understanding the interaction of adaptive and monostable and bistable threshold processes. *IET Syst Biol*, 5(2):81–

94, Mar 2011a. doi: 10.1049/iet-syb.2009.0061. URL http://dx.doi.org/10.1049/iet-syb.2009.0061.

Daniel D Seaton and J. Krishnan. The coupling of pathways and processes through shared components. *BMC Syst Biol*, 5:103, 2011b. doi: 10.1186/1752-0509-5-103. URL http://dx.doi.org/10.1186/1752-0509-5-103.

Jesus Seco, Carles Ferrer-Costa, Josep M. Campanera, Robert Soliva, and Xavier Barril. Allosteric regulation of pkc?: understanding multistep phosphorylation and priming by ligands in agc kinases. *Proteins*, 80(1):269–280, Jan 2012. doi: 10.1002/prot.23205. URL http://dx.doi.org/10.1002/prot.23205.

L. A. Segel. On the validity of the steady state assumption of enzyme kinetics. *Bull Math Biol*, 50(6):579–593, 1988.

Pil Joon Seo, Shin-Young Hong, Sang-Gyu Kim, and Chung-Mo Park. Competitive inhibition of transcription factors by small interfering peptides. *Trends Plant Sci*, 16(10):541–549, Oct 2011. doi: 10.1016/j.tplants.2011.06.001. URL http://dx.doi.org/10.1016/j.tplants.2011.06.001.

Ann-Bin Shyu, Miles F. Wilkinson, and Ambro van Hoof. Messenger rna regulation: to translate or to degrade. *EMBO J*, 27(3):471–481, Feb 2008. doi: 10.1038/sj.emboj.7601977. URL http://dx.doi.org/10.1038/sj.emboj.7601977.

Amoolya H. Singh, Denise M. Wolf, Peggy Wang, and Adam P. Arkin. Modularity of stress response evolution. *Proc Natl Acad Sci U S A*, 105(21):7500–7505, May 2008. doi: 10.1073/pnas.0709764105. URL http://dx.doi.org/10.1073/pnas.0709764105.

Sungmin Son, Amit Tzur, Yaochung Weng, Paul Jorgensen, Jisoo Kim, Marc W. Kirschner, and Scott R. Manalis. Direct observation of mammalian cell growth and size regulation. *Nat Methods*, 9(9):910–912, Sep 2012. doi: 10.1038/nmeth.2133. URL http://dx.doi.org/10.1038/nmeth.2133.

E. D. Sontag. Remarks on feedforward circuits, adaptation, and pulse memory. *IET Syst Biol*, 4(1):39–51, Jan 2010. doi: 10.1049/iet-syb.2008.0171. URL http://dx.doi.org/10.1049/iet-syb.2008.0171.

David G. Spiller, Christopher D. Wood, David A. Rand, and Michael R H. White. Measurement of single-cell dynamics. *Nature*, 465(7299):736–745, Jun 2010. doi: 10.1038/nature09232. URL http://dx.doi.org/10.1038/nature09232.

Keith A. Spriggs, Martin Bushell, and Anne E. Willis. Translational regulation of gene expression during conditions of cell stress. *Mol Cell*, 40(2):228–237, Oct 2010. doi: 10.1016/j.molcel.2010.09.028. URL http://dx.doi.org/10.1016/j.molcel.2010.09.028.

K. Sriram, G. Bernot, and F. Kepes. A minimal mathematical model combining several regulatory cycles from the budding yeast cell cycle. *IET Syst Biol*, 1(6):326–341, Nov 2007.

Jon M. Steichen, Ganesh H. Iyer, Sheng Li, S Adrian Saldanha, Michael S. Deal, Virgil L Woods, Jr, and Susan S. Taylor. Global consequences of activation loop phosphorylation on protein kinase a. *J Biol Chem*, 285(6):3825–3832, Feb 2010. doi: 10.1074/jbc.M109.061820. URL http://dx.doi.org/10.1074/jbc.M109.061820.

Jörg Stelling, Uwe Sauer, Zoltan Szallasi, Francis J Doyle, 3rd, and John Doyle. Robustness of cellular functions. *Cell*, 118(6):675–685, Sep 2004. doi: 10.1016/j.cell.2004.09.008. URL http://dx.doi.org/10.1016/j.cell.2004.09.008.

A. M. Stock, V. L. Robinson, and P. N. Goudreau. Two-component signal transduction. *Annu Rev Biochem*, 69:183–215, 2000. doi: 10.1146/annurev.biochem.69.1.183. URL http://dx.doi.org/10.1146/annurev.biochem.69.1.183.

Charles H. Streuli. Integrins and cell-fate determination. *J Cell Sci*, 122(Pt 2):171–177, Jan 2009. doi: 10.1242/jcs.018945. URL http://dx.doi.org/10.1242/jcs.018945.

Jesse Stricker, Scott Cookson, Matthew R. Bennett, William H. Mather, Lev S. Tsimring, and Jeff Hasty. A fast, robust and tunable synthetic gene oscillator. *Nature*, 456 (7221):516–519, Nov 2008. doi: 10.1038/nature07389. URL http://dx.doi.org/10.1038/nature07389.

Naoyuki Sugiyama, Hirofumi Nakagami, Keiichi Mochida, Arsalan Daudi, Masaru Tomita, Ken Shirasu, and Yasushi Ishihama. Large-scale phosphorylation mapping reveals the extent of tyrosine phosphorylation in arabidopsis. *Mol Syst Biol*, 4:193, 2008. doi: 10.1038/msb.2008.32. URL http://dx.doi.org/10.1038/msb.2008.32.

Lijun Sun and Zhijian J Chen. The novel functions of ubiquitination in signaling. *Curr Opin Cell Biol*, 16(2):119–126, Apr 2004. doi: 10.1016/j.ceb.2004.02.005. URL http://dx.doi.org/10.1016/j.ceb.2004.02.005.

Barbara Szomolay and Vahid Shahrezaei. Bell-shaped and ultrasensitive dose-response in phosphorylation-dephosphorylation cycles: the role of kinase-phosphatase complex formation. *BMC Syst Biol*, 6(1):26, Apr 2012. doi: 10.1186/1752-0509-6-26. URL http://dx.doi.org/10.1186/1752-0509-6-26.

Masahiro Takahashi, Tatsuo Shibata, Toshio Yanagida, and Yasushi Sako. A protein switch with tunable steepness reconstructed in escherichia coli cells with eukaryotic signaling proteins. *Biochem Biophys Res Commun*, 421(4):731–735, May 2012. doi: 10.1016/j.bbrc.2012.04.071. URL http://dx.doi.org/10.1016/j.bbrc.2012.04.071.

Amos Tanay, Roded Sharan, Martin Kupiec, and Ron Shamir. Revealing modularity and organization in the yeast molecular network by integrated analysis of highly heterogeneous genomewide data. *Proc Natl Acad Sci U S A*, 101(9):2981–2986, Mar 2004. doi: 10.1073/pnas.0308661100. URL http://dx.doi.org/10.1073/pnas.0308661100.

Susan S. Taylor and Alexandr P. Kornev. Protein kinases: evolution of dynamic regulatory proteins. *Trends Biochem Sci*, 36(2):65–77, Feb 2011. doi: 10.1016/j.tibs.2010.09.006. URL http://dx.doi.org/10.1016/j.tibs.2010.09.006.

Craig J Thalhauser and Natalia L Komarova. Signal response sensitivity in the yeast mitogen-activated protein kinase cascade. *PLoS One*, 5(7):e11568, 2010. doi: 10.1371/journal.pone.0011568. URL http://dx.doi.org/10.1371/journal.pone.0011568.

Matthew Thomson and Jeremy Gunawardena. Unlimited multistability in multisite phosphorylation systems. *Nature*, 460(7252):274–277, Jul 2009. doi: 10.1038/nature08102. URL http://dx.doi.org/10.1038/nature08102.

Benjamin P. Tu, Andrzej Kudlicki, Maga Rowicka, and Steven L. McKnight. Logic of the yeast metabolic cycle: temporal compartmentalization of cellular processes. *Science*, 310(5751):1152–1158, Nov 2005. doi: 10.1126/science.1120499. URL http://dx.doi.org/10.1126/science.1120499.

John J Tyson and Bela Novak. Temporal organization of the cell cycle. *Curr Biol*, 18(17): R759–R768, Sep 2008. doi: 10.1016/j.cub.2008.07.001. URL http://dx.doi.org/10.1016/j.cub.2008.07.001.

John J. Tyson, Katherine C. Chen, and Bela Novak. Sniffers, buzzers, toggles and blinkers: dynamics of regulatory and signaling pathways in the cell. *Curr Opin Cell Biol*, 15(2): 221–231, Apr 2003.

Hideki Ukai and Hiroki R. Ueda. Systems biology of mammalian circadian clocks. *Annu Rev Physiol*, 72:579–603, 2010. doi: 10.1146/annurev-physiol-073109-130051. URL http://dx.doi.org/10.1146/annurev-physiol-073109-130051.

Fausto Ulloa and James Briscoe. Morphogens and the control of cell proliferation and patterning in the spinal cord. *Cell Cycle*, 6(21):2640–2649, Nov 2007.

Tanya Vavouri, Jennifer I. Semple, Rosa Garcia-Verdugo, and Ben Lehner. Intrinsic protein disorder and interaction promiscuity are widely associated with dosage sensitivity. *Cell*, 138(1):198–208, Jul 2009. doi: 10.1016/j.cell.2009.04.029. URL http://dx.doi.org/10.1016/j.cell.2009.04.029.

Domitilla Del Vecchio, Alexander J Ninfa, and Eduardo D Sontag. Modular cell biology: retroactivity and insulation. *Mol Syst Biol*, 4:161, 2008. doi: 10.1038/msb4100204. URL http://dx.doi.org/10.1038/msb4100204.

Reiner A. Veitia, Samuel Bottani, and James A. Birchler. Cellular reactions to gene dosage imbalance: genomic, transcriptomic and proteomic effects. *Trends Genet*, 24(8):390–397, Aug 2008. doi: 10.1016/j.tig.2008.05.005. URL http://dx.doi.org/10.1016/j.tig.2008.05.005.

Barry Wark, Brian Nils Lundstrom, and Adrienne Fairhall. Sensory adaptation. *Curr Opin Neurobiol*, 17(4):423–429, Aug 2007. doi: 10.1016/j.conb.2007.07.001. URL http://dx.doi.org/10.1016/j.conb.2007.07.001.

Darren J. Wilkinson. Stochastic modelling for quantitative description of heterogeneous biological systems. *Nat Rev Genet*, 10(2):122–133, Feb 2009. doi: 10.1038/nrg2509. URL http://dx.doi.org/10.1038/nrg2509.

Alejandro Wolf-Yadlin, Mark Sevecka, and Gavin MacBeath. Dissecting protein function and signaling using protein microarrays. *Curr Opin Chem Biol*, 13(4):398–405, Oct 2009. doi: 10.1016/j.cbpa.2009.06.027. URL http://dx.doi.org/10.1016/j.cbpa.2009.06.027.

Jin Yang and William S. Hlavacek. Scaffold-mediated nucleation of protein signaling complexes: elementary principles. *Math Biosci*, 232(2):164–173, Aug 2011. doi: 10.1016/j.mbs.2011.06.003. URL http://dx.doi.org/10.1016/j.mbs.2011.06.003.

Qiong Yang, Bernardo F. Pando, Guogang Dong, Susan S. Golden, and Alexander van Oudenaarden. Circadian gating of the cell cycle revealed in single cyanobacterial cells. *Science*, 327(5972):1522–1526, Mar 2010. doi: 10.1126/science.1181759. URL http://dx.doi.org/10.1126/science.1181759.

T. M. Yi, Y. Huang, M. I. Simon, and J. Doyle. Robust perfect adaptation in bacterial chemotaxis through integral feedback control. *Proc Natl Acad Sci U S A*, 97(9):4649–4653, Apr 2000.

Shadia Zaman, Soyeon Im Lippman, Xin Zhao, and James R Broach. How saccharomyces responds to nutrients. *Annu Rev Genet*, 42:27–81, 2008. doi: 10.1146/annurev.genet.41.110306.130206. URL http://dx.doi.org/10.1146/annurev.genet.41.110306.130206.

Shadia Zaman, Soyeon I. Lippman, Lisa Schneper, Noam Slonim, and James R. Broach. Glucose regulates transcription in yeast through a network of signaling pathways. *Mol Syst Biol*, 5:245, 2009. doi: 10.1038/msb.2009.2. URL http://dx.doi.org/10.1038/msb.2009.2.

Eric E. Zhang and Steve A. Kay. Clocks not winding down: unravelling circadian networks. *Nat Rev Mol Cell Biol*, 11(11):764–776, Nov 2010. doi: 10.1038/nrm2995. URL http://dx.doi.org/10.1038/nrm2995.

Qiang Zhang and Melvin E. Andersen. Dose response relationship in anti-stress gene regulatory networks. *PLoS Comput Biol*, 3(3):e24, Mar 2007. doi: 10.1371/journal.pcbi.0030024. URL http://dx.doi.org/10.1371/journal.pcbi.0030024.